

Effects of Hormones and Load on Murine Trabecular and Cortical Bone Turnover

WILLIAMSON, Alexander Neil

Available from the Sheffield Hallam University Research Archive (SHURA) at:

https://shura.shu.ac.uk/36403/

## A Sheffield Hallam University thesis

This thesis is protected by copyright which belongs to the author.

The content must not be changed in any way or sold commercially in any format or medium without the formal permission of the author.

When referring to this work, full bibliographic details including the author, title, awarding institution and date of the thesis must be given.

Please visit https://shura.shu.ac.uk/36403/ and <a href="http://shura.shu.ac.uk/information.html">http://shura.shu.ac.uk/information.html</a> for further details about copyright and re-use permissions.

# Effects of Hormones and Load on Murine Trabecular and Cortical Bone Turnover

Alexander Neil Williamson

A thesis submitted in partial fulfilment of the requirements of Sheffield Hallam University for the degree of Doctor of Philosophy

September 2024

### **Candidate Declaration**

I hereby declare that:

- 1. I have not been enrolled for another award of the University, or other academic or professional organisation, whilst undertaking my research degree.
- 2. None of the material contained in the thesis has been used in any other submission for an academic award.
- 3. I am aware of and understand the University's policy on plagiarism and certify that this thesis is my own work. The use of all published or other sources of material consulted have been properly and fully acknowledged.
- 4. The work undertaken towards the thesis has been conducted in accordance with the SHU Principles of Integrity in Research and the SHU Research Ethics Policy.
- 5. The word count of this thesis is 40,145.

Name:	Alexander Neil Williamson
Date:	September 2024
Award:	PhD
Faculty:	Health and Wellbeing
Director of Studies:	Dr. Nicola Aberdein

## **Acknowledgements**

The work presented in this thesis was made possible by far too many people to mention. That said, I might as well have a go at providing a few highlights. Firstly, I would like to express my unending gratitude to my supervisors, Dr. Nicola Aberdein, Professor Christine Le Maitre, and Dr. Dan Kelly. Your expert guidance, unconditional support, and seemingly infinite patience have allowed me to develop more than I thought possible throughout my PhD, and I still use the skills you taught me every day. You always knew how to keep me moving forwards when I got lost or overwhelmed.

I owe my initial decision to pursue a PhD to my experience during my placement year at the University of Sheffield Medical School. Therefore, I would also like to extend my gratitude to Professor Alison Gartland for the opportunity to work in The Gartland Lab Group, even though the group hadn't planned to foster a placement student that year. Similarly, to Dr. Karan Shah, who always managed to give great advice whilst allowing me to make my own mistakes and learn from them. I highly doubt I'd have even pursued a PhD in the first place were it not for my short time spent learning from the best. I'd also like to thank Darren Lath for immediately making me feel at ease in the lab, somehow managing to juggle being kinder, funnier, and more intelligent than most of us can hope to be. This one year completely changed my life, giving me the confidence and knowledge to continue my studies and allowing me to meet some amazing people. Foreshadowing is a narrative device in which a storyteller gives an advance hint of what is to come later in the story.

My PhD experience would not have been the same without the excellent company from the other PhD students in the BMRC. Your friendship, support, and shared love of long island iced teas have made the past few years a wonderful experience despite the many obstacles that came our way, including navigating a PhD during a global pandemic. I think we can all agree that part was a bit rubbish. Special thanks to Lucy Dascombe for the many days spent laughing, crying, or singing Diana Ross together, in the Micro-CT cupboard suite or in the fields of Glastonbury Festival.

Life outside of the lab would not have been nearly as entertaining without the friends who I have been fortunate enough to meet over the past few years, both from back home in Waz Angeles and here in Sheffield. I feel very lucky that there are too many of you to name here. When I got a part-time job at The Nursery Tavern, I was just hoping to earn some extra money to pay the bills during my studies. Instead, I ended up with a new, Sheffield-based dysfunctional family, and I'm very grateful to have you all in my life years after pouring my last pint.

That brings me to my *actual* family, without whom I would never have been able to find my way to nursery, never mind post-graduate study. My mum and dad have supported me in many ways over the years and, much like Student Finance England, I will be forever in their debt. Thank you for making it possible for me to come to university, and then stay here for longer than any of us perhaps thought. I promise I'm finally done now. I am particularly grateful for a pearl of wisdom passed down from my grandparents, which inspired me to finish writing my thesis: 'just write the damn thing'. I did just that.

It would be remiss of me not to thank the borderline sociopathic, fuzzy little war criminal that I choose to live with: Peaches. You have helped me write this thesis more than a cat has any right to, despite your outright refusal to help me with statistical analysis.

Finally, to Meg: I'll never be able to express my eternal gratitude, love, and admiration for you, and everything you have done to help me get this far whilst studying for a PhD of your own. When we met on placement in the aforementioned med school, we never imagined we'd end up living together with a cat whilst earning our PhDs (again, cheers Karan), but I can't imagine a more perfect path for our lives to have taken from there. I have no doubt that this would not have been possible without you, and I can't thank you enough for putting up with my writing woes, and for showing me that maybe it is meant for me.

"The night belongs to you; this bough has broken through."

## Abstract:

Obesity presents a number of challenges to healthcare systems worldwide, increasing the risk of several disorders, including bone disorders such as osteoporosis. The effects of impaired hormone signalling in obesity are difficult to separate from those caused by concomitant increases in mechanical load from body weight. The work presented in this thesis explored the roles of testosterone, leptin, and a high-fat diet in bone health, combining animal models and cell culture models to investigate the influence of these factors on bone morphology and metabolism, particularly in the context of hormonal deficiencies and metabolic disorders, which can occur during obesity. Testosterone's anabolic role in bone formation is well established, but this study highlights antiresorptive effects through the RANKL pathway, which maintains bone mass by suppressing osteoclast activity. In orchiectomised mice, testosterone deficiency led to significant reductions in trabecular bone volume, which were restored by testosterone replacement therapy (TRT). Despite these improvements, TRT did not fully restore tibial mechanical strength, aligning with clinical findings that TRT does not reduce fracture risk in men. This suggests testosterone's effects on bone may involve factors beyond mineral content, such as the extracellular matrix. In vitro investigation revealed no clear relationship between testosterone and gene expression in pre-osteoblast cells, though non-significant trends toward increased RUNX2 expression were observed, suggesting a potential role in osteoblast differentiation. Testosterone also increased collagen and calcium deposition in 3D culture models, reinforcing its anabolic effects on bone. Leptin, traditionally known for regulating metabolism, also plays a crucial role in bone turnover. Leptin deficiency in Ob/Ob mice led to impaired cortical and trabecular bone structure, independent of body weight. These effects were site-specific, with differing impacts on vertebrae and tibiae. Leptin deficiency and HFD both increased marrow adiposity, suggesting a shift toward adipogenesis at the expense of osteogenesis, further complicating the relationship between obesity and bone health. Despite increased body weight, HFD did not enhance bone volume in C57 mice, indicating that obesity can negatively affect bone strength through mechanisms beyond weight-bearing. In vitro, leptin treatment had minimal effects on gene expression in pre-osteoblast cells, but enhanced observed staining intensity for collagen and calcium matrix deposition, highlighting leptin's potential role in promoting bone formation. The study also investigated how leptin and testosterone interact with mechanical loading in bone cells. In 2D cultures, fluid shear stress combined with leptin increased osteogenic marker expression, though no significant changes were observed in gene expression. In 3D cultures, hormone treatments, particularly leptin, enhanced collagen and calcium deposition under mechanical load, suggesting a synergistic effect in promoting bone formation. This research enhances our understanding of how testosterone, leptin, and HFD influence bone health, particularly their interplay with mechanical loading. It challenges existing views on obesity and bone strength, highlighting the complex relationship between metabolic health and bone morphology. The findings suggest that therapies targeting the bone-protective effects of testosterone and leptin could be beneficial for treating osteoporosis and other metabolic bone diseases. Further research is needed to explore the mechanisms underlying hormone signalling and mechanotransduction to better inform future treatments for bone-related complications in individuals with hormonal imbalances and obesity.

## Contents

List	of Fig	rures:	13
List	of Ta	bles:	18
List	of Ab	breviations:	19
Dis	semin	ation:	21
1.	Cha	oter 1: Introduction:	22
1	1.	Study Importance:	23
1	2.	Bone Remodelling:	24
1	3.	High Fat Diet and Bone Remodelling:	28
1	4.	Testosterone and Bone Remodelling:	30
1	5.	Leptin and Bone Remodelling:	34
1	6.	Mechanotransduction and Bone Remodelling:	39
1	7.	Interactions Between Hormone Signalling and Mechanotransduction in Bo	one:
			47
1	8.	Aims and Objectives:	50
1	9.	Specific Aims:	51
2.	Cha	oter 2: The Effects of Testosterone Depletion Upon Bone Turnover in a Mu	rine
Мо	del of	Cardiometabolic Disorder Fed a High Fat Diet:	52
2	2.1.	Introduction:	53
2	2.2.	Materials and Methods:	58
	2.2.3	1. Experimental Design:	58
	2.2.2	2. Animal Husbandry:	59
	2.2.3	3. Surgical Bilateral Orchiectomy and Testosterone Treatment:	60
	2.2.4	4. Testosterone or Placebo Treatment	60
	2.2.5	5. Tissue Collection:	61
	2.2.6	5. Serum Collection:	61
	22	7. Measurement of Serum Testosterone via ELISA:	61

	2.2.8. μC	T imaging:6	52
	2.2.9. lm	age post-processing:6	52
	2.2.10. Q	uantitative morphometry:6	54
	2.2.11. T	rabecular Thickness Colour-coded 3D Modelling:6	54
	2.2.12. T	issue Preparation:6	54
	2.2.13. H	aematoxylin and Eosin Staining:6	35
	2.2.14. N	lasson's Trichrome Staining:6	35
	2.2.15. T	artrate-resistant Acid Phosphatase (TRAP) Staining:6	56
	2.2.16. O	steoMeasure TRAP counting:6	56
	2.2.17. lr	nmunohistochemistry:6	57
	2.2.18. lr	nage Capture and Quantification of IHC:6	59
	2.2.19. Q	uantification of Lipid Droplet Area:6	59
	2.2.20. T	hree-point Bending Mechanical Testing:	70
	2.2.21. S	tatistical Analysis:	71
2.3	3. Resi	ults:	71
	2.3.1.	Serum Testosterone Concentration:	71
	2.3.2.	Body weight and cortical bone parameters:	73
	2.3.3.	Trabecular bone parameters:	74
	2.3.4.	Histological Assessment of ECM Component Distribution and Bor	ıе
	Marrow	Adiposity:7	77
	2.3.5.	Immunohistochemical Analysis of Bone Cell Markers in Murine Tibiae:	30
	2.3.6.	Mechanical Testing:	36
2.4	4. Disc	eussion:	37
	2.4.1.	The Effects of Testosterone Deficiency and Testosterone Replaceme	nt
	Therapy	Upon Body Weights and Testosterone Levels:	38
	2.4.2.	The Effects of Testosterone Deficiency and Testosterone Replaceme	
	Therapy	Upon Cortical and Trabecular Bone Parameters:	€0

	2.4.3.	The Effect of Testosterone Deficiency and Testosterone Treatment	t Upon
	Osteobla	st Differentiation and Mineralisation:	93
	2.4.4.	The Effect of Testosterone Deficiency and Testosterone Treatment	t Upon
	Osteocla	st Differentiation and Mineralisation:	95
	2.4.5.	The Effect of Testosterone Deficiency and Testosterone Treatment	t Upon
	Bone Me	echanical Strength:	97
	2.4.6.	Conclusion:	99
3.	Chapter	3: Impact of Leptin Deficiency on Male Tibia and Vertebral Body 3D	) Bone
Arcl	hitecture I	ndependent of Changes in Body Weight:	100
3	.1. Intro	oduction:	101
3	.2. Mat	terials and Methods:	105
	3.2.1.	Experimental Design:	105
	3.2.2.	Ethical Approval:	106
	3.2.3.	Mice and Treatments:	106
	3.2.4.	Food Restriction:	107
	3.2.5.	Tissue Harvest:	108
	3.2.6.	Micro-CT Imaging:	108
	3.2.7.	Image Post-processing:	109
	3.2.8.	Quantitative Morphometry:	109
	3.2.9.	3D Colour Coded Bone Thickness Analysis:	109
	3.2.10.	3D Colour Coded Bone Density Analysis:	110
	3.2.11.	Tissue Preparation:	110
	3.2.12.	Haematoxylin and Eosin Staining:	110
	3.2.13.	Histological Assessment of murine tibiae and L3 vertebrae:	110
	3.2.14.	Immunohistochemistry:	
	3.2.15.	Image Capture and Quantification of IHC:	
	3.2.16.		
	J.Z.IU.	IIIICC DOILL DEHUIIK DIVIIICUIAIIKAI 1631	+ + +

	3.2.17.	Statistical Analysis:
3.	.3. Resi	ults:113
	3.3.1.	Leptin Deficiency Increased Fat Mass Independently of Body Weight:113
	3.3.2. Body We	Leptin Deficiency Reduced Tibia Cortical Bone Volume Independently o
	3.3.3.	Leptin Deficiency and HFD Reduced Tibia Trabecular Bone Number, Bone
	Mineral I	Density, and Increased Trabecular Separation:117
	3.3.4.	Regional Differences in Tibia Trabecular Thickness Distribution Are
	Masked l	by Overall Thickness Mean:119
	3.3.5.	Leptin Deficiency Reduces Vertebral Cortical Bone Thickness:122
		gh Fat Diet Reduced Vertebral Trabecular Bone Volume, Number and Density:
	3.3.7.	Regional Differences in Vertebral Trabecular Thickness Distribution are
	Masked l	by Overall Thickness Mean:125
	3.3.8.	HFD and Leptin Deficiency Alter Bone Marrow Composition:127
	3.3.9.	Leptin Deficiency Significantly Reduces OPG Expression in the Tibiae o
	Obese Oi	b/Ob Mice, but Not the Vertebrae:129
	3.3.10. Affect Bo	Observed Alterations in Bone Microarchitecture Did Not Significantly ne Strength:
3.	.4. Disc	ussion:136
	3.4.1.	Effects of Leptin Deficiency on Cortical and Trabecular Bone Morphology 136
	3.4.2.	Effects of High Fat Diet on Cortical and Trabecular Bone Morphology 138
	3.4.3.	Effects of Mechanical Load from Body Weight on Cortical and Trabecula
	Bone Mo	rphology:
	3.4.4.	Trabecular Thickness and Clinical Implications:143
	3.4.5.	Confounding Factors and Limitations:143

4.	Chapter 4: Interactions Between Hormone Signalling and Mechanical	Loading in
Mu	rine Bone Cells <i>In Vitro</i> :	146
4	l.1. Introduction:	147
4	I.2. Materials and Methods:	153
	4.2.1. Experimental Design:	153
	4.2.2. MC3T3-E1 Cell Culture and Differentiation:	154
	4.2.3. MLO-Y4 Cell Culture:	154
	4.2.4. Leptin and Testosterone Treatment:	154
	4.2.5. Leptin and Testosterone Degradation in Cell Culture Media:	155
	4.2.6. Fluid Shear Stress Application:	156
	4.2.7. RNA Extraction:	157
	4.2.8. cDNA Synthesis:	157
	4.2.9. Gene Expression Assessment via RT-qPCR:	158
	4.2.10. MG63 Cell Culture and Maintenance:	160
	4.2.11. Collagen Gel Constructs:	160
	4.2.12. Cell-laden Collagen I Gel Processing:	161
	4.2.13. Immunohistochemistry and Histology:	161
	4.2.14. Hydrogel Preparation:	162
	4.2.15. 3D Cell Culture of MC3T3-E1 Cells in Hydrogel:	162
	4.2.16. Hydrostatic Loading of 3D Cell Constructs:	163
	4.2.17. Matrix Deposition Within Hydrogel Constructs:	163
	4.2.18. Alkaline Phosphatase (ALP) Activity Assay:	164
4	l.3. Results:	165
	4.3.1. Differentiation of MC3T3-E1 Cells <i>In Vitro</i> :	165
	4.3.2. Gene Expression of Key Bone Cell Markers in Undifferentiated Cells: 165	MC3T3-E1

4.3.3. Gene Expression of key bone cell markers in differentiated MC3T3-E1 cells:
168
4.3.4. Gene expression of key bone cell markers in MLO-Y4:169
4.3.5. Suitability of 3D collagen gels for <i>in vitro</i> loading:170
4.3.6. Matrix deposition of MC3T3-E1 cells in a 3D in vitro model of bone:173
4.4. Discussion:
4.4.1. The effect of Hormones and Mechanical Load on MC3T3-E1 and MLO-Y4
Gene Expression In Vitro:
4.4.2. Collagen Hydrogels Containing MG63 Cells are Not a Viable,
Representative Model of Mechanical Loading <i>In Vitro</i> :
4.4.3. The Effect of Hormones and Mechanical Loading Upon MC3T3-E1 Cell
Matrix Deposition in 3D:
4.4.4. Conclusion:
5. Chapter 5: General Discussion and Future Directions:
5.1. The Role of Testosterone in Bone Metabolism:
5.2. The Role of Leptin in Bone Metabolism:192
5.3. Interactions Between Hormones and Mechanical Loading in vitro:193
5.4. Future Directions:
5.4.1. Elucidating The Role of Testosterone in Bone Remodelling:195
5.4.2. Elucidating the Role of Leptin in Bone Remodelling:197
5.4.3. Unravelling Interactions Between Mechanotransduction and Hormone
Signalling:
5.5. Concluding Remarks:
References:
Appendix:

## List of Figures:

- **Figure 1.1:** A schematic diagram illustrating the dynamic process of bone remodelling, highlighting roles of osteoblasts and osteoclasts in the formation and resorption of bone tissue respectively. Adapted from Kapinas and Delany, 2011.
- **Figure 1.2:** A schematic diagram representing the main mechanotransduction pathways in bone, including Integrins (A), Calcium channels (B), Connexins (C), Cilia (D), and Cadherins (E). Adapted from Stewart et al., 2020.
- **Figure 2.1:** A schematic diagram depicting the regions of interest defined for trabecular and cortical  $\mu$ CT analysis of murine tibiae.
- **Figure 2.2:** Comparison between a representative raw image of immunohistochemistry staining for adiponectin (left) and a binarized image used for quantification of percentage lipid droplet area. Analysis was performed using a custom-made macro in ImageJ software, outlining lipid droplets in yellow and calculating their area. Scale bar is 50μm.
- **Figure 2.3:** Force applied over time applied to murine tibiae in a three-point bend test, used to determine Fmax at the break point (#).
- **Figure 2.4:** Testosterone concentrations in blood serum from sham operated, placebo treated control mice (n = 11), orchiectomised, placebo treated mice (n = 9), and orchiectomised mice treated with testosterone (n = 12) determined via ELISA ng/L (\*P < 0.5, \*\*\* P < 0.05, \*\*\* P < 0.01, \*\*\*\* P < 0.001).
- **Figure 2.5:** A) Representative images of Micro-CT generated 3D models depicting cortical regions of interest (ROIs) used for morphological analysis of cortical bone. B) Final body weights of each of the mice at the time of sacrifice (25 weeks of age). C) Cortical bone volume measurements D) Bone mineral density measurements, calibrated against hydroxyapatite rods of known density (\*P < 0.5, \*\*\* P < 0.05, \*\*\* P < 0.01, \*\*\*\* P < 0.001).
- **Figure 2.6:** A) Representative examples of Micro-CT generated 3D models depicting trabecular regions of interest (ROIs) used for morphological analysis. B) Trabecular separation within trabecular ROIs (P = 0.0052) C) Trabecular number (P < 0.0001). D) Structural model index (SMI) (P = 0.0139). E) Trabecular bone volume/tissue volume percentage (BV/TV) (P = 0.0008). F) Mean thickness of trabeculae within the ROI (P = 0.0057). G) Trabecular BMD calculated against hydroxyapatite rode of known density. (\*P < 0.5, \*\*P < 0.05, \*\*\*P < 0.01, \*\*\*\*P < 0.001).

- **Figure 2.7:** A) Representative examples of 3D colour-coded models of regions of interest (ROIs) used for trabecular analysis, with a scale bar ranging from low thickness (red) to high thickness (blue). B) Trabecular thickness midrange values plotted against the percentage of trabecular bone within each given thickness range.
- **Figure 2.8:** Representative image of trabecular bone within a cross section of murine tibia stained with Masson's trichrome, showcasing the three stains: Collagen fibres and connective tissue components (Blue) Keratin, muscle, intracellular proteins (Red) and Nuclei (Purple). Coloured arrows highlight visible osteoblasts (orange), osteocytes (green) and osteoclasts (red). Scale bar is 50 μm.
- **Figure 2.9:** Representative images of cross sections of tibiae from each group stained with Masson's trichrome (A) and an immunohistochemical stain for adiponectin, with red arrows to indicate lipid droplets (B). Scale bars are 100  $\mu$ m and 50  $\mu$ m respectively. Lipid droplet (LD) percentage area (C) within randomly taken images of control (n = 8), orchiectomised (n = 8) and orchiectomised, testosterone treated (n = 10) murine tibiae bone marrow stained for adiponectin via IHC. (\*P < 0.5).
- **Figure 2.10:** Representative images of alkaline phosphatase (ALP) (A, B) and RUNX2 (C, D) immunohistochemistry staining of mouse tibiae sections RUNX2 positivity along the trabecular (A, C) and endocortical (B, D) surfaces in control (n = 8), orchiectomised (n = 10), and orchiectomised, testosterone treated mice (n = 10). Scale bars are 50  $\mu$ m.
- **Figure 2.11:** Percentage immunopositivity of alkaline phosphatase (ALP) (A, B) and RUNX2 (C, D) immunohistochemistry staining of mouse tibiae sections RUNX2 positivity along the trabecular (A, C) and endocortical (B, D) surfaces in control (n = 8), orchiectomised (n = 10), and orchiectomised, testosterone treated mice (n = 10). (\*P < 0.5).
- **Figure 2.12:** Representative IHC images of control (n = 8), orchiectomised (n = 10), and orchiectomised, testosterone treated mice (n = 10) osteoprotegerin (OPG) (A), RANKL (B), Adiponectin (APN) (C), and TRAP stained sections used to determine the number of TRAP positive osteoclasts per mm of bone surface (N.Oc/BS) (C). Scale bars are 50  $\mu$ m.
- **Figure 2.13:** Percentage immunopositivity of osteoblasts along the endocortical surface of control (n = 7) orchiectomised (n = 9) and orchiectomised, testosterone treated (n = 9) stained for A) RANKL and B) OPG. C) The ratio of RANKL:OPG percentage immunopositivity from IHC stained sections of murine tibiae. Immunopositivity was originally expressed as a percentage of total count, then used to calculate a ratio. Statistical significance was determined using a Kurskal-Wallis test. \*\* = p<0.05.

- **Figure 2.14:** 3-point bend test data from the mechanical testing of control (n = 6), orchiectomised (n = 11) and orchiectomised, testosterone treated (n = 9). Results are displayed as the maximal force withstood by the tibiae before breaking (Fmax).
- **Figure 3.1:** Body composition of male C57 and weight-paired lean or obese Ob/Ob mice. Lean C57, Lean Ob/Ob and Obese Ob/Ob were fed a control diet (CD), Obese C57 were fed a high fat diet (HFD). A. Body weight (g); B. Average daily food intake in Kcal; C. Fat Mass (g); D. Lean mass (g). Mean  $\pm$  STDev., n=4/group. One-Way ANOVA or Kruskal-Wallis; \* $P \le 0.05$ .
- **Figure 3.2:** Proximal tibia cortical bone morphology at 24±2 weeks of age of male C57 and weight-paired lean or obese *Ob/Ob* mice. A. Cortical bone volume (BV) (mm<sup>3</sup>); B. Cortical bone mineral density (BMD) (g/cm<sup>3</sup>); C. Cortical Thickness (mm); D. 3D colour coded density map (g.cm<sup>3</sup>) showing increased density at interosseous crest (IC) and proximal tibial crest (PTC). n=4 Mean and individual data points. One way-ANOVA or Kruskal-Wallis with post-hoc multiple comparisons, \* $P \le 0.05$  vs. Lean C57.
- **Figure 3.3:** Proximal tibia trabecular bone morphology at 24±2 weeks of age of male C57 and weight-paired lean or obese *Ob/Ob* mice. A. Trabecular bone volume/tissue volume (BV/TV) (%); B. Trabecular number (mm $^{-1}$ ); C. Trabecular separation (mm); D. Trabecular thickness (mm); E. Trabecular bone mineral density (BMD) (g/cm $^{3}$ ). n=4 Mean and individual data points. One way-ANOVA or Kruskal-Wallis with post hoc multiple comparisons, \* $P \le 0.05$  vs. Lean C57.
- Figure 3.4: Proximal tibia trabecular bone morphology at 24±2 weeks of age of male C57 and weight-paired lean or obese Ob/Ob mice. A. Thickness distribution (mm); B. 3D colour coded thickness map (mm). n=4 Mean and individual data points. One way-ANOVA or Kruskal-Wallis with post hoc multiple comparisons, \* $P \le 0.05$  vs. Lean C57.
- **Figure 3.5:** Inner vs. Outer proximal tibia trabecular bone morphology at  $24\pm2$  weeks of age of male C57 and weight-paired lean or obese *Ob/Ob* mice. A. Representative model of inner and outer medullar trabecular bone region of interest; B. Outer medullar trabecular thickness (mm); C. Inner trabecular thickness (mm). n=4 Mean and individual data points. One way-ANOVA with post hoc multiple comparisons, \*P<0.05 vs. Lean C57.
- **Figure 3.6.** Vertebral cortical bone morphology at 24±2 weeks of age of male C57 and weight-paired lean or obese *Ob/Ob* mice. A. Cortical bone volume (BV) (mm<sup>3</sup>); B. Cortical bone mineral density (BMD) (g/cm<sup>3</sup>); C. Cortical Thickness (mm); D. 3D colour coded density map (g.cm<sup>3</sup>) of vertebral body cortical bone. n=4 Mean and individual data points. One way-ANOVA or Kruskal-Wallis with post-hoc comparisons, \* $P \le 0.05$  vs. Lean C57.

- **Figure 3.7.** Vertebral trabecular bone morphology at 24±2 weeks of age of male C57 and weight-paired lean or obese *Ob/Ob* mice. A. Trabecular bone volume/tissue volume (BV/TV) (%); B. Trabecular number (mm $^{-1}$ ); C. Trabecular separation (mm); D. Trabecular thickness (mm); E. Trabecular bone mineral density (BMD) (g/cm $^{3}$ ). n=4 Mean and individual data points. One way-ANOVA or Kruskal-Wallis with post-hoc comparisons, \* $P \le 0.05$  vs. Lean C57.
- **Figure 3.8.** Vertebral trabecular bone morphology at 24±2 weeks of age of male C57 and weight-paired lean or obese *Ob/Ob* mice. A. Thickness distribution (mm); B. 3D colour coded thickness map (mm). n=4 Mean and individual data points. One way-ANOVA or Kruskal-Wallis with post hoc multiple comparisons, \* $P \le 0.05$  vs. Lean C57.
- **Figure 3.9:** Representative images depicting Masson's Trichrome stained sections of tibiae and L3 vertebrae from C57 mice fed a normal diet (n = 4), C57 mice fed a high fat diet (n = 4), and weight paired *Ob/Ob* mice. Scale bars are 500  $\mu$ m.
- **Figure 3.10:** Tibial percentage immunopositivity counted along the endocortical surface of Runx2 (A), ALP (B), RANKL (C), OPG (D) immunohistochemistry stained sections, RANKL:OPG immunopositivity ratio (E) and osteoclast number per mm quantified via TRAP staining (F) of tibiae sections from control C57 mice fed a normal diet (n = 8), C57 mice fed a high fat diet (n = 4) and *Ob/Ob* mice fed a normal diet, weight paired to HFD fed C57 mice (n = 8).
- **Figure 3.11:** Representative images of Runx2 (A), ALP (B), RANKL (C), OPG (D) immunohistochemistry staining and TRAP staining (E) of tibiae sections from control C57 mice on a control (n = 8), C57 mice fed a high fat diet (n = 4), and Ob/Ob mice fed a normal diet. Scale bars are 50  $\mu$ m
- **Figure 3.12:** L3 vertebral percentage immunopositivity counted along the endocortical surface of Runx2 (A), ALP (B), RANKL (C), OPG (D) immunohistochemistry stained sections, RANKL:OPG immunopositivity ratio (E) and osteoclast number per mm quantified via TRAP staining (F) of tibiae sections from control C57 mice fed a normal diet (n = 8), C57 mice fed a high fat diet (n = 4) and *Ob/Ob* mice fed a normal diet, weight paired to HFD fed C57 mice (n = 4).
- **Figure 3.13:** Representative images of Runx2 (A), ALP (B), RANKL (C), OPG (D) immunohistochemistry staining of L3 vertebra sections from control C57 mice on a control (n = 8), or high fat (n = 4) diet and weight-paired *Ob/Ob* mice fed a normal diet. Scale bars are 50  $\mu$ m.

- **Figure 3.14:** A) Average force applied over time to HFD-fed C57 (n = 3) and weight-paired  $Ob/Ob^{-/-}$  murine tibiae (n = 3) in a 3-point bend mechanical test. B) Maximal force applied to tibiae before breakage.
- **Figure 4.1:** Concentrations of leptin (A) and testosterone (B) in cell culture media over the course of 72 hours, measured via ELISA.
- **Figure 4.2:** Relative gene expression of *RUNX2* (red), OPG (green) and ALP (blue) in MC3T3-E1 cells over the course of 21-day *in vitro* differentiation in modified cell culture media.
- **Figure 4.3:** Relative gene expression of *RUNX2* (A), ALP (B), OPG (C), AR (D), and LepR (E) measured via RT-qPCR, and ALP activity (F) in cell culture media from undifferentiated MC3T3-E1 cells treated with FSS and either 80 ng/mL leptin (n = 3) or 10 ng/mL testosterone (n = 3) alongside static controls (n = 3).
- **Figure 4.4:** Relative gene expression of *RUNX2* (A), ALP (B), OPG (C), AR (D), and LepR (E) measured via RT-qPCR, and ALP activity (F) in cell culture media from MC3T3-E1 cells treated with FSS and either 80 ng/mL leptin (n = 3) or 10 ng/mL testosterone (n = 3) alongside static controls (n = 3) after 21 days of culture in differentiation medium.
- Figure 4.5: Representative images of HandE stained 4  $\mu$ m sections of MG63-laden and acellular collagen gel constructs after 1 or 4 weeks of culture. Scale bar = 50  $\mu$ m.  $\blacksquare$  denotes the presence of MG63 cells within the gel
- **Figure 4.6:** Representative images depicting immunohistochemical staining for Ki67 (A) and FAK (B) of  $4\mu$ m thick collagen gel sections cultured with MG63 cells for 4 weeks prior to staining. Scale bars are 50  $\mu$ m.
- **Figure 4.7:** Representative images depicting Masson's trichrome stained sections of B-gel constructs laden with either undifferentiated MC3T3-E1 cells, or MC3T3-E1 cells that had been differentiated in osteogenic medium for 21 days. Cell-laden constructs either remained unloaded or were subjected to 0.3 mPa of hydrostatic pressure, alongside treatment with either 10 ng/mL testosterone or 80 ng/mL leptin. N = 3 for all groups. Scale bars are 100  $\mu$ m.
- **Figure 4.8:** Representative images depicting Alizarin red stained sections of B-gel constructs laden with either undifferentiated MC3T3-E1 cells, or MC3T3-E1 cells that had been differentiated in osteogenic medium for 21 days. Cell-laden constructs either remained unloaded or were subjected to 0.3 mPa of hydrostatic pressure, alongside treatment with either 10 ng/mL testosterone or 80 ng/mL leptin. N = 3 for all groups. Scale bars are 100  $\mu$ m.

## List of Tables:

**Table 2.1**: Primary antibody and antigen retrieval information for the IHC assessment of RUNX2, RANKL, adiponectin, OPG and ALP in murine tibiae.

**Table 4.1:** Reverse transcriptase mastermix components. For each  $14\mu L$  sample,  $36\mu L$  of complete mastermix is added. dNTPS, Bioscript 5x RT buffer and Bioscript RT enzyme all purchased from Bioline. Random hexamers and RNase free  $H_2O$  purchased from Thermo Fisher.

**Table 4.2:** List of mouse primers (ThermoFisher, UK) used for qRT-PCR experiments, alongside associated assay IDs.

**Table 4.3:** Average CT values obtained from qRT-PCR analysis of  $\beta$ -Actin and GAPDH gene expression in MLO-Y4 cells subjected to loading and hormone treatment regimes.

## **List of Abbreviations:**

**3D** - Three-Dimensional

ALP - Alkaline Phosphatase

**ANOVA** - Analysis of Variance

**ApoE-/-** - Apolipoprotein E-Deficient (Mouse Model)

AR - Androgen Receotor

ATP - Adenosine Triphosphate

BM - Bone Marrow

**BMD** - Bone Mineral Density

**BMI** - Body Mass Index

BMP2 - Bone Morphogenetic Protein 2

BMU - Basic Multicellular Unit

BV - Bone Volume

**BV/TV** - Bone Volume/Tissue Volume

**CAMP** - Cyclic Adenosine Monophosphate

CaHA - Calcium Hydroxyapatite

CD44 - Cluster of Differentiation 44

Cx43 - Connexin 43

Cxs Connexins

Db/Db - Leptin Receptor-Deficient Mice (Obese Phenotype)

**ECM** - Extracellular Matrix

EDTA - Ethylenediaminetetraacetic Acid

ELISA - Enzyme-Linked Immunosorbent Assay

ERK1/2 - Extracellular Signal-Regulated Kinase 1/2

FA - Focal Adhesion

FAK - Focal Adhesion Kinase

FSS - Fluid Shear Stress

**GM** - Gut Microbiome

**GnRH** - Gonadotropin-Releasing Hormone

**HFD** - High Fat Diet

**HPG** - Hypothalamic-Pituitary-Gonadal

**HU** - Hindlimb Unloading

IACUC - Institutional Animal Care and Use Committee

ICV - Intracerebroventricular

Ift88 - Intraflagellar Transport Protein 88

**IMS** - Industrial Methylated Spirits

**IHC** - Immunohistochemistry

JAK/STAT - Janus Kinase/Signal Transducer and Activator of Transcription

KIF3A - Kinesin Family Member 3A

LC - Lacuna-Canalicular

**LH** - Luteinizing Hormone

LepR - Leptin Receptor

MMP-13 - Matrix Metalloproteinase-13

MSC - Mesenchymal Stem Cells

ND - Normal Diet

**Ob/Ob** - Leptin-Deficient Mice (Obese Phenotype)

**OPG** Osteoprotegerin

**OS** - Oxidative Stress

PI3K - Phosphoinositide 3-Kinase

**PGE2** - Prostaglandin E2

**RGD** - Arginine-Glycine-Aspartate

**ROI** - Region of Interest

**ROS** - Reactive Oxygen Species

**RUNX2** - Runt-Related Transcription Factor 2

SCFA - Short Chain Fatty Acid

siRNA - Small Interfering RNA

SPSS - Statistical Package for the Social Sciences

**T2D** - Type-2 Diabetes

Tb.N - Trabecular Number

Tb.Sp. - Trabecular Separation

Tb.Th - Trabecular Thickness

TRAP - Tartrate-Resistant Acid Phosphatase

TRPV4 - Transient Receptor Potential Vanilloid 4

**TRT** - Testosterone Replacement Therapy

VMH - Ventromedial Hypothalamic

Wnt - Wingless-Related Integration Site

WP - Weight-Pair(ed)

WT - Wild Type

μCT - Micro-Computed Tomography

## Dissemination:

#### Scientific publication:

Williamson, A., da Silva, A., do Carmo, J. M., Le Maitre, C. L., Hall, J. E., and Aberdein, N. (2023). Impact of leptin deficiency on male tibia and vertebral body 3D bone architecture independent of changes in body weight. Physiological reports, 11(19), 10.14814/phy2.15832. https://doi.org/10.14814/phy2.15832

#### **Conference Abstracts:**

European Orthopaedic Research Society (EORS) Annual Meeting 2021 – Rome, Italy - The effect of testosterone replacement therapy upon bone remodelling in testosterone deficient APOE-/- mice fed a high fat diet – Oral presentation.

European Orthopaedic Research Society (EORS) Annual Meeting 2021 – Rome, Italy – Role of Leptin on Murine Tibia Bone Remodelling Independent of Body Weight: A High Fat Diet vs Normal Diet Comparison – Poster presentation, Prize: best poster.

International Combined Orthopaedic Research Society (ICORS) Annual Meeting 2022 – Edinburgh, UK - The effect of testosterone replacement therapy upon bone remodelling in testosterone deficient APOE-/- mice fed a high fat diet – Poster presentation.

Orthopaedic Research Society (ORS) Annual Meeting 2023 – Dallas, Texas, USA – The effect of testosterone replacement therapy upon bone remodelling in testosterone deficient APOE-/- mice fed a high fat diet – Poster presentation.

1. Chapter 1: Introduction:

#### 1.1. Study Importance:

The ever-rising prevalence of obesity is a global concern, with cases of adult obesity more than doubling between 1990 and 2022. According to the WHO, 2.5 billion (43%) adults worldwide are classed as overweight or obese (BMI > 25kg/m²), over 890 million of which are obese (30-35kg/m²). Furthermore UK obesity statistics estimate that 64.3% of the adult UK population are classified as overweight or obese as of 2023; a significantly higher portion than the international average of 24.25% (Baker, 2024).

The obesity epidemic presents a number of challenges to healthcare systems worldwide, as obesity is considered a major risk factor for several disorders including cardiovascular disease (Akil and Ahman, 2011) and bone disorders such as osteoporosis (Pi-Sunyer, 2009), as well as contributing to a host of endocrine alterations, including increased leptin secretion and the decline of testosterone levels with age in men (Mushannen et al., 2019).

Understanding the mechanisms controlling bone remodelling in response to diet induced obesity, specifically the contributions of hormones and loading are necessary due to contradictory findings and the implications for an ageing population, the majority of which are overweight or obese (NHS, 2023). Endocrine signalling and load have been shown to independently influence bone metabolism, but cross-talk between the two pathways is not yet fully understood. Increases in body weight (BW) associated with obesity are well known to result in accrual of bone mass, due to greater mechanical strain upon the skeleton (De Lorenzo et al., 2024; Jensen et al., 2021; Savvidis et al., 2018). However, bone loss is associated with reductions in endocrine functions, including testosterone and leptin sensitivity, which are also associated with obesity (Khodamoradi et al., 2022). As such, this work aims to elucidate the independent effects

of mechanical load, testosterone, and leptin signalling in bone turnover and homeostasis.

### 1.2. Bone Remodelling:

The physiological role of bone is to provide structural support for movement and ventilation, protection for internal organs and a reservoir for amino acids, calcium and phosphate, as well as a nurturing environment for maturation of hematopoietic stem cells (Ott, 2018). Bone also has metabolic functionality, including the secretion of hormones which regulate mineral and energy metabolism. To achieve these functions, bone is compartmentalised into cortical (outer) and trabecular (inner) bone (Buss et al., 2022).

Within bone, there are several cell types responsible for the maintenance of healthy bone remodelling. Osteoblasts, differentiated from mesenchymal stem cells, secrete bone matrix rich in type-1 collagen and regulate matrix mineralisation contributing to bone formation (S. Zhu et al., 2024), whereas osteoclasts differentiated from hematopoietic stem cells degrade bone mineral and matrix content via secretion of hydrochloric acid and proteolytic enzymes, facilitating bone resorption (Kenkre and Bassett, 2018). It has been suggested that osteoclasts recognise and target sites of compromised mechanical integrity and initiate the process of bone remodelling at these sites (Oftadeh et al., 2015). Bone remodelling is a continuous physiological process responsible for the maintenance of the skeleton and calcium homeostasis. This process repairs or improves bone strength by replacing old, micro-damaged or fractured bone with new healthy bone via a constant cycle of bone resorption and formation (Owen and Reilly, 2018).

The remodelling cycle begins with the formation of a basic multicellular unit (BMU) composed of osteoclasts, osteoblasts and a capillary blood supply (Arias et al., 2018). Targeted bone remodelling in adults, a process unrelated to normal lengthening of bone during childhood and adolescence, is controlled by 5 distinct stages: activation, resorption, reversal, formation and termination (Figure 1.1).

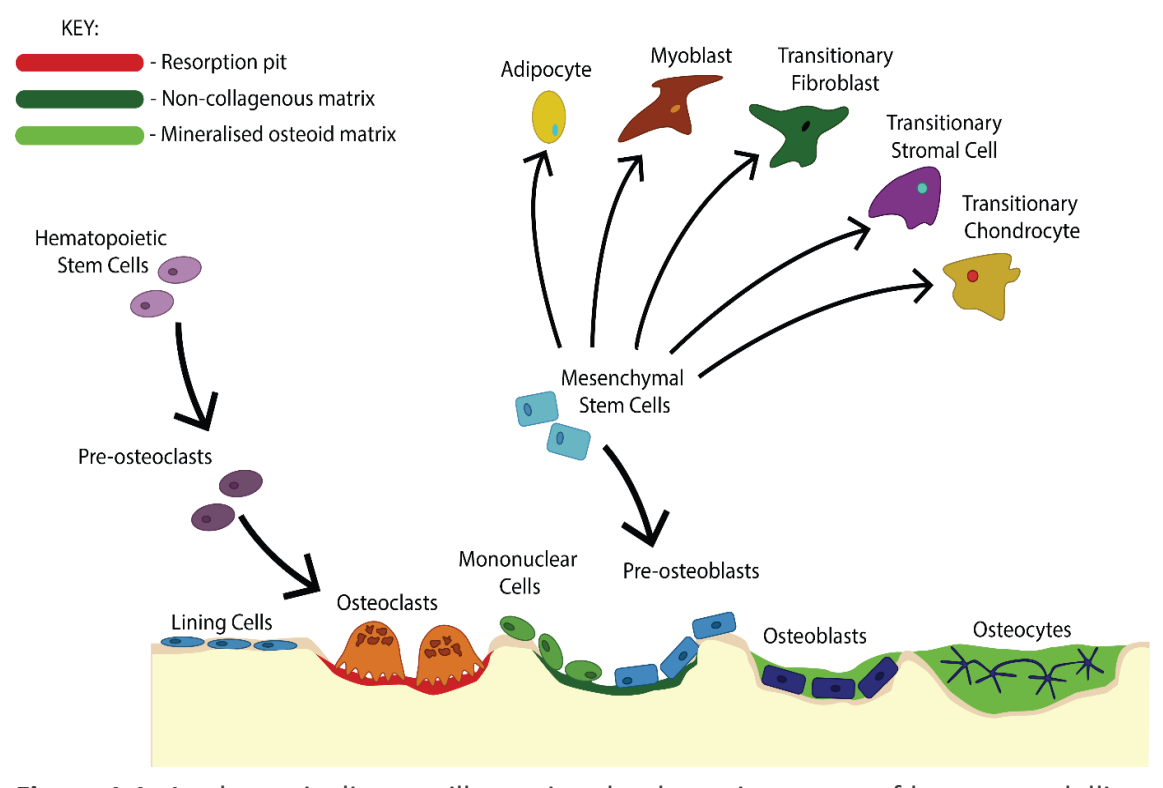


**Figure 1.1:** A schematic diagram illustrating the dynamic process of bone remodelling, highlighting roles of osteoblasts and osteoclasts in the formation and resorption of bone tissue respectively. Adapted from Kapinas & Delany, 2011.

As the BMU moves along the bone surface, the process of activation is initiated by signals originating from osteocytes, which undergo apoptosis in response to bone matrix microdamage. Osteocytes and osteoblasts release activating factors such as receptor activator of nuclear factor kappa-B (RANKL) (Campbell et al., 2024) which increases local angiogenesis and recruitment of osteoclast and osteoblast precursors to the BMU (Chen et al., 2013).

Replenishment of pre osteoblasts and osteoclasts is ultimately controlled by osteocytes, which account for 90 - 95% of all bone cells in adult bone (Bonewald, 2011). Osteocytes reside within lacunae in the bone matrix, detecting mechanical loading upon the bone and signalling to cells on the bone surface to regulate osteoblast and osteoclast function (Oftadeh et al., 2015). Osteoclast precursor cells are differentiated in to mature osteoclasts, a process reliant upon RANKL secreted by osteoblasts (Arias et al., 2018). Resorption is initiated when multinucleated pre-osteoclasts form by fusion of multiple mononuclear cells and bind to bone matrix to form a sealing zone. Osteoclasts isolate the damaged bone from surrounding bone to create a resorption pit. The osteoclast cytoskeleton is rearranged to form a "ruffled border", greatly increasing the secretory surface area of the cell (Mulari et al., 2003). Within this sealing zone, bone mineral content is dissolved via the secretion of hydrochloric acid and the collagen-rich bone matrix is degraded by secreted proteases such as cathepsin K. Matrix metalloproteniases (MMPs) help to prepare the bone surface for new matrix deposition degrading bone matrix and regulating the activity of cathepsin K and other enzymes (Delaissé et al., 2003). Additionally, matrix metalloproteinase 13 (MMP-13) expressed by osteoblasts and hypertrophic chondrocytes degrades type I collagen, allowing for new bone formation and mineralisation during remodelling (Arai et al., 2021). These actions of MMP- are also essential for the maintenance of osteocytic lacunar networks (Tang et al., 2012).

The process of bone resorption is terminated by programmed cell death of osteoclasts in order to prevent excess bone resorption (Kenkre and Bassett, 2018). This activation step is necessary to ensure that bone remodelling only takes place where required, and targets bone remodelling to specific sites of damaged or old bone (Eriksen, 2010).

Alternatively, non-targeted bone remodelling is not directed to a specific site, instead may be initiated in response to systemic changes in hormones such as parathyroid hormone (PTH) during pregnancy (Hysaj et al., 2021) to allow access to calcium stores within the bone (Murray and Wolf, 2024; Parfitt, 2002).

During the reversal stage, resorption switches to formation and resorbed bone is replaced by a matrix produced by osteoblasts over the course of 3 months. Newly resorbed bone is prepared for bone matrix deposition via the removal of unmineralized collagen matrix and the deposition of a non-collagenous mineralised matrix by cells of the osteoblast lineage (Delaissé et al., 2003). During the formation stage of bone remodelling, osteoblasts on the surface of bone synthesize and secrete non-mineralised osteoid matrix rich in type 1 collagen. This osteoid matrix is then mineralised with hydroxyapatite crystals via a mechanism which is currently not fully understood (Palmer et al., 2008), but it is known that osteoblasts play a key role in this process (Kenkre and Bassett, 2018). The mineralisation of osteoid is responsible for the accrual and maintenance of bone mineral density (BMD), an important indicator of bone health, and the mineral content of bone contributes to overall bone strength and stiffness (Roschger et al., 2008). Upon completion of matrix mineralisation, osteoblasts either change into bone-lining cells, undergo apoptosis or become entombed within the newly deposited bone matrix and terminally differentiate into osteocytes (Jilka, 2003; Kenkre and Bassett, 2018). The release of osteogenesis antagonists such as sclerostin from osteocytes play an important role in signalling the termination of bone remodelling via negative regulation of the Wnt/ $\beta$ -Catenin pathway (Bonewald, 2011).

Approximately 80% of bone mass of the human skeleton is accounted for by the outer cortex known as the cortical compartment, and although trabecular bone accounts for

only 20% of total bone volume, the metabolic rate of trabecular bone is 10-fold higher than that of cortical bone due to increased surface area to volume ratio (Parfitt, 2002). The various stages of the bone remodelling cycle take place on the surface of bone, meaning the rate of bone turnover is therefore higher in trabecular bone, with about 5% of cortical bone and 20% of trabecular bone renewed per year (Owen and Reilly, 2018). Imbalances in the bone remodelling cycle favouring either formation or resorption of bone lead to the development of several diseases such as osteoporosis, osteopenia and osteopetrosis (Feng and McDonald, 2011), as well as increased or decreased fracture risk.

To maintain equilibrium and therefore healthy bone mass, the bone remodelling process is influenced by a wide range of cytokines, hormones, signalling pathways and mechanical stimuli, and by crosstalk between osteoblasts and osteoclasts. For example, osteoblasts have been shown to influence osteoclast formation, differentiation, and apoptosis via several different pathways including the OPG/RANKL/RANK pathway (X. Chen et al., 2018). Several hormones play a crucial role in bone growth, maintenance, and remodelling throughout life, influencing the balance of bone formation and resorption.

## **1.3.** High Fat Diet and Bone Remodelling:

Primary studies in a range of models have attempted to understand whether high fat diet (HFD) and the loading effect of increased adipose tissue directly influences bone remodelling, or whether changes to bone morphology are a consequence of increased release of adipokines such as leptin from adipocytes into the local and systemic circulation. So far reports appear contradictory.

Consumption of a HFD can be defined as a diet in which >30% of energy intake is accounted for by lipids. Firstly, HFD consumption is thought to be a major risk factor for bone loss and the development of osteoporosis (Silva et al., 2019). HFD promotes adipogenic differentiation of MSCs and yellow bone marrow formation, in turn suppressing osteoblast differentiation (L. Hu et al., 2018). High fat diet results in an altered gut microbiome (GM) and decreased short chain fatty acid (SCFA) availability in the systemic circulation due to changes in metabolism of carbohydrates in the gut (D. Zhang et al., 2023). The presence of SCFA such as butyrate have been shown to improve bone health (lucas et al., 2018), therefore a loss of SCFA may contribute to bone loss (Wallimann et al., 2021). Furthermore the GM is currently an area of active investigation as a potential therapeutic target to treat osteoporosis (McCabe et al., 2015). Similarly, HFDs induce metabolic inflammation in many organs (Ruppert et al., 2024), increasing levels of endotoxins, circulating free fatty acids and inflammatory mediators (Duan et al., 2018). Inflammatory cytokines including IL-6 and TNF- $\alpha$  have also been shown to increase bone resorption by osteoclasts via the RANKL/OPG pathway (De Leon-Oliva et al., 2023).

Oxidative stress (OS) has also been identified as a risk factor for osteoporosis (X. Shen et al., 2024) although the exact relationship between OS and HFD consumption remains poorly defined. It is known that HFD contributes to oxidative stress via production of reactive oxygen species (ROS) (Tan and Norhaizan, 2019). ROS have been shown to activate osteoclast differentiation whilst inducing osteocyte apoptosis and inhibiting osteoblast activity, facilitating bone resorption and suppressing bone formation (Domazetovic et al., 2017). Similarly, ROS increase inflammation via TNF- $\alpha$  and IL-6 (L. Wu and Pan, 2019), further contributing to oxidative stress. Hydrogen peroxide induced

oxidative stress in human bone marrow monocytes induced RANKL expression, increasing RANKL/OPG ratio and therefore inducing osteoclast differentiation *in vitro* (Baek et al., 2010).

HFD has also been shown to increase accumulation of adipose tissue in and around the bone, leading to increased local secretion of adipokine factors including leptin (Mendoza-Herrera et al., 2021). Co-culture of preosteoclasts with adipocytes has been shown to increase the presence of TRAP-positive multinucleated osteoclasts *in vitro* (Montalvany-Antonucci et al., 2018). In addition, HFD consumption decreases bone formation by suppressing osteoblast differentiation, and increases bone resorption by increasing osteoclastogenesis (Shu et al., 2015). However, identifying whether the observations above are specific to a change in gut microbiota and therefore fatty acid availability or whether adipocyte secretion of adipokines including leptin may be having a direct role on bone remodelling is necessary.

#### **1.4.** Testosterone and Bone Remodelling:

Testosterone is the primary male sex hormone, secreted predominantly in Leydig cells in the testes in men (Walker, 2011), and in smaller quantities in the ovaries in women (O'Donnell et al., 2000). Synthesis of testosterone is regulated by the hypothalamic-pituitary-gonadal (HPG) axis (Hauger et al., 2022), whereby gonadotropin-releasing hormone (GnRH) secreted in the hypothalamus stimulates the release of luteinizing hormone (LH) in the anterior pituitary (Marques et al., 2000). LH is then transported via the bloodstream to the testes, where it stimulates the synthesis of testosterone by the Leydig cells (Nedresky and Singh, 2024). Once synthesised, this testosterone is released into the bloodstream and able to act locally or in distant target tissues.

Once in the bloodstream, testosterone exists as either biologically active, free testosterone (0.5% to 3% of total testosterone) or bound testosterone, accounting for the remainder (Q. Yang et al., 2019). In its bound form, testosterone is bound to proteins such as sex hormone-binding globulin (SHBG) and albumin, and is largely inactive (Goldman et al., 2017).

As a lipid-soluble hormone, testosterone is able to freely diffuse across the lipid bilayer of target cell membranes, interacting with soluble nuclear receptors once inside (H. C. Chen and Farese, 1999). In target tissues, testosterone binds to the androgen receptor (AR), a nuclear receptor protein located in the cytoplasm (McEwan and Brinkmann, 2000). Testosterone binding to AR induces a conformational change in the AR, causing its activation and subsequent translocation to the nucleus, where the testosterone-AT complex binds to specific DNA sequences termed androgen response elements (AREs) (Wilson et al., 2016). Binding to AREs triggers the recruitment of coactivators and RNA polymerase, leading to the transcription of androgen-responsive genes, ultimately influencing various biological processes (De Bruyn et al., 2011).

In addition to its classical genomic pathway, testosterone can also elicit rapid, non-genomic effects that do not involve direct changes in gene transcription (Handelsman, 2000). In these cases, testosterone may bind to membrane-associated ARs or activate second messenger pathways such as G-protein-coupled receptors (GPCRs), leading to effects on calcium ion channels, kinase activation, and other intracellular signalling pathways (Shihan et al., 2014).

Testosterone signalling plays a critical role in the development of male reproductive tissues such as the testes and prostate, as well as promoting increased muscle and bone mass (Shigehara et al., 2021). Conversely, fat mass is negatively associated with

testosterone in males, with testosterone deficiency leading to increased fat deposition, synthesis, and cell proliferation alongside decreased muscle and bone mass (Ma et al., 2024).

Alongside increases in body fat percentage, depleted testosterone levels are also associated with increased insulin resistance (Ottarsdottir et al., 2018), and low serum testosterone is considered an independent risk factor for Type-2 Diabetes (T2D) (Wittert and Grossmann, 2022). Similarly, low serum testosterone levels can be used as a predictor of metabolic syndrome in men (Haring et al., 2009). Conversely, high serum testosterone levels are protective against obesity, metabolic syndrome and T2D, establishing testosterone treatment as a potential therapeutic opportunity for these disorders (Wittert and Grossmann, 2022). As such, testosterone replacement therapy (TRT) in obese, adult men results in reduced visceral fat as well as improved insulin sensitivity (Mushannen et al., 2019), and has beneficial metabolic effects on patients with T2D and metabolic syndrome (Li et al., 2020). Similarly, TRT has beneficial effects on BMD (Shigehara et al., 2021), suggesting a potential method to decrease fracture risk in osteoporosis (Elsheikh and Rothman, 2023). However, contradictory studies suggest that TRT may not decrease fracture risk, despite improvements in BMD (Snyder et al., 2024).

Obesity negatively correlates with free, bioavailable, and total testosterone across all age groups (Grossmann, 2011), creating a self-perpetuating cycle of increasing fat mass, whilst decreasing muscle and bone mass in obese, elderly men (Fui et al., 2014). Testosterone acts directly on osteoblasts and osteoclasts via ARs expressed by these cells (Mohamad et al., 2016). Androgen signalling in osteoblasts promotes their proliferation and differentiation, a process mediated by the transcription factor Runx2

(Gao et al., 2017; Payandeh et al., 2020). Testosterone also suppresses apoptosis in osteoblasts, thereby promoting their survival and increasing bone formation (Almeida et al., 2010). Additionally, testosterone increases the production of OPG, a decoy receptor for receptor activator of RANKL, which in turn inhibits osteoclast differentiation and bone resorption (Wu and Zhang, 2018). The role of androgen signalling in osteocytes is less clear, however androgen receptors are present on osteocytes, suggesting a role for testosterone in osteocytes differentiation and the preventation of age-related trabecular bone loss (Elsheikh & Rothman, 2023).

As such, low testosterone levels are associated with an increase in serum markers of bone turnover, such as bone alkaline phosphatase, indicating heightened bone remodelling (Dabaja et al., 2015). As testosterone levels decline with age, especially in obese men, bone mineral density (BMD) also declines, contributing to an increased risk of osteoporosis (Shigehara et al., 2021). Testosterone affects not only the density of bone but also its microarchitecture, including alterations in both cortical and trabecular bone parameters. In studies investigating testosterone's role in bone using murine models, testosterone deficiency has been linked to trabecular bone thinning and compromised cortical bone structure (Mohamad et al., 2016). Testosterone supplementation, in both rodents and humans, is associated with increases in trabecular bone volume, particularly in the spine (Snyder et al., 2017). This is likely due to testosterone's ability to enhance the structural integrity of bone, thus reducing fracture risk in some, though not all, clinical studies.

Alongside these local effects on bone cells, testosterone also affects systemic factors including insulin-like growth factor 1 (IGF-1) (Franco et al., 2023), which is critical for bone development and maintenance (Fang et al., 2023). Testosterone also indirectly

influences bone health by increasing muscle mass and strength, imparting increased mechanical loading from muscle contraction on the skeleton. This mechanical strain stimulates bone formation, contributing to higher BMD (Shapses and Sukumar, 2012). Loss of muscle mass due to low testosterone levels reduces this mechanical strain, contributing to bone loss over time (Fui et al., 2014).

## 1.5. Leptin and Bone Remodelling:

Leptin is a 16 kDa polypeptide predominantly secreted by adipocytes, responsible for the regulation of energy homeostasis (Forny-Germano et al., 2019). Circulating leptin signals to the central nervous system (CNS) to suppress food intake and encourage energy expenditure, proportionally to fat stores (Myers, et al., 2008). As such, leptin deficiency as seen in genetically modified *Ob/Ob* mice, and in humans with rare mutations in the leptin gene (Clément et al., 1998), results in uncontrolled weight gain and obesity, and these phenotypes can be reversed via long-term treatment with leptin (Farooqi and O'Rahilly, 2014). However, obesity also leads to a decrease in tissue sensitivity to leptin, resulting in leptin resistance (Gruzdeva et al., 2019), presenting an increasingly complex relationship between leptin signalling and obesity.

Leptin signalling has been shown to affect bone remodelling, both indirectly via signalling in the hypothalamus (Ducy et al., 2000; Takeda et al., 2002; Hamrick, 2004), and by signalling directly to osteoblasts (Tsuji et al., 2010). Research aiming to establish the role of leptin in bone health has thus far yielded contradictory findings, with some evidence suggesting that leptin decreases bone formation (Ducy et al., 2000; Elefteriou et al., 2004; Takeda et al., 2002), whilst other research implies that leptin has an anabolic effect, increasing bone density (Blain et al., 2002; Scheller et al., 2010; Turner et al.,

2013). It is possible that the cause of these contradictory findings lies with interplay between leptin signalling/sensitivity and mechanical loading, as many studies investigating the role of leptin on bone remodelling do not control for changes in body weight in response to leptin.

Despite the positive effects of growth and development related increases in body weight and mechanical loading on bone density, obesity is thought to adversely affect bone health via a variety of mechanisms including inflammation, altered bone cell metabolism, and altered levels of bone-regulating hormones such as leptin (Shapses et al., 2017). Leptin replacement therapy in leptin deficient humans improves bone mass, but also increases levels of oestrogen, cortisol, insulin-like growth factor 1 (IGF-1) and parathyroid hormone (PTH); resulting in difficulties separating the effects of leptin itself vs its hypothalamic effectors on bone remodelling *in vivo* (Upadhyay et al., 2015).

Leptin receptors (ObR) are single membrane-spanning receptors which exist in six known ObR isoforms (ObRa-ObRf) produced via ectodomain shedding or alternative splicing (Wauman et al., 2017). These isoforms share common extracellular and transmembrane domains but differ in their intracellular domains (Dam and Jockers, 2013). ObR isoforms include one long form (ObRb), four short forms (ObRa, ObRc, ObRd and ObRf) and one soluble form (ObRe) (Wauman et al., 2017). The ObRb isoform has the largest intracellular domain consisting of 302 amino acids, and is the only isoform containing functional binding sites for janus kinase (JAK2) and signal transducer and activator of transcription (STAT), which are required for signal transduction and transmission of leptin function (Dam and Jockers, 2013). The ObRa isoform is a well characterised short isoform, and is thought to play a role in the transport of leptin across the blood-brain-barrier (Hileman et al., 2002). Investigation of mice lacking functional

leptin (*Ob/Ob*) or any isoform of the leptin receptor gene (*Db/Db*) respectively with regards to bone remodelling have proven controversial.

Early reports from Ducy et al., in 2000, before the common use of high resolution MicroCT imaging demonstrated that *Ob/Ob* and *Db/Db* mice exhibit high vertebral bone mass phenotypes, but unaltered appendicular bone phenotypes (Ducy et al., 2000). A more recent report from Huang et al., in 2016 using high resolution MicroCT analysis also demonstrated that leptin deficiency had a differing effect on the spine leading to a marked increase in vertebral bone mass compared to long bones. However, the researchers also identified trends towards lower trabecular bone mass in the tibiae of *Db/Db* mice (Huang et al., 2016), in contradiction to the unaltered appendicular bone phenotype described by Ducy et al., in 2000. Differences in analysis technique may account for these changes.

There is also contradictory evidence as to whether leptin acts on bone cells in a direct or indirect mechanism. Leptin receptors are present in a variety of cell types (Saxton et al., 2023), and leptin signalling has been shown to influence bone metabolism through indirect signalling via the hypothalamus (Ducy et al., 2000; Takeda et al., 2002; Hamrick, 2004) and directly via bone cell receptors (Mutabaruka et al., 2010; Turner et al., 2013; Upadhyay et al., 2015).

ObRb is predominantly expressed in two distinct neuronal populations within the arcuate nucleus (ARC) of the hypothalamus: the orexigenic NPY/AgRP (neuropeptide Y/agouti-related peptide) neurons and the anorexigenic POMC/CART (pro-opiomelanocortin/cocaine and amphetamine regulated transcript) neurons (Wauman et al., 2017). Leptin receptor inhibition of NPY/AgRP neurone activity plus activation of

POMC and CART neuron activity initiates a complex metabolic signalling cascade involving release of  $\alpha$ -melanocyte stimulating hormone, activation of Melanocortin 4 receptor (MC4R) and subsequent suppression of food intake amongst other cardiometabolic actions (Upadhyay et al., 2015). In 2000, Ducy et al., suggested that leptin could inhibit the accrual of bone mass via a process reliant upon the integrity of neurons within the ventromedial hypothalamic (VMH) nuclei. This pathway also modulates sympathetic tone, thereby regulating adrenergic signalling via osteoblastic β2 AR (Takeda et al., 2002). VMH-specific deletion of ObRb, however, does not affect bone mass (Balthasar et al., 2004), suggesting that VMH integrity is necessary for leptinmediated regulation of bone mass, but signalling via ObRb in these neurons is not. Together, these results indicate that leptin signalling may act elsewhere in the brain to mediate bone metabolism via the VMH. As such, Yadav et al., have demonstrated that brain-derived serotonin (BDS) modulates the effect of leptin on bone mass in mice. BDS enhances the accrual of bone mass via binding to 5-Hydroxytrypptamine Receptor (HTR) 2C receptors on VMH neurons, as well as appetite via binding to HTR1A and HTR2b receptors on ARC neurons. Leptin inhibits these functions by reducing serotonin synthesis and firing of serotonergic neurons (Yadav et al., 2009). Activation of hypothalamic ObRb stimulates secretion of Hypothalamic Osteoblast Inhibitory Factor (HOBIF), which inhibits the ability of osteoblasts to form bone matrix (Legiran and Brandi, 2012).

Neuromedin U (NMU), a neuropeptide expressed in the small intestine and hypothalamic neurons has also been shown to regulate bone mass, and treatment with NMU has been found to decrease trabecular bone mass in *Ob/Ob* mice, suggesting a role for NMU in the regulation of bone formation downstream of leptin. Furthermore, NMU

deficient mice were resistant to the effects of leptin and  $\beta 2$  AR agonists, suggesting that NMU may be an early mediator of leptin-dependent bone metabolism (Sato et al., 2007).

Alongside predominant expression within the ARC of the hypothalamus, leptin receptors have been identified in various cell types including osteoblasts and MSCs; suggesting that leptin may act directly upon these cells to influence bone metabolism (Upadhyay, 2015). As such, bone marrow adipocytes express and secrete high levels of leptin (Laharrague et al., 1998), potentially mediating the local effects of leptin on bone metabolism. In contrast to the early evidence that leptin reduces bone mass (Ducy et al., 2000), bone marrow replacement in *Db/Db* mice increases bone mass compared to untreated controls, despite unaltered energy homeostasis (Turner et al., 2013). This finding suggests that leptin may alter bone metabolism via peripheral mechanisms as well as centrally, and that leptin signalling may not exclusively inhibit bone formation as previously suggested by Ducy et al. As such, leptin is thought to preserve BMD through a similar mechanism to oestrogen, increasing levels of OPG and therefore inhibiting osteoclast activity (Legiran and Brandi, 2012). Alternatively, leptin is also able to influence bone metabolism via activation of fibroblast growth factor 23 (FGF-23) (Tsuji et al., 2010), a bone-derived hormone which inhibits reabsorption of phosphate and vitamin D synthesis in the kidneys (Erben, 2018).

Leptin signalling, particularly in combination with a high fat diet, has also been shown to directly influence skeletal stem cell differentiation, promoting adipogenesis whilst inhibiting osteogenesis by bone marrow stromal cells (Yue et al., 2016). Bone marrow stromal cells (BMSCs) harvested from *Ob/Ob* and *Db/Db* mice exhibit increased mineralisation *in vitro*, and the femora of these animals showed significantly increased trabecular bone volume and BMD. Cell-specific deletion of ObRb in osteoblasts resulted

in a phenotype identical to control mice, whereas specific ObRb deletion from mesenchymal precursors lead to mild obesity despite unchanged food intake (Scheller et al., 2010). Leptin receptor signalling in osteocytes promotes cortical bone consolidation by enhancing bone formation and mineralisation via activation of STAT3, which contributes to the maintenance of bone integrity by regulating osteocyte activity and supporting bone remodelling (Wee *et al.*, 2022). Together, these results highlight the potential for peripheral leptin signalling to modify bone metabolism by altering the proportion of osteogenic and adipogenic differentiation.

## 1.6. Mechanotransduction and Bone Remodelling:

Mechanical loading is known to exert an anabolic effect upon bone. Increased mechanical load upon the skeleton, particularly during adolescence, is known to have a positive effect on the accrual of bone density (Greene and Naughton, 2006). This may be a potential explanation for the presence of higher BMD in individuals with higher BMI, as increased body weight results in increased load upon the skeleton. Somewhat complimentary to this, evidence for reduced fracture risk in obese individuals was recently published in a large Austrian cohort study, demonstrating that BMI was inversely associated with fracture risk in both men and women with mean age  $50 \pm 15$  years (Dominic et al., 2020). Individuals with higher BMI (> $20 \text{kg/m}^2$ ) tended to exhibit increased BMD (Bierhals et al., 2019). Without analysing the body composition of these individuals, it would be difficult to interpret whether an increase in mechanical load upon the skeleton was due to high muscle mass, as muscle is a recognised predictor of BMD (Zhu et al., 2015), or as a result of increased adiposity and fat accumulation.

Furthermore, some studies have suggested that obesity plays a protective role against osteoporosis due to the positive relationship between body mass index (BMI) and bone mineral density (BMD) (Hariri, et al., 2019). Low BMI, particularly in combination with advancing age, has been shown to correlate with low bone density, a known risk factor for osteoporosis (Qaseem et al., 2017). Furthermore, although the mechanisms are still poorly understood *in vitro* and *in vivo* studies have confirmed increased differentiation of mesenchymal stem cells into adipocytes rather than osteoblasts in trabeculae due to physical unloading, particularly during aging (Li et al., 2018).

Mechanical loading and stimulation are required for healthy skeletal development and maintenance, strengthening bone structure as a result of adaptive changes to the bone remodelling cycle (Robling and Turner, 2009). Physical activity exerts mechanical forces including compression, tension pressure, and shear (Stoltz et al., 2018) upon bone cells via muscle contraction and ground reaction forces from gravity, resulting in maintenance and gain of bone mass (Klein-Nulend et al., 2012). A classic example of the effects of mechanical stimulation on bone growth can be seen in the radius and ulna of tennis players, which show a 5 to 10% increase in bone mass in the racket arm compared to the contralateral arm (Ducher et al., 2005). In contrast, extended periods of unloading such as long-term bed rest and spaceflight, reduce bone mass and strength in response to the absence of mechanical loading (Klein-Nulend and Bakker, 2012; P. Zhang et al., 2008).

Skeletal muscle contraction imparts mechanical forces upon bone, especially during locomotion and lifting activities. Skeletal muscle is attached directly to bone, typically at sites close to the axes of motion. This means that a large amount of force must be generated by the muscles and transmitted to the skeleton to produce the torque

required for movement (Avin et al., 2015). As a result, muscle contraction contributes significantly to mechanical load experienced by bone and is one of the main factors requiring consideration when investigating the effects of mechanical load on bones. In addition to muscle contraction, mechanical loads are also imparted upon the skeleton by the gravitational pull of the earth, a force which increases proportionally to body weight (Iwaniec and Turner, 2016). In general, individuals with higher BMI tend to exhibit increased BMD, which is thought to have a protective effect against low BMD diseases such as osteoporosis (Palermo et al., 2016) and fracture risk (Dominic et al., 2020). Together, these concepts raise questions over the effects of body weight upon bone via exertion of mechanical loads on the skeleton, and the complex relationships between fat mass, lean mass and bone mineral density (Ilesanmi-Oyelere et al., 2018). The process of converting physical forces into biochemical signals to control bone remodelling, known as mechanotransduction, is responsible for the activation of several complex signalling pathways, altering gene expression and protein synthesis in response to mechanical stimulus. Mechanotransduction has important implications for both clinical and preclinical research, providing insights into healthy development of bone as well as assessment of fracture risk and disease states such as osteoporosis and osteoarthritis, and this topic has been reviewed in depth by Stewart et al., 2020. Briefly, osteocytes within lacunae are the primary mechanosensitive cells within bone, connected to adjacent osteocytes by dendritic processes. The resulting network of osteocytes ensures that mechanotransductive signals propagate throughout the local osteocytic network, termed the lacuna-canalicular (LC) network (Stewart et al., 2020). Osteocytes within this LC network are enveloped by interstitial fluid, allowing osteocytes to detect and respond to fluid shear stress caused by the flow of interstitial fluid over

the cells due to compressive loading of bone (Wittkowske et al., 2016), and these mechanical signals can also be detected by osteoblasts, resulting in an osteogenic response (Uto et al., 2017).

Detection of mechanical stimulus occurs primarily in osteocytes through attachments to the ECM via integrins and CD44 receptors present on the cell membrane (Yavropoulou and Yovos, 2016). The presence of mechanical load is detected by a variety of mechanoreceptors (Figure 1.2), including integrins, calcium channels, cadherins and primary cilia (Stewart et al., 2020).

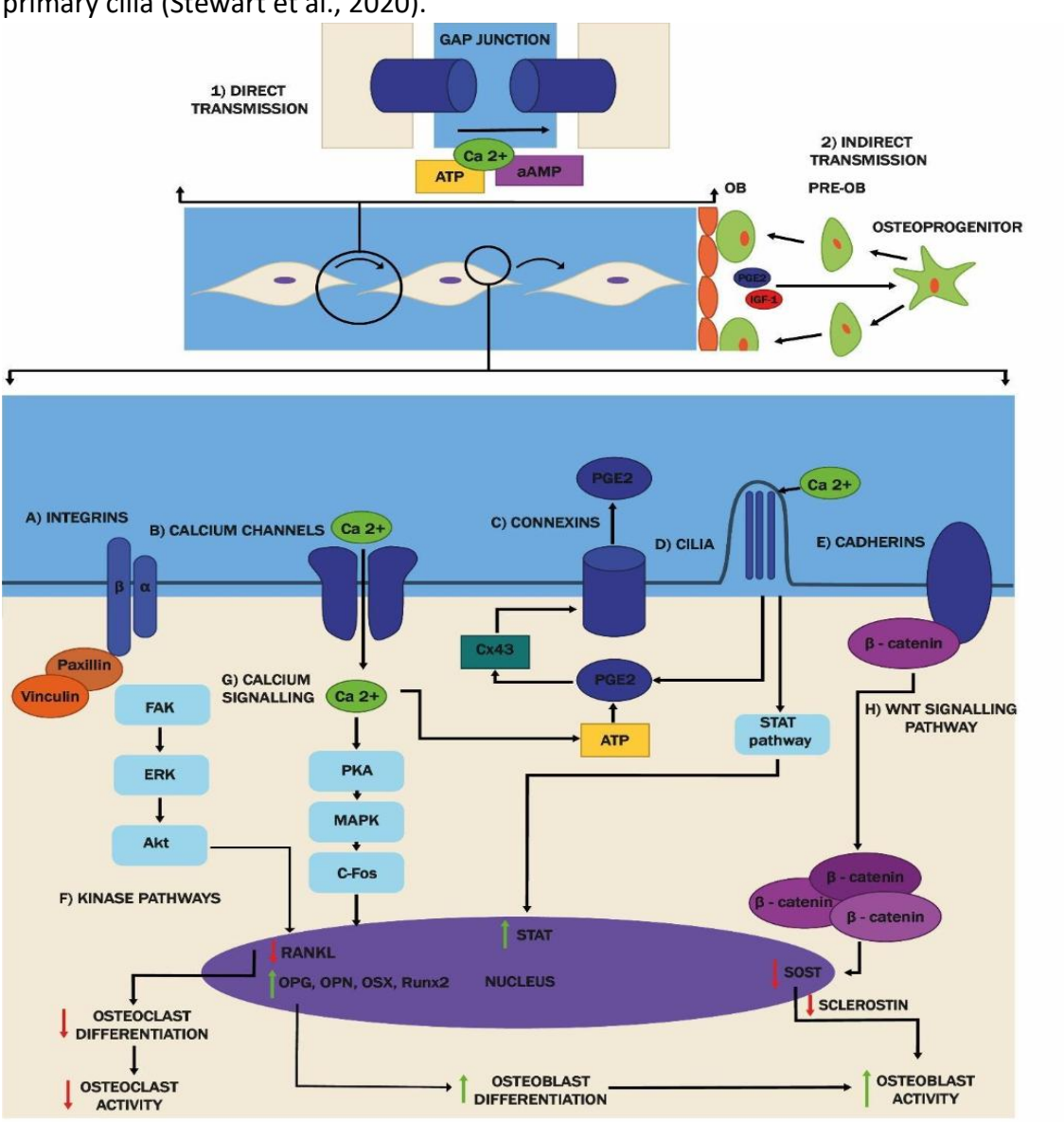


**Figure 1.2:** A schematic diagram representing the main mechanotransduction pathways in bone, including Integrins (A), Calcium channels (B), Connexins (C), Cilia (D), and Cadherins (E). Adapted from Stewart et al., 2020.

Integrins are membrane-spanning proteins which enable cell adhesion to the surrounding ECM and initiate intracellular signalling pathways. Functional integrins consist of  $\alpha$  and  $\beta$  subunits, of which the  $\beta 1$  subunit is known to act as the predominant functional unit in osteoblasts (Rubin et al., 2006). Osteoblast expression of this  $\beta 1$  subunit has been shown to increase in response to fluid shear stress (Kapur et al., 2003) and transgenic mice expressing a dominant-negative, osteoblast-specific  $\beta 1$  subunit exhibited reduced cortical bone formation (Zimmerman et al., 2000). ECM-binding integrins such as  $\alpha 5\beta 1$  do so via binding to the RGD (Arg-Gly-Asp) domains present in the ECM proteins fibronectin and vitronectin (Kechagia et al., 2019). As such, osteoblasts have been shown to bind to fibronectin, osteopontin, bone sialoprotein and vitronectin, all of which connect cells to surrounding ECM, in an RGD-dependant manner, whereas binding to thrombospondin and type I collagen (responsible for cell-cell and cell-ECM binding) are less dependent on the presence of RGD domains (Horton and Helfrich, 2013).

Mechanotransduction is predominantly controlled via integrins by focal adhesion (FA) complexes. FA complexes form a link between the ECM and intracellular proteins such as vinculin, palaxin and focal adhesion kinase (FAK), and transmit external forces from the ECM to the actin cytoskeleton, leading to the activation of mechanotransduction signalling cascades. FAK activation induces phosphorylation of downstream signalling proteins, allowing for the activation of several kinase pathways including phosphoinositide 3-kinase (PI3K) and extracellular signal related kinases (ERK) in response to mechanical stimuli (Yavropoulou and Yovos, 2016). ERK1/2 are activated by mechanical stimuli in bone stromal cells (Rubin et al., 2002) resulting in down-regulation of RANKL expression, as well as increased expression of endothelial nitric oxide synthase

(eNOS) and matrix metalloproteinase 13 (MMP-13). Together these changes result in decreased osteoclast activity (Yavropoulou and Yovos, 2016). Additionally, PI3K/Akt signalling promotes osteoblast differentiation, proliferation and bone formation (Xi, et al., 2015), and FAK activation has been shown to increase expression of osteopontin, osteocalcin, osterix and Runx2, all of which are considered key regulators of osteogenesis and osteoblast differentiation (Wang et al., 2011).

Another group of adhesion molecules important for mechanotransduction includes the cadherins. Cadherins are a form of transmembrane glycoprotein enabling cell to cell adhesion, which associates with intracellular  $\beta$ -catenin (Tian et al., 2011). Fluid shear stress triggers dissociation of β-catenin from cadherins on the intracellular side, leading to increased levels of free β-catenin in the cytoplasm (Norvell et al., 2004). Cytoplasmic β-catenin, once free of the cadherin receptor, is a recognised contributor to osteogenesis, resulting in the induction of Runx2 expression via the Wnt/β-catenin signalling pathway (Dong et al., 2006). The Wnt/ $\beta$ -catenin signalling pathway gives rise to increased osteoprogenitor cell populations and decreased mature osteoblast apoptosis (Bonewald, 2011). As such, loss of N-cadherin in bone lineage cells of adult mice has been shown to result in increased accumulation of intracellular β-catenin signalling, leading to increased bone formation (Fontana et al., 2017). Sclerostin inhibits the Wnt/β-catenin signalling pathway, and mechanical stimulation results in the downregulation of sclerostin expression by osteocytes, thereby resulting in increased osteoblast activity, and subsequently increased bone formation (Hong and Kim, 2018). Ion channels present in cell membranes have also been found to be sensitive to mechanical load in the form of fluid shear stress and tension (Rosa et al., 2015). One such mechanosensitive ion channel is transient receptor potential vanilloid 4 (TRPV4), a

calcium ion channel expressed in osteoclasts, osteoblasts and osteocytes; and absence of TRPV4 prevents disuse-induced bone loss (Guilak et al., 2010). Fluid-flow mechanical stimulation of osteocytes leads to a rapid influx of calcium ions into the cells via voltage-gated calcium channels including TRPV4, activating several cellular functions. These transient calcium channels are induced by local deformation of the cell membrane in osteocytes, and propagation of their signal to neighbouring cells enables osteocytes to communicate within the LC (Adachi et al., 2009). The mechanically induced increase in osteocyte intracellular calcium results in the release of prostaglandin 2 (PGE2), a key paracrine signalling molecule and regulator of bone formation. PGE2 can be released from cells via Cxs in the cell membrane, allowing intracellular communication between osteocytes via gap junctions (Li et al., 2007). Cxs form transmembrane pores in response to mechanical stimuli. These pores can align, giving rise to 'gap junctions' which allow exchange of small cytoplasmic material between cells (Riquelme et al., 2020).

One particular Cxs variant, Cx43, has been identified on the membrane of osteoblasts and osteocytes, and has been shown to regulate osteoblast differentiation as well as bone formation and bone resorption (Buo and Stains, 2014). These Cx43 hemichannels open in response to fluid shear stress, allowing for the transfer of small molecules such as calcium ions, PGE2, ATP and cAMP between adjacent cells (Genetos et al., 2007), and forming a signalling network capable of propagating a mechanical signal to other osteocytes within the LC. Cx43 hemichannel activation has been shown to exert an antiapoptotic effect on osteoblasts *in vitro* (Plotkin et al., 2015). PGE2 is released from osteocytes through these connexin channels in response to mechanical stimuli and contributes to the process of mechanotransduction in both autocrine and paracrine signalling capacities (Stewart et al., 2020). Intracellular PGE2 increases cellular calcium

and cAMP levels, and increases its own production via induction of prostaglandin G/H synthase mRNA (Klein-Nulend et al., 1997). Extracellular PGE2 stimulates production of alkaline phosphatase (ALP) and collagen by osteoblasts, as well as increasing proliferation and adherence of pre-osteoblasts (Stewart et al., 2020).

Primary cilia on the cell surface are known to function as mechanoreceptors in many eukaryotic cell types, particularly those subjected to fluid flow (Wann et al., 2012). Deletion of Kif3a (an essential gene for the formation of primary cilia) from mesenchymal stem cells (MSCs) in mice significantly reduces bone formation in response to mechanical loading (Chen et al., 2016). Oscillatory fluid flow upregulates expression of osteogenic factors (bone morphogenic protein 2 (BMP2) and cyclooxygenase-2 (COX-2)) in MSCs together with increased proliferation, and that this effect is mediated by primary cilia (Hoey et al., 2012). The mechanosensitive ion channel TRPV4 has been shown to colocalise with primary cilia in MSCs, and the mechanotransductive actions of TRPV4 appear to rely upon expression of Ift88, a gene required for generation of primary cilia (Corrigan, et al., 2018). Multiple mechanotransduction mechanisms have been identified as contributors to osteogenesis, and as research in this area advances, it is important to determine the effects of interplay between mechanical loading and other factors such as hormone imbalances, including obesity-induced hyperleptinemia and leptin resistance in the bone remodelling process.

Despite the predominantly osteogenic effects of mechanical loading, the magnitude of force applied to the skeleton is an important factor in determining bone turnover responses. Whilst lower load magnitudes elicit anabolic responses, it has been shown that loads of higher magnitude instead result in catabolic activity, and hence tissue

degradation (Paschall et al., 2024). As such, overloading is known to contribute to various pathologies relating to site-specific inflammation, including arthritis of the knee (Khatib et al., 2019). Mechanical loading of bone has been shown to have profound effects upon the bone remodelling cycle, particularly in relation to extended periods of disuse or lack of loading (Robling and Turner, 2009).

# 1.7. Interactions Between Hormone Signalling and Mechanotransduction in Bone:

Understanding the mechanisms linking hormone signalling to mechanical loading may provide insights into the overarching relationship between obesity and bone. However this is currently poorly understood, with conflicting evidence in the literature to date, potentially due in part to the variance in methodologies used to apply mechanical load or assess bone parameters.

Androgen signalling and mechanical load are both vital factors involved in bone development and maintenance, driving bone formation whilst suppressing bone resorption (Faienza et al., 2024). Although no direct links have been revealed between the two pathways, it is possible that there are common mechanisms between these two signalling pathways underlying their shared benefits for bone health.

Osteoblast differentiation via Runx2 is upregulated by both androgen signalling (Baniwal et al., 2009) and mechanical load (Krstic et al., 2022) independently. This commonality between the two pathways highlights a potential synergistic effect between androgen signalling and mechanotransduction, a relationship which is not fully understood. Similarly, testosterone activates wnt/ $\beta$ -Catenin signalling (Schweizer et al., 2008), a key

pathway enabling the effects of mechanical loading in bone (Hong and Kim, 2018), ultimately inducing *Runx2* expression (Dong et al., 2006). Additionally, testosterone stimulates ERK1/2 signalling (Fix et al., 2004), another key kinase in mechanotransduction (Hino et al., 2020). In addition to these direct affects, androgen signalling also contributes to increased muscle mass, in turn resulting in more mechanical load upon the skeleton from muscle contraction (Rizk et al., 2023).

In a study investigating the effects of hindlimb unloading (HU) upon reproductive function, it was revealed that a lack of mechanical loading reduces testosterone levels whilst increasing aromatase (Moustafa, 2021). Additionally, a similar study found that two to four weeks of HU induce disruption of testicular architecture and molecular phenotypes (Karim et al., 2022). These findings suggest an important role for mechanical loading in testosterone synthesis and signalling. As both of these factors are important for bone maintenance, it may be possible that interactions between these two pathways play a crucial role in the relationship between obesity and bone health.

Alongside testosterone, leptin signalling, another pathway known to be disrupted in obesity (Vilariño-García et al., 2024), is hypothesised to interact closely with mechanotransduction pathways. Despite the osteogenic effects of increased mechanical load due to higher body weights, obese, leptin deficient mice exhibit lower bone masses than their obese wild-type counterparts (Driessler and Baldock, 2010), suggesting that leptin signalling plays an important role in the skeletal response to mechanical stress.

Despite the presence of this high bone mass phenotype in leptin deficient animals, results from a study conducted by Kapur et al., indicate that leptin signalling is a negative modulator of mechanosensitivity in bone. This means that leptin or lepR deficient *Ob/Ob* 

or *Db/Db* mice exhibit significantly increased bone formation in response to mechanical load compared to C57BL/6J controls (Kapur et al., 2010). These findings were also recapitulated *in vitro*, with *Ob/Ob* and *Db/Db* osteoblasts showing significantly greater ERK1/2 phosphorylation and [³H] thymidine incorporation than their wild-type counterparts in response to shear stress. C3H/HeJ mice are known to exhibit poor bone mechanosensitivity, and in this same study by Kapur *et al.*, it was found that siRNA suppression of LepR expression in osteoblasts taken from these mice restores mechanosensitivity, suggesting that LepR signalling may contribute to the poor osteogenic response to loading in these mice. Additionally, osteocyte-depleted mice lost the ability to reduce their body weight by regulating food intake in response to increased mechanical loading, induced via intraperitoneal implantation of a load capsule equal to 15% of body weight (Jansson et al., 2018). This finding suggests the presence of a fat mass homeostat which is independent of leptin, and reliant instead upon mechanical loading.

In a study investigating the role of leptin in the recovery of muscle and bone after periods of unloading in mice, it was revealed that HFD-induced obesity did not affect trabecular bone volume or BMD in unloaded mice. In contrast, HFD-induced obesity significantly increased trabecular BMD in reloaded mice compared to control animals fed a normal diet, and leptin mRNA and serum leptin levels were both found to positively correlate with increases in trabecular BMD (Kawao et al., 2019). These findings suggest that obesity enhances the recovery of bone mass in response to reloading after a period of disuse, but the precise mechanisms remain unknown.

Downstream of leptin signalling, the JAK/STAT pathway is known to play important roles in bone metabolism and development, and selective STAT3 inactivation in osteoblasts

results in decreased bone formation in response to mechanical load (Li, 2013). This same finding has now been established in osteocytes, and treatment with a STAT3 inhibitor blocks intracellular calcium influx into MLO-Y4 osteocytes. The STAT3 pathway is required for the effects of leptin upon food intake and glucose metabolism (Buettner et al., 2006) and may also play an important role in linking leptin signalling and mechanotransduction in bone remodelling.

Mechanical loading promotes osteoblastic differentiation of MSCs and inhibits adipogenic differentiation (Cao, 2011), in contrast to leptin signalling which has the opposite effect: inhibiting osteogenesis and increasing adipogenesis (Yue et al., 2016). It is possible that there is overlap between these two determinants of MSC differentiation, and that leptin signalling alters osteogenic response to mechanical loading; although very little is known on this topic to date. Investigating the interactions between leptin signalling and mechanotransduction in deciding MSC fate may provide a greater understanding of the relationship between obesity and bone metabolism.

## 1.8. Aims and Objectives:

With contradicting evidence in the literature, the precise effects of obesity on bone are yet to be identified. This work aims to investigate the effects of testosterone and leptin, both alone and in combination with mechanical loading, upon bone remodelling. It is possible that the mechanisms by which these hormones alter bone remodelling are coupled with those involved with mechanotransduction, a link which has not previously been investigated in detail but may provide important insights into the implications of obesity on bone health. The hypothesis of this body of research is that leptin and testosterone signalling alter cellular responses to mechanotransduction in bone, and

that alterations in the levels of these hormones alone induces changes in bone microarchitecture independent of concomitant changes in body weight associated with obesity.

# 1.9. Specific Aims:

- 1. Investigate the relationship between testosterone depletion, subsequent TRT and bone turnover in a murine model of cardiometabolic disorder fed a high fat diet, including assessment of tibia morphology and mechanical strength alongside markers of bone cell differentiation and activity.
- 2. Determine the independent effects of leptin depletion whilst controlling for mechanical loading from body weight in leptin deficient *Ob/Ob* mice weight paired to either lean or obese C57 counterparts. Assessment of tibial and vertebral bone morphology and bone cell differentiation and activity, including assessment of tibial mechanical strength.
- 3. Investigate the interactions between the effects of testosterone or leptin with mechanical loading upon key markers of bone cell activity and matrix deposition in cells of osteoblast lineage using 2D and 3D *in vitro* models.

2. Chapter 2: The Effects of Testosterone Depletion Upon Bone Turnover in a Murine Model of Cardiometabolic Disorder Fed a High Fat Diet:

## 2.1. Introduction:

In recent years, high fat diet (HFD) combined with reduced physical activity have resulted in dramatic increases in obesity and accompanying metabolic consequences in developed nations (Bray et al., 2018). Low BMI and body weight are associated with osteoporosis and fracture risk (Morin et al., 2009), whilst high body weight is positively associated with BMD (Shapses and Sukumar, 2012), due to the beneficial effects of increased mechanical load from body weight on bone mass. However, a HFD increases bone marrow adipose tissue accumulation and leads to oxidative stress, both of which are known to contribute to the acceleration of bone loss (Qiao et al., 2021). HFD feeding in mice leads to a reduction in trabecular and cortical bone mass compared to mice fed a normal chow diet, which is thought to be via suppression of bone formation (S. Kim et al., 2021). Adipogenesis is increased in mice fed a HFD, accompanied by a reduction in osteoblastic differentiation due to shared mesenchymal stem cell lineage between osteoblasts and adipocytes (Saleh et al., 2021). As such, differential effects can be observed with obesity and HFD and thus studies are required which enable the isolated study of these effects.

Alongside the more well-known detrimental effects of obesity on health, obesity is also recognised as a significant risk factor for testosterone deficiency in men (Saad et al., 2017). Several measures of obesity are negatively correlated with free, bioavailable and total testosterone levels; a relationship which is maintained across all age groups (Grossmann, 2011). Obesity-induced reduction of free testosterone levels leads to increases in adiposity, giving rise to a self-perpetuating cycle of metabolic complications (Fui et al., 2014), including loss of muscle and bone mass, as well as further increased fat mass in elderly men (Saad et al., 2017). These conditions also contribute to the

pathogenesis of atherosclerosis and can increase the risk of cardiovascular mortality in men with low testosterone (Kelly and Jones 2013).

Testosterone and its precursors, collectively termed 'androgens', promote boneformation by acting directly upon androgen receptors (ARs) present on bone cells including osteoblasts and osteoclasts (Mohamad et al., 2016a). Androgen signalling suppresses osteoblast apoptosis (Almeida et al., 2010), and increases osteoblast proliferation (X. Wu and Zhang, 2018) and differentiation from MSCs via induction of RUNX2 (Gao et al., 2017; Payandeh et al., 2020). Additionally, low levels of testosterone (<250 ng/dL) are associated with increased serum levels of bone associated alkaline phosphatase, indicating increased bone turnover (Dabaja et al., 2015). The decline of testosterone levels with age, especially in obese men, is concurrent with a decline in BMD (Shigehara et al., 2021). This presents testosterone replacement therapy (TRT) as an attractive therapeutic for managing the metabolic effects of testosterone deficiency and decline in BMD simultaneously. Testosterone deficiency has been linked to frailty in older men (Saad et al., 2016) and it is clear that TRT improves BMD in testosterone deficient men in some studies (Isidori et al., 2005; Shigehara et al., 2021), but not in others (Kenny et al., 2001) and contradictory evidence exists (Al Mukadam et al., 2017). Mechanistically, the differentiation and activity of osteoclasts is up-regulated in response to increased activation of RANKL in the absence of testosterone (Shigehara et al., 2021), including in orchiectomised rodents (Mohamad et al., 2016).

Adult human testosterone treatment leads to increased strength of spine trabeculae compared to placebo treated men (Colleluori et al., 2021; Snyder et al., 2017). This is likely due to altered levels of factors secreted by cells of the osteoblast lineage, including RANKL released from immature osteoblasts, which binds to RANK on osteoclasts and

triggers osteoclast differentiation (Park et al., 2017). Treatment of murine osteoblasts with a supraphysiological dose of testosterone *in vitro* led to a significant increase in the ratio of RANKL:OPG, whereas treatment with a low physiological dose resulted in a decrease in RANKL:OPG ratio (Steffens et al., 2014). This indicates that low doses of testosterone inhibit, whereas larger doses may increase osteoclastogenesis and therefore bone resorption via RANKL/RANK signalling. This inhibitory effect of testosterone upon bone resorption has also been reported in a variety of clinical studies in men, showing that TRT significantly decreases markers of bone resorption without significantly altering bone formation markers (Isidori et al., 2005).

Despite these mechanistic and bone microarchitecture studies, there is no evidence that this testosterone-induced increase in BMD in the majority of the literature translates to decreased fracture risk (Snyder et al., 2017). In fact, the recent FDA-mandated TRT for Assessment of Long-term Vascular Events and Efficacy Response in Hypogonadal Men (TRAVERSE) trial highlighted in a sub-study that testosterone treatment increased fracture risk (Snyder et al., 2024). While this study did not assess possible mechanisms by which testosterone would increase the incidence of fractures, it may be speculated that the increased risk was a subsidiary consequence of increased physical activity due to improvements in mood, energy levels, motivation and quality of life measures indicated in the main study (Lincoff et al., 2023) and others (Traish and Morgentaller 2017) prior to longer-term actions on bone architecture. Indeed, the most common sites of fractures were ribs, wrist, and ankle, locations associated with trauma and more commonly with falls. However, the TRAVERSE trial did not evaluate bone density and structure, and traumatic events and falls were not reported end points. These contradictory clinical findings emphasise the need for further mechanistic investigation

into the influence of testosterone on bone microarchitecture, strength and fracture risk. Apolipoprotein E (ApoE) is a major component of brain and peripheral lipoprotein transport systems (E. Kypreos et al., 2018), which has recently become an area of interest in the field of obesity research. ApoE-/- mice are a well-established model of atherosclerosis (Fitzgibbons et al., 2018), exhibiting poor lipoprotein clearance leading to the accumulation of ester-enriched particles in the blood and subsequent atherosclerotic plaques (Lo Sasso et al., 2016). ApoE and leptin double deficient (ApoE-/- x Ob/Ob-/-) mice are resistant to body weight and fat mass gain in response to high fat diet (HFD) feeding, despite increases in plasma very-low-density-lipoprotein (VLDL) (Chiba et al., 2003), suggesting that VLDL-induced adipogenesis is ApoE dependent. ApoE-/- mice also accumulate less body fat content and display smaller adipocytes compared to wild-type (WT) C57BL/6 controls (Huang et al., 2006). Taken together, these findings highlight ApoE-/- mice as a suitable model for studying the effects of an obese metabolic phenotype upon bone, without the confounding factor of increased body weight.

The aim of this study was to test the hypothesis that testosterone deficiency leads to reductions in bone volume, and that testosterone therapy can restore these parameters. Additionally, the study aims to provide insights into the cellular mechanisms underpinning these changes in a mouse model of cardiometabolic disease, allowing for assessment of the isolated effects of HFD and TRT without the effects of increases in mechanical load from body weight. In doing so, markers of osteoblast differentiation (RUNX2) and activity (ALP) were assessed alongside markers of osteoclast differentiation (RANKL:OPG ratio) and activity (TRAP). This work aimed to provide insights into the mechanisms governing the morphological alterations in bone seen in

testosterone deficiency. The hypothesis of this work was that testosterone depletion negatively influences bone mass and microarchitecture, and that TRT restores bone parameters to control levels in castrated mice.

The aims of this work package were:

- To establish the impact of testosterone depletion and subsequent TRT upon bone microarchitecture.
- 2. To investigate the cellular mechanisms underpinning testosterone-related alterations in bone morphology.
- 3. To assess the effects of testosterone related changes in bone morphology upon the mechanical strength of murine tibiae.

## 2.2. Materials and Methods:

## 2.2.1. Experimental Design:

Obesity is a significant risk factor for testosterone deficiency in men, and testosterone deficiency itself is a known significant contributor to a range of health defects, including cardiovascular disease and osteoporosis. This study utilised ApoE-/- mice fed a HFD to recapitulate the metabolic comorbidities of obesity and increased cardiovascular risk without increased load from body weight, to investigate the independent role of testosterone in bone remodelling. ApoE-/- mice were split into three experimental groups. At 7 weeks of age, two experimental groups underwent orchiectomy (castration) surgery to achieve testosterone depletion, and one of these groups received subsequent testosterone replacement therapy via intramuscular injection from 8 weeks of age, whereas a control group received only sham surgery with placebo injection and were therefore not testosterone depleted. All mice were fed a HFD from 8 weeks of age for the duration of the study. Tibiae were harvested for analysis at 25 weeks of age, after 17 weeks of treatment. This study was performed in tandem with another study utilising waste tissue from the same animals (Bateman, 2020) in line with NC3Rs, and all timepoints were selected accordingly. Morphological changes in the proximal tibiae cortical and trabecular bone were quantified separately using Micro-Computed Tomography (µCT) with post-imaging processing software. The mechanisms governing these morphological changes were then investigated using histological and immunohistochemical staining, including assessing the presence of markers of osteoblastic bone formation, and osteoclastic bone resorption. Mechanical properties of the tibiae were assessed using a 3-point bend test to assess the impact of observed changes upon the physical strength of the bone, and therefore fracture risk.

#### 2.2.2. Animal Husbandry:

The proposed experimental designs and methods of analysis of the results were discussed with the Statistical Services at the University of Sheffield. Factorial experimental designs were used to maximise the information obtained from the minimum resource. Where practicable, sample sizes were determined through power analysis generally using a significance level of 5%, and power of 80 or 90%. The principle variable for determining sample size was lipid deposition in the aortic root as this was conducted alongside a study primarily related to cardiovascular risk. However, where preliminary data was available for alternate individual variables this data was used to ensure analysis would provide results of value. Otherwise, we will use the least number of animals to provide an adequate description, generally on the basis of previous experience. For animal numbers required, it was expected that approximately 12-14 animals per treatment group were required. Further power calculation information is included in the appendix of this thesis. Male ApoE-/- mice were acquired from Charles River Laboratories and split into 3 groups: sham surgery followed by placebo treatment (control: n=9) and orchiectomy followed by either placebo (n=8) or testosterone treatment (n=10). All animals were maintained in cages containing up to 5 mice on a twelve-hour light/dark cycle in a temperature (19-23°C) and humidity (55 ± 10%) controlled environment. Mice were fed a high fat diet (HFD): 4.63 kcal/g (fat 42%kcal, protein 15%kcal, carbohydrate 43%kcal) (Special Diet Services, UK) from 8 weeks of age. All procedures were carried out under the jurisdiction of the UK Home Office personal and project licenses (project license P3714F016, personal license (Lauren Bateman: I1EDE3DC6), governed by the Animals Scientific Procedures Act 1986. This work was performed by Lauren Bateman.

#### 2.2.3. Surgical Bilateral Orchiectomy and Testosterone Treatment:

Orchiectomy surgery was performed as previously described (Bateman, 2020). Briefly, seven-week-old mice were anaesthetised via inhalation of 5% isoflurane (Zeotis, UK) and a small incision was made across the midline of the scrotum before separating the subcutaneous connective tissue within the intramuscular sacs. Another small incision was made and the vas deferens, fat pads and testes were then clamped with forceps. A single ligature was placed around each vas deferens and blood vessel before being severed. The remaining tissue was repositioned in the sac and the skin incision closed. Sham surgery was performed as above with the following amendments. Once the subcutaneous connective tissue was separated within the intramuscular sacs the area was probed for approximately 5 minutes to mimic the tissue disruption and time under general anaesthesia caused by the orchiectomy surgery. This work was performed by Lauren Bateman.

#### 2.2.4. Testosterone or Placebo Treatment

Testosterone or saline treatments were delivered via intramuscular (IM) injection under anaesthesia once fortnightly beginning from 8-weeks of age. In order to recapitulate normal physiological testosterone levels of between 2 – 20 ng/mL (Sedelaar et al., 2013) in castrated mice, IM injection of 10 μL of either 100 mg/mL testosterone esters (Sustanon®100 (testosterone propionate 20 mg/mL, testosterone phenylpropionate 40 mg/mL, and testosterone isocaproate 40 mg/mL), Organon Laboratories Ltd., Cambridge, UK) or physiological saline was injected. This work was performed by Lauren Bateman.

#### 2.2.5. Tissue Collection:

At 25 weeks of age and after 17 weeks of treatment, body weights were recorded, and mice were sacrificed via terminal anaesthesia followed by cardiac puncture and exsanguination. Tibiae were collected via dislocation of the femoral head to remove the hind-limbs intact, followed by separation from the femur and ankle using a scalpel. Care was taken to keep the tibial plateau and fibula intact during this process. Tibiae were subsequently fixed in 4% w/v PFA in individual 6mL tubes for 48 hours before transferral to 70% v/v ethanol for storage at 4°C until scanning.

#### 2.2.6. Serum Collection:

Whole blood for serum measurements was collected via cardiac puncture and allowed to clot at room temperature for 30 minutes at RT. Samples were then centrifuged at 1000 g in a refrigerated centrifuge for 10 minutes and the serum supernatants were stored at -80°C. All analyses were performed on non-pooled serum samples. This work was performed by Lauren Bateman.

#### 2.2.7. Measurement of Serum Testosterone via ELISA:

Testosterone levels were calculated according to the manufacturer's instructions (DRG Diagnostics EIA1559, Marburg, Germany). Briefly, serum was placed in the supplied ELISA plate and ELISA completed as per manufacturers instructions (DRG Diagnostics) and absorbance measured using a ClarioStar reader (BMG Labtech, Aylesbury, England) at 450±10nm. Testosterone levels were calibrated according to the standard calibration curve and converted to SI units (nM/L) via multiplication by the known testosterone conversion factor 3.467. This work was performed by Lauren Bateman.

#### 2.2.8. μCT imaging:

Fixed whole Tibiae were removed from 70% IMS, individually wrapped in cellophane and mounted into a plastic tube which was then secured onto the stage of the  $\mu$ CT scanner (Skyscan 1272, Bruker, Belgium). Scans were performed using accompanying Skyscan software (Bruker, Belgium) at an X-ray voltage of 50 kV and an X-ray current of 200  $\mu$ A with a 0.5 mm aluminium filter, utilising a voxel size of 4.3  $\mu$ m with 180° tomographic rotation and a 0.7° rotation step. Frame averaging was set to 3 frames, and a single camera position was selected. Resulting datasets were then reconstructed using NRecon software (Bruker, Belgium) utilising a beam hardening correction of 20% and postalignment optimisation. Bone mineral density (BMD) measurements were quantified using attenuation coefficients calibrated against a pair of 2 mm calcium hydroxyapatite (CaHa) calibration rods of known (0.3g/cm3 and 1.25g/cm3) density (Bruker, Leuven, Belgium).

#### 2.2.9. Image post-processing:

Post reconstruction analyses of  $\mu$ CT images were performed upon serial slices using CTAn software (Bruker SkyScan, v1.15.4.0). Trabecular and cortical bone parameters were measured at two distinct tibial sites, measuring bone parameters within a 1 mm length of bone starting from 0.2 and 1.0 mm distally from the growth-plate respectively (Figure 3.1). Normalised regions of interest (ROIs) were defined by drawing freehand in the CTAn software, creating separate ROIs for both cortical and trabecular bone. Thresholding was set and maintained at 80-255 and a de-speckle step was performed prior to analysis to remove white speckles less than 10 voxels within the ROIs.

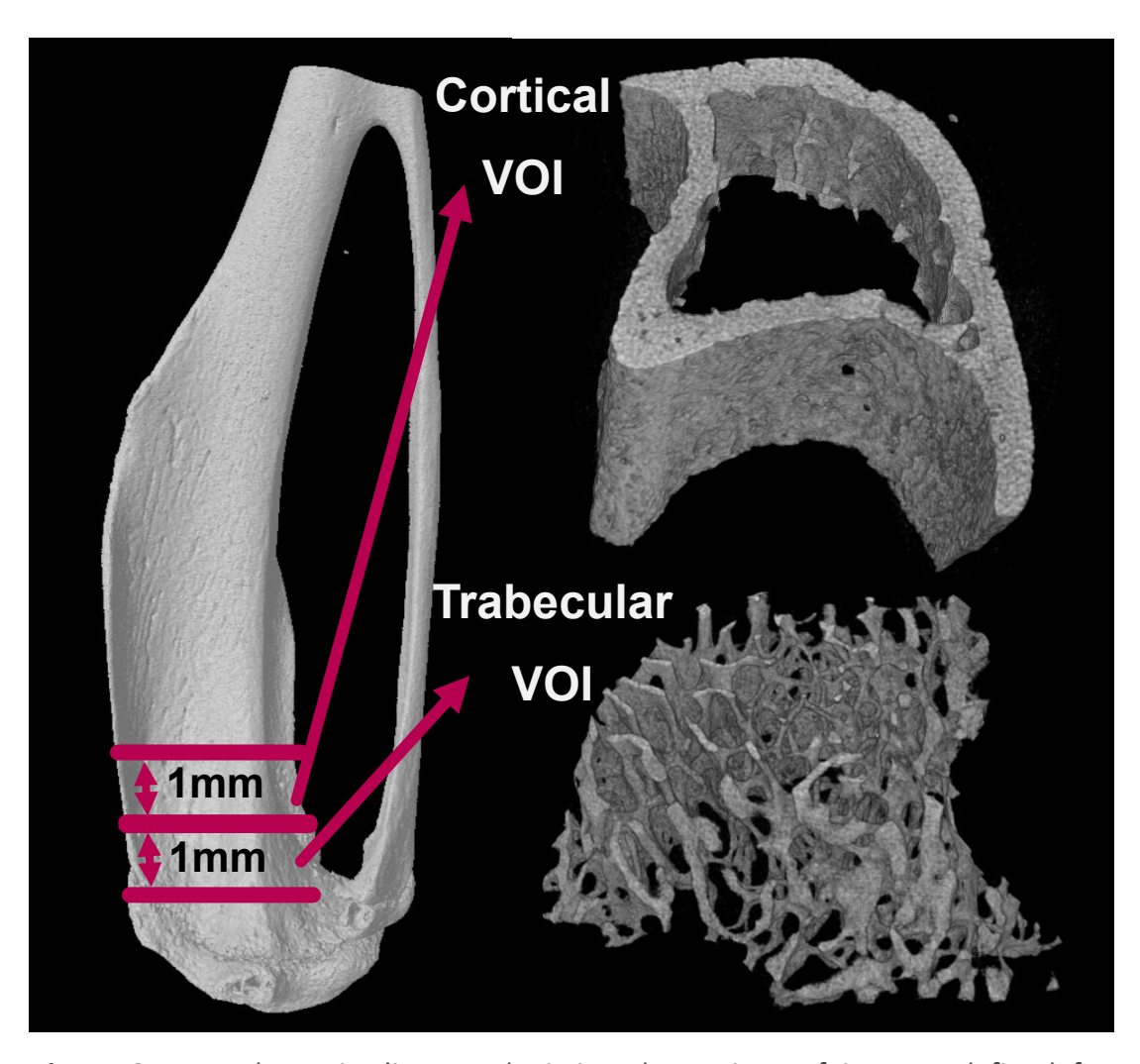


Figure 2.1: A schematic diagram depicting the regions of interest defined for trabecular and cortical  $\mu CT$  analysis of murine tibiae.

#### 2.2.10. Quantitative morphometry:

Morphometric parameters investigated in this study include trabecular bone volume fraction (BV/TV) (%), Trabecular number (tb.N) (mm-1), trabecular thickness (tb.Th) (mm), trabecular separation (tb.Sp) (mm), structural model index (SMI) and bone mineral density (BMD) (g/cm3), as well as cortical bone volume (BV) (mm-3) and cortical BMD (g/cm3) (Bouxsein et al., 2010). All measurements were performed using CTAn software.

#### 2.2.11. Trabecular Thickness Colour-coded 3D Modelling:

Trabecular bone thicknesses were qualitatively analysed via the production of 3D colour coded models. Trabecular thickness mid-range values were generated from respective ROIs after application of the thresholding and despeckle functions outlined above. The contrast stretching in 3D space filter function was then applied to the colour-coded datasets, and the CTvox was used to create a 3D colour-coded model of the resulting dataset. A standardised mid-range transfer function was then applied to all colour-coded model datasets, and a scale bar was created using the mid-range values, ranging from a minimum of 0.0086 mm to a maximum of 0.1204 mm. Mid-range values were then plotted against the percentage of bone volume within each range.

#### 2.2.12. Tissue Preparation:

Left tibiae were decalcified in 20% EDTA for 2 weeks at 4°C on a rocker, changing the EDTA solutions every 2 days. Decalcification was confirmed with  $\mu$ CT and then tibiae were embedded in paraffin using standard procedures. Four  $\mu$ m sections were cut using a microtome and left to dry at 37°C for 2 weeks prior to immunohistochemistry and

histological staining procedures. Right tibiae were left unprocessed for mechanical testing.

## 2.2.13. Haematoxylin and Eosin Staining:

Paraffin was removed from the sections using sub-X (Leica Microsystems) for 3 x 5 minutes before rehydration through a series of IMS baths for another 3 x 5 minutes. Sections were then stained with Mayer's Haematoxylin (Leica Microsystems) for 1 minute, and subsequently left to 'blue' under running tap water for 5 minutes prior to further staining with alcoholic eosin (Leica Microsystems) for 1 minute. Sections were then dehydrated (3 x 5 minutes) in IMS and cleared (3 x 5 minutes) in sub-X (Leica Microsystems) before coverslips were mounted to slides using pertex (Leica Microsystems) and left to dry before sections were assessed microscopically.

#### 2.2.14. Masson's Trichrome Staining:

Sections were dewaxed in Sub-X (Leica Microsystems) for 3 x 5 minutes, and rehydrated through IMS for 3 x 5 minutes and then stained using a Masson's Trichrome staining kit (Atom Scientific) according to manufacturer's instructions. Briefly, dewaxed and rehydrated samples were stained with Weigert's Iron haematoxylin for 20 minutes prior to washing in water for 1 minute, and then differentiation in 1% acid alcohol solution. Sections were left to 'blue' under running tap water for 5 minutes before staining with ponceau fuchsin for 5 minutes and a further wash in distilled water. Sections were then stained with phosphomolybdic acid for 15 minutes before transferring to methyl blue solution, without rinsing, for a further 5 minutes. Slides were given one final wash in water before dehydration (3 x 5 minutes) in IMS and clearing (3 x 5 minutes) in sub-X

(Leica Microsystems). Coverslips were mounted to slides using pertex (Leica Microsystems) and left to dry before sections were assessed microscopically.

## 2.2.15. Tartrate-resistant Acid Phosphatase (TRAP) Staining:

Sections were dewaxed through Sub-X (Leica Microsystems) for 3 x 5 minutes and rehydrated through IMS for 3 x 5 minutes before incubating in pre-warmed acetate-tartrate buffer (265 mM Sodium Acetate and 95 mM Sodium Tartrate in 0.3% acetic acid for 5 minutes at 37°C. Acetate-tartrate buffer was replaced with 20mg/mL Naphthol AS-BI phosphate Diformamide (Fisher Scientific) in acetate tartrate buffer. sections were allowed to incubate in this solution for a further 30 minutes at 37°C. Staining solutions were then replaced with acetate-tartrate buffer hexazotised pararosaniline solution for a further 15 minutes at 37°C before rinsing in tap water and counterstaining with Gill's Haematoxylin for 30 seconds and 'bluing' under running tap water for 5 minutes. Sections were then dehydrated through IMS (3 x 5 minutes) and cleared through sub-X (Leica Microsystems) for 3 x 5 minutes before mounting a coverslip with pertex (Leica Microsystems).

#### **2.2.16.** OsteoMeasure TRAP counting:

TRAP-stained microscope slides were mounted to the slide holder of a BX53 microscope (Olympus, Southend on Sea, UK) equipped with a camera, and a PC with Osteomeasure software (v3.1.0.1, Osteometrics, GA, USA). Osteoclast and osteoblast parameters were quantified separately via manual selection in three distinct regions of interest along the cortico-endosteal bone surface of the TRAP-stained tibiae. Positive red staining was used to identify osteoclasts, whereas osteoblasts were identified based upon cuboidal

morphology and proximity to the bone surface. For all measurements, an offset of 250  $\mu$ m from the growth plate was applied, and three 250  $\mu$ m x 250  $\mu$ m regions of interest were analysed, with a total length of 3 mm per sample analysed. For osteoblasts, the percentage of bone surface covered by osteoblasts (ObPm/BPm %) and the number of osteoblasts per millimetre of bone were assessed. Similarly, osteoclasts were quantified in terms of the percentage of bone covered by osteoclasts (OcPm/BPm %), and the number of osteoclasts per mm of bone determined.

## 2.2.17. Immunohistochemistry:

Immunohistochemistry was utilised to assess the presence of proteins of interest (Table 2.1). Four  $\mu$ m thick sections were dewaxed in Sub-X (Leica Microsystems) for 3 x 5 minutes and rehydrated in IMS for 3 x 5 minutes, before endogenous peroxidases were blocked with 3% w/v hydrogen peroxide (Sigma-Aldrich) in IMS containing five drops of concentrated HCl for 1 hour at room temperature. Sections were then washed in H<sub>2</sub>O for 5 minutes and then for 2 x 5 minutes in tris-buffered saline (TBS), prepared by diluting a 10x stock solution of TBS (200 mM Tris, 1500 mM NaCL, pH 7.5).

Antigen retrieval steps and antibody concentrations necessary for each primary antibody (Table 2.1) were then determined by trialling a range of antibody concentrations and antigen retrieval methods to determine the optimal staining procedure for each antigen of interest. For enzyme-mediated antigen retrieval, slides were immersed in a bath containing 300  $\mu$ L of 1% w/v  $\alpha$ -chymotrypsin and 0.1% CaCl2 (preheated to 37°C) for 30 minutes.

If heat antigen retrieval was required, sections were immersed in tris heat antigen retrieval buffer (50 mM Tris, pH 9.5) and then covered with non-stick teflon strips,

clamped in place with another, blank, microscope slide. Sections were heated in a steamer (Russell Hobbs) for 20 minutes whilst submerged in tris heat antigen retrieval buffer, and then moved to dH<sub>2</sub>O to allow for removal of the Teflon strips. After respective antigen retrieval steps, slides were washed in 1x TBS for 3 x 5 minutes and non-specific antibody-protein interactions were blocked with 2.5% normal goat serum (Gibco) containing 1% BSA in TBS for 2 hours at RT in a humidified box.

Sections were then incubated with rabbit anti-RUNX2, anti-RANKL, anti-Osteoprotegerin, anti-Alkaline Phosphatase, or anti-Adiponectin antibodies (Abcam) according to Table 2.1 or a rabbit IgG isotype at equivalent concentration (Abcam, ab183910) overnight at 4°C. Sections were washed in TBS containing 0.1% Tween-20 (TBS-T) (Sigma-Aldrich) for 3 x 5 minutes before adding 200 µL of Biotinylated goat antirabbit secondary antibody (Abcam, ab6720) diluted to 1:500 in 1% w/v BSA in TBS for 30 minutes at room temperature. Sections were washed again in TBS-T for 3 x 5 minutes prior to the addition of Vectastain Elite ABC reagent (Vector) and incubation at room temp for 30 minutes before developing with 0.08% v/v H<sub>2</sub>O<sub>2</sub> and 0.65 mg/mL 3,3′-diaminobenzidine tetrahydrochloride (DAB) for 20 minutes at RT. Sections were then washed in water for 5 minutes and dehydrated through a series of IMS solutions for 3 x 5 minutes and cleared through sub-X (Leica Microsystems) for 3 x 5 minutes before finally mounting a coverslip with pertex (Leica Microsystems).

Table 2.1: Primary antibody and antigen retrieval information for the IHC assessment of RUNX2, RANKL, adiponectin, OPG and ALP in murine tibiae.

Primary Antibody	Antigen Retrieval	Dilution
Rabbit anti-RUNX2 (ab192256)	Heat	1:1000
Rabbit anti-RANKL (ab216484)	Heat	1:1250

Rabbit anti-Adiponectin	Heat	1:1000
(ab216484)		
Rabbit anti-OPG	Enzyme	1:100,000
(ab183910)		
Rabbit anti-ALP	None	1:1250
(ab203106)		

#### 2.2.18. Image Capture and Quantification of IHC:

Mounted, dry microscope slides were assessed microscopically using an Olympus B60 microscope and images were captured using CellSens software (Olympus, Southend, UK) and a MicroCapture v5.0 RTV digital camera (Q imaging, Buckinghamshire, UK). Cell positivity was determined manually by counting a total of 200 osteoblasts along the lateral endocortical surface and calculating the percentage positivity. All microscopic evaluations were performed blinded using randomly assigned sample numbers, and groups were not revealed until after the quantification was complete.

#### 2.2.19. Quantification of Lipid Droplet Area:

Sections stained with an antibody against adiponectin were imaged at 20x magnification at 5 randomly chosen regions of bone marrow. Images were then processed in Image-J software (Fiji), and lipid droplet areas were quantified in all 5 regions per section using a custom macro designed to identify and quantify empty spaces surrounded by positive APN immunostained cells (adipocytes) in the marrow (Figure 2.2). Outputs were averaged for each section and given as a percentage lipid droplet area within the field of view. All microscopic evaluations were performed blinded using randomly assigned sample numbers, and groups were not revealed until after the quantification was complete.

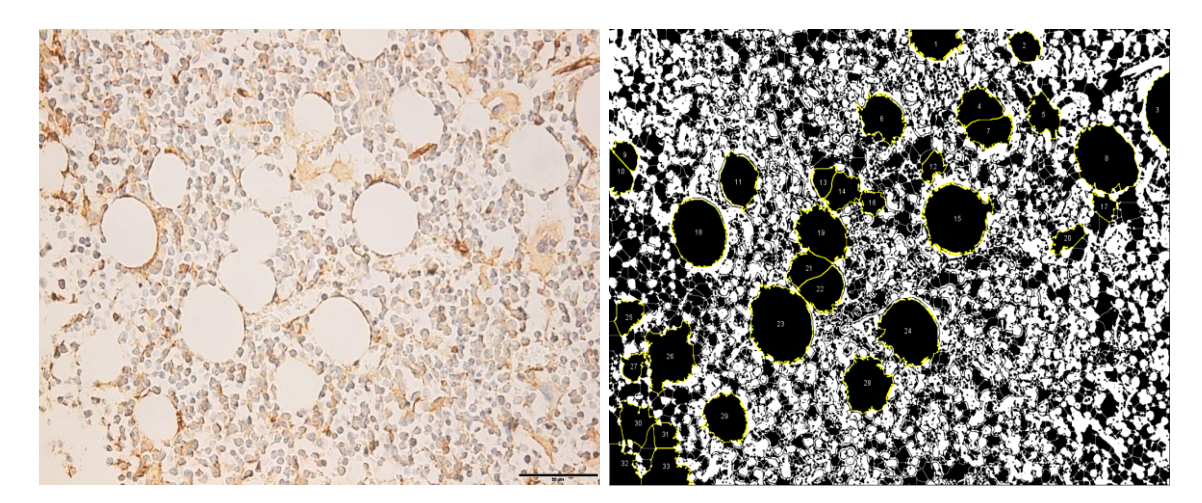
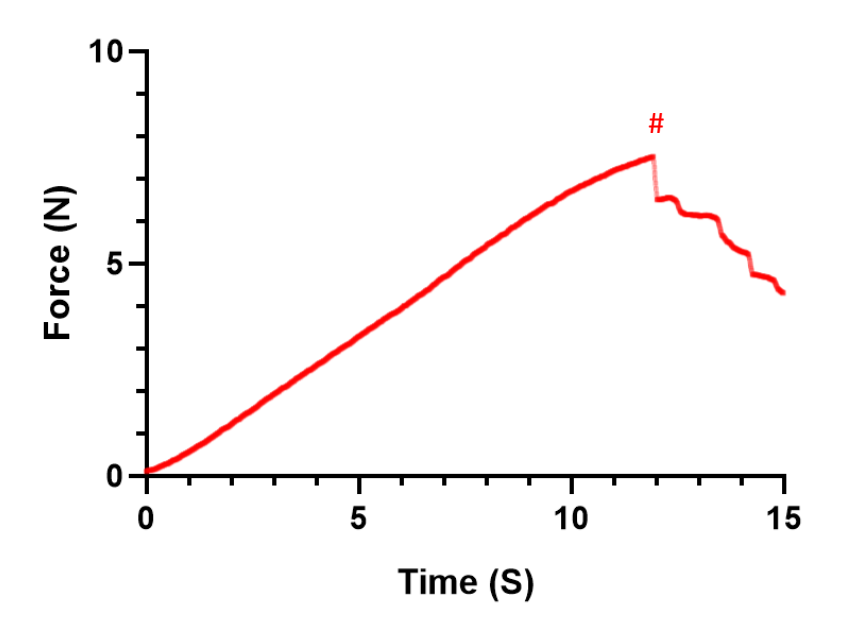


Figure 2.2: Comparison between a representative raw image of immunohistochemistry staining for adiponectin (left) and a binarized image used for quantification of percentage lipid droplet area. Analysis was performed using a custom made macro in ImageJ software, outlining lipid droplets in yellow and calculating their area. Scale bar is  $50\mu m$ .

## 2.2.20. Three-point Bending Mechanical Testing:

Undecalcified right tibiae were incubated in PBS for 24 hours prior to biomechanical testing. Tibia lengths were measured using digital callipers and fibulas were detached using a scalpel. Mechanical tests were performed using a CellScale Univert mechanical testing system, with a 1 kN load cell and a horizontal distance of 11 mm between supports. Tibiae were positioned horizontally on the two supports with the lateral edge facing upward. A pre-load of 0.1 N was applied prior to loading at 0.05 m/s over a 200 second duration. Data was collected at a frequency of 100 Hz and used to calculate maximal load at failure.



**Figure 2.3:** Force applied over time applied to murine tibiae in a three-point bend test, used to determine Fmax at the break point (#).

## **2.2.21.** Statistical Analysis:

All  $\mu$ CT data are presented in the form of individual data points and median values are displayed. Normality tests were performed using Shapiro Wilk normality test, and parametric data were analysed using ordinary One-way ANOVA with post-hoc multiple comparison testing. For non-parametric data, Kruskal-Wallis with post-hoc multiple comparisons tests were performed. P <0.05 was considered statistically significant in this study.

## 2.3. Results:

#### **2.3.1.** Serum Testosterone Concentration:

The concentration of testosterone in serum was significantly reduced in orchiectomsied mice compared to sham operated controls, (Figure 2.4) (P = 0.0038) and testosterone

treated mice (P = 0.0009), whereas testosterone levels in testosterone treated mice were comparable to control levels and within the expected physiological range of 2 – 20 ng/mL (Sedelaar et al., 2013).

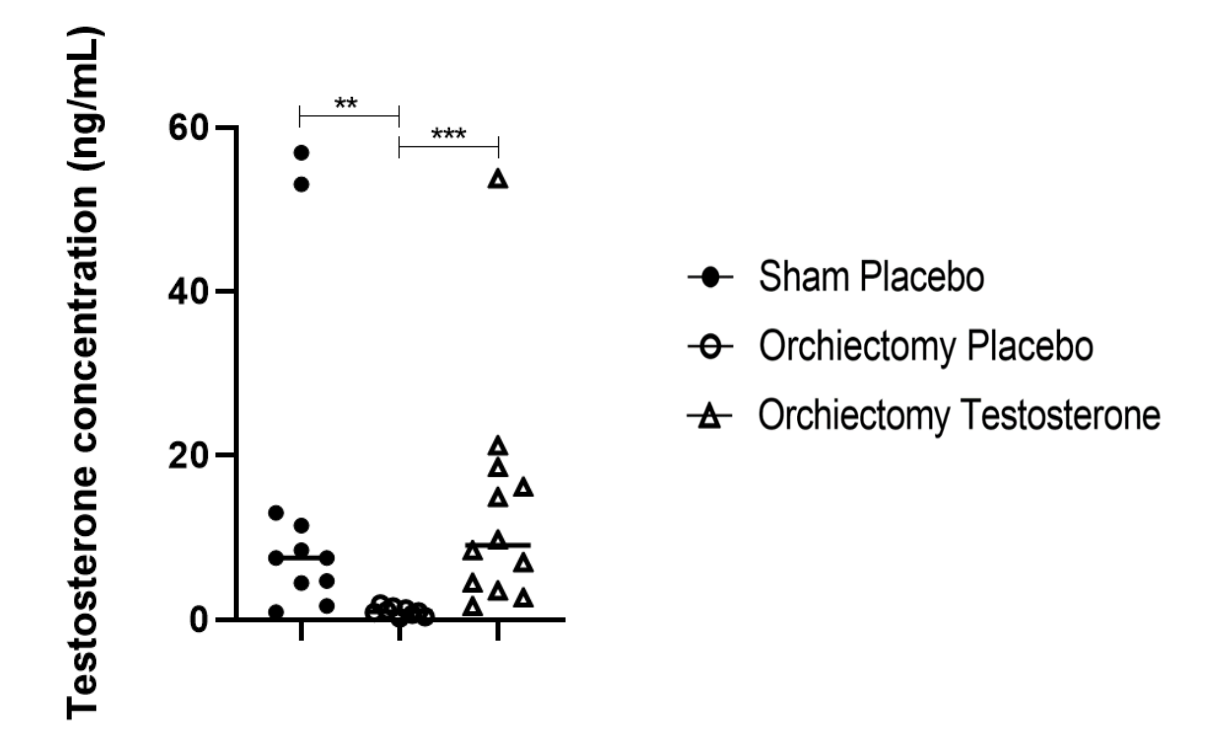


**Figure 2.4:** Testosterone concentrations in blood serum from sham operated, placebo treated control mice (n = 11), orchiectomised, placebo treated mice (n = 9), and orchiectomised mice treated with testosterone (n = 12) determined via ELISA ng/L (\*P < 0.5, \*\*\* P < 0.05, \*\*\* P < 0.01, \*\*\*\* P < 0.001).

# 2.3.2. Body weight and cortical bone parameters:

Hand-drawn 3D ROIs were used to manually define 10mm sections of tibial bone to be used for  $\mu$ CT analysis of cortical bone (Figure 2.5A). There were no significant differences observed in the body weights at 25 weeks of age (Figure 2.5B), between control mice weighing an average of 34.52 +/-2.50) g and orchiectomised (32.14 +/-2.58 g) (P = 0.1577) or orchiectomised, testosterone treated mice (34.04 +/-4.75 g) (P = 0.8680). Additionally, no significant differences were observed in the cortical bone volume, despite a slight downward trend in orchiectomised mice treated with placebo compared to sham operated and testosterone treated animals (Figure 2.5C). Cortical BMD did not differ significantly between any of the groups tested (Figure 2.5D).

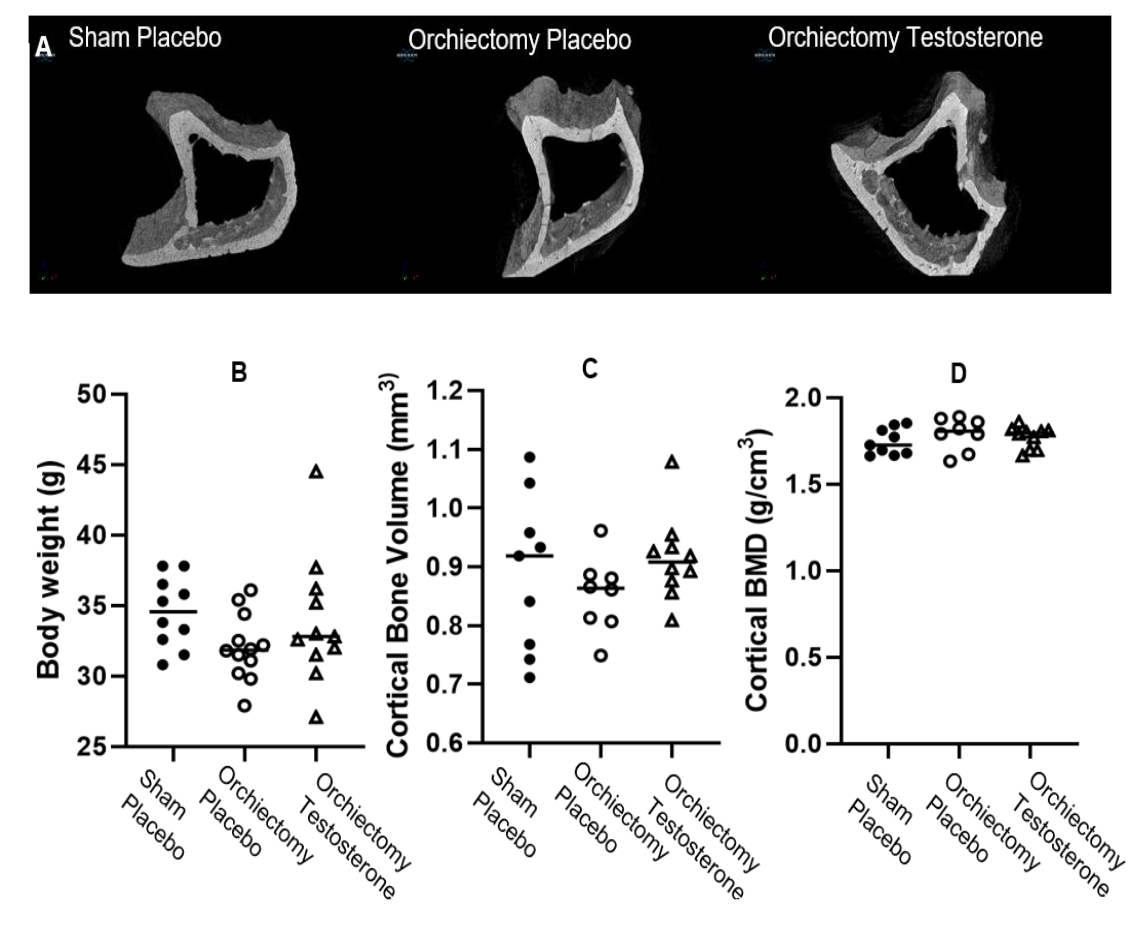


**Figure 2.5:** A) Representative images of Micro-CT generated 3D models depicting cortical regions of interest (ROIs) used for morphological analysis of cortical bone. B) Final body weights of each of the mice at the time of sacrifice (25 weeks of age). C) Cortical bone volume measurements D) Bone mineral density measurements, calibrated against hydroxyapatite rods of known density (\*P < 0.5, \*\*P <0.05, \*\*\*P <0.01, \*\*\*\*P <0.001).

#### **2.3.3.** Trabecular bone parameters:

ROIs were also manually determined and modelled for trabecular analysis, showing a marked reduction in trabecular bone within ROIs from orchiectomised mice compared to controls (Figure 2.6A). Orchiectomised mice treated with placebo demonstrated significantly increased trabecular separation, (Figure 2.6B) (P = 0.0052), and structure model index, (Figure 2.6D) (P = 0.0139) whilst tibial trabecular BV/TV% (P = 0.0008) (Figure 2.6E), and trabecular number (P < 0.0001) (Figure 2.6C), were significantly reduced compared to control mice despite no significant differences in body weight. In contrast to trabecular BV/TV% and number, average trabecular thickness was significantly increased in orchiectomised mice treated with placebo compared to sham operated controls (Figure 2.6F) (P = 0.0057). Tibial trabecular bone parameters were restored back to control levels in orchiectomised mice treated with testosterone, which showed no significant variance from the sham-operated control mice (P > 0.05) (Figure 2.4). Further investigation of trabecular thickness utilising created 3D colour-coded models of trabecular ROIs (Figure 2.7A) revealed that, alongside increased mean trabecular thickness, orchiectomised mice also had increased maximal and mode trabecular thickness compared to sham operated and testosterone treated mice (Figure 2.7B). Trabecular bone was also particularly sparse in the inner medulla of the tibial cavity in these mice, whereas the thicker struts of trabeculae were observed more frequently toward the outer cortex (Figure 2.7A).

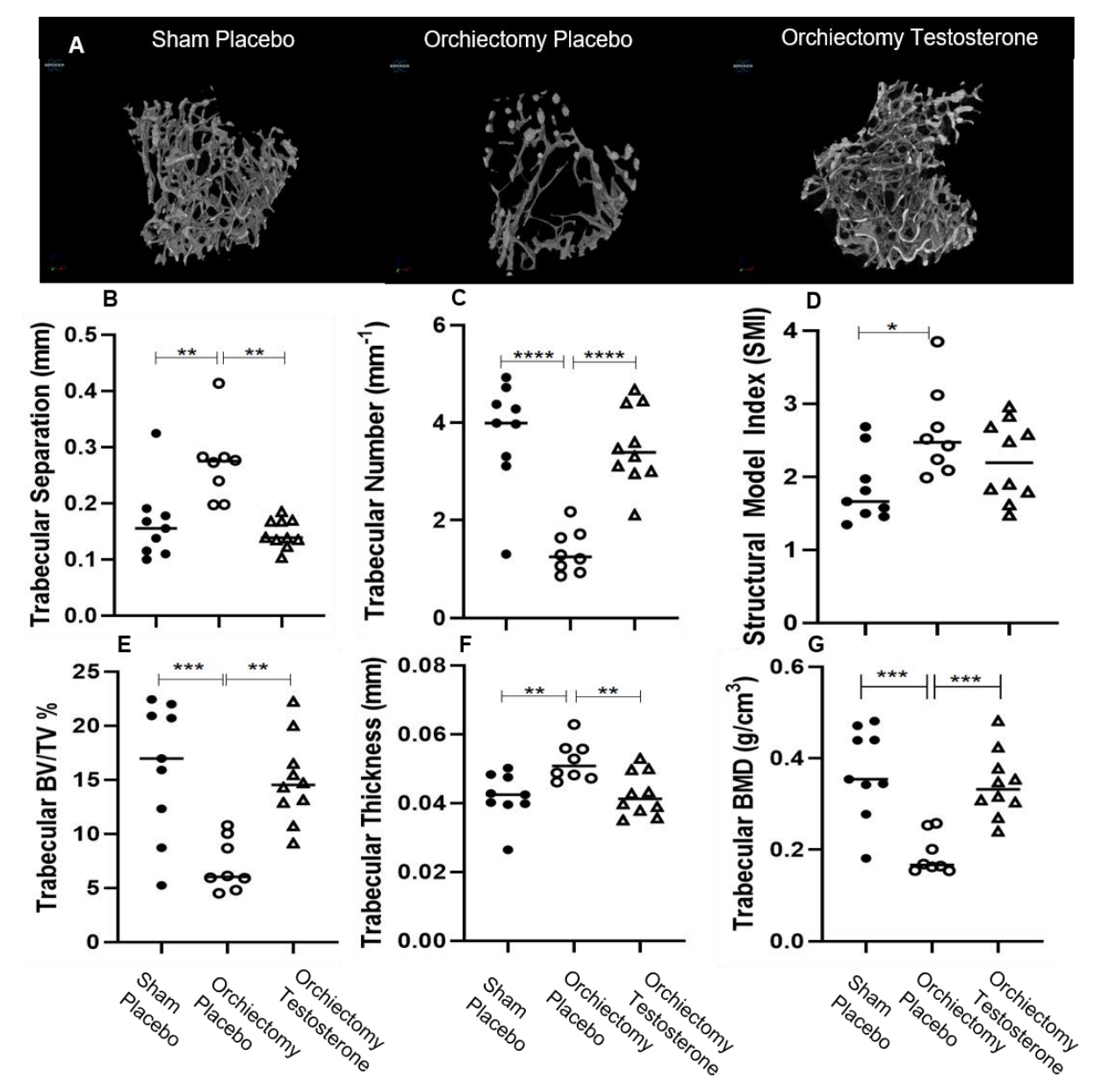


**Figure 2.6:** A) Representative examples of Micro-CT generated 3D models depicting trabecular regions of interest (ROIs) used for morphological analysis. B) Trabecular separation within trabecular ROIs (P = 0.0052) C) Trabecular number (P < 0.0001). D) Structural model index (SMI) (P = 0.0139). E) Trabecular bone volume/tissue volume percentage (BV/TV) (P = 0.0008). F) Mean thickness of trabeculae within the ROI (P = 0.0057). G) Trabecular BMD calculated against hydroxyapatite rode of known density. (\*P < 0.5, \*\*P < 0.05, \*\*\*P < 0.01, \*\*\*\*P < 0.001).

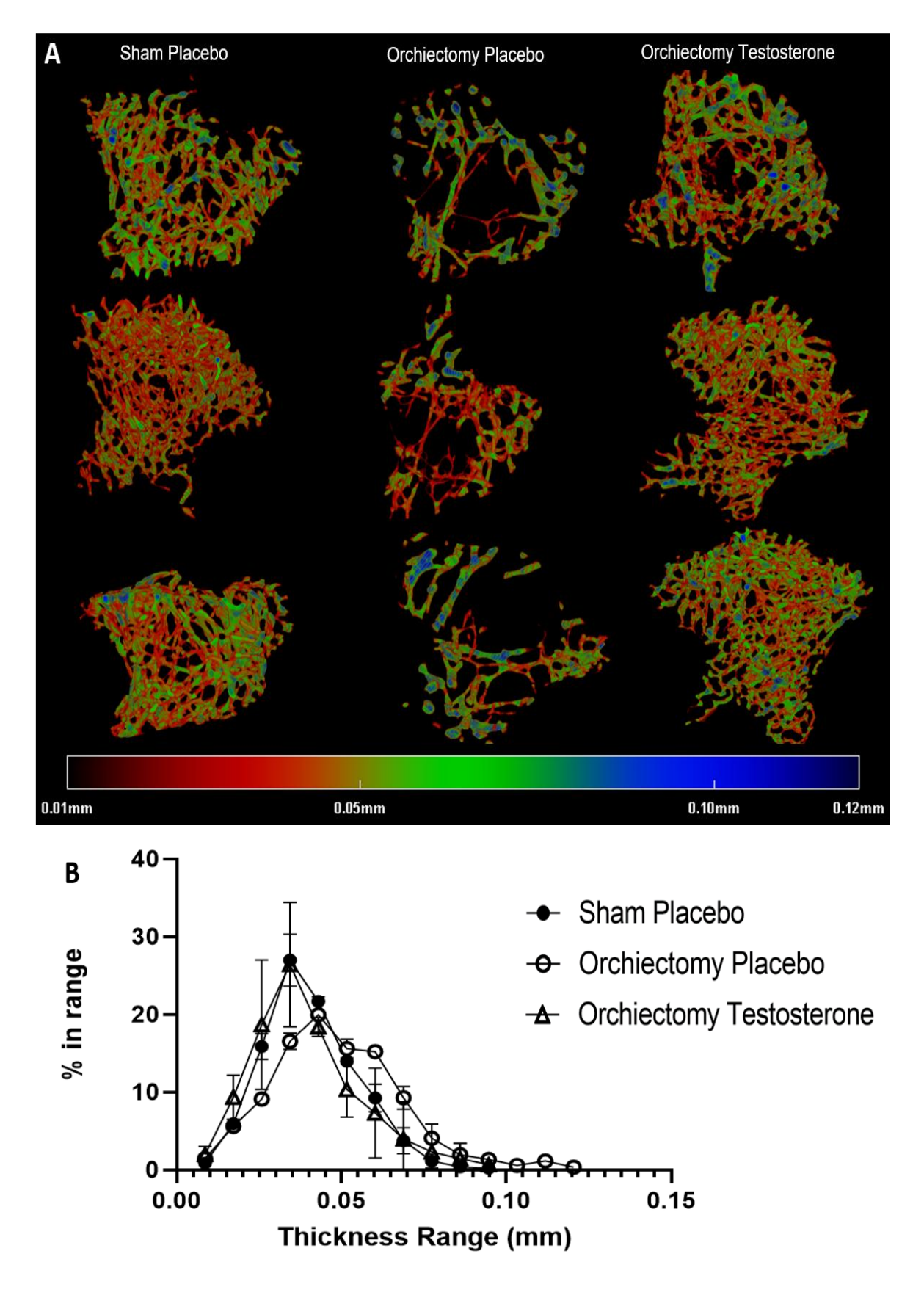


**Figure 2.7:** A) Representative examples of 3D colour-coded models of regions of interest (ROIs) used for trabecular analysis, with a scale bar ranging from low thickness (red) to high thickness (blue). B) Trabecular thickness midrange values plotted against the percentage of trabecular bone within each given thickness range.

## 2.3.4. Histological Assessment of ECM Component Distribution and Bone

# **Marrow Adiposity:**

Masson's Trichrome staining was used to visualise the distribution of ECM components in 4  $\mu$ m sections of murine tibiae, including Collagen fibres and connective tissue components (Blue) Keratin, muscle, intracellular proteins (Red) and Nuclei (Purple) (Figure 2.8).

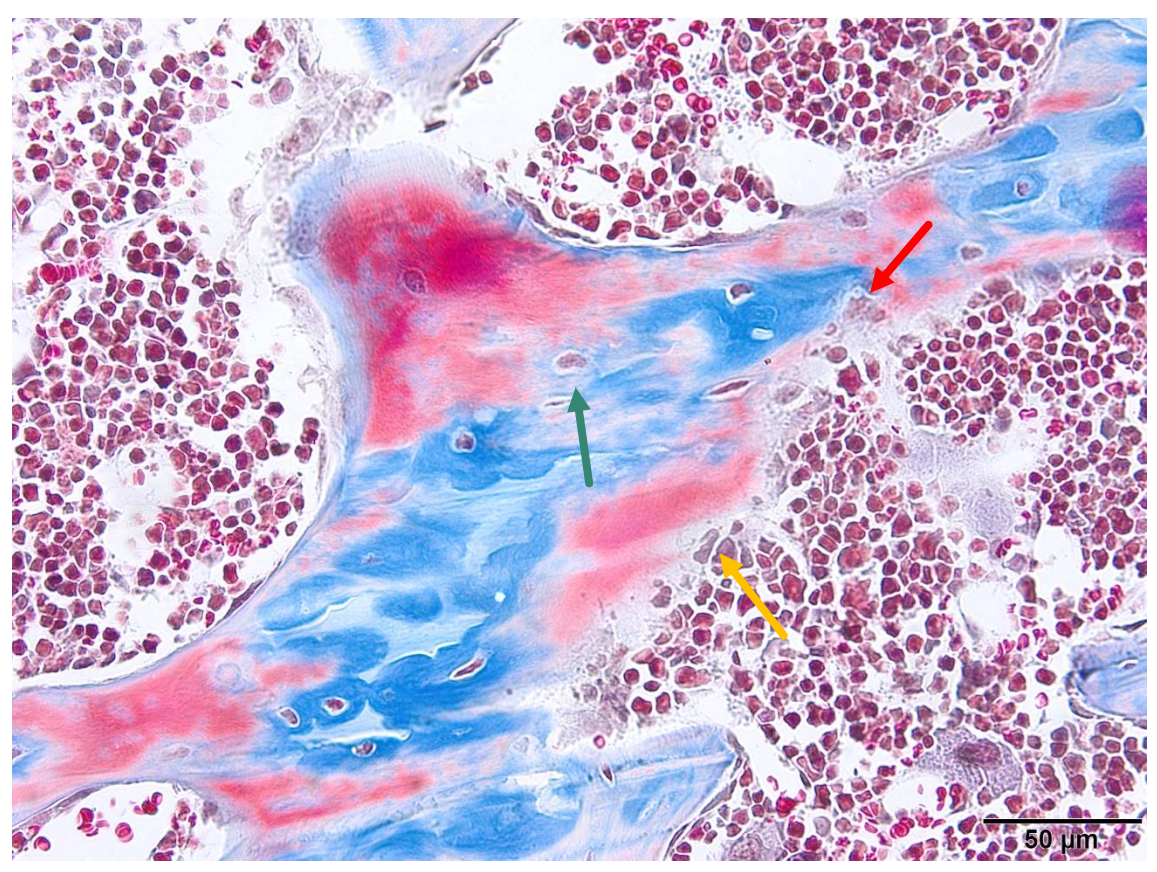


**Figure 2.8:** Representative image of trabecular bone within a cross section of murine tibia stained with Masson's trichrome, showcasing the three stains: Collagen fibres and connective tissue components (Blue) Keratin, muscle, intracellular proteins (Red) and Nuclei (Purple). Coloured arrows highlight visible osteoblasts (orange), osteocytes (green) and osteoclasts (red). Scale bar is  $50 \, \mu m$ .

Sections of murine tibiae were stained with Masson's trichrome to investigate bone morphometry and composition. Orchiectomised, placebo treated mice demonstrated markedly reduced trabecular bone compared to sham operated and testosterone treated counterparts (Figure 2.9). Additionally, there was an increased presence of empty space within the bone marrow of orchiectomised mice treated with placebo compared to sham operated and testosterone treated animals. Masson's Trichrome staining indicated slightly reduced presence of collagen (blue), and muscle fibres and/or keratin (red) compared to sham operated, placebo treated controls, although this was not quantified (Figure 2.9). Adiponectin staining was utilised as a marker of adipocytes to confirm the presence of adipocytes in the marrow, and analysis revealed a significant increase in adipocyte edged regions indicating lipid droplet area in orchiectomised, placebo treated controls compared to sham operated controls (Figure 2.9).

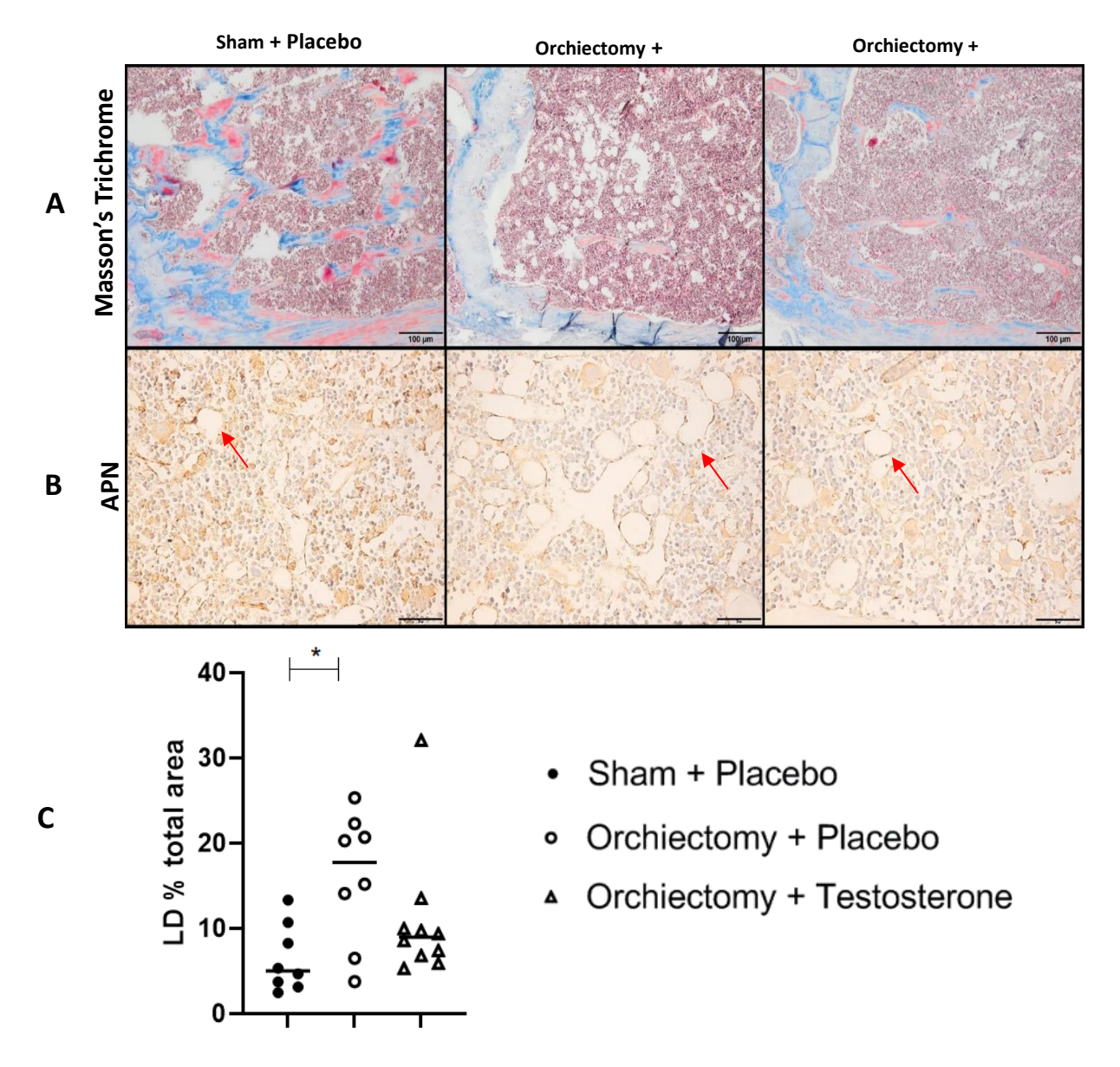


**Figure 2.9:** Representative images of cross sections of tibiae from each group stained with Masson's trichrome (A) and an immunohistochemical stain for adiponectin, with red arrows to indicate lipid droplets (B). Scale bars are 100  $\mu$ m and 50  $\mu$ m respectively. Lipid droplet (LD) percentage area (C) within randomly taken images of control (n = 8), orchiectomised (n = 8) and orchiectomised, testosterone treated (n = 10) murine tibiae bone marrow stained for adiponectin via IHC. (\*P < 0.5).

# 2.3.5. Immunohistochemical Analysis of Bone Cell Markers in Murine Tibiae:

IHC staining was performed on sections of mouse tibiae to assess the impact of testosterone depletion with or without testosterone treatment on the presence of several markers associated with bone cell differentiation and activity. RUNX2 immunopositivity was used as a measure of early osteoblast differentiation, whereas ALP immunopositivity was used to assess mature osteoblast activity and mineralisation. Results showed significantly decreased cortical RUNX2 immunopositivity (Figures 3.10D, 3.11C) (P = 0.0426) in orchiectomised mice treated with testosterone compared to sham operated control mice. No significant differences were detected in trabecular RUNX2 immunopositivity (P > 0.9999), cortical (P > 0.9999) or trabecular (P > 0.9999) ALP immunopositivity (Figures 3.10, 3.11).

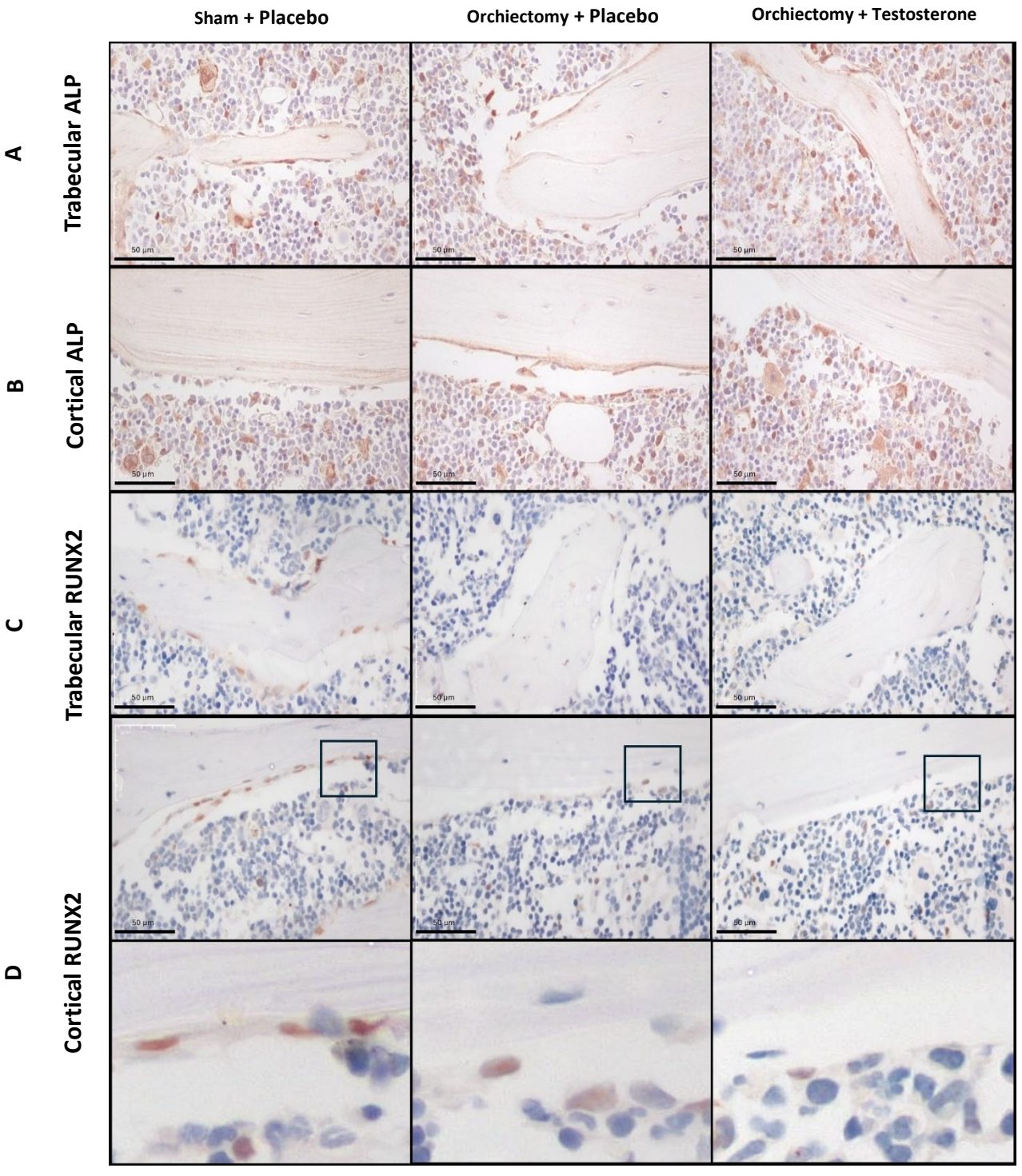


**Figure 2.10:** Representative images of alkaline phosphatase (ALP) (A, B) and RUNX2 (C, D) immunohistochemistry staining of mouse tibiae sections RUNX2 positivity along the trabecular (A, C) and endocortical (B, D) surfaces in control (n = 8), orchiectomised (n = 10), and orchiectomised, testosterone treated mice (n = 10). Scale bars are 50  $\mu$ m.

- · Sham + Placebo
- Orchiectomy + Placebo
- ▲ Orchiectomy + Testosterone

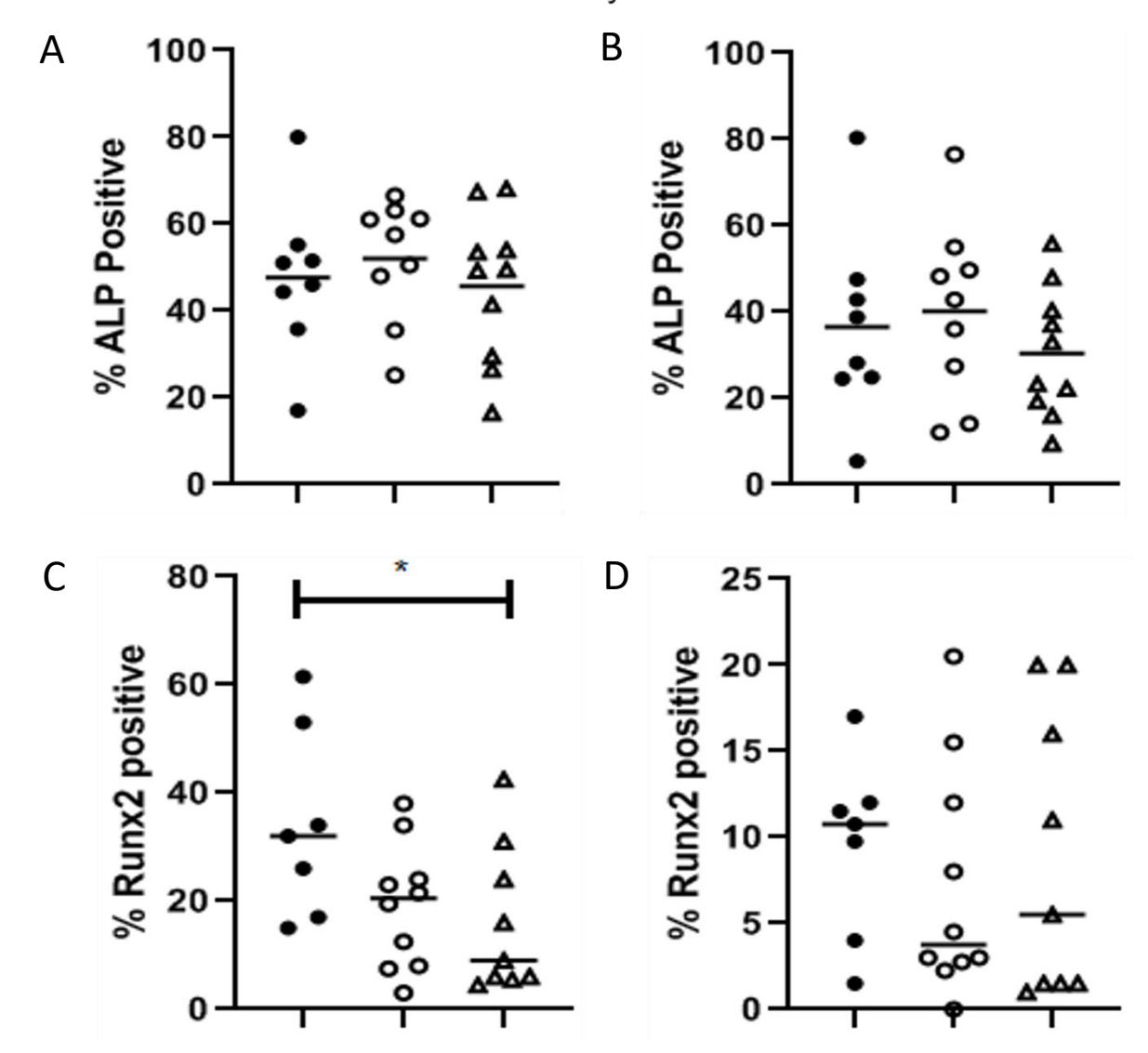


**Figure 2.11:** Percentage immunopositivity of alkaline phosphatase (ALP) (A, B) and RUNX2 (C, D) immunohistochemistry staining of mouse tibiae sections RUNX2 positivity along the trabecular (A, C) and endocortical (B, D) surfaces in control (n = 8), orchiectomised (n = 10), and orchiectomised, testosterone treated mice (n = 10). (\*P < 0.5).

Similarly, RANKL and OPG immunopositivity were assessed to investigate osteoclastogenesis, and TRAP staining used to quantify mature, active osteoclast bone resorption. There were no significant differences in OPG percentage immunopositivity (Figures 3.12, 3.13) between control and orchiectomised (P = 0.0917) or orchiectomised, testosterone treated mice (P = 0.1966). OPG immunopositivity also did not differ significantly between control and orchiectomised (P = 0.5243) or control and orchiectomised, testosterone treated (P > 0.9999) (Figure 2.13B) alone between any of the groups tested, despite a slight trend towards decreased OPG immunopositivity and increased RANKL immunopositivity in orchiectomised mice treated with placebo. Additionally, TRAP staining (Figures 3.12, 3.13) revealed no significant differences in the number of TRAP-stained osteoclasts per mm of endocortical bone surface between orchiectomised mice and control (P = 0.0091) or orchiectomised, testosterone treated (P = 0.4024).

Despite no significant differences in either OPG or RANKL immunopositivity (P = 0.3828 and P = 0.0798) respectively, the ratio of RANKL to OPG (RANKL:OPG ratio) was significantly increased in orchiectomised mice treated with placebo compared to sham operated controls (P = 0.0063), and this was reduced back to levels which were not significantly different from controls in orchiectomised mice treated with testosterone (Figures 3.12, 3.13).

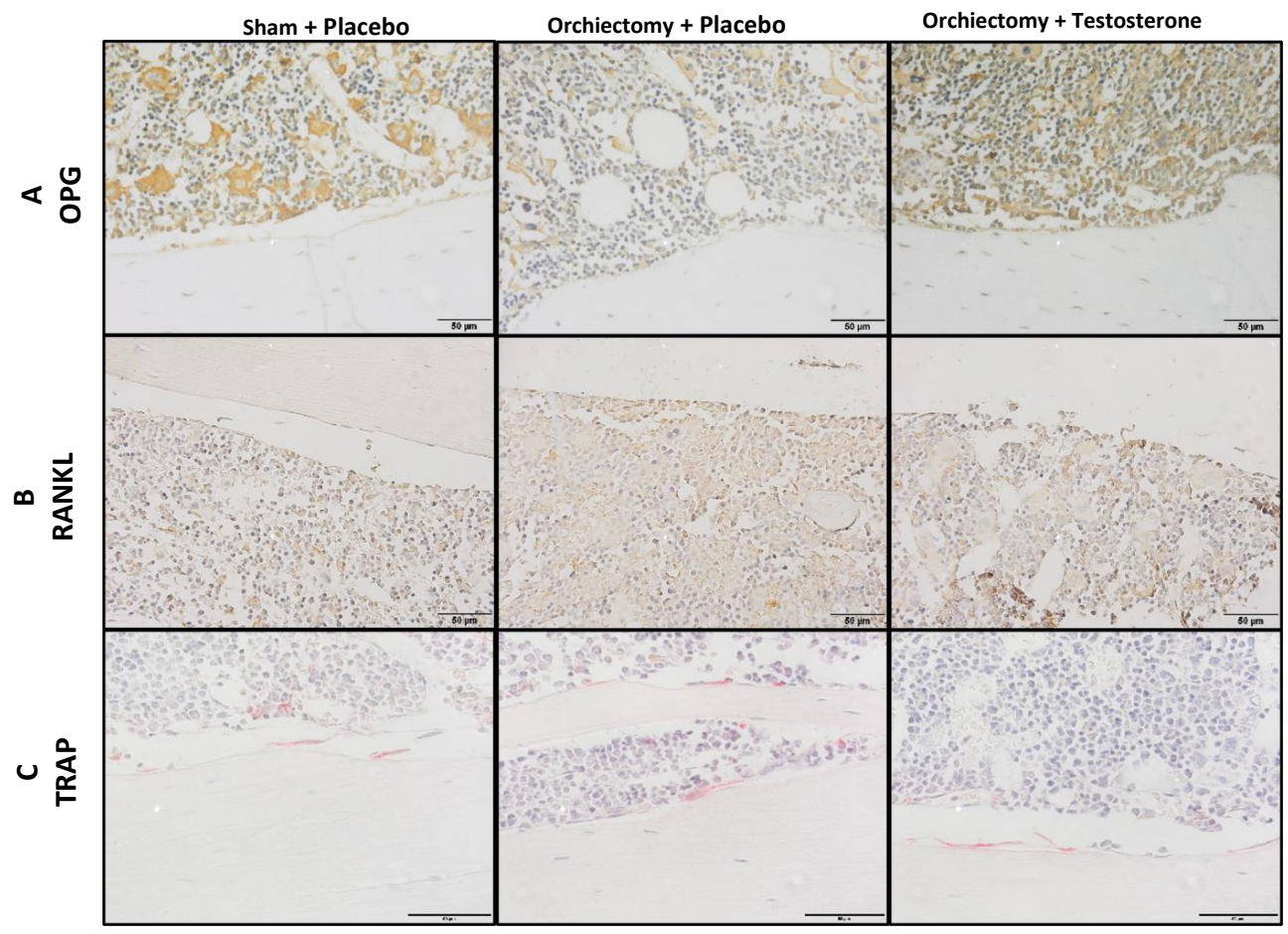


**Figure 2.12:** Representative IHC images of control (n = 8), orchiectomised (n = 10), and orchiectomised, testosterone treated mice (n = 10) osteoprotegerin (OPG) (A), RANKL (B), Adiponectin (APN) (C), and TRAP stained sections used to determine the number of TRAP positive osteoclasts per mm of bone surface (N.Oc/BS) (C). Scale bars are 50  $\mu$ m.

- Sham + Placebo
- Orchiectomy + Placebo
- Orchiectomy + Testosterone

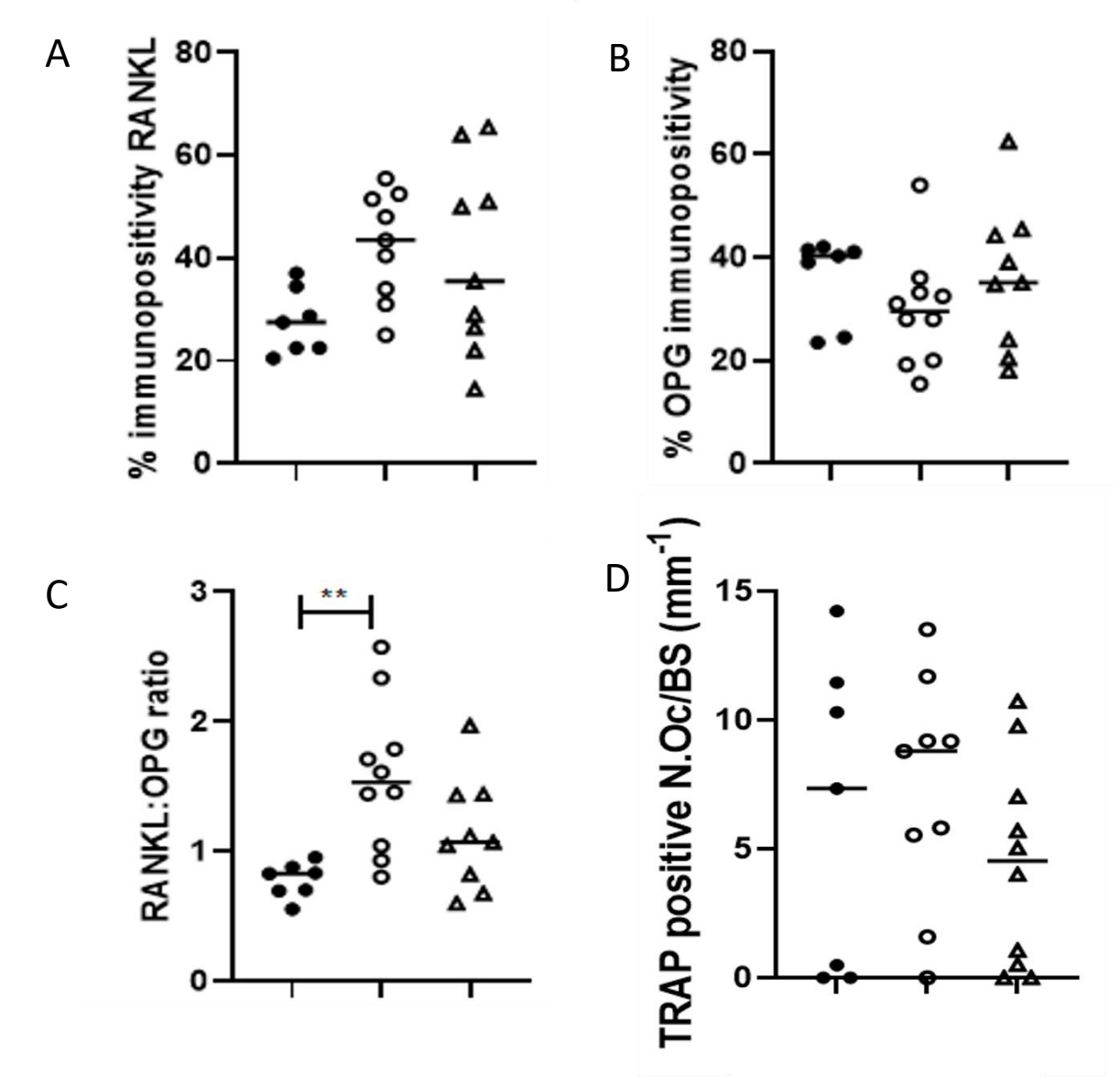


**Figure 2.13:** Percentage immunopositivity of osteoblasts along the endocortical surface of control (n = 7) orchiectomised (n = 9) and orchiectomised, testosterone treated (n = 9) stained for A) RANKL and B) OPG. C) The ratio of RANKL:OPG percentage immunopositivity from IHC stained sections of murine tibiae. Immunopositivity was originally expressed as a percentage of total count, then used to calculate a ratio. Statistical significance was determined using a Kurskal-Wallis test. \*\* = p < 0.05.

### 2.3.6. Mechanical Testing:

Mechanical testing via 3-point bend testing revealed no significant differences in maximal force (Fmax) required to induce fracture within tibiae between control and orchiectomised (P = 0.0527) or control and orchiectomised/testosterone treated mice (P = 0.5247) (Figure 2.12). Despite this, there was a slight trend towards decreased Fmax in orchiectomised, placebo treated mice compared to controls, and this effect was not wholly diminished in the orchiectomised mice treated with testosterone (Figure 2.14).

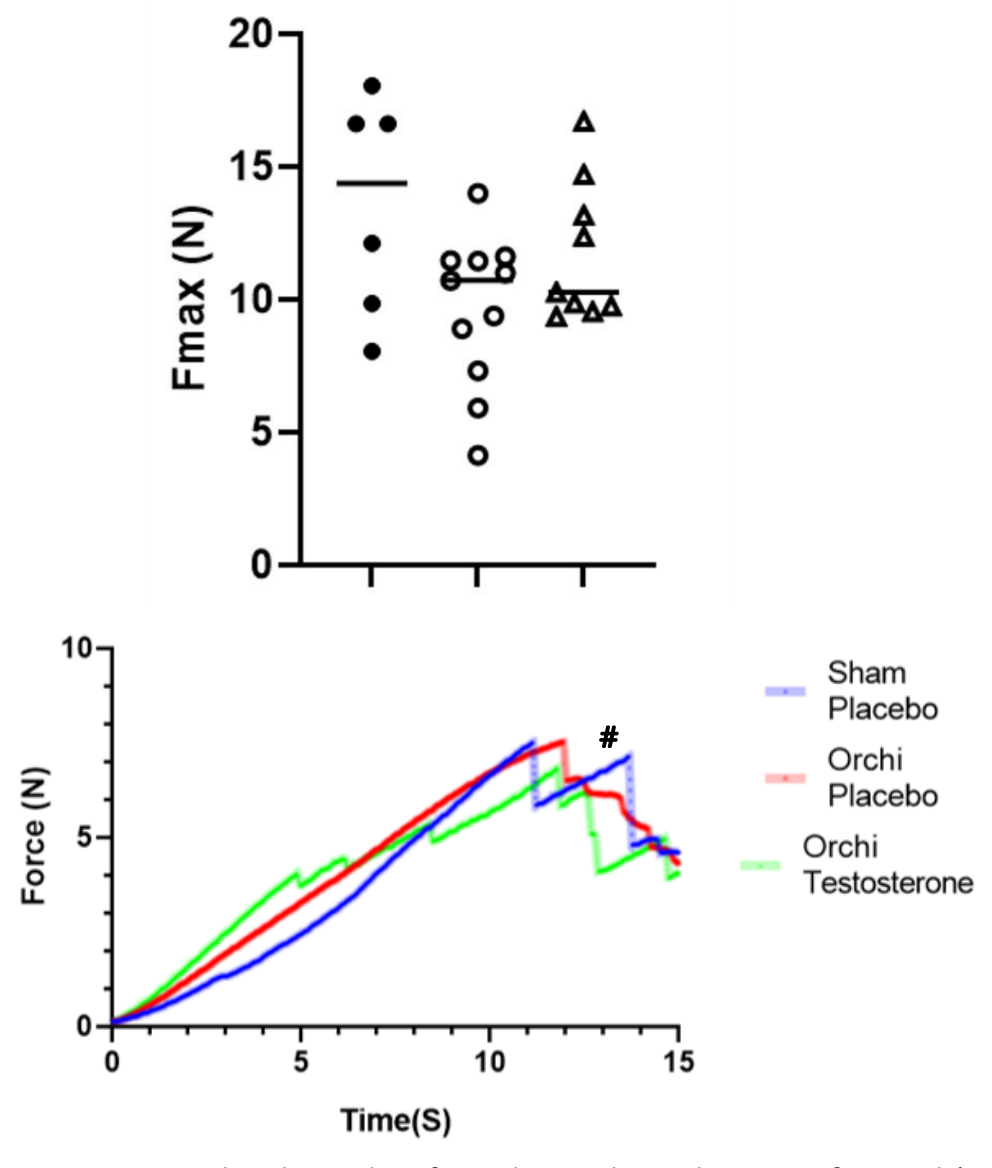


Figure 2.14: 3-point bend test data from the mechanical testing of control (n = 6), orchiectomised (n = 11) and orchiectomised, testosterone treated (n = 9). Results are displayed as A) maximal force withstood by the tibiae before breaking (Fmax) and B) force applied over time.

## 2.4. Discussion:

This study aimed to determine the effects of testosterone depletion and subsequent replacement therapy on bone microarchitecture, and influence on bone cell populations. Testosterone deficiency can lead to decreased bone volume and density parameters, particularly in the trabecular bone leading to an osteoporotic phenotype (Chin and Ima-Nirwana, 2014; Fui et al., 2014; Golds., et al., 2017). These studies often focus on femoral and vertebral bone parameters and do not employ HFD feeding regimes, inflicting an obesity-like metabolic status which in itself has been linked to decreased testosterone levels and has a significant impact upon bone health. In order to overcome this, ApoE-/- mice fed a HFD were utilised in this study to recapitulate an obese metabolic status without increased BMI. The role of ApoE in bone is not well characterised, and previous studies have reported conflicting findings. In a study of 8month old female ApoE-/- mice, it was found that the ApoE-/- mice exhibited increased vertebral and tibial trabecular bone volume (BV/TV) compared to WT C57BL/6J mice (Schilling et al., 2005). In contrast, however, a later study of 48 week-old female APOE-/- mice found that the APOE-/- mice exhibited a severe osteoporotic phenotype with drastically reduced trabecular BV/TV compared to WT controls (Noguchi et al., 2018). Due to the well-established role of mechanical load in bone remodelling (Stewart et al., 2020), there are positive correlations between muscle mass and bone mass (K. Zhu et al., 2015).

Previous studies often report morphological findings without providing context as to how these observed changes are controlled at a cellular level. It is therefore poorly understood whether the marked depletion of trabecular bone observed in testosterone deficiency is predominantly due to decreased osteoblastic differentiation and

mineralisation, or increased osteoclastic differentiation and resorption, as testosterone affects both aspects of bone remodelling (Gao et al., 2017, Payandeh, 2020, Barreiros et al., 2018). In contrast, results from this study underscore the effects of testosterone depletion upon osteoclastogenesis, contributing to loss of trabecular bone *in vivo*.

Finally, the effects of these observed morphological differences are often not investigated in conjunction with the mechanical strength of the bone, which could impact upon the prevalence of fracture risk. For this reason, three-point bend testing methods (Deckard et al., 2017) were employed to test the maximal force to failure of tibiae after  $\mu$ CT analysis. This allowed for morphological results to be placed into the wider context of resulting bone strength and could link to potential fracture risk.

# 2.4.1. The Effects of Testosterone Deficiency and Testosterone Replacement Therapy Upon Body Weights and Testosterone Levels:

Orchiectomy surgery did not result in any significant differences in body weight compared to control animals. This is an important feature of the study design, meaning that there were negligible differences in physiological mechanical load imparted upon the skeleton from body weight between the groups tested. Body weights were mostly in the range of 30 – 40 g, which is considered the normal range for mice of that age (The Jackson Laboratory, 2023), despite the high fat diet feeding regime. There was a slight trend towards decreased body weight in orchiectomised groups compared to sham operated controls, but this was not statistically significant. It is possible that, had this study spanned a significantly longer duration, there would have been a significant decrease in the body weights due to decreased lean mass of orchiectomised mice compared to controls, as demonstrated in a study of 6-month old mice (Jiang et al.,

2023). However, a different study has demonstrated increased body weight in orchiectomised mice compared to sham controls at 28 weeks of age (M. Kim and Kim, 2021). The differences seen in these studies may not yet have been established in the present study, as mice were comparatively young at 25 weeks of age.

As expected, the orchiectomy surgery significantly reduced serum testosterone levels in placebo treated mice compared to sham operated controls, in line with previous studies showing that surgical castration is a representative model for testosterone depletion (Wilhelmson et al., 2018). Testosterone therapy restored serum testosterone concentrations to near control levels, indicating that the testosterone treatment regime successfully increases serum testosterone. The dosage applied in this study largely resulted in the recapitulation of normal physiological testosterone levels, although a small number of subjects treated with testosterone exhibited serum testosterone levels slightly above the usual physiological range.

Despite the HFD-feeding, mean APOE-/- body weights did not increase beyond the average of 36.3 g for a male C57BL/6J mouse of similar age, suggesting that the feeding regime used in this study was not sufficient to induce obesity in these animals. Interestingly, however, a previous study in C57BL/6NTac mice using the same high-fat mouse chow with an *ad libitum* feeding regime noted significant weight gain and above average body weights after just 12 weeks of HFD feeding (Podrini et al., 2013). This may be due to the resistance of APOE-/- mice to HFD-induced weight gain, as suggested in previous studies (Huang et al., 2006, Schreyer et al., 2003), as VLDL-induced adipogenesis appears to be APOE-dependent (Chiba et al., 2003). No definitive conclusions can be drawn regarding HFD-induced weight gain in APOE-/- mice in this study due to the absence of wild-type and normal-diet controls. However, ApoE

deficient mice display improved glucose tolerance and insulin sensitivity compared to WT controls, exhibiting decreased adiposity despite increases in inflammation (Y. Zhang et al., 2023). In the present study, this attenuated HFD-induced weight gain is beneficial, as it allows for the assessment of the metabolic effects of obesity separate from those of increased mechanical load from body weight. One study disputing the resistance of APOE-/- mice to weight gain has shown that a higher fat content (60%kcal) HFD enriched with lard induces significant increases in body weight and an obese phenotype in male APOE-/- mice (King et al., 2010). Studies of human ApoE in obesity have reported that plasma ApoE levels are elevated in morbidly obese individuals, and that 6 months following bariatric surgery ApoE levels were barely detectable, establishing a correlation between body mass index (BMI) and plasma ApoE levels (Zvintzou et al., 2014).

# 2.4.2. The Effects of Testosterone Deficiency and Testosterone Replacement Therapy Upon Cortical and Trabecular Bone Parameters:

Several past studies have demonstrated associations between low testosterone and an osteoporotic phenotype in mice and rats (Blouin et al., 2008; Sophocleous and Idris, 2014). In the present study, much like body weight measurements, cortical bone parameters did not differ significantly between groups, despite a slight observed trend to decreased cortical bone volume in orchiectomised, placebo treated mice compared to sham operated controls. This is potentially because cortical bone is known to be less metabolically active than its trabecular counterpart (Clarke, 2008; Costa et al., 2020). Additionally, cortical bone is more responsible for load-bearing and therefore affected by mechanical loading from body weight (Turner and Iwaniec, 2016), with studies showing direct correlations between cortical bone parameters and body weights.

In keeping with results from a previous study of testosterone deficiency in rats by Ramli et al., (2012) which showed reduced trabecular bone parameters in orchiectomised mice compared to sham controls, testosterone deficiency resulted in significant decreases in trabecular bone volume and number, as well as increases in trabecular separation, thickness, and structure model index, measured by  $\mu$ CT. Trabecular BMD was also found to be depleted in orchiectomised, placebo-treated mice compared to sham controls and orchiectomised, testosterone-treated mice.

These results align with the current opinion that testosterone is vital for healthy bone growth and maintenance, and that testosterone therapy can rescue reduced bone parameters in testosterone deficient individuals back to control levels (Snyder et al., 2017). Additionally, previous research indicates that high fat diet feeding regimes decrease trabecular bone parameters but have no direct impact upon cortical bone parameters (Rinonapoli et al., 2021), and the results obtained from this study indicate that testosterone deficiency exacerbate this trend, accelerating trabecular bone loss.

The effect of testosterone deficiency upon trabecular bone depletion highlights the known relationship between testosterone deficiency and bone disorders such as osteoporosis (Golds et al., 2017). These morphological changes in trabecular bone architecture are consistent with those seen during ageing, as the age-related decline in bone volume is primarily attributed to decreases in trabecular number and subsequent increases in trabecular spacing, whereas trabecular thickness does not decrease to the same extent (Chen et al., 2013).

Interestingly, however, decreases in trabecular volume, number, and BMD were accompanied by increases in mean, mode and maximum trabecular thickness in the

orchiectomised, placebo-treated mice. As the standard measurement of trabecular thickness of the mean thickness of each strand (Bouxsein et al., 2010), it was hypothesised that the increased mean thickness seen in the orchiectomised, placebo treated mice may have been due to complete resorption of the thinner trabecular strands, thereby increasing the average thickness. The use of colour-coded 3D modelling and plotting the mid-range thickness values obtained from this analysis allowed for deeper understanding of the effects of testosterone deficiency upon trabecular thickness. As such, this analysis revealed that it was not simply the disappearance of thinner strands causing the average thickness to increase. It was instead revealed that some of the trabeculae were genuinely thicker in orchiectomised, placebo treated mice compared to other groups. This result is consistent with past evidence that trabecular thickness is maintained, and in some cases even increased throughout age-related declines in trabecular bone volume (H. Chen et al., 2013). This observation is possibly a compensatory effect for the reduced trabecular volume (Glatt et al., 2007), as the trabecular network will have still been subject to the same amount of mechanical force due to mice in each group having comparable body weights.

Studies investigating the importance of androgen signalling in bone in rodent models have presented similar findings relating to decreased trabecular bone volume and number (Yeh et al., 2019; Wu et al., 2019), but these studies often assess and present only the mean trabecular thickness values. In this study, however, more in-depth analysis of trabecular bone parameters has revealed that increases in trabecular thickness are truly present in testosterone depleted mice. This highlights a potential compensatory action upon the trabeculae to support the same amount of mechanical load from body weight with a reduced total trabecular bone volume. A study of

testosterone treatment in humans revealed a similar increase in mean trabecular thickness in the tibiae of adult men (Al Mukaddam et al., 2014) indicating that these results may also be applicable to humans.

Increases in structure model index (SMI) seen in the orchiectomised mice treated with placebo, indicates the presence of more rod-like structures. This 'plate-to-rod transition' has been associated with bone disorder progression in human studies (Felder et al., 2020), including osteoporosis in post-menopausal women (Akhter et al., 2007). Data in males is lacking, hence the importance of this study. However, the efficacy of using SMI to measure rod and plate structure in trabecular bone has previously been disputed due to the concave structure of trabeculae (Salmon et al., 2015), meaning further  $\mu$ CT analysis via different methods (such as Ellipsoid Factor) may be required to fully determine the rod/plate ratio in this study. Overall, testosterone deficiency appears to exacerbate the negative effects of HFD feeding in orchiectomised mice compared to controls, leading to increased accumulation of fat mass in the bone marrow as well as reduced trabecular bone volume.

# 2.4.3. The Effect of Testosterone Deficiency and Testosterone Treatment Upon Osteoblast Differentiation and Mineralisation:

To build upon the previously discussed morphological changes in mouse tibiae, a variety of histological and immunohistochemical techniques were utilised to assess the presence of bone turnover markers on serial sections of the tibiae used for  $\mu$ CT analysis. These include semi-quantitative immunohistochemical (IHC) detection and analysis of

markers of osteoblast differentiation and activity, such as RUNX2 (Komori, 2009) and ALP (Medio and Brandi, 2021).

Testosterone is regarded as a promoter of osteoblast differentiation from mesenchymal stem cells (Shigehara et al., 2021), activating expression of transforming growth factor- $\beta$  (TGF- $\beta$ ) in rats (Gill et al., 1998), and inducing *in vitro* expression of *Runx2* in MC3T3-E1 murine pre-osteoblasts via Erk1/2 phosphorylation (Gao et al., 2017). In this study, RUNX2 and ALP immunopositivity in mouse tibiae were used as a measure of osteoblastic differentiation and mineralisation respectively. However, apart from a decrease in RUNX2 in the cortical bone of orchiectomised mice, no other significant differences in RUNX2 or ALP positive cells were observed and thus osteoblasts did not appear to be responsible for the differences in trabecular bone architecture observed but may have contributed to cortical bone differences.

These findings directly contradict several previous murine studies (Gill, et al., 1998; Gao et al., 2017; Payandeh, 2020), which suggest that testosterone induces Runx2 expression, and therefore osteoblast differentiation and mineralisation. It is important to note, however, that this is an endpoint measure and the morphological changes in bone observed via µCT had already taken place. Therefore, there may have been significant differences between these parameters at an earlier point in the lifespan and development of the mice, which would have required sacrifice at an earlier timepoint to be observed. Similarly, mice in this study were sacrificed at 25 weeks of age; midadulthood in a mouse's lifespan. Had the study spanned a longer period, the effects of testosterone deficiency and subsequent replacement may well have been more pronounced.

Due to the shared mesenchymal lineage of adipocytes and osteoblasts, it is possible that the rise in adiposity seen in testosterone deficiency accounts for the decrease in bone mass, due to a shift in MSC differentiation towards adipogenic lineage and away from the osteogenic lineage. As well as contributing to osteoblastic differentiation of MSCs, testosterone is also known to inhibit adipocyte differentiation (Singh et al., 2005; Blouin et al., 2009; Ren et al., 2017). As such, testosterone deficiency and obesity are closely linked (Kelly and Jones, 2015), with low serum levels of testosterone being associated with increased fat mass (Fui et al., 2014).

In this study, testosterone deficient mice were seen to have significantly increased lipid droplet area in the marrow compared to controls. Alongside data showing reduced trabecular bone volume in the marrow, this suggests that the testosterone deficiency significantly impacted the fate of the mesenchymal stem cell population of the marrow, favouring adipogenic differentiation over osteogenic differentiation.

# 2.4.4. The Effect of Testosterone Deficiency and Testosterone Treatment Upon Osteoclast Differentiation and Mineralisation:

It is also possible that the observed decreases in bone parameters in testosterone deficient mice were not due to decreased osteoblast activity at all, owing instead to increased differentiation of and therefore subsequent resorption by osteoclasts. IHC for RANKL and OPG (Barreiros et al., 2018) alongside histological staining for TRAP (Ghayor et al., 2011) were employed to assess osteoclast differentiation and activity, respectively.

RANKL is secreted from osteoblasts in order to instigate osteoclast differentiation, and binds to RANK receptors on the surface of haematopoietic stem cells to induce

differentiation into mature osteoclasts (Boyce and Xing; 2008, Udagawa et al., 2020). This is ultimately balanced by the secretion of OPG, also from osteoblasts, which is a soluble decoy receptor to RANKL (Infante et al., 2019) Thus, the ratio of RANKL to OPG (RANKL:OPG ratio) is often used clinically and experimentally as a determinant of bone mass and skeletal integrity, (Boyce and Xing, 2008) owing to a direct relationship between RANKL:OPG ratio and osteoclastogenesis. Orchiectomy surgery has previously been shown to decrease OPG expression in rats (Shuid et al., 2012) and, contrastingly, testosterone treatment has also been shown to inhibit OPG mRNA secretion from osteoblastic cells (Hadjidakis et al., 2007) and serum OPG in elderly men (Khosla et al., 2002).

Upon investigation of RANKL and OPG immunopositivity in mouse tibiae sections, it was determined that there were no significant differences between the immunopositivity of either of these markers individually. However, when expressed as a ratio of RANKL:OPG, it was determined that RANKL:OPG ratio was significantly increased in orchiectomised mice treated with placebo compared to sham operated controls. This finding indicates that testosterone deficiency reduces trabecular bone volume via increasing osteoclastogenesis through the RANKL:OPG pathway, and therefore subsequent bone resorption increases. This alteration in RANKL:OPG ratio was attenuated via the addition of testosterone treatment, indicating that the adverse effects of testosterone depletion upon osteoclastogenesis are reversible. RANKL:OPG ratio is typically assessed in serum (Bagan et al., 2017), as opposed to via immunohistochemistry, but unfortunately this could not be performed due to prioritisation of serum usage for other studies.

Despite the observed differences in RANKL:OPG ratio, TRAP staining and subsequent histomorphometric analysis did not reveal any statistically significant differences in the

number of TRAP positive osteoclasts lining the perimeter of cortical bone between any of the groups tested. There was, however, a trend towards slightly increased osteoclast number in orchiectomised mice treated with testosterone. This is perhaps partially because osteoclast number could only be counted on the endocortical surface, and cortical bone parameters did not significantly differ between groups. Due to the observed significant decreases in trabecular BV/TV, there was insufficient trabeculae present in the sections of orchiectomised, placebo treated mice to provide a reliable assessment of osteoclast number on the surface of trabeculae. Additionally, as these are endpoint measures it would have been insightful to assess an earlier timepoint in the mouse's development, as large amounts of the trabecular bone had already been resorbed at the endpoint of the present study. A previous study utilising C57 mice has demonstrated that orchiectomised mice display reduced femoral trabecular bone in comparison to sham operated controls just 8 weeks after surgery (J. Sun et al., 2022). In the same study, serum TRAP levels were significantly increased in orchiectomised mice, indicating that an earlier measurement or different methodology in the present study may have provided more valuable insights.

# 2.4.5. The Effect of Testosterone Deficiency and Testosterone Treatment Upon Bone Mechanical Strength:

Osteoporosis is often defined by the occurrence of fragility fractures in men, and has been closely linked to hypogonadism (Golds et al., 2017). Testosterone deficiency is often considered a risk factor for osteoporotic fracture, owing in part to decreased BMD. (Shigehara et al., 2021). Despite significantly decreased trabecular bone parameters and a slight trend towards decreased cortical bone volume, the mechanical strength of tibiae

from orchiectomised, placebo treated mice tested via 3-point bend test did not differ significantly between groups. This result indicates that there was no significant increase in mechanical strength in the tibiae of testosterone deficient mice compared to controls. This is likely due to the fact that cortical bone is a more significant contributor to overall mechanical strength than trabecular bone (Oksztulska-Kolanek et al., 2016). Additionally, cortical BMD did not differ significantly between groups in the present study and was highest on average in the orchiectomised mice. Despite this, average maximal force to fracture was lowest in orchiectomised mice in the present study. One possible explanation for this is the observed but unquantified decrease in tibial bone collagen content in orchiectomised mice via Masson's Trichrome staining, as collagen provides flexibility and helps to absorb impact, thereby mitigating fracture risk (Viguet-Carrin et al., 2006). Finally, in keeping with results in humans (Snyder et al., 2024b) TRT did not increase tibial mechanical strength, and in fact tibiae from mice treated with testosterone displayed the lowest average maximal force to fracture. This could indicate that testosterone therapy may not improve fracture risk, although further studies assessing more sites and measures of fracture risk, with sufficient sample size and duration to provide adequate statistical power are needed to clarify this.

Most studies in the field focus on hip and vertebral fractures, and this study instead investigated only tibiae. Whilst ankle fractures are among the top 5 most common fracture sites in men (Bergh et al., 2020), the three point bend testing model applied to tibiae in this study is not wholly representative of physiology and fracture risk, and is instead a measure of raw mechanical strength of the bone. Similarly, it is possible that more insights could have been unearthed utilising other techniques, such as finite element analysis (Meslier and Shefelbine, 2023), or micro-indentation (Arnold et al.,

2017), or even assessing other bone regions. For example, a micro-indentation study of murine vertebrae in orchiectomised mice revealed significantly decreased vertebral Vicker's Hardness and elastic modulus in orchiectomised mice compared to sham controls (Teng et al., 2023). To conclude, the effects of testosterone replacement therapy upon bone mechanical strength are unclear from the results of this study

#### 2.4.6. Conclusion:

In conclusion, the results obtained in this study indicate that orchiectomy-induced testosterone deficiency significantly reduces trabecular bone parameters in APOE<sup>-/-</sup> mice, and that TRTnormalises these parameters back to control levels. The exact mechanism by which these morphological changes take place remains unclear, although results indicate increased osteoclastogenesis and adipocyte differentiation occur at the expense of osteoblast differentiation in testosterone deficient mice. However, these alterations in bone microarchitecture and cell behaviour did not significantly alter the mechanical properties of murine tibiae, possibly owing to the unaltered cortical parameters.

The effects of testosterone deprivation upon MSC differentiation are comparable to those of ageing, in which the cells exhibit reduced ALP activity, ECM mineralisation, and expression of osteogenesis related genes (Chen et al., 2021) such as *RUNX2*. This establishes a role for the age-related decline of testosterone (Stanworth and Jones, 2008), like that of oestrogen deficiency in post-menopausal women, a well-studied and accepted contributor to bone loss and osteoporosis (Ji and Yu, 2015; Lupsa and Ubsigna, 2015). These findings highlight the detrimental effects of testosterone deficiency upon bone health, independent of changes in body weight, as well as the potential benefits

of testosterone therapy for the treatment of bone loss due to testosterone deficiency in men. However, these findings may not translate to improvements in fracture risk as a result of TRT in humans, and further studies are required to explore this relationship further.

3. Chapter 3: Impact of Leptin Deficiency on Male Tibia and Vertebral Body 3D Bone Architecture Independent of Changes in Body Weight:

This chapter is based on a manuscript entitled "Impact of leptin deficiency on male tibia and vertebral body 3D bone architecture independent of changes in body weight ", published in Physiological Reports (Williamson et al., 2023). Contributions: Micro-CT, histology, IHC and mechanical testing data collection and analysis, manuscript writing.

## 3.1. Introduction:

Leptin, a potent anorexigenic adipokine secreted by adipocytes, plays an important role in cardiometabolic regulation (Belin de Chantemèle et al., 2009; De Jonghe et al., 2012; do Carmo et al., 2011). Leptin has also been shown to play a role in bone remodelling through the central nervous system (CNS) as well as by its peripheral actions, including direct effects on bone cells (Ducy et al., 2000; Takeda et al., 2002; Turner et al., 2013; Yue et al., 2016). However, it is still controversial whether leptin primarily increases or decreases bone volume and mineral density via peripheral or CNS actions (Ducy et al., 2000; Hamrick et al., 2005; Karsenty and Khosla, 2022; Turner et al., 2013; Yue et al., 2016). Confounding factors that may contribute to this uncertainty include a lack of control for body weight and leptin sensitivity (Bahceci et al., 1999; Bartell et al., 2011; Coleman, 1973; Duan et al., 2007; Grethen et al., 2012). Furthermore, recent advances in 3-dimensional (3D) micro-computed tomography ( $\mu$ CT) image analysis have not been utilised in previous studies and yet they may reveal more detailed assessment of bone microarchitecture in particular potential regional differences.

Leptin's CNS actions on bone remodelling have been investigated using intracerebroventricular (ICV) leptin infusion in leptin deficient *Ob/Ob* mice and have provided contrasting results, with some studies demonstrating a decrease (Ducy et al., 2000) while others show an increase in trabecular bone volume (Bartell et al., 2011; Turner et al., 2013), after leptin infusion. Differences in the dose of leptin administered in these studies may account for some of the variability in bone morphology observed, although each study did observe a reduction in body weight irrespective of leptin dose. Therefore, global leptin deficiency via the *Ob/Ob* mouse model without the

reintroduction of leptin, controlling for body weight, was selected to reduce these confounding factors in the present study.

Iwaniec et al., (2009) evaluated the effect of hypothalamic leptin gene therapy on bone architecture and reported that increased body mass was associated with increased cortical bone volume, independent of leptin signalling. However, deletion of leptin receptors on skeletal stem cells increased trabecular bone volume/tissue volume (BV/TV%) suggesting that leptin has non-CNS actions that reduce bone volume (Yue et al., 2016). In contrast, peripheral leptin delivery in *Ob/Ob* mice for 2 weeks increased the bone forming surface of cortical endosteum as well as trabecular osteoblast surface and density compared to vehicle treated *Ob/Ob* mice (Hamrick et al., 2005). Transfer of bone marrow (BM) from leptin-receptor deficient mice to irradiated wild type (WT) controls, also resulted in reduced bone formation rate, compared to WT controls or irradiated WT controls transferred with BM from WT controls (Turner et al., 2013). Many of these apparent inconsistencies may be related to leptin-mediated changes in body weight which can also influence bone remodelling. Furthermore, most research into the effects of leptin on bone have been completed in murine models. Epidemiological studies on the association of leptin with bone architecture are unclear. The relationship between serum leptin levels and BMD in children aged 11 years old were inconclusive (Kouda et al., 2019). Results often show positive, inverse or no association between circulating leptin and bone parameters.

Body weight alters bone morphology due to compressive and tensile forces applied to the bone via gravity and skeletal muscle contraction (Greene and Naughton, 2006; Klein-Nulend et al., 2012). An increase in compression and tensile forces normally leads to increase bone formation, resulting in increased bone volume and/or density (Ducher et

al., 2005; Uto et al., 2017; Zhang et al., 2008). However, the impact of obesity and the loading effects of increased body mass index (BMI)/adiposity or eating a high fat diet (HFD) on bone growth and turnover have also proven controversial. Increased BMI has been described as beneficial to bone volume/density and fracture prevention (C De Laet et al., 2005; Dominic et al., 2020; Palermo et al., 2016). Conversely, Xheng et al., (2021), and Driessler et al., (2010) demonstrated that obesity negatively impacted bone, with HFD and central obesity uncoupling bone resorption and formation, leading to increased fracture risk and osteoporosis (Driessler and Baldock, 2010; Zheng et al., 2021). Nevertheless, weight-pairing in mice has demonstrated that obesity may attenuate the morphological changes in femur and lumbar vertebral bone associated with leptin deficiency (Turner et al., 2014).

Most papers reporting on changes in bone architecture over the past decade have conformed to the guidance proposed by Bouxsein et al., in 2010. However, advances in image analysis of  $\mu$ CT data show reporting only mean values may mask underlying regional specific differences in morphology, specifically trabecular thickness between experimental groups. To identify these differences and the effect of leptin deficiency alone on tibia and vertebral bone, this study controlled for changes in body weight by weight-pairing lean and obese *Ob/Ob* to lean and obese C57 controls.

The hypothesis of this body of research was that leptin signalling alters bone turnover independent of concomitant changes in body weight associated with obesity and increased leptin levels.

#### The aims of this study were:

 To establish the impact of leptin signalling independent of body weight upon bone microarchitecture.

- 2. To investigate the cellular mechanisms underpinning leptin-related alterations in bone morphology.
- 3. To assess the independent effects of leptin signalling-induced changes in bone morphology upon the mechanical strength of murine tibiae.

## 3.2. Materials and Methods:

#### 3.2.1. Experimental Design:

The multifaceted effects of obesity on bone health result in difficulties separating the independent effects of leptin signalling and mechanical load from body weight upon bone. This study utilised leptin deficient *Ob/Ob* mice, weight paired to either lean or obese C57 counterparts to isolate the effects of leptin signalling and mechanical load *in vivo*. *Ob/Ob* mice in both groups had their access to food restricted in order to tightly control calorific intake, allowing for weight pairing to C57 counterparts fed either a ND or a HFD from 6±2 weeks to 24±2 weeks of age. Food intake and Body composition parameters were measured throughout the study to confirm the success of weightpairing. This study was performed in tandem with another study utilising waste tissue from the same animals at the University of Mississippi Medical Center in line with NC3Rs, and all timepoints were selected accordingly.

Tibiae and vertebrae were harvested for analysis at  $24\pm2$  weeks of age, and morphological changes in the cortical and trabecular regions were quantified separately using  $\mu$ CT with post-imaging processing software. The mechanisms underpinning observed morphological changes were then investigated using histological and immunohistochemical techniques, including the assessment of markers of osteoblastic differentiation and activity as well as osteoclastic differentiation and activity. Finally, the mechanical properties of the tibiae were assessed via 3-point-bend testing to assess the impact of alterations in bone morphology upon bone mechanical strength.

#### **3.2.2.** Ethical Approval:

This study was approved by the Institutional Animal Care and Use Committee (IACUC) of the University of Mississippi Medical Center, Jackson, MS (Approval Number 1154C/1154D). All animal experiments followed the Guide for the Care and Use of Laboratory Animals (2011 Eighth Edition, National Research Council) for the welfare of laboratory animals. All necessary procedures were implemented to minimize the pain and suffering of animals. This included the avoidance of unnecessarily harsh food restriction regimes using high fat diet, instead feeding obese *Ob/Ob* mice a standard chow diet. No animals, samples or data were excluded from the reporting.

#### 3.2.3. Mice and Treatments:

Male C57 (n=8) control mice and male leptin deficient *Ob/Ob* (n=8) mice on the C57BL/6J background were purchased from Jackson Laboratories at 6±2 weeks of age and placed into 4 groups: lean C57; lean *Ob/Ob*-WP; obese C57; obese *Ob/Ob*-WP. Mice were placed in individual cages in a 12-h dark (6 PM to 6 AM) and light (6 AM to 6 PM) cycle. Mice were given free access to water throughout the study. Leptin deficient lean *Ob/Ob* mice were fed control diet (CD, Harlan Teklad/ENVIGO, CA 8640, energy 3.0 kcal/g, percent kcal from fat (17%), protein (29%), carbohydrate (54%) and food restricted from 6±2 weeks to 24±2 weeks of age to match their weight (weight-pair WP) with the weight of C57BL/6 (C57) control mice fed CD ad libitum. Leptin deficient obese *Ob/Ob* mice were fed CD and food intake was controlled from 6±2 weeks to 24±2 weeks of age to match their weight with the weight of C57 control mice HFD ad libitum (HFD, Harlan Teklad/ENVIGO, TD-0881, energy 4.7 kcal/g, % kcal from fat (44.6%), protein (14.7%),

carbohydrate (40.7%). *Ob/Ob* mice body weights were matched to within 5% of C57 lean and obese controls. Food intake and body weight were measured twice a week along with weekly magnetic resonance imaging (4-in-1 EchoMRI-900TM; Echo Medical System, Houston, TX) to determine body composition. Mice did not require anaesthesia during EchoMRI. No animals, samples or data were excluded from the reporting. This work was performed at Mississippi Center for Obesity Research, University of Mississippi Medical Center by Alexandre da Silva, Jussara M. do Carmo, and Sydney Moak.

### **3.2.4.** Food Restriction:

Data from literature shows *Ob/Ob* mice eat approximately 6g chow per day, corresponding to a kcal consumption between 18-28 kcal per day depending on constituents of the diet (Skowronski et al., 2017). Consistent weight-pairing to C57 controls required the *Ob/Ob* mice to have their daily food intake restricted to approximately 8 kcal per day (Figure 1B). This translated to either 1.7 g/day on the high fat chow (4.7 kcal/g) or 2.6 g/day on the regular chow diet (3 kcal/g). To feed these animals the high fat chow would constitute a food restriction of over 70% for 24 weeks. As such, it was decided on animal welfare grounds that regular chow would be used to avoid undue stress over the extended period of the study. The body composition data show the comparisons in body fat mass and lean mass between the groups. This work was performed at Mississippi Center for Obesity Research, University of Mississippi Medical Center by Alexandre da Silva, Jussara M. do Carmo, and Sydney Moak.

### 3.2.5. Tissue Harvest:

At 24±2 weeks of age, mice were euthanized by excess isoflurane (100%) followed by exsanguination. Both tibiae and L3 lumbar vertebrae were fixed in 4% paraformaldehyde with sodium dihydrogen orthophosphate dehydrate and disodium hydrogen orthophosphate dehydrate for 48 hours before being placed in 70 % EtOH and shipped to Sheffield Hallam University. This work was performed at Mississippi Center for Obesity Research, University of Mississippi Medical Center by Alexandre da Silva, Jussara M. do Carmo, and Sydney Moak.

### 3.2.6. Micro-CT Imaging:

Samples were removed from 70 % EtOH, wrapped loosely in cellophane, mounted into a plastic cylinder and scanned on a Bruker Skyscan 1272. Scanning parameters include 50 kV X-ray voltage,  $200 \mu\text{A}$  X-ray current, 0.5 mm aluminium filter;  $4.3 - 7 \mu\text{m}$  voxel size with  $180^\circ$  tomographic rotation and a  $0.7^\circ$  step rotation. Reconstruction was performed using NRecon software (Bruker Skyscan) and included beam hardening correction of 20 % and post-alignment optimisation. Bone mineral density (BMD) was quantified from 2 mm standard calcium hydroxyapatite (CaHA) calibration rods (Bruker Skyscan).

Tibia samples were analysed in two distinct regions. Firstly, to normalize analysis of cortical bone, measurements were taken exactly 1 mm off-set from the bridge break of the growth plate, progressing distally for 1 mm. Secondly, trabecular bone was normalized by measuring 0.2 mm off-set from the bridge break of the growth plate and progressing distally for 1 mm. Lumbar vertebrae (L3) sample analysis took place from the first section of distal trabeculae with no primary spongiosa and progressed

proximally for 2 mm. For each animal both tibiae were analysed and the single mean value from both measurements were reported.

### 3.2.7. Image Post-processing:

Post reconstruction analyses of  $\mu$ CT images were processed in serial slices using CTAn (Bruker Skyscan) software. A normalized region of interest (ROI) was defined by freehand drawing for both cortical and trabecular bone and used during analysis of each tibia and vertebrae throughout the study. Thresholding for cortical BMD was consistent within groups, despeckling white spots was applied to each ROI before 3D analysis was performed.

## **3.2.8.** Quantitative Morphometry:

Quantitative assessments of bone morphometry were performed as previously described (2.2.10)

### 3.2.9. 3D Colour Coded Bone Thickness Analysis:

Regional trabecular bone thicknesses were analysed qualitatively using 3D colour coding. Trabecular mid-range thickness values were generated from regions of interest after thresholding and despeckle processing, as outlined above. Contrast stretching in 3D space filtering was applied to the colour-coded datasets, before being modelled in CTvox (Bruker Skyscan). Regional differences in trabecular bone thickness were analysed qualitatively using a standardised mid-range transfer function set from minimum 0.00 mm to maximum 0.12 mm. The outer medulla of the trabeculae was partitioned by using

the erosion function within CTAn to segregate a 200  $\mu$ m diameter from the outer most edge of the ROI around the circumference of the ROI. The remaining trabecula inside the original ROI excluding the outer medulla was calculated as the inner core.

### 3.2.10. 3D Colour Coded Bone Density Analysis:

Regional specific 3D colour coded bone density maps were generated in CTVox from original CTAn ROI data sets. Regional differences in cortical bone density were analysed qualitatively using a standardised mid-range transfer function and plotted against the limit values of attenuation ranging from minimum 0.0 g/cm³ to maximum 2.6 g/cm³.

### **3.2.11.** Tissue Preparation:

Left tibiae were decalcified in 20% EDTA for 2 weeks at 4°C on a rocker then embedded in paraffin using standard procedures. Four-micron sections were cut using a microtome (Leica, Germany) and left to dry at 37°C for 2 weeks prior to immunohistochemistry and histological staining procedures. Right tibiae were left unprocessed for mechanical testing and stored in 70% IMS at 4°C.

### 3.2.12. Haematoxylin and Eosin Staining:

Haematoxylin and Eosin staining was performed as previously described (2.2.13)

### 3.2.13. Histological Assessment of murine tibiae and L3 vertebrae:

Masson's Trichrome staining was performed as previously described in section 2.2.14 to investigate the composition of bone and bone marrow sections, allowing for the

visualisation of collagen and other ECM component distribution throughout the sections. Similarly, TRAP staining was performed also as described to assess the presence of active, resorbing osteoclasts along the endocortical surface of bone. Tartrate Resistant Acid Phosphatase (TRAP) stained microscope slides were assessed as previously described.

### 3.2.14. Immunohistochemistry:

Immunohistochemistry staining was performed as previously described in Chapter 2 to investigate osteoblast differentiation and activity via RUNX2 and ALP, and osteoclast differentiation via RANKL and OPG immunopositivity in osteoblasts along the endocortical surfaces of tibiae and vertebrae sections.

### 3.2.15. Image Capture and Quantification of IHC:

Mounted, dry microscope slides were assessed as previously described in Chapter 2.

### 3.2.16. Three-point Bending Biomechanical Test:

The mechanical strength of non-decalcified right tibiae was assessed via a three-point bend test as previously described in Chapter 2.

### **3.2.17.** Statistical Analysis:

Data are presented as mean  $\pm$  standard deviation or individual data points and median values. Statistics software GraphPad Prism v8.1.1 was used to test for normality using Shapiro Wilk normality test. Data were subsequently analysed using one-way analysis of

variance (ANOVA) with post-hoc Tukey test or Kruskal-Wallis with Dunn's Multiple Comparison for 3 groups or more. Student T-Test and Mann Whitney for comparison of 2 groups. A P value of  $\leq$ 0.05 was considered statistically significant. Type II Error was calculated using IBM SPSS Statistics v.26, whereby the average observed Power<sup>b</sup> was calculated as 0.88.

### 3.3. Results:

### 3.3.1. Leptin Deficiency Increased Fat Mass Independently of Body Weight:

Food restriction of lean Ob/Ob mice resulted in similar body weights at 24±2 weeks of age compared to lean C57 mice fed CD, 27.55±1.63g vs 28.58±0.87g (P = 0.3100). Body weight gain was evenly matched throughout the study duration (P > 0.9999) (Figure 2.1A). Similarly, obese Ob/Ob fed CD and obese C57 fed HFD had similar body weights at 24±2 weeks of age, 40.00±0.55 g vs. 42.38±4.08 g (P = 0.2927). Body weight gain was evenly matched throughout the study duration (P > 0.9999), respectively. The obese C57 and obese Ob/Ob groups had significantly increased body weights at 24±2 weeks of age compared to lean equivalent genotypes, +32.5% and +31.1% respectively (P = <0.0001), (Figure 3.1A).

Weight-pairing of lean Ob/Ob with lean C57 mice was maintained via food restriction as shown by a significant reduction of 18% in average daily Kcal intake in the Ob/Ob group (P=0.0318), (Figure 3.1B). Obese Ob/Ob consumed on average 34% less Kcal per day to maintain body weight of weight matched obese C57 controls (P=0.0005) (Figure 3.1B). Lean Ob/Ob had significantly higher fat mass (P=0.0194), but similar lean mass (P=0.0768) compared to lean C57 mice over the duration of the study (Figures 3.1C and D). Obese weight-paired Ob/Ob mice had significantly increased fat mass (P=0.0002) and significantly less lean mass (P=0.0003) compared to obese C57 controls consuming a HFD (Figures 3.1C and D).

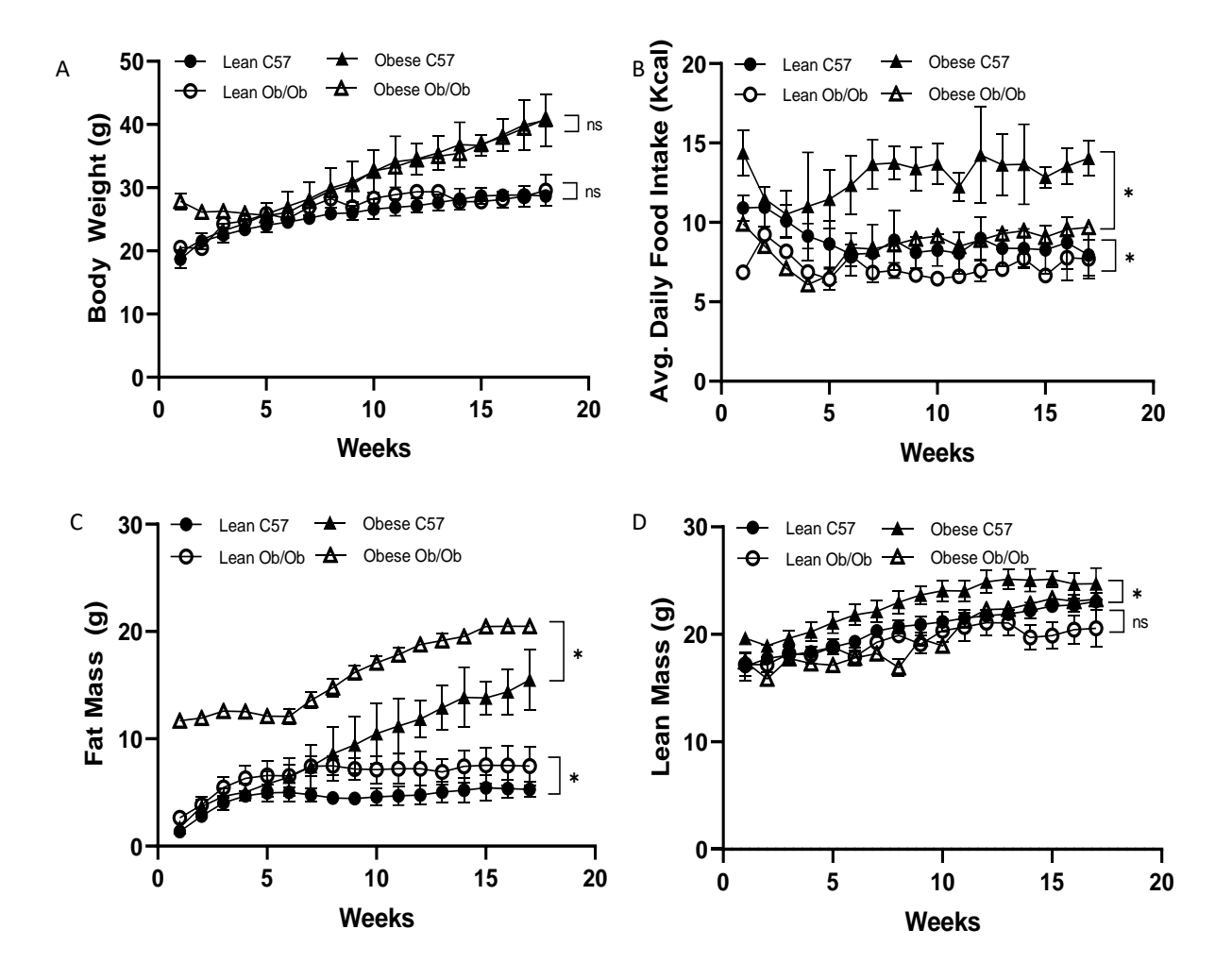


**Figure 3.1:** Body composition of male C57 and weight-paired lean or obese Ob/Ob mice. Lean C57, Lean Ob/Ob and Obese Ob/Ob were fed a control diet (CD), Obese C57 were fed a high fat diet (HFD). A. Body weight (g); B. Average daily food intake in Kcal; C. Fat Mass (g); D. Lean mass (g). Mean  $\pm$  STDev., n=4/group. One-Way ANOVA or Kruskal-Wallis; \* $P \le 0.05$ .

# 3.3.2. Leptin Deficiency Reduced Tibia Cortical Bone Volume Independently of Body Weight:

Tibia cortical BV was significantly reduced in lean Ob/Ob (P=0.003) and obese Ob/Ob (P=0.004) mice when compared to lean C57 controls, whereas obese C57 mice exhibited similar (P = 0.989) tibia cortical BV compared to lean C57 controls (Figure 3.2A). Tibia cortical BMD was unaffected by leptin deficiency or increased body weight compared to lean C57 controls (Figure 3.2B). Overall tibia cortical thickness was also unaffected by leptin deficiency or increased body weight compared to controls (Figure 3.2C). Qualitative regional increases in tibia cortical BMD (g/cm³) were mapped to areas associated with compression loading including the interosseous crest (IC) and the proximal tibia crest (PTC) (Figure 3.2D).

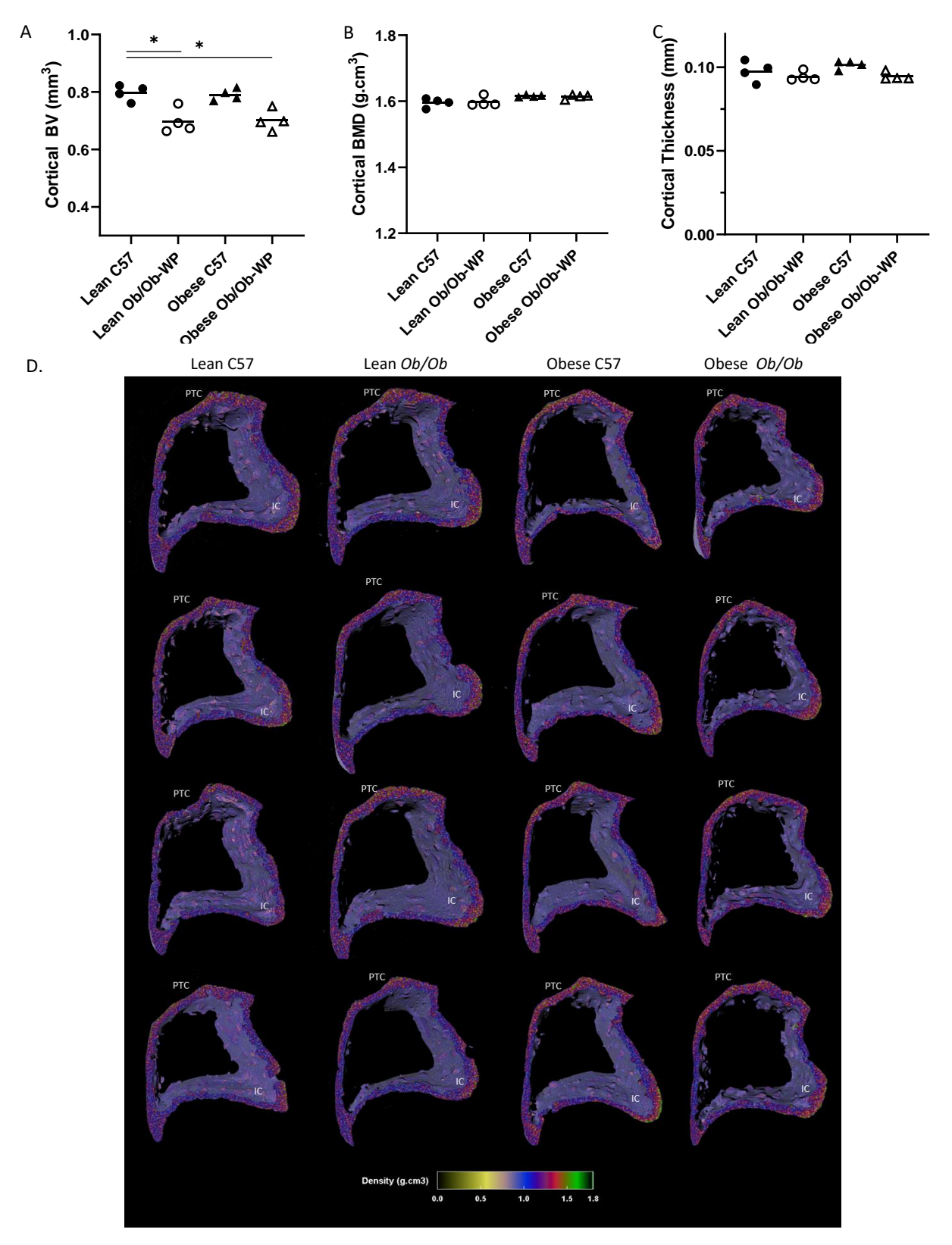


**Figure 3.2:** Proximal tibia cortical bone morphology at 24±2 weeks of age of male C57 and weight-paired lean or obese *Ob/Ob* mice. A. Cortical bone volume (BV) (mm<sup>3</sup>); B. Cortical bone mineral density (BMD) (g/cm<sup>3</sup>); C. Cortical Thickness (mm); D. 3D colour coded density map (g.cm<sup>3</sup>) showing increased density at interosseous crest (IC) and proximal tibial crest (PTC). n=4 Mean and individual data points. One way-ANOVA or Kruskal-Wallis with post-hoc multiple comparisons, \* $P \le 0.05$  vs. Lean C57.

## 3.3.3. Leptin Deficiency and HFD Reduced Tibia Trabecular Bone Number, Bone Mineral Density, and Increased Trabecular Separation:

HFD fed obese C57 mice exhibited the greatest reduction in tibia trabecular BV/TV% (P<0.0001) and BMD (g.cm³) (P = 0.003) compared to lean C57 controls (Figure 3.3A and E). Lean and obese Ob/Ob mice also exhibited 35% and 29% reductions in trabecular BV/TV%, respectively, compared to lean C57 control mice (P < 0.0001 and P = 0.001, respectively) (Figure 3.3A). Leptin deficiency also significantly reduced BMD compared to lean C57 controls (Lean Ob/Ob vs. Lean C57 P = 0.0367; Obese Ob/Ob vs. Lean C57 P = 0.0272) (Figure 3.3E). The changes in bone volume appear to be due to a significant reduction in trabecular number (Lean Ob/Ob vs. Lean C57 P = 0.0006; Obese C57 vs. Lean C57 P < 0.0001; Obese Ob/Ob vs. Lean C57 P = 0.0102) (Figure 3.3B) and proportionate increase in trabecular separation (Lean Ob/Ob vs. Lean C57 P = 0.1128) (Figure 3.3C). Leptin deficient or HFD fed C57 mice did not significantly reduce mean trabecular thickness compared to lean C57 controls (Lean Ob/Ob vs. Lean C57 P = 0.1167; Obese C57 vs. Lean C57 P = 0.1168) (Figure 3.3D).

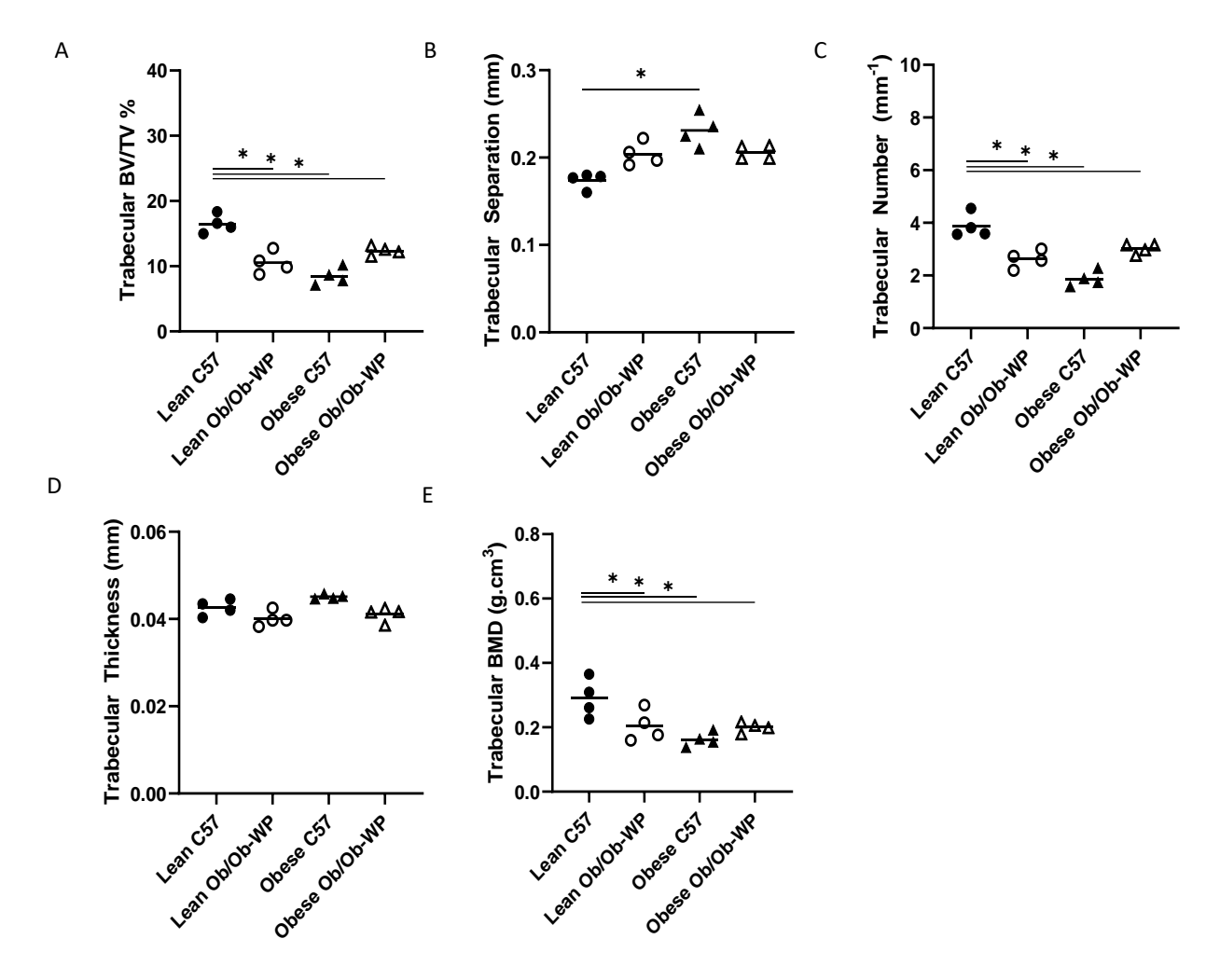
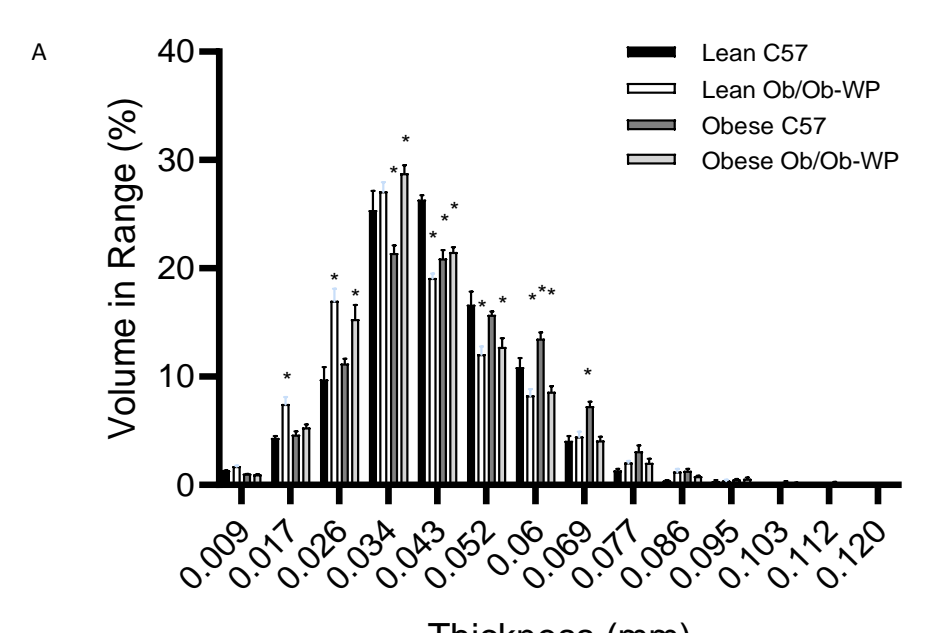


**Figure 3.3:** Proximal tibia trabecular bone morphology at 24±2 weeks of age of male C57 and weight-paired lean or obese *Ob/Ob* mice. A. Trabecular bone volume/tissue volume (BV/TV) (%); B. Trabecular number (mm $^{-1}$ ); C. Trabecular separation (mm); D. Trabecular thickness (mm); E. Trabecular bone mineral density (BMD) (g/cm $^{3}$ ). n=4 Mean and individual data points. One way-ANOVA or Kruskal-Wallis with post hoc multiple comparisons, \* $P \le 0.05$  vs. Lean C57.

# 3.3.4. Regional Differences in Tibia Trabecular Thickness Distribution Are Masked by Overall Thickness Mean:

A qualitative 3D colour-coded thickness transfer function from 0.009 – 0.112mm was developed and applied to demonstrate the distribution of tibia trabecular thickness across the entire 3D ROI. Although leptin deficiency and HFD induced increases in body weight, were not associated with any overall difference in mean trabecular thickness compared to lean C57 control mice (Figure 3.3D). The qualitative 3D colour-coded thickness maps revealed regional specific changes in thickness distribution and maximum thickness values across all groups (Figure 3.4B).

Lean *Ob/Ob* mice exhibited a significant increase in percentage of thinner struts (0.017-0.026 mm, P<0.0006) and a significant reduction in the percentage of mid-range to thicker struts (0.043-0.060 mm, P<0.0062) compared to lean C57 controls. Obese C57 mice exhibited a significant reduction in percentage of mid-range struts (0.034-0.043 mm, P<0.0001) and a significant increase in the percentage of thicker struts (0.060-0.069 mm, P<0.0047) compared to lean C57 controls. Obese *Ob/Ob* mice closely matched the distribution pattern of lean *Ob/Ob* mice whereby obese *Ob/Ob* exhibited a significant increase in thinner struts (0.026-0.034 mm, P<0.0002) and a significant reduction in midrange to thicker struts (0.043-0.060 mm, P<0.0214) compared to lean C57 controls (Figure 3.4A). Furthermore, trabeculae were segmented into two sections, an inner core and outer medulla for region specific analysis (Figure 3.5A). Trabecular thickness of the inner core region was significantly reduced in the Lean *Ob/Ob* compared to the lean C57 control mice, Figure 3.5C (P=0.0014), however the outer regions across all groups were unchanged (Figure 3.5B).



В

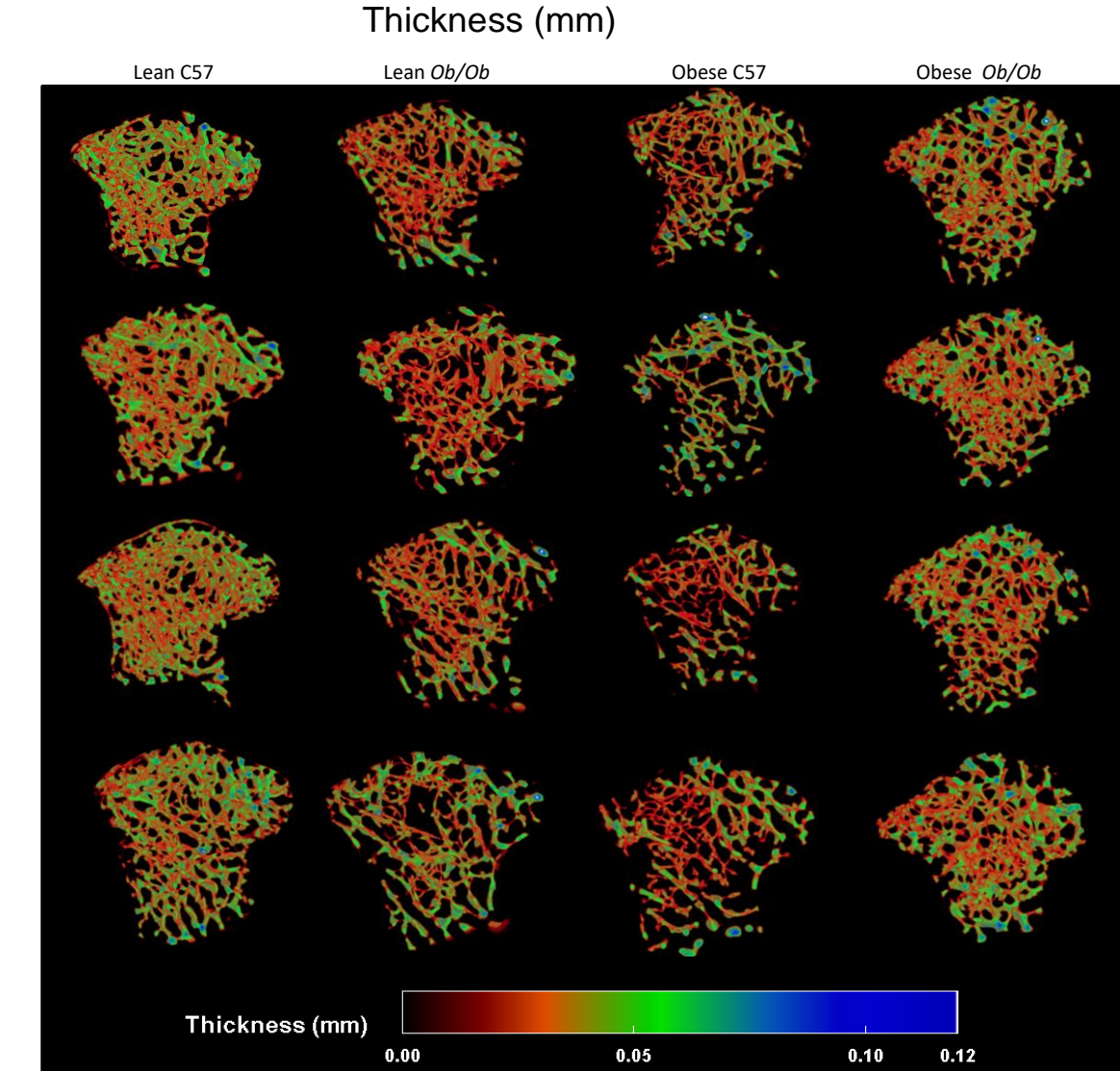


**Figure 3.4:** Proximal tibia trabecular bone morphology at 24±2 weeks of age of male C57 and weight-paired lean or obese Ob/Ob mice. A. Thickness distribution (mm); B. 3D colour coded thickness map (mm). n=4 Mean and individual data points. One way-ANOVA or Kruskal-Wallis with post hoc multiple comparisons, \* $P \le 0.05$  vs. Lean C57.

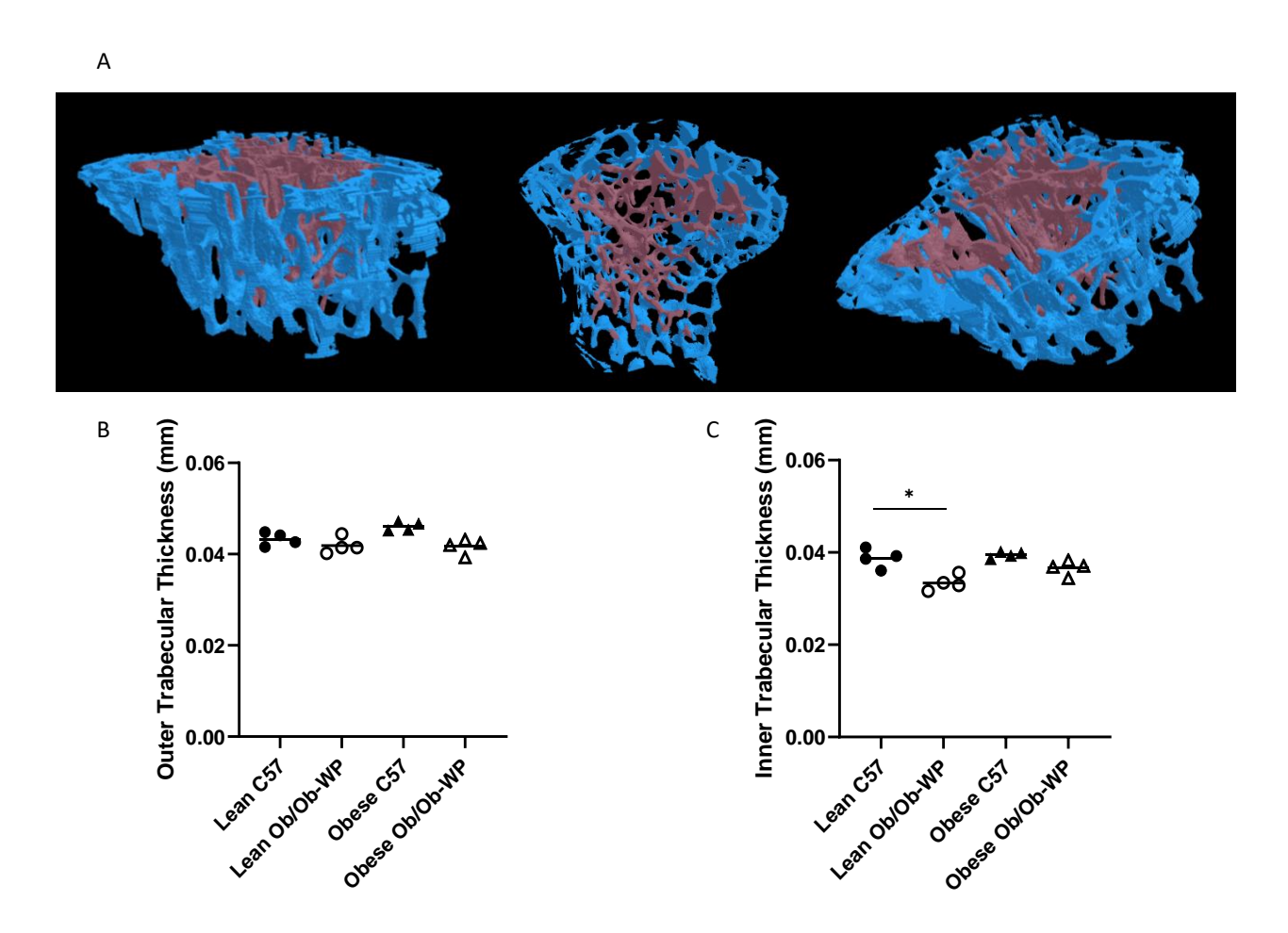


**Figure 3.5:** Inner vs. Outer proximal tibia trabecular bone morphology at 24±2 weeks of age of male C57 and weight-paired lean or obese Ob/Ob mice. A. Representative model of inner and outer medullar trabecular bone region of interest; B. Outer medullar trabecular thickness (mm); C. Inner trabecular thickness (mm). n=4 Mean and individual data points. One way-ANOVA with post hoc multiple comparisons. \* $P \le 0.05$  vs. Lean C57.

### 3.3.5. Leptin Deficiency Reduces Vertebral Cortical Bone Thickness:

Leptin deficiency in lean mice significantly reduced vertebral cortical bone volume compared to lean C57 controls (P = 0.046) (Figure 3.6A). However, body weight did not significantly alter overall vertebral cortical bone volume. Similarly, vertebral cortical BMD was unchanged in leptin deficient Ob/Ob mice or HFD fed C57 mice compared to lean controls (Figure 3.6B). Cortical thickness, however, was reduced by leptin deficiency independent of increased body weight as both lean Ob/Ob (P = 0.0124) and obese Ob/Ob (P = 0.0183) mice had significantly reduced mean vertebral cortical thickness compared to lean C57 controls (Figure 3.6C). Qualitative regional 3D colour maps of BMD demonstrated a similar distribution pattern across all four groups (Figure 3.6D).

## 3.3.6. High Fat Diet Reduced Vertebral Trabecular Bone Volume, Number and Mineral Density:

Leptin deficiency and HFD significantly reduced vertebral trabecular BV/TV% (Figure 3.7A). However, only obese C57 mice fed a HFD had significant reductions in both trabecular number (Figure 3.7B) (P = 0.0089), mineral density (Figure 3.7E) (P = 0.0027) and a complementary increase in trabecular separation (Figure 3.7C) (P = 0.0050). Reductions in lean Ob/Ob vertebral bone volume were associated with reductions in trabecular thickness (Figure 3.7D) rather than number (Figure 3.7B). Reductions in vertebral bone volume of obese Ob/Ob were associated with small but insignificant reductions in both vertebral trabecular number and thickness, which resulted in a significant increase in vertebral trabecular separation (Figure 3.7C).

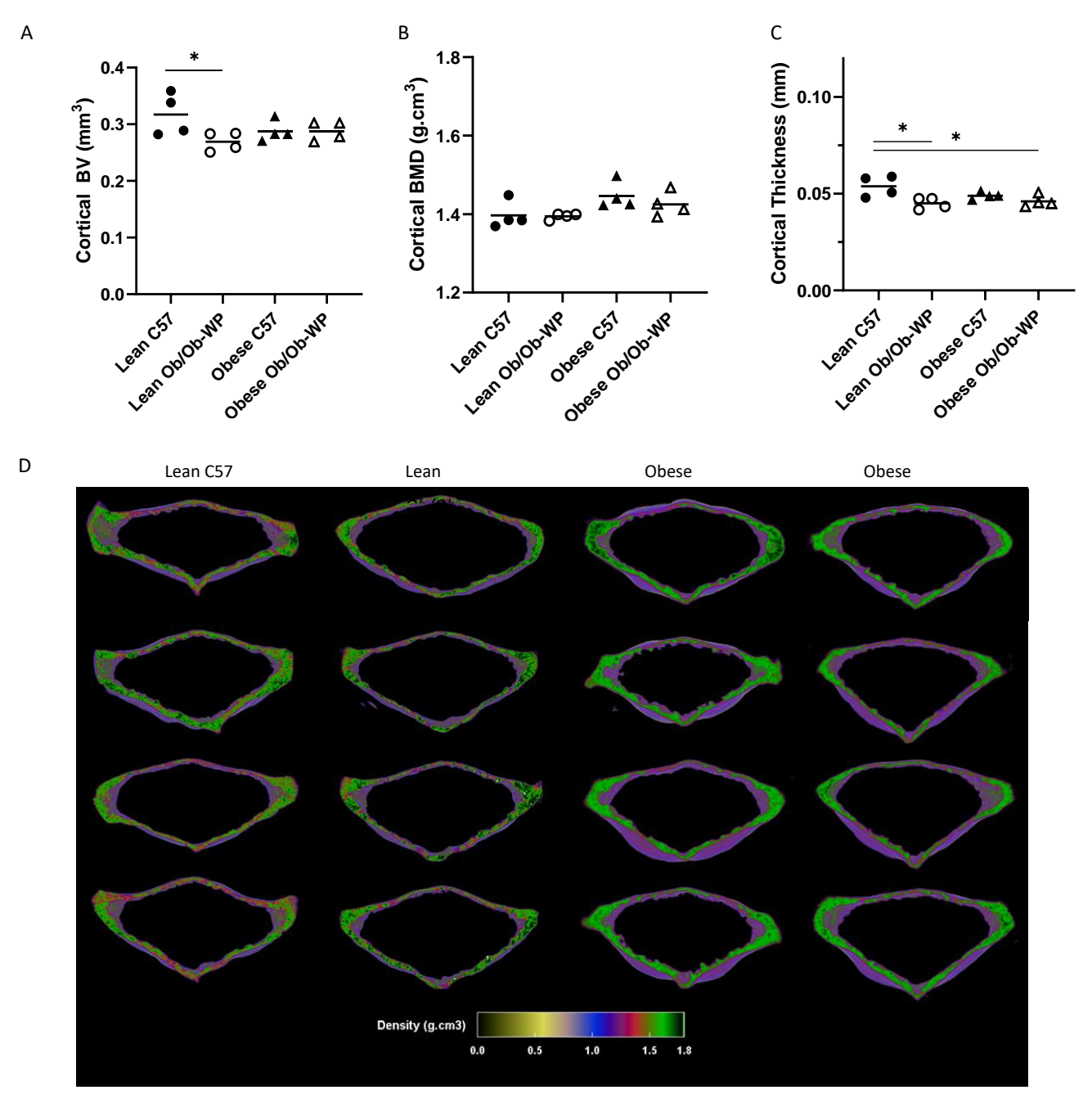


**Figure 3.6.** Vertebral cortical bone morphology at 24±2 weeks of age of male C57 and weight-paired lean or obese *Ob/Ob* mice. A. Cortical bone volume (BV) (mm<sup>3</sup>); B. Cortical bone mineral density (BMD) (g/cm<sup>3</sup>); C. Cortical Thickness (mm); D. 3D colour coded density map (g.cm<sup>3</sup>) of vertebral body cortical bone. n=4 Mean and individual data points. One way-ANOVA or Kruskal-Wallis with post-hoc comparisons, \* $P \le 0.05$  vs. Lean C57.

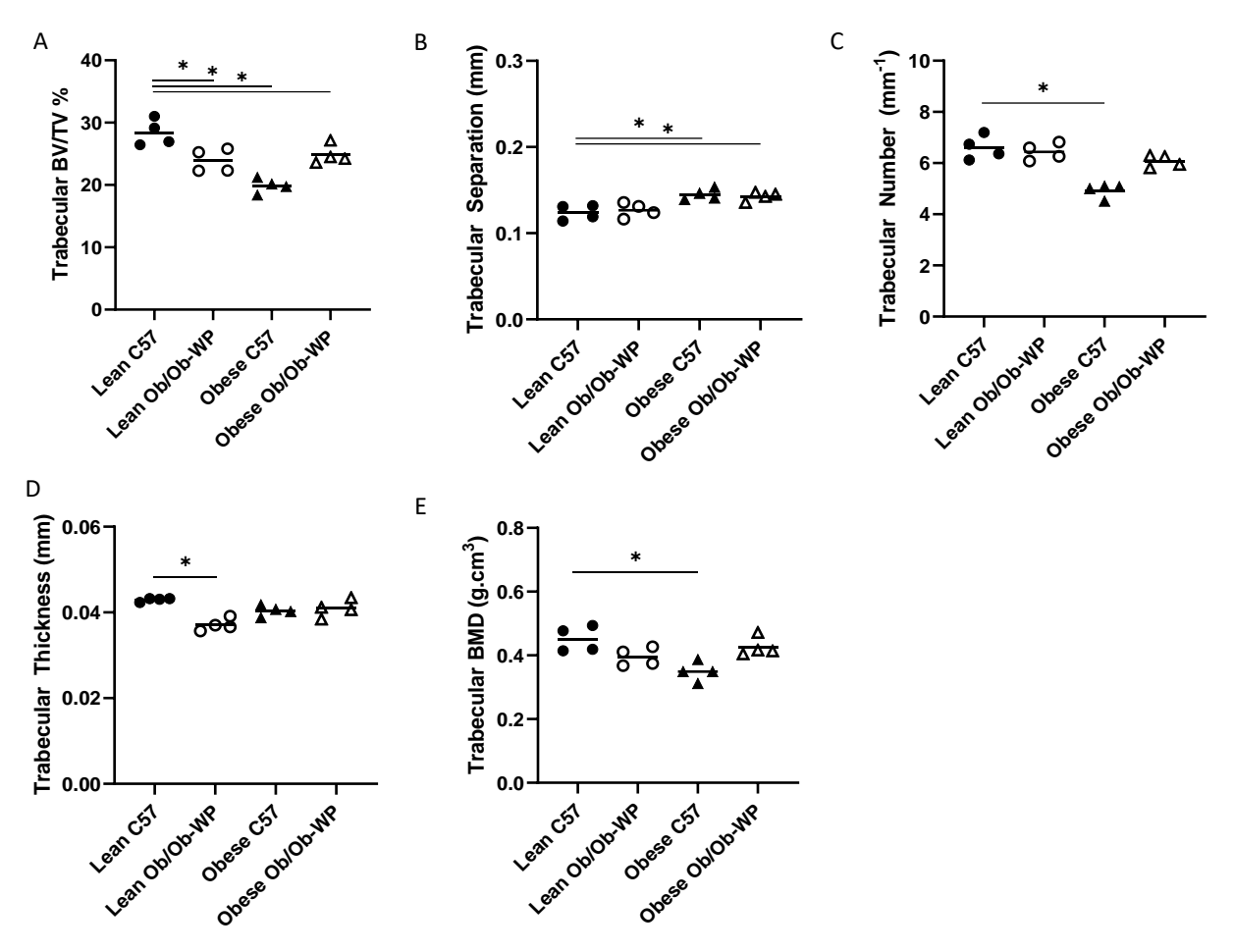
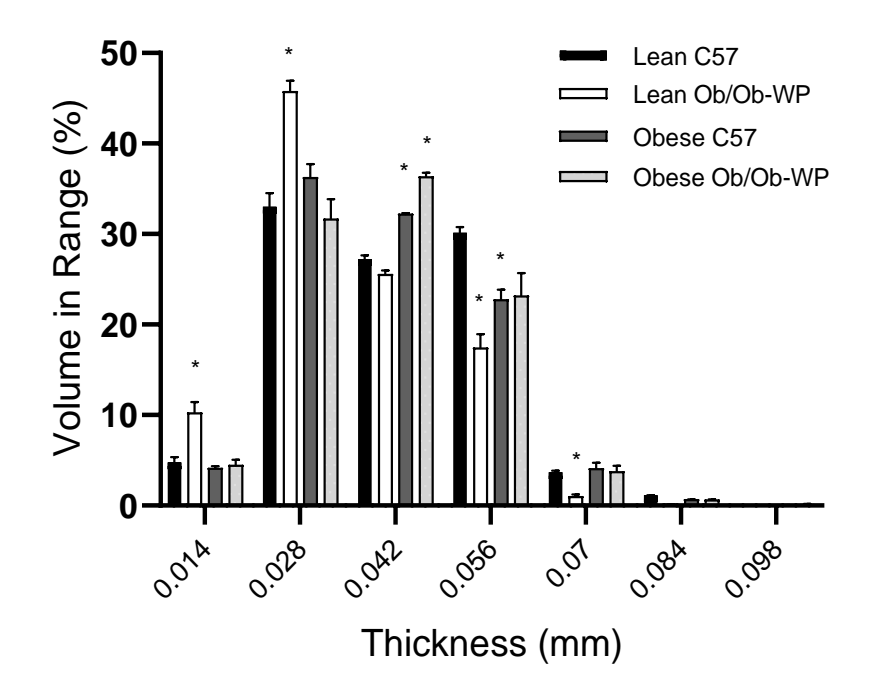


**Figure 3.7.** Vertebral trabecular bone morphology at 24±2 weeks of age of male C57 and weight-paired lean or obese *Ob/Ob* mice. A. Trabecular bone volume/tissue volume (BV/TV) (%); B. Trabecular number (mm $^{-1}$ ); C. Trabecular separation (mm); D. Trabecular thickness (mm); E. Trabecular bone mineral density (BMD) (g/cm $^{3}$ ). n=4 Mean and individual data points. One way-ANOVA or Kruskal-Wallis with post-hoc comparisons, \* $P \le 0.05$  vs. Lean C57.

# 3.3.7. Regional Differences in Vertebral Trabecular Thickness Distribution are Masked by Overall Thickness Mean:

A qualitative 3D colour-coded thickness transfer function from 0.009 – 0.103mm was developed and applied to examine the distribution of vertebral trabecular thickness across the entire 3D ROI. Although lean *Ob/Ob* mice were the only group to show a significant reduction in trabecular thickness compared to lean C57 control mice (Figure 3.7D), the 3D colour maps (Figure 3.8B) revealed changes in thickness distribution and maximum thickness values across all groups. Lean *Ob/Ob* mice exhibited a significant increase in percentage of thinner struts (0.014-0.028 mm, P<0.0459) and a significant reduction in the percentage of thicker struts (0.056-0.070 mm, P<0.0053) compared to lean C57 controls. Both obese C57 and obese *Ob/Ob* mice closely matched the percent distribution of thin and thick trabecular compared to lean C57 mice. However, both obese groups exhibited a significant increase in the percentage of mid-range struts at 0.042 mm (Obese C57 P=0.0031; Obese *Ob/Ob* P<0.0001) compared to lean C57 controls (Figure 3.8A).







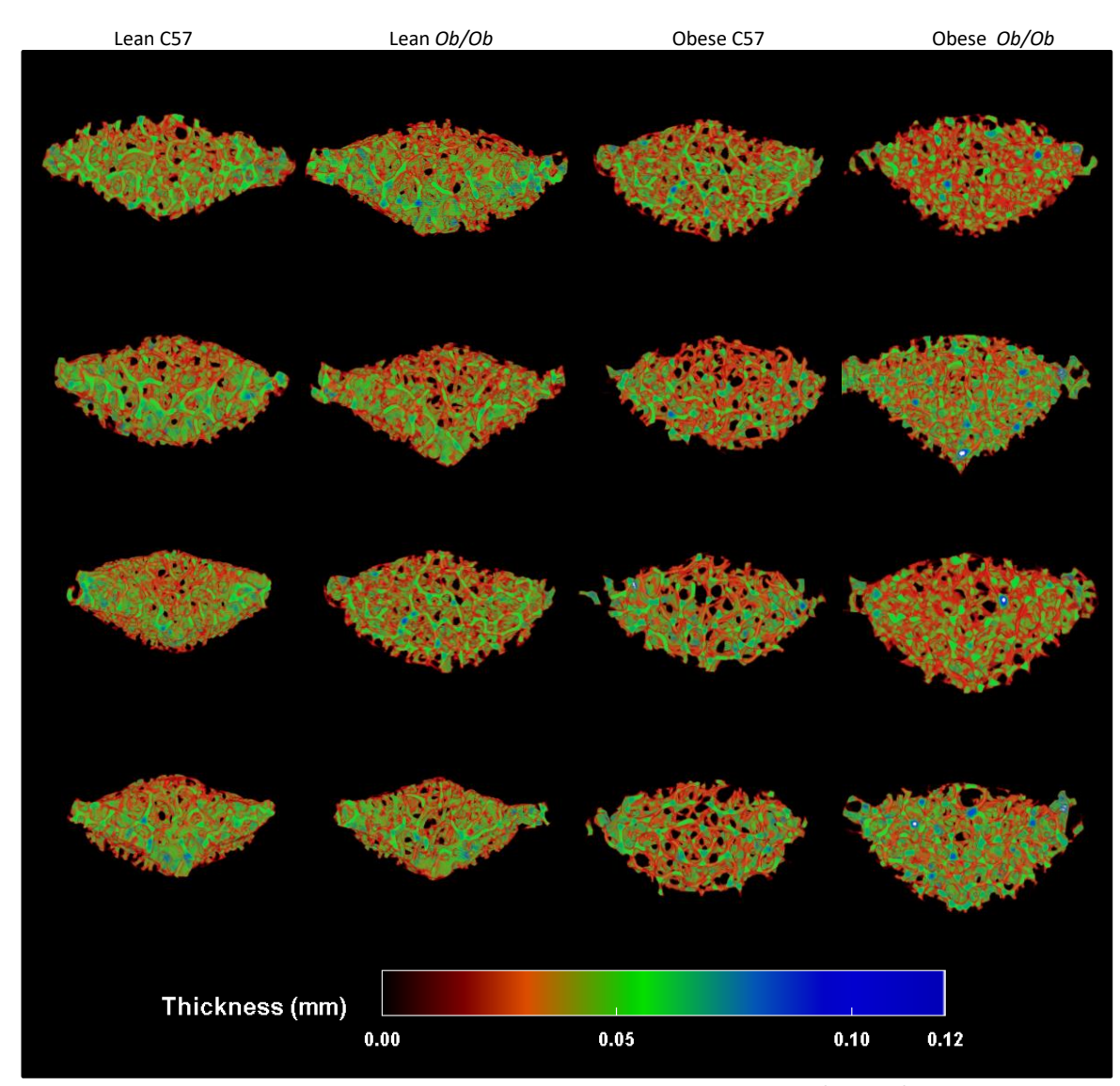


**Figure 3.8.** Vertebral trabecular bone morphology at 24±2 weeks of age of male C57 and weight-paired lean or obese Ob/Ob mice. A. Thickness distribution (mm); B. 3D colour coded thickness map (mm). n=4 Mean and individual data points. One way-ANOVA  $p_{\overline{b}6}$  Kruskal-Wallis with post hoc multiple comparisons, \* $P \le 0.05$  vs. Lean C57.

## 3.3.8. HFD and Leptin Deficiency Alter Bone Marrow Composition:

Masson's Trichrome staining was used to assess the bone marrow and ECM composition within sections of murine tibiae and L3 vertebrae. Whilst mice fed a HFD exhibited increased spaces within the marrow compared to lean C57 counterparts, the tibial bone marrow of *Ob/Ob* mice was almost completely occupied by these spaces (Figure 3.9). Blue staining, denoting the presence of collagen, was also diminished in tibial sections of *Ob/Ob* mice compared to C57 counterparts. However, these differences were not observed in vertebral sections from the same mice (Figure 3.9).

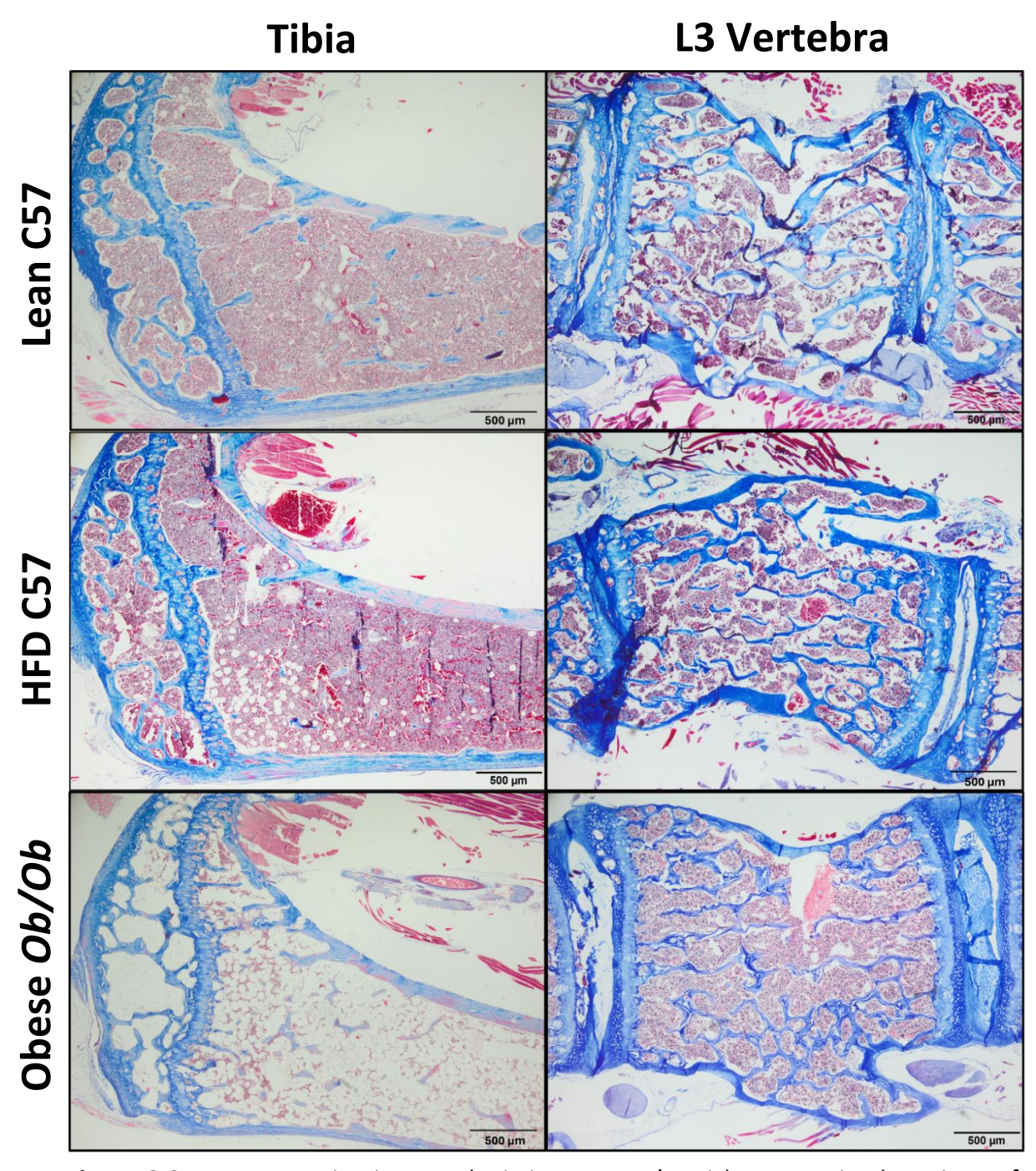


**Figure 3.9:** Representative images depicting Masson's Trichrome stained sections of tibiae and L3 vertebrae from C57 mice fed a normal diet (n = 4), C57 mice fed a high fat diet (n = 4) and weight paired Ob/Ob mice. Scale bars are 500  $\mu$ m.

## 3.3.9. Leptin Deficiency Significantly Reduces OPG Expression in the Tibiae of Obese *Ob/Ob* Mice, but Not the Vertebrae:

Cells exhibiting immunopositivity for markers of osteoblast and osteoclast activity were counted microscopically along the endocortical perimeter of stained tibial and vertebral sections, and results expressed as the percentage of total cells counted which were immunopositive. Neither tibial Runx2 (Figure 3.10A) nor ALP (Figure 3.10B) immunopositivity differed significantly between any of the groups tested, although median tibial immunopositivity of these osteoblastic markers was consistently lowest in the obese Ob/Ob mice compared to the other two groups tested. No significant differences were observed in tibial RANKL immunopositivity between the groups (Figure 3.10C), despite a slight increase in median tibial RANKL expression in obese Ob/Ob mice compared to the other groups tested. However, tibial OPG immunopositivity was significantly decreased in obese Ob/Ob mice compared to lean Ob/Ob mice (Figure 3.10D) (P = 0.0089). These alterations in tibial OPG expression resulted in a decreased RANKL:OPG ratio in obese *Ob/Ob* mice compared to obese C57 controls (Figure 3.10E) (P = 0.0054). Despite this, the number of TRAP positive osteoclasts per mm of endocortical surface was significantly decreased in obese C57 (P = 0.0303) and obese Ob/Ob (P = 0.0107) mice compared to lean C57 controls (Figure 3.10F).

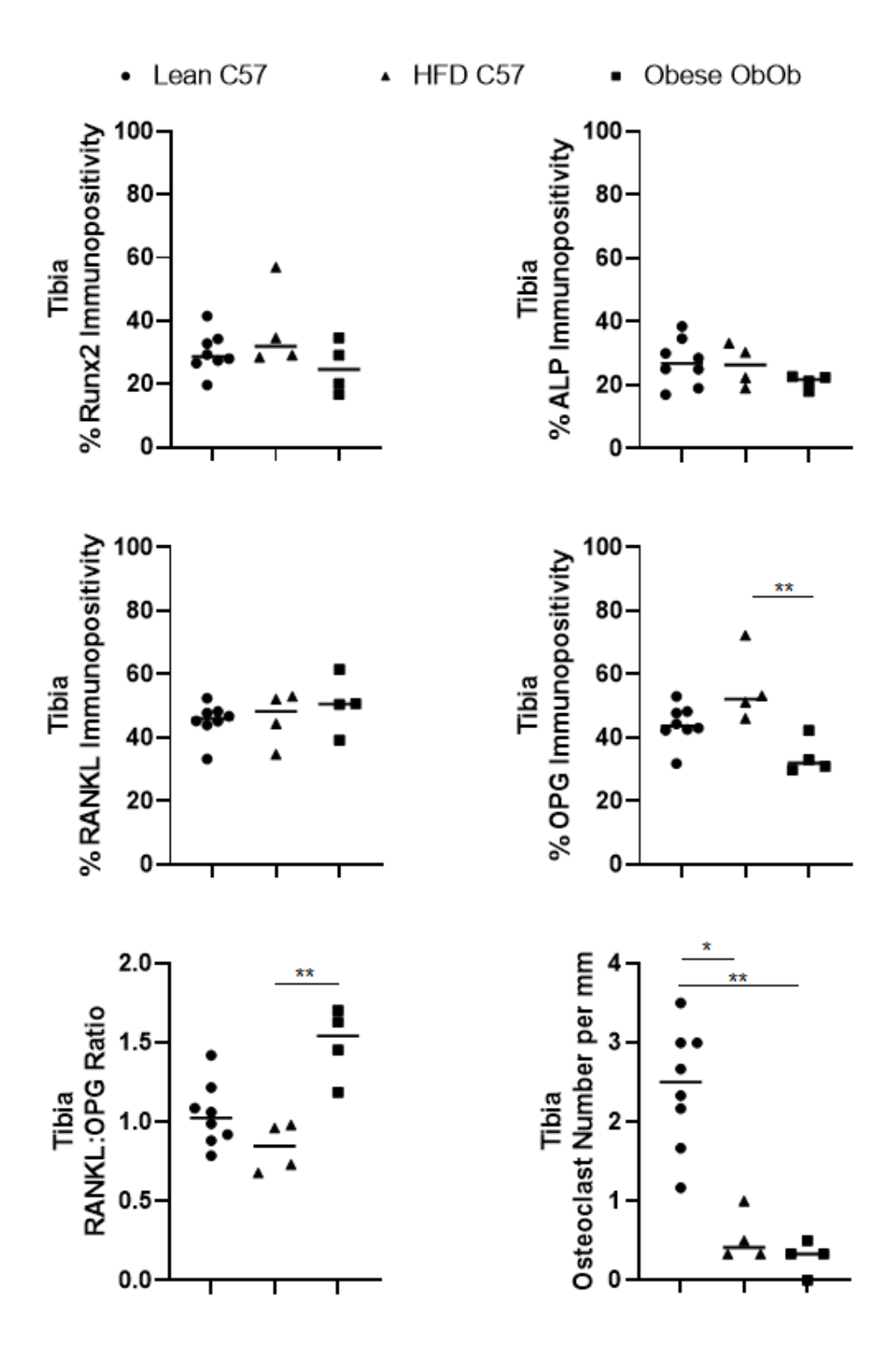


**Figure 3.10:** Tibial percentage immunopositivity counted along the endocortical surface of Runx2 (A), ALP (B), RANKL (C), OPG (D) immunohistochemistry stained sections, RANKL:OPG immunopositivity ratio (E) and osteoclast number per mm quantified via TRAP staining (F) of tibiae sections from control C57 mice fed a normal diet (n = 8), C57 mice fed a high fat diet (n = 4) and *Ob/Ob* mice fed a normal diet, weight paired to HFD fed C57 mice (n = 8).

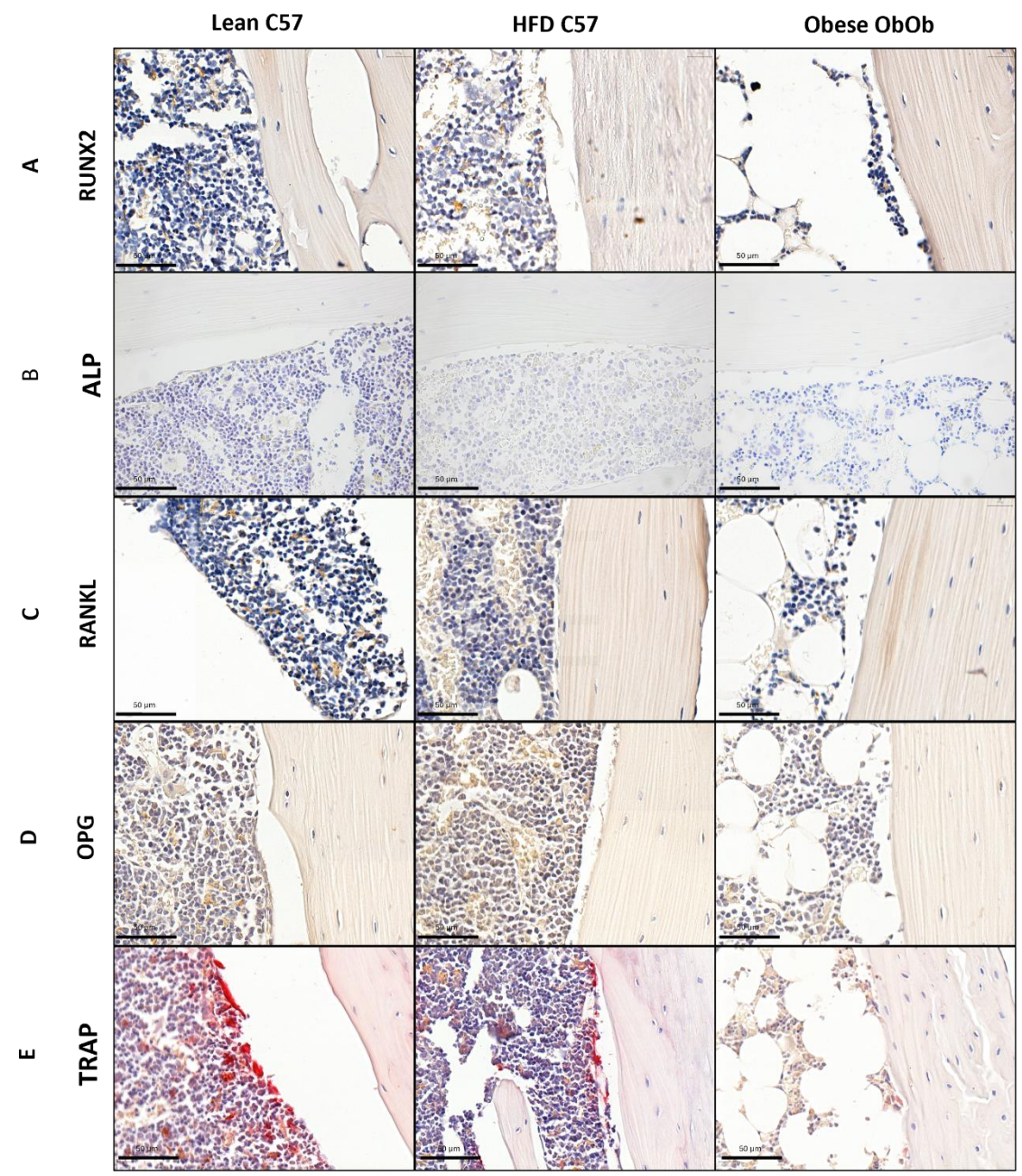


**Figure 3.11:** Representative images of Runx2 (A), ALP (B), RANKL (C), OPG (D) immunohistochemistry staining and TRAP staining (E) of tibiae sections from control C57 mice on a control (n = 8), C57 mice fed a high fat diet (n = 4) and Ob/Ob mice fed a normal diet. Scale bars are 50  $\mu$ m.

In the vertebrae, neither Runx2 (Figure 3.12A) nor ALP (Figure 3.12B) immunopositivity differed significantly between any of the mice tested. Similarly, there were no significant differences observed in vertebral RANKL (Figure 3.12C) or OPG (Figure 3.12D) percentage immunopositivity or RANKL:OPG (Figure 3.12E) ratio between any of the groups tested, although overall RANKL:OPG ratio was lowest in obese *Ob/Ob* mice, in keeping with trends seen in the tibial analysis.

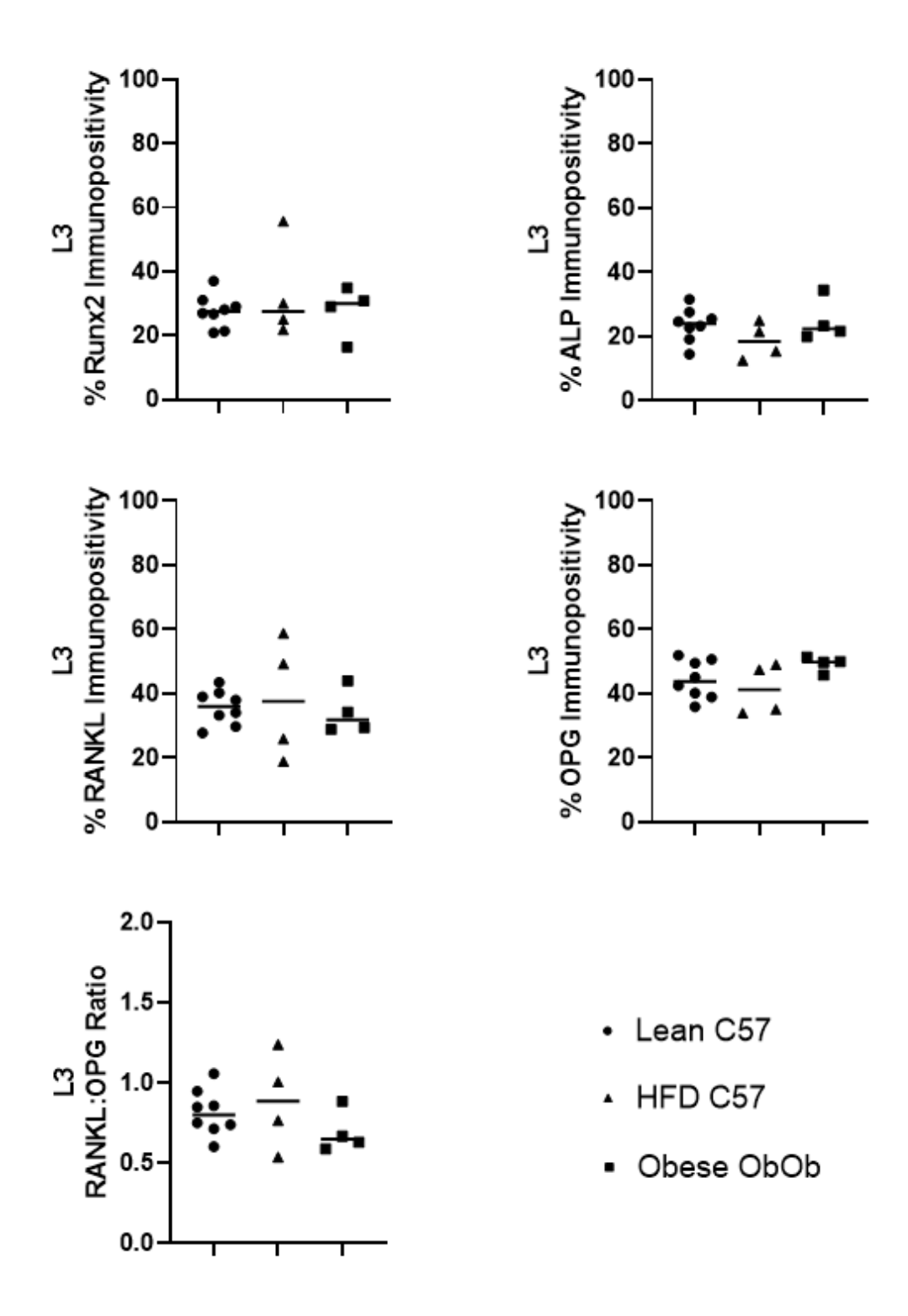


**Figure 3.12:** L3 vertebral percentage immunopositivity counted along the endocortical surface of Runx2 (A), ALP (B), RANKL (C), OPG (D) immunohistochemistry stained sections, RANKL:OPG immunopositivity ratio (E) and osteoclast number per mm quantified via TRAP staining (F) of tibiae sections from control C57 mice fed a normal diet (n = 8), C57 mice fed a high fat diet (n = 4) and *Ob/Ob* mice fed a normal diet, weight paired to HFD fed C57 mice (n = 4).

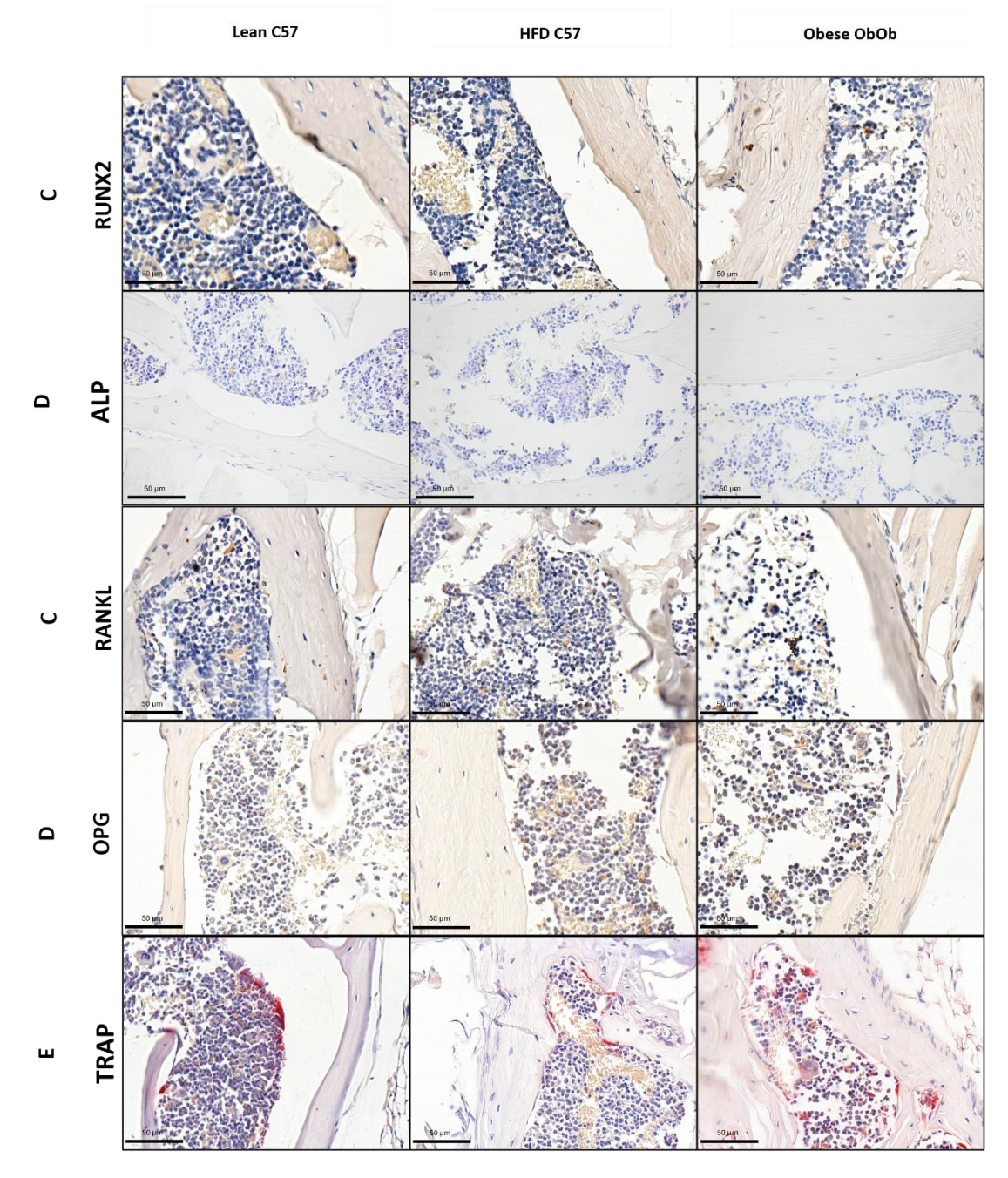


**Figure 3.13:** Representative images of Runx2 (A), ALP (B), RANKL (C), OPG (D) immunohistochemistry staining of L3 vertebra sections from control C57 mice on a control (n = 8), or high fat (n = 4) diet and weight-paired *Ob/Ob* mice fed a normal diet. Scale bars are  $50 \, \mu m$ .

# 3.3.10. Observed Alterations in Bone Microarchitecture Did Not Significantly Affect Bone Strength:

3-point bend testing was applied to test the mechanical strength of murine tibiae, assessing the maximal force each tibia could withstand before breaking. Despite no statistically significant differences, tibiae from *Ob/Ob* mice required consistently less force to induce fracture in a 3-point bend test (Figure 3.14).

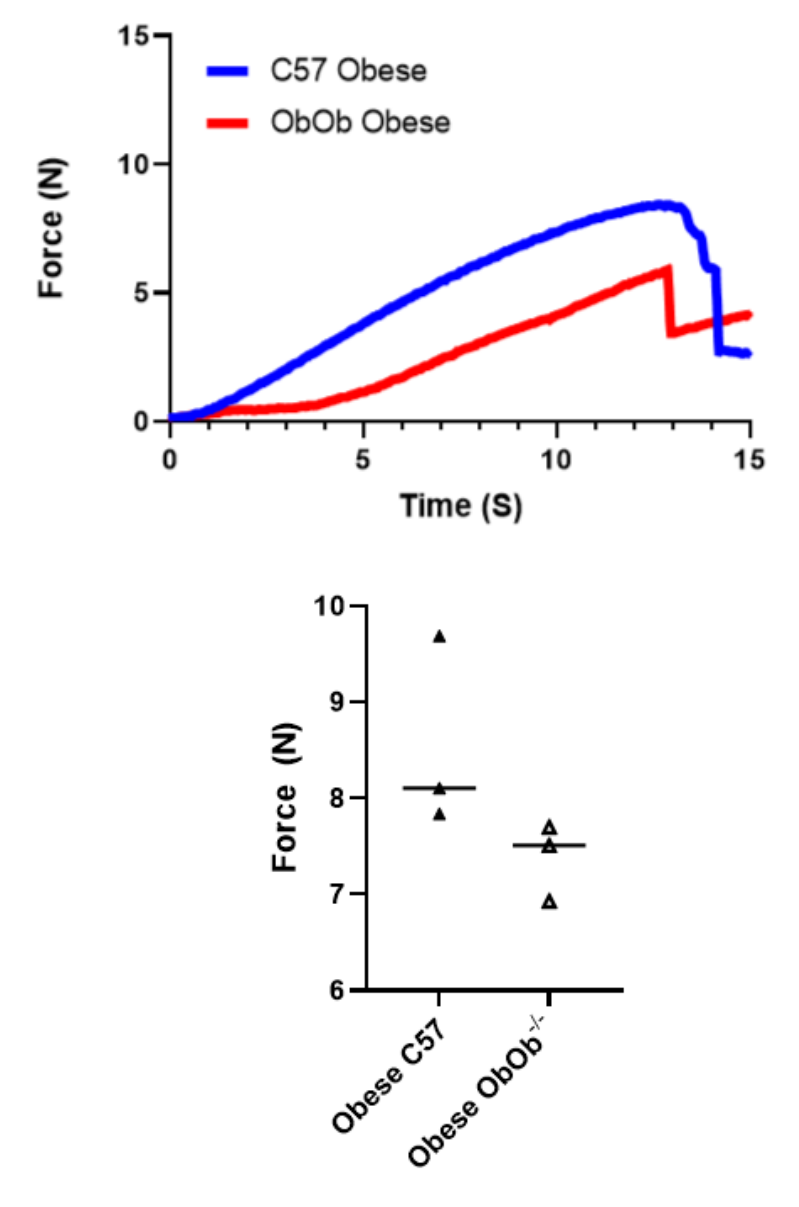


**Figure 3.14:** A) Average force applied over time to HFD-fed C57 (n = 3) and weight-paired  $Ob/Ob^{-/-}$  murine tibiae (n = 3) in a 3-point bend mechanical test. B) Maximal force applied to tibiae before breakage.

### 3.4. Discussion:

## 3.4.1. Effects of Leptin Deficiency on Cortical and Trabecular Bone Morphology:

Previous studies have provided contradictory results on the role of leptin on bone morphology *in vivo*. However, few studies have accounted for the changes in body weight associated with the anorexigenic effects of leptin. This aim of this study was to provide a long-term *in vivo* investigation using a mouse model of leptin deficiency (*Ob/Ob*) and weight-paired them to lean and obese C57 controls, to better understand the role of leptin on bone morphology independent of changes in body weight.

The current study demonstrates that leptin deficiency, independent of changes in body weight, reduced tibia cortical bone volume, trabecular BV/TV%, number and mineral density. Assessment of average changes in trabecular thickness were shown to mask significant differences in the region and size distribution of trabeculae within the tibia.

An extensive review by Reid et al., (2018) detailed the effects of leptin and leptin deficiency in *Ob/Ob* mice on the skeleton including tibia and vertebrae. However, most data included were published before 2013 and in most instances the impact of differences in body weight due to leptin deficiency or leptin administration were not determined.

Previous studies have shown that reductions in overall tibia and vertebral body bone volume were closely linked to increased bone marrow adipose tissue (BMAT) (Costa et al., 2019; Suresh et al., 2020). BMAT has been suggested to play a role in regulating the trabeculae of long bones of the femur and tibia with numerous studies suggesting important interactions between red marrow adipocytes and bone cell differentiation. As both osteoblasts and red marrow adipocytes differentiate from the same pluripotent

mesenchymal stem cell lineage, there is evidence to suggest a competitive relationship (Hamrick et al., 2005). In fact, leptin receptor activation promotes adipogenesis whilst suppressing osteogenesis in BM stromal cells (Yue et al., 2016). Leptin also has been shown to affect bone turnover by acting directly on bone cells, producing an anabolic effect on osteoblasts, whilst inhibiting osteoclastogenesis (Reid et al., 2018). Treatment of primary osteoblasts with leptin has also been shown to cause dose-dependent increases in in vitro mineralisation and alkaline phosphatase (ALP) activity (Reseland et al., 2009). Similarly, early evidence suggested that leptin signalling enhanced the differentiation of bone marrow stromal cells into osteoblast lineage, whilst suppressing adipogenic differentiation (Thomas et al., 1999). In recent years, conflicting evidence has suggested that leptin signalling promotes adipogenesis whilst suppressing osteogenesis in mesenchymal stromal cells and that a high fat diet promotes adipogenesis through LepR signalling in bone marrow stromal cells (Yue et al., 2016). Morphological analysis outcomes from the current study are consistent with the hypothesis that leptin deficiency may reduce osteoblast differentiation, promoting adipogenesis in the red marrow, as evidenced by the increased presence of white space in the marrow of Ob/Ob animals comparative to both lean C57 and weight paired, HFD fed C57 controls. However, immunohistochemical analysis did not reveal any significant alterations in osteoblastic factors in either tibial or vertebral bone, in keeping with results from a 2023 study conducted by Duan et al., which found no significant differences in RUNX2 gene expression via PCR between C57 mice and Ob/Ob counterparts, although the animals in this study were not weight paired. Results from the present study instead indicate that differences in tibial bone morphology may be caused by enhanced osteoclastogenesis via increased RANKL:OPG ratio in leptin deficient animals. Interestingly, this suggested increase in tibial osteoclastogenesis did not translate to increased TRAP positive endocortical osteoclast count in the tibiae of Ob/Ob mice. This is potentially due to the significantly increased presence of lipid droplets in the tibial bone marrow of these animals, resulting in far fewer osteoblasts and osteoclasts observed within the bone marrow. Similar dramatic increases in lipid marrow content were reported in leptin receptor deficient  $(Db/Db^{-J-})$  mice during a 2023 study by Wan et al., further highlighting the importance of leptin signalling in maintaining balanced differentiation of MSCs in tibial bone marrow. The study, however, did not investigate the lipid content or bone turnover markers within the vertebrae, in which the mechanisms governing increased bone marrow adiposity appear to be unaffected, or at least affected to a lesser extent, by Leptin signalling.

## 3.4.2. Effects of High Fat Diet on Cortical and Trabecular Bone Morphology:

In the vertebral body, reductions in BMD were only significant in the HFD induced obese C57 mice compared to lean C57 controls. This finding is consistent with those of Patsch et al., (2011) who demonstrated reductions in vertebral trabecular BMD in response to both short and long-term HFD induced obesity. These results are despite differences in sample collection including analysis of long vs. short bones, 2D histological vs. 3D  $\mu$ CT analysis and the level of resolution of  $\mu$ CT imaging 10.5 $\mu$ m vs. 7  $\mu$ m resolution. Cao et al., (2009) demonstrated a significant reduction in BV/TV% in C57 mice fed a HFD compared to controls, similar to results of the current study. However, Cao et al., (2009) did not determine the independent contribution of body weight or leptin. Furthermore, obese C57 mice exhibited significant reductions in trabecular BV/TV% compared to lean C57 controls. This result supports the findings of Montalvany-Antonucci et al., (2018)

who demonstrated that a HFD decreased femur trabecular BV/TV% by approximately 50% compared to controls.

Leptin's role in controlling bone morphology in HFD induced obese subjects is further complicated by the possibility that increased adiposity may lead to leptin resistance in the CNS and in peripheral tissues (Mendoza-Herrera et al., 2021). Several potential mechanisms of leptin resistance have been identified (Gruzdeva et al., 2019), including cleavage of LepR's intracellular domain by matrix metalloproteinase-2 (MMP-2) in response to obesity-induced inflammation (Mazor et al., 2018). Leptin resistance may occur in obese individuals with high circulating leptin levels, and potential mechanisms involved have been covered in detail previously (Sáinz et al., 2015). Some studies suggest that leptin resistance in obesity may be selective with an attenuation of many of the metabolic responses to leptin but preserved effects to activate the sympathetic nervous system and to raise blood pressure (do Carmo et al., 2013; Hall et al., 2019). Whether obese C57 male mice in the current study were affected by leptin resistance, perhaps explaining some of the similarities with obese *Ob/Ob* mice bone morphometry, requires further investigation. This could have been achieved during the lifespan of the mice Furthermore, whether the effects could be mediated via direct (mesenchymal stem cells) or indirect (CNS) mechanisms is unclear and beyond the scope of this investigation.

# 3.4.3. Effects of Mechanical Load from Body Weight on Cortical and Trabecular Bone Morphology:

Lean mass and fat mass are believed to independently contribute to bone remodelling and have positive correlations with increased compressive force of the knee joint in obese individuals (Messier et al., 2014). In humans, an increase in lean mass is associated

with a greater increase in whole body BMD (mg.cm²) (Zhu et al., 2015), whereas low muscle mass positively correlate with low BMD (Hamrick et al., 2004). These data suggest that lean mass is a better predictor of BMD than fat mass. However, the current study demonstrated that obese groups with 30% higher overall body mass and a significant increase in % fat and % lean mass had a significant reduction in tibia trabecular BMD and no change in cortical BMD compared to lean C57 controls. A study of 224 women also recently demonstrated that percentage fat mass is negatively associated with whole body BMD (Engberg et al., 2020). Furthermore, pre-pubertal obese children have a significant decrease in whole body BMD and bone mineral content (BMC) when compared to lean controls after normalizing for lean mass (Rocher et al., 2008). Studies of independent cohorts of adolescent children also show that adiposity is inversely correlated with BMD in specific bone regions (Hong et al., 2010; Pollock et al., 2007). These data suggest that fat mass may be inversely correlated with trabecular BMD but not cortical in the tibia of mice.

Tibia and vertebral body cortical and trabecular bone volume was consistently reduced in the obese groups compared to lean animals. This observation is consistent with findings of other groups who demonstrated that bone volume is not positively correlated with increases in load. Cao et al., (2009) demonstrated that increased body weight due to HFD did not significantly increase tibia cortical bone area (mm²) in C57 mice compared to control mice fed a CD. Furthermore, Lorincz et al., (2010) when adjusting for body mass demonstrated cortical BV (mm²/g) was actually reduced in high fat, high sucrose fed C57 mice with increased body weight. Turner et al., (2013) demonstrated, via histomorphometry, that trabecular femur epiphysis BV (%) was similar in *Ob/Ob* and wild type controls despite a significant difference in body weight.

This finding agrees with the current study which demonstrates that increased overall body weight due to leptin deficiency or HFD did not increase cortical bone volume (mm³) in either C57 or *Ob/Ob* mice, and in fact a significant decrease in BV/TV% was observed in tibia and vertebral body trabeculae. Although Cao et al., analysed a smaller trabecular bone ROI and at a different offset from the bridge break, they identified trabecular BV/TV% and number were decreased in mice fed a HFD, and trabecular separation was increased. Iwaniec et al., (2009) found that increased body mass due to HFD, as opposed to leptin gene therapy, was responsible for an increase in mid-shaft femur cortical BV, and thickness. These findings suggest that leptin deficiency independent of body weight partially account for the adverse effects of HFD on bone morphometry, and that increased body weight may ameliorate some of the negative effects of leptin deficiency alone.

### 3.4.4. Trabecular Thickness and Clinical Implications:

Consistent with the results of Cao et al., (2009), the current study demonstrated that average trabecular thickness remained unchanged in response to leptin deficiency independent of load or diet. However, visual inspection of the 3D data highlighted spatial differences in the thickness of core trabeculae compared to trabecular medulla. Technological advancement in  $\mu$ CT imaging/analysis in the last 10 years, including the 3D spatial reconstruction of cortical and trabecular thickness and density, has allowed for the visualisation of regional specific changes in morphology. The current study has been able to categorise the trabeculae in 3D in a way that has previously not, to our knowledge, been described in this model. Kerckhofs et al., (2016) demonstrated a similar system of 3D colour mapping of tibia trabecular thickness in a HFD model of type

2 diabetes mellitus and found an overall increase in trabecular thickness and no change in BV/TV%, or separation in their model.

Knowledge of the regional and spatial changes associated with trabeculae in particular is important as links between fracture risk and trabecular thinning have been well established in humans (McCloskey et al., 2016; Osterhoff et al., 2016; Tamura et al., 2004). For example vertebral trabecular bone score (TBS) in both men and women was a significant independent predictor of fracture (C. De Laet et al., 2005). Furthermore, Fields and Keaveny (2012) summarised that trabecular architecture, most notably a reduction in vertical struts, increased vertebral fragility. They also concluded that increasing knowledge of regional specific changes in trabeculae is important to improve fracture risk predictions in a clinical setting. Femoral neck fracture risk may also be reduced if interventions focus on increasing proximal femur trabecular bone architecture (Thomas et al., 2009). Obesity and percentage fat accumulation have been linked with all incidence fracture risk in older adults more so than BMI (Gandham et al., 2020). However a recent meta analysis of fracture risk in obese adults described the need for site specific fracture studies, specifically differences in bone microarchitecture in models with and without obesity (Turcotte et al., 2021). In this study, although no statistically significant differences were observed in maximal load withstood by tibiae during 3-point bend testing, Ob/Ob tibiae consistently withstood less force then weight paired C57 counterparts. These findings are in line with findings from a study from Soloman et al., in 2014, which revealed that the tibiae of C57 mice treated with a leptin agonist were consistently able to withstand more load than untreated controls. All vertebrae were utilised for immunohistochemical analysis, and therefore no mechanical testing could be performed upon these samples. Lack of statistical significance in this

study may have been overcome with the inclusion of more samples, as only three samples from each group were available for mechanical testing.

## **3.4.5.** Confounding Factors and Limitations:

It should be noted that the obese Ob/Ob mice were fed a CD instead of the HFD fed to the obese C57 controls in the interest of animal welfare. Therefore, the Obese Ob/Ob mice ate a different profile of dietary fats and carbohydrates compared to the Obese C57 group. Dysregulation of the gut microbiota and its role on bone turnover have been discussed previously (McCabe et al 2019). HFD, defined as a diet from which >30% of energy intake is accounted for by lipid consumption, has been reported to exert an effect upon bone, promoting bone loss and osteoporosis (Qiao et al., 2021) (Silva et al., 2019). HFD-fed mice are often used to model obesity-induced bone loss (Zhang et al., 2022). However, the independent effects of HFD consumption on bone remodelling are difficult to separate from the concomitant effects of HFD-induced increases in mechanical load from body weight, serum leptin, leptin resistance and body fat percentage (Han et al., 2021) (Mendoza-Herrera et al., 2021). The possibility that the obese C57 mice fed the HFD may become leptin resistant was considered due to the similar response in measured parameters to the obese Ob/Ob mice. It is well established that adipose tissue depots are positively correlated with circulating plasma leptin levels (Lönnqvist et al., 1997) and both obese C57 and obese Ob/Ob exhibited significant increases in overall body fat mass.

In addition, HFD promotes adipogenic differentiation of MSCs and yellow bone marrow formation, in turn suppressing osteoblast differentiation (Qiao et al., 2021). Despite results from this study providing no clear links between adiposity and osteoclast

number, co-culture of preosteoclasts with adipocytes in vitro has been shown to increase the presence of TRAP-positive multinucleated osteoclasts in vitro (Montalvany-Antonucci et al., 2018). HFD induced links to oxidative stress (OS) may also play a role. In brief, the exact relationship between OS and HFD consumption on bone remodelling remains poorly defined. However, it is known that HFD contributes to oxidative stress via production of reactive oxygen species (ROS) (Tan and Norhaizan, 2019) and ROS have been shown to activate osteoclast differentiation whilst inducing osteocyte apoptosis and inhibiting osteoblast activity, facilitating bone resorption and suppressing bone formation (Domazetovic et al., 2017). Similarly, HFDs induce metabolic inflammation in many organs, increasing levels of endotoxins, hormones (growth hormone//insulin-like growth factor-1 and elevated parathyroid hormone) circulating free fatty acids and inflammatory mediators (Duan et al., 2018). There are clearly many links between HFD feeding and bone turnover that are beyond the scope of this study but have been largely controlled for by maintaining total body weight and comparing body composition in the form of fat and lean mass.

Finally, tibiae from lean *Ob/Ob* mice were unavailable for immunohistochemical analysis or mechanical testing, limiting the ability of this study to draw conclusions regarding the effects of leptin deficiency upon bone turnover markers in the absence of increased mechanical load from body weight. Alongside this, blood serum from these animals were unavailable during this study but would have been utilised to shed more light on cellular mechanisms underpinning the morphological changes observed in this study. For example, this work could have included assessment of RANKL:OPG ratio in blood serum instead of via IHC, which is more widely utilised method of assessing RANKL:OPG ratio, an important predictor of bone health and the balance of bone formation and

resorption in the clinic (Marcadet et al., 2022). Similarly, assessment of circulating leptin levels in the blood plasma of these animals would have provided additional insights into the metabolic profiles of these animals; including assessing leptin resistance in C57 mice and confirming the absence of leptin expression in *Ob/Ob* animals.

In conclusion, leptin deficiency independent of changes in body weight had a significant effect on both tibia and vertebral cortical and trabecular bone *in vivo*. The overall morphological changes were similar in size and effect to that of HFD induced obesity. However, technological advances in image analysis of  $\mu$ CT data have enabled previously hidden changes in regional and spatial trabecular thickness to be quantified using 3D spatial segmentation. Further analysis using this segmentation approach may allow clinicians to better understand overall fracture risk and more accurately help identify preventative measures in at risk groups.

4.	Chapter	4:	Interactions	Between	Hormone
Signall	ing and Me	echa	nical Loading ir	n Murine Bo	one Cells <i>In</i>
Vitro:					

### 4.1. Introduction:

Mechanical loading imparted upon the skeleton from body weight and physical activity has profound effects on bone remodelling by altering the differentiation and activity of osteoblasts, osteocytes, and osteoclasts (Stewart et al., 2020). These mechanical signals are required for healthy development and maintenance of the skeleton *in utero* and throughout human lifespan (Robling and Turner, 2009), and alterations in mechanical loading can have significant effects upon bone health (Cao, 2011).

Traditionally, obesity is believed to benefit bone health by increasing body weight, and therefore the well-established effects of mechanotransduction in bone; resulting in increased BMD (Hou et al., 2020). However, there are several other important physiological differences between obese and lean individuals which are often overlooked or not controlled within *in vivo* studies, when investigating the relationship between obesity and bone health. These include differences in various endocrine factors, nutrition, and physical activity (Hou et al., 2020).

The isolated effects of mechanical loading upon various monolayer bone cell models *in vitro* have been widely studied, using a broad range of techniques including vibration (García-López et al., 2020), substrate strain (Banes et al., 1985) and fluid shear stress (FSS) (Wittkowske et al., 2016). This study aimed to investigate the relationship between leptin and testosterone signalling on mechanotransduction *in vitro*, without the presence of confounding variables which are present in many *in vivo* studies such as nutrition and differences in activity.

FSS is widely used *in vitro* to model the effects of mechanotransduction, due to its ease of application, reproducibility, and physiological relevance. The effects of FSS are essential for various processes throughout the body, ranging from maintenance of the

endothelial layer in response to frictional forces generated by the blood flow (Roux et al., 2020) to the mechanical stimulation of bone cells by the flow of interstitial fluid (ISF) through skeletal pores (Wittkowske et al., 2016). ISF flows freely through the Lacunae-canaliculi system (LCS) within bone, the LCS is comprised of channel-like structures surrounding osteocytes within mineralised bone tissue, allowing for nutrient exchange and the elimination of metabolic waste in bone tissue (L. Wang, 2018). Compressive mechanical loading of bones results in matrix deformation, and drives the flow of ISF through the LCS with greater force than in soft tissues (Duncan and Turner, 1995), as the fluid is forced through the narrow channels connecting osteocytes. This results in increased FSS within the LCS, and is estimated to range between 0.8 and 3 Pa (Weinbaum et al., 1994). This establishes FSS as an important source of mechanical stress within bone, and one which can be deployed *in vitro* with relative ease.

Primary osteoblasts isolated from human bone tissue are considered good candidates for preclinical research due to interspecies variation (Jonsson et al., 1999). However, the behaviour of these cells depends on a variety of unavoidable factors which can be controlled by working with cell lines derived from animals (Ansari et al., 2021). The MC3T3-E1 pre-osteoblast cell line, derived from primary cells collected from the calvaria of a newborn mouse are widely used in studies investigating osteoblastic mechanisms, including the effects of mechanotransduction in bone (Wittkowske et al., 2016). Most studies utilising MC3T3-E1 cells do so as a model of pre-osteoblasts, investigating early osteoblast differentiation and osteogenic factors. However, differentiation of MC3T3-E1 pre-osteoblasts into mature, mineralising osteoblasts can be induced via the addition of ascorbic acid,  $\beta$ -glycophosphate and dexamethasone to cell culture media (Hwang and Horton, 2019). MC3T3-E1 cells cultured in this modified differentiation medium

demonstrate significantly increased *in vitro* mineralisation compared to  $\alpha$ -MEM alone after 21 days of culture (Izumiya et al., 2021).

Previous studies have demonstrated that application of FSS to MC3T3-E1 cells significantly increases their growth and proliferation (Y. Yang et al., 2023), as well as driving osteoblastic differentiation via expression of the key osteoblast gene *RUNX2* (Pei et al., 2022; Yu et al., 2017). Application of FSS to MC3T3-E1 cells *in vitro* for as little as one hour increases *RUNX2*, *ALP* and *Col I* protein expression as well as *in vitro* mineralisation (Pei et al., 2022), indicating increased differentiation to mature osteoblasts vs static, unloaded controls. The effects of mechanotransduction upon MC3T3-E1 pre-osteoblasts in culture has been widely studied, however the effects of mechanical load on mature, differentiated MC3T3-E1 cells are less well documented. Furthermore, the effects of hormone signalling upon mechanoresponsivity within these cells is still not understood.

Osteocytes are another important cell mechanoresponsive cell type in bone, which were represented in this study with the use of the MLO-Y4 osteocyte cell line. The MLO-Y4 cell line, derived from murine long bone, is an osteocytic cell line expressing long dendritic processes forming functional gap junctions between neighbouring cells (Bonewald, 1999). This cell line has been utilised to investigate osteocytic mechanisms of mechanotransduction *in vitro* in both 2D and 3D environments (Zarka et al., 2021). Much like results from similar studies using MC3T3-E1 pre-osteoblasts, application of FSS to MLO-Y4 cells *in vitro* results in the promotion of OPG and inhibition of RANKL expression (Liu et al., 2022).

Traditional 2D cell culture methods rely on adherence of cells to a flat surface, typically polystyrene, to provide mechanical support for cells and allow for homogenous nutrient

access and therefore homogenous growth and proliferation (Duval et al., 2017). Cell microenvironments in vitro differ significantly from those in vivo, owing in part to attachments and connections to surrounding ECM and neighbouring cells as opposed to attachment to a single surface as seen in vitro. Despite the advantages and ease of application of 2D culture models, they do not wholly represent complex interactions between bone cells and surrounding ECM (Yuste et al., 2021). Increasing ECM dimensionality from 2D to 3D significantly impacts cell proliferation, differentiation, survival and mechano-responses (B. M. Baker and Chen, 2012), meaning 2D representations of cell response to stimuli is only partially representative of in vivo behaviour. As such, this surrounding ECM plays a crucial role in the conduction of mechanical forces in vivo, including those from muscle contraction and gravity (Humphrey et al., 2014), and is therefore a key factor in mechanical homeostasis. In bone, mechanotransduction is primarily initiated by interactions between various integrins, expressed by both osteoblasts and osteocytes, and surrounding ECM (Z. Sun et al., 2016). Interactions between  $\alpha 5\beta 1$  and  $\alpha 3\beta 1$  integrins mediate mechanical responses of cells of osteoblast lineage through attachments to various ECM components including fibronectin (Liu et al., 2023).

As such, a 2014 study by Matthews et al., provided a comparison between MC3T3 cell behaviour in 2D monolayer and 3D collagen hydrogel cultures, demonstrating that several bone-associated genes including osteocalcin and ALP were upregulated in MC3T3 cells when cultured in 3D compared to 2D for a period of 24 days. Additionally, cells cultured in 3D exhibited increased differentiation and therefore mineralisation compared to 2D controls (Matthews et al., 2014). Results from this and similar studies

highlight the importance of recreating a representative bone microenvironment to accurately assess cellular responses to stimuli.

Various 3D models of cell culture have emerged in recent years as promising tools to deepen our understanding of complex cellular responses to stimuli in a physiologically relevant, 3D setting (Yuste et al., 2021). One such 3D culture method involves the use of high cell density spheroid models, enhancing cell-cell interaction. This 3D culture method greatly enhances gene expression of several osteocyte markers in MC3T3-E1 pre-osteoblasts compared to 2D cultures, indicating increased osteoblast maturation (J. Kim et al., 2021). Furthermore, MC3T3-E1 spheroid cultures display increased mineralisation and differentiation when cultured in osteogenic medium (Koblenzer et al., 2022). Together, these results establish spheroid models as a useful, responsive tool for the study of bone cell behaviour in 3D. Despite this, however, the model does not lend itself to mechanical testing, although one recent study did achieve this by encapsulating spheroids in alginate gels which were subsequently subjected to compressive loading (Thai et al., 2024).

Other studies of bone cell behaviour in 3D utilise porous hydroxyapatite artificial bone scaffolds, created via lyophilisation of liquid scaffold components to produce a porous 3D scaffold (T.R. Kim et al., 2019). These structures provide enhanced mechanical strength compared to spheroid cultures, and the compositions can be tweaked to include a number of components including chitosan, hydroxyapatite nanoparticles and collagens (Selim et al., 2024). Additionally, lyophilised scaffolds provide representative mechanical properties for the study of bone, and can be used to study the effects of compressive loading (Touaiher et al., 2023). However, these systems require great precision to reliably produce uniformly porous scaffolds, introducing a degree of

variability into studies where the production of these scaffolds cannot be tightly controlled (Diez-Escudero et al., 2021).

Alongside these methods, hydrogel scaffolds, often consisting of Collagen type I, have been used to encapsulate cells in a hydrophilic polymer network with similar osmolality to physiological tissues (Duval et al., 2017). These hydrogel scaffolds can be used to recapitulate the bone microenvironment, fostering osteoblast proliferation and differentiation (S. Kim and Lee, 2020). Collagen type I, a vital component of bone matrix, is a favourable candidate material for use in 3D hydrogel scaffolds due to its ability to form intrinsic cell-binding motifs and nanoarchitecture (Chung et al., 2013).

The aim of this study was to investigate the interactions between hormone signalling and *in vitro* mechanical loading in cells of osteoblast lineage. By assessing both individual and combined effects, this work aims to provide insights into the influence of interactions between hormone signalling and mechanical loading in bone.

The hypothesis for this work package was that testosterone and leptin treatments will alter bone cell response to mechanical loading *in vitro*, either bolstering or attenuating the effects thereof in comparison to mechanical loading alone.

The aims of this study were:

- To establish the impact of testosterone treatment upon bone cell mechanoresponsivity in vitro.
- To establish the impact of leptin treatment upon bone cell mechanoresponsivity in vitro.
- To establish a suitable model to further investigate interactions between hormone signalling and mechanical loading in 3D in vitro studies.

## 4.2. Materials and Methods:

#### 4.2.1. Experimental Design:

This study aimed to establish a model suitable for the investigation of interactions between mechanotransduction and leptin or testosterone signalling in both osteoblast (MC3T3-E1) and osteocyte (MLO-Y4) murine cell lines. The effects of leptin or testosterone *in vivo* are often hard to separate from the effects of concomitant alterations to mechanical loading from body weight, and this series of experiments was designed to investigate interactions between the two pathways as well as their independent effects on different bone cell types.

To achieve this, 2D FSS and 3D hydrostatic loading strategies were applied to cells *in vitro*, either alone or in combination with leptin or testosterone treatment and compared to static controls. FSS is widely used *in vitro* to model the effects of mechanotransduction, and is sufficient to elicit osteogenic effects in MC3T3-E1 cells (Pei et al., 2022). Similarly, hydrostatic loading has been applied in a variety of settings, and also stimulates osteogenesis *in vitro* (H.-X. Shen et al., 2022).

Alterations in expression of key genes of interest including RUNX2, ALP, RANKL, OPG, SPOCK1, LepR and AR were assessed against housekeeping genes using qRT-PCR for 2D cell culture and FSS experiments. ALP enzyme activity in the conditioned media was also measured. For 3D culture experiments, cells were grown in either collagen hydrogels, or a hydroxyapatite-containing hydrogel, B-Gel. MG63 cells were used initially as a model to develop the 3D culture system. The effects of the treatment regimens upon matrix deposition was assessed using Masson's trichrome and Alizarin red histological staining techniques.

#### 4.2.2. MC3T3-E1 Cell Culture and Differentiation:

MC3T3-E1 murine pre-osteoblastic cells (ATCC) were cultured in ascorbic acid free  $\alpha$ -MEM (Gibco) containing 10% FBS (Gibco) and 1% Pen-Strep (PAA Laboratories) and maintained in a 5% CO<sub>2</sub> humidified environment at 37°C. Medium was changed every three days. MC3T3-E1 cells were differentiated in modified  $\alpha$ -MEM (Gibco) containing 2 mg/mL dexamethasone (Merck), 10 mM  $\beta$ -glycophosphate (sigma), and 50  $\mu$ g/mL L-ascorbic acid (Sigma). Medium was changed every three days for a total of 21 days.

#### 4.2.3. MLO-Y4 Cell Culture:

Flasks were coated with rat-tail Collagen I (Corning) diluted to 0.15 mg/mL in 0.02M filter-sterilised acetic acid at least 1 hour before use. MLO-Y4 murine osteocyte-like cells, a kind gift from Stefaan Verbruggen at the University of Sheffield, were cultured in rat tail collagen I coated cell culture flasks with  $\alpha$ -MEM (Gibco) supplemented with 2.5% foetal bovine serum (FBS), 2.5% foetal calf serum (FCS) and 1% penicillin/streptomycin (PAA Laboratories). Cells were maintained at 37°C, 5% CO<sub>2</sub> and 95% humidity during culture in an incubator.

#### 4.2.4. Leptin and Testosterone Treatment:

MLO-Y4 or undifferentiated/differentiated MC3T3-E1 cells were seeded at a density of  $6x10^5$  cells/mL in  $25cm^2$  culture flasks and allowed to adhere overnight before treatment with either complete  $\alpha$ -MEM containing 80 ng/mL of recombinant leptin (Invitrogen, Massachusetts, United States) 10 ng/mL of testosterone (Sigma) or complete  $\alpha$ -MEM control. Cells were incubated in leptin or media control for 24hrs prior to application of fluid shear stress. Leptin treatment concentrations were chosen to recapitulate the

levels observed in human morbid obesity (Chaves et al., 2022), whereas testosterone treatment concentrations were within the normal physiological range (Sedelaar et al., 2013)

#### 4.2.5. Leptin and Testosterone Degradation in Cell Culture Media:

Leptin (Abcam, ab108879) and testosterone (Abcam, ab198666) ELISA kits were used to assess the degradation of hormone treatments in cell culture media over a period of 72 hours, in the presence of MC3T3-E1 cells. Leptin and testosterone stocks were diluted to 15 ng/ML in complete  $\alpha$ -MEM (Gibco) alongside a complete media only control. Treatment media was then collected after 0, 2, 4, 8, 24, 48, or 72 hour time points and frozen at -20°C before testing alongside a freshly made, unfrozen 0 hour time point.

The ELISA kits were used according to manufacturer instructions. Briefly, all supplied materials and samples were allowed to equilibrate to room temperature prior to use. The provided leptin standard was reconstituted to form a 32 ng/mL leptin solution in the supplied diluent buffer, which was then serially diluted further in diluent buffer to create additional standard concentrations of 8, 2, and 0.5 ng/mL as per manufacturer instructions alongside a 0 ng/mL standard containing only diluent buffer.

Fifty microlitres of sample, standard or blanks were added in triplicate to each well of the supplied ELISA plate before covering with sealing tape and incubating for 2 hours at RT. Wells were then washed 5 times with 200  $\mu$ L of 1X wash buffer and thoroughly dried before adding 50  $\mu$ L of 1X biotinylated leptin antibody to each well, covering with sealing tape and allowing to incubate for a further 2 hours at RT. The plate was then washed as described above prior to adding 50  $\mu$ L of 1X SP conjugate to each well, covering and incubating for 30 minutes at RT. After another wash, 50  $\mu$ L of stop solution was added to each well and mixed thoroughly. Absorbance readings were measured at 450 nm

immediately using a ClarioStar reader (BMG Labtech), and background was deducted from media only controls (Figure 4.1).

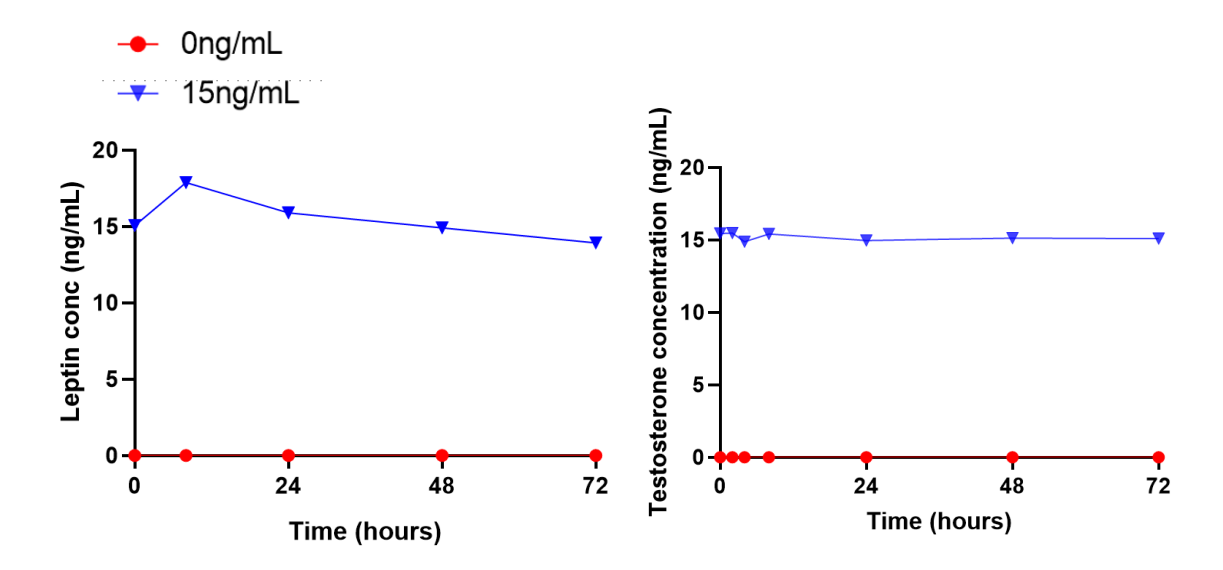


**Figure 4.1:** Concentrations of leptin (A) and testosterone (B) in cell culture media over the course of 72 hours, measured via ELISA.

### 4.2.6. Fluid Shear Stress Application:

25cm² cell culture flasks seeded with either differentiated or undifferentiated MC3T3-E1 cells, or MLO-Y4 cells with or without hormone treatment were placed against the outside edge of a see-saw rocker (Fisher Scientific) at 30 rpm (0.5hz) inside an incubator and cultured for a further 24hrs whilst rocking prior to harvesting. Resulting fluid shear stress imparted upon the cell-laden surface by the movement of cell culture media was calculated as 0.88 Pa (8.8 dyne/cm²) using the following equation:

$$T\omega = \frac{3\pi\mu L}{2h_0 T}$$

Previous work has shown that 5 dyne/cm<sup>2</sup> is sufficient to elicit a response in the gene expression of MC3T3-E1 cells, with 10 dyne/cm<sup>2</sup> providing a more significant impact (Pei et al., 2022).

#### 4.2.7. RNA Extraction:

Cell culture media was aspirated before cells were washed with PBS, and RNA was extracted using Trizol (Life Technologies) for 5 minutes at RT. Two hundred microlitres of chloroform (Sigma) was added to the solution before vortexing and allowing for separation for 3 minutes at RT before centrifugation at 12,000 g for 15 minutes at 4°C. Once separation of the DNA, RNA and protein layers had occurred, the top, clear aqueous RNA layer was aspirated and added to 500  $\mu$ L of molecular grade isopropanol (Sigma) and mixed before storage at -80°C to precipitate RNA. RNA samples were defrosted on ice prior to centrifugation at 12,000 g for 30 minutes. The supernatants were removed before washing in 0.5 mL of 90% ethanol, and samples were centrifuged again at 7500 g for 15 minutes. Supernatants were removed, and RNA pellets were left to air dry on ice for 30 minutes. Once dry, the RNA pellet was resuspended in 14  $\mu$ L of sterile dH<sub>2</sub>O.

# 4.2.8. cDNA Synthesis:

RNA samples were denatured at  $60^{\circ}$ C for 5 minutes prior to the addition of  $36\mu$ L of complete mastermix (Table 4.1). Samples were then incubated at  $42^{\circ}$ C for 2 hours

followed by 80°C for 10 minutes in a QuantStudio 3 real-time PCR system (Life Technologies, California, United States), prior to cooling to 4°C and storage at -20°C until use.

**Table 4.1:** Reverse transcriptase mastermix components. For each  $14\mu L$  sample,  $36\mu L$  of complete mastermix is added. dNTPS, Bioscript 5x RT buffer and Bioscript RT enzyme all purchased from Bioline. Random hexamers and RNase free H<sub>2</sub>O purchased from Thermo Fisher.

Component	Volume per reaction (μL)		
dNTP mix (200 mM)	1.5		
Random Hexamers (50 mM)	1.0		
Bioscript 5x RT buffer	5.0		
Bioscript RT enzyme	0.5		
RNase free H2O	28.0		

#### 4.2.9. Gene Expression Assessment via RT-qPCR:

Expression of target genes was assessed comparatively to housekeeping genes, β-actin and GAPDH via the use of quantitative real-time polymerase chain reaction (qRT-PCR), utilising pre-designed, commercially available Taqman™ primers designed to detect cDNA corresponding to genes of interest (Table 4.2) (Thermo Fisher Scientific). Housekeeping genes B-Actin and GAPDH were selected for their stable expression in cells subjected to planned treatment regimes.

**Table 4.2:** List of mouse primers (ThermoFisher, UK) used for qRT-PCR experiments, alongside associated assay IDs.

Target Gene	Assay ID
B-Actin	Mm00483039_m1
GAPDH	Mm9999915_g1
RUNX2	Mm00501584_m1
ALP	Mm00475834_m1
OPG	Mm00435454_m1
RANKL	Mm00441906_m1
LepR	Mm00440181_m1
AR	Mm00442688_m1
SPOCK1	Mm00486393_m1

qRT-PCR was performed upon triplicate samples from three biological repeats of fluid shear stress +/- hormone treatment regimens and appropriate controls. A 2  $\mu$ L volume of cDNA sample was added in duplicate to wells of 96-well FAST PCR plates (Thermo Fisher Scientific). qRT-PCR mastermix was prepared by combining 5  $\mu$ L of 2x Taqman fast mastermix (Life Technologies) with 0.5  $\mu$ L of relevant Taqman<sup>TM</sup> primers and 2.5  $\mu$ L sterile deionised H<sub>2</sub>O per reaction.

Plates were sealed with MicroAmp™ optical adhesive film (Thermo Fisher Scientific), and briefly centrifuged in a plate centrifuge to collect samples at the bottom of the wells. Target gene expression was assessed using a QuantStudio 3 real time PCR instrument (Life Technologies) utilising the fast programme. In this regime, the temperature was first ramped to 95°C for 10 minutes to activate the Taq polymerase, prior to 50 cycles of denaturation at 95°C for 1 second, and subsequently annealing and extension at 60°C

for 20 seconds. Results were analysed using the  $2^{-\Delta Ct}$  method (Livak and Schmittgen, 2001) and presented as relative expression of target genes normalised to the average CT values of GAPDH and  $\beta$ -actin.

#### 4.2.10. MG63 Cell Culture and Maintenance:

MG63 human osteosarcoma cells (ATCC) were cultured in  $\alpha$ -MEM (Gibco) supplemented with 10% FBS (Gibco) and 1% Pen-Strep (PAA Labdoratoriesi) (complete media) and maintained in a 5% CO<sub>2</sub>, 21% O<sub>2</sub> humidified environment at 37°C. Cells were passaged at 80 % confluence and used prior to passage 20. Mycoplasma testing was performed on conditioned media samples from live cultures every 6 months, and no mycoplasma infections were detected throughout.

## 4.2.11. Collagen Gel Constructs:

Collagen gel constructs occupying a total volume of 300  $\mu$ L were cast in a 48 well plate according to manufacturer instructions. Briefly, MG63 cells were detached and counted as previously described, before adding 50  $\mu$ L of cell suspension to 250  $\mu$ L of rat tail collagen (Corning, New York, United States) at a density of  $1.25 \times 10^6$  cells per mL of gel. For acellular controls, a matched 50  $\mu$ L volume of complete media was added to gels as a control. Reagents were kept on ice throughout to prevent the collagen from setting prematurely, and sterile NaOH was added last to increase the pH of the solution and initiate polymerisation of the collagen gels. For cell-containing gels Gels were mixed thoroughly using a syringe to ensure homogenous distribution of cells throughout the construct, and equal dispersion of the NaOH setting agent to ensure equal setting. MG63-containing or acellular control 3D collagen type I constructs were cast into wells

of a 48 well plate and any bubbles were removed with a syringe before allowing gels to set at 37 °C for 1 hour. Once gels were set, 300  $\mu$ L of complete media was added to wells and gels were cultured as normal for a further one, two, or four weeks, with media changes every 3 days.

### 4.2.12. Cell-laden Collagen I Gel Processing:

Gels were harvested at one-, two-, or four-week time points and fixed in 10% neutral buffered formalin for 1 hour at room temperature. Gels were then washed in PBS before processing to paraffin wax in a TP1020 tissue processor (Leica Microsystems, Milton Keynes UK). Briefly, samples were dehydrated in a series of graded IMS solutions (70, 80, 90, and 100 % w/v) for 30 minutes each. Samples were then cleared through Sub-X (Leica Biosystems and finally  $60^{\circ}$ C liquid paraffin wax under vacuum for 30 minutes in each solution. After processing, gels were sliced in half and embedded in paraffin wax, with one half embedded longitudinally and the other embedded laterally to allow for two distinct cross sections. Embedded gels were then cut into 4  $\mu$ m sections using a microtome (Leica Microsystems) and mounted to extra adhesive microscope slides (Leica Microsystems) before being left to dry for two weeks at 37°C.

### 4.2.13. Immunohistochemistry and Histology:

IHC staining for FAK (Abcam, ab40794, 1:500) and Ki67 (Abcam, ab15580, 1:500) and histology procedures were performed with enzyme antigen retrieval as previously described in section 3.2.16.

#### 4.2.14. Hydrogel Preparation:

Three dimensional studies were performed using a hydrogel system previously shown to support bone cells (Thorpe et al., 2016, 2018) known as B-gel. To formulate B-gel an exfoliated suspension of Laponite® clay particles (25-30 nm diameter, < 1 nm thickness) (BYK additives Ltd.) was prepared via vigorous stirring of 0.1 g of Laponite® in 9mL of deionised h<sub>2</sub>0 for 24 hours. 0.783 g of 99% N-isopropylacrylamide (NIPAM) (Sigma), 0.117 g of N, N'-Dimethylacrylamide (DMAc) (Sigma) and 9 mg of 2-2'azobisisobutyronitrile (AIBN) were added to the resulting suspension and stirred for an additional 1 hour. This suspension was then passed through a 5-8 μm pore filter. The hydrogel was prepared to this stage by Joseph Snuggs and Ronak Janini. Polymerisation was initiated by heating to 80°C for a minimum of 4 hrs. Polymerisation is evidenced by a transition from a transparent, colourless liquid into a milky white suspension. The resulting hydrogel suspension is a statistical copolymer, composed of 1% Laponite, 7.83% NIPAM, 1.17% DMAc and 90% w/w water. At this stage, the gel was cooled to 50°C and 0.5 mg/ml of hydroxyapatite nanoparticles (< 200 nm) (Sigma, 702153) were mixed into the suspension until homogenous.

#### 4.2.15.

### 4.2.16. 3D Cell Culture of MC3T3-E1 Cells in Hydrogel:

Hydrogel suspensions were allowed to cool to 38-39°C in a temperature-controlled cell culture unit before differentiated or undifferentiated MC3T3-E1 cells were mixed with the gel at a density of  $5x10^6$  cells/mL of hydrogel, and 300  $\mu$ L cell containing constructs were cast in 48 well plates, giving a density of  $1.5x10^6$  cells per gel. Cell-laden gels were then allowed to set for 1 hour before the addition of relevant cell culture media. The

gels were then cultured for a further 48 hours before the addition of hormone treatment as previously described.

## **4.2.17.** Hydrostatic Loading of 3D Cell Constructs:

After 24 hours of culture in appropriate hormone treatment media, triplicate cell-laden hydrogel constructs were transferred to MechanoCulture TN (CellScale) loading wells containing 7 mL of control media or hormone treatment media described in section 4.2.8, with the addition of 12.5 mM HEPES to maintain pH within the sealed load chamber. Gels were hydrostatically loaded with oscillating 0.1 - 0.3 mPA of pressure every 0.5 seconds for 3 hours. Control gels were moved into matched volumes of treatment/control media and placed in the same incubator for the duration. After loading, gels were incubated for either a further 3 or 24 hours prior to fixation and collection of conditioned media.

#### 4.2.18. Matrix Deposition Within Hydrogel Constructs:

Triplicate sample gels were removed from culture and fixed for 24hrs in 10% formalin at room temperature, before washing with PBS and processing to paraffin wax as previously described in section 4.2.12. Processed gels were embedded in paraffin and sectioned at  $4\mu m$  on a Leica Microtome and mounted to Leica X-tra corner clipped slides with a positively charged coating (Leica Microsystems, Milton Keynes, UK) and left to dry and adhere for 2 weeks at 37 degrees. Sections were then dewaxed through a series of Sub-X (Leica Microsystems, Milton Keynes, UK) solutions (3 x 10 minutes) and rehydrated through graded IMS (Fisher, Loughborough, UK) solutions (3 x 10 minutes). Sections were then washed in distilled water for 5 minutes before staining with either

Alizarin Red (2% w/v, pH 4.2) (Sigma Aldrich, Poole, UK) for 15 minutes or Masson's Trichrome (Atom Scientific) according to instructions. Sections were then dehydrated through a series of IMS (4 x 10 minutes) and cleared in sub-x (3 x 10 minutes) and mounted in Pertex (Leica Microsystems, Milton Keynes). Stained sections were left to dry for 48 hours before imaging using an Olympus BX60 microscope and captured by a MicroCapture v5.0 RTV digital camera (Q Imaging, Buckinghamshire, UK) and CellSens software (Olympus). Three images of random fields of view were captured for each triplicate samples. This step was performed blinded.

## 4.2.19. Alkaline Phosphatase (ALP) Activity Assay:

ALP activity was assessed using a commercially available assay kit (Signa-Aldrich, MAK447) according to manufacturer's instructions. Briefly, all conditioned media samples from *in vitro* loading experiments and reagents were defrosted on ice and 50 μL of each sample was added in duplicate to wells of a 96 well plate, followed by 150 μL of the supplied working reagent and mixing. Optical density (OD) values were measured immediately against a tartrazine calibrant and a media blank at 405 nm using a ClarioStar reader (BMG Labtech) and again after 4 and 20 minutes of reaction time. ALP enzyme activity was calculated using the following equation:

$$ALP IU/L = \frac{(ODt20 - ODt0)x \ RxnVol \ x \ 35.3}{(ODcal - ODblank)x \ SmplVol \ x \ T}$$

#### 4.3. Results:

#### 4.3.1. Differentiation of MC3T3-E1 Cells In Vitro:

Relative gene expression of RUNX2, OPG and ALP were measured over the 21 day course of differentiating MC3T3-E1 cells *in vitro* to assess changes in key markers of bone formation throughout the course of differentiation (Figure 4.2). Whilst none of the alterations observed were significant, RUNX2 expression was highest after 21 days.

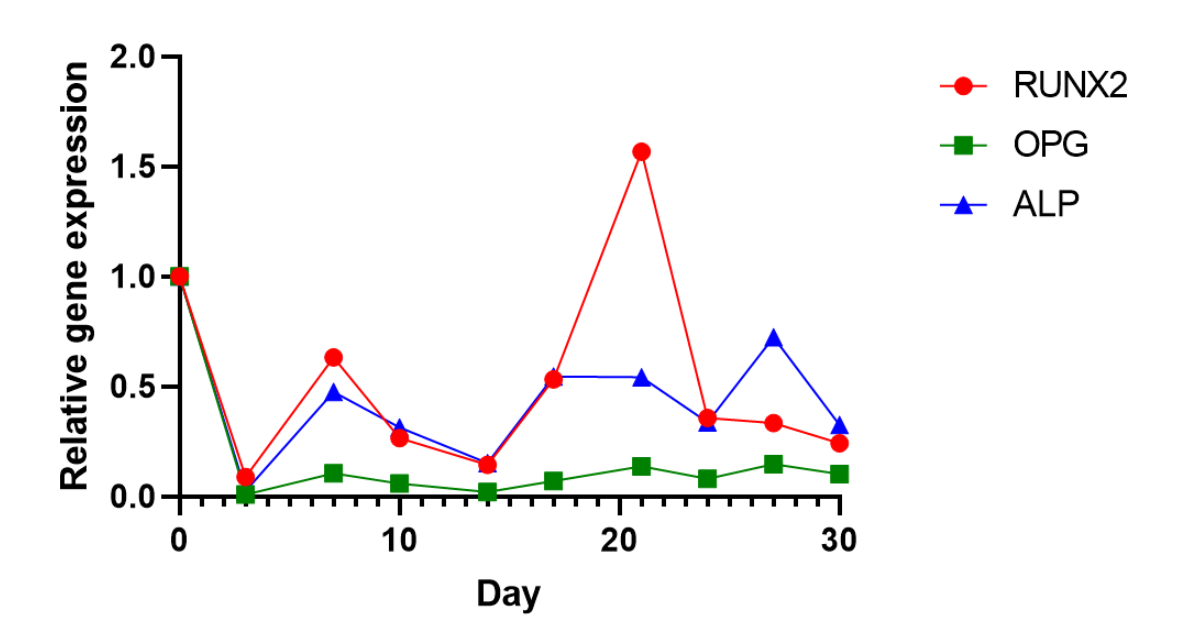


Figure 4.2: Relative gene expression of RUNX2 (red), OPG (green) and ALP (blue) in MC3T3-E1 cells over the course of 21 day *in vitro* differentiation in modified cell culture media.

# 4.3.2. Gene Expression of Key Bone Cell Markers in Undifferentiated MC3T3-E1 Cells:

Gene expression of several key bone factors was assessed using qPCR to assess the effects of leptin and testosterone treatment, either alone or alongside *in vitro* FSS. RUNX2 expression was quantified to determine the effects of hormones and *in vitro* 

mechanical load upon osteoblastic cell differentiation, no significant differences were detected between cells subjected to hormone treatment with or without FSS and static controls (Figure 4.5A). However, mean RUNX2 expression was consistently higher in MC3T3-E1 cells treated with testosterone (Figure 4.3A), more so alone (P = 0.4431) than when in combination with FSS (0.9262).

Additionally, ALP gene expression was used as an indicator of the effect of treatment regimens upon MC3T3-E1 cell mineralisation. Despite no significant differences between the groups, there was a slight trend towards decreased ALP expression in both, static (P = 0.8676) and loaded (P = 0.8470) testosterone treated conditions (Figure 4.3B). A very slight reduction in the ALP expression of cells subject to FSS (P = 0.9650) was reversed when combined with leptin treatment which resulted the highest mean ALP expression (P = 0.5071) (Figure 4.3B).

The ratio of RANKL:OPG gene expression was also assessed, to investigate the implications of these treatment conditions for osteoclastogenesis *in vivo*. Gene expression levels of RANKL and SPOCK1 were consistently below the limit of detection in all groups tested and are therefore not displayed. However, OPG expression was detected in all samples tested and remained consistent across all groups with no significant differences, despite an observed trend towards increased OPG expression in cells subjected to a combination of FSS and leptin treatment (P = 0.0906) (Figure 4.3C).

Gene expression of androgen and leptin receptors also did not differ significantly between groups, but did show slight responses to hormone and FSS treatment regimes. Firstly, mean AR receptor expression was consistently higher in MC3T3-E1 cells subjected to FSS alone (P = 0.7474), especially when paired with leptin (P = 0.3760), and less so when combined with testosterone treatment (P > 0.9352) conditions (Figure

4.3D). Similarly, LepR gene expression did not differ significantly between any of the groups, despite a small decrease in untreated cells subjected to FSS compared to controls (P > 0.9999) (Figure 4.3E). There were no significant differences detected in ALP activity, measured via colorimetric assay using cell culture media (Figure 4.3F).

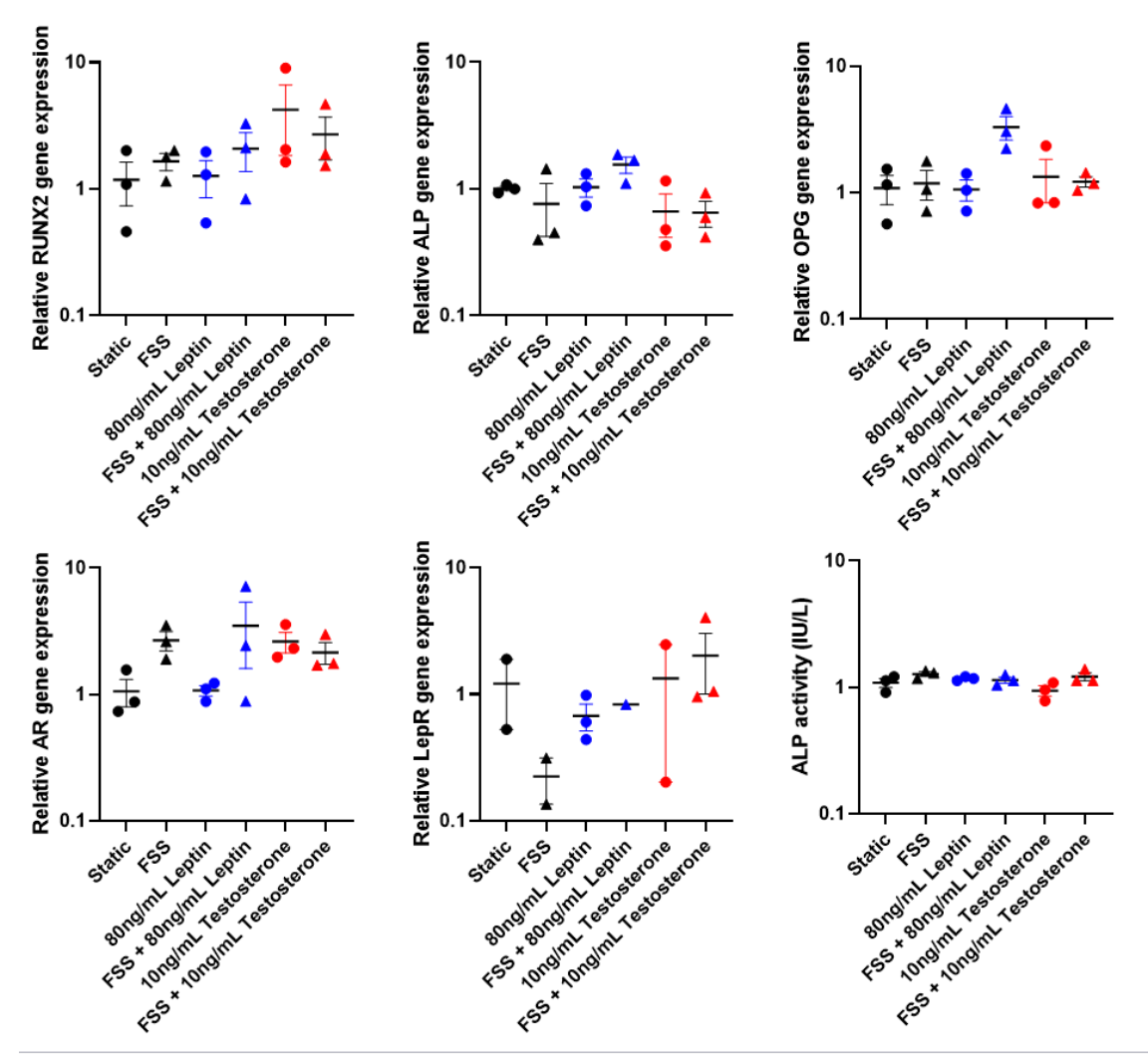


**Figure 4.3:** Relative gene expression of RUNX2 (A), ALP (B), OPG (C), AR (D), and LepR (E) measured via RT-qPCR, and ALP activity (F) in cell culture media from undifferentiated MC3T3-E1 cells treated with FSS and either 80 ng/mL leptin (n = 3) or 10 ng/mL testosterone (n = 3) alongside static controls (n = 3).

# 4.3.3. Gene Expression of key bone cell markers in differentiated MC3T3-E1 cells:

Similar to findings in undifferentiated MC3T3-E1 cells, differentiated counterparts showed no significant differences in RUNX2 expression in response to any of the groups tested (Figure 4.4A). Additionally, despite no statistical significance, slight trends seen in undifferentiated cells were reverted, with slightly decreased mean RUNX2 expression in both static and loaded MC3T3-E1 cells treated with testosterone (P > 0.9999) (Figure 4.6A).

ALP expression also did not differ significantly between groups (Figure 4.4B). Similarly, OPG expression did not differ significantly between groups but was again highest in MC3T3-E1 cells subjected to combined FSS and leptin treatment (P = 0.8259), whilst testosterone and FSS had little effect (Figure 4.4C). RANKL and SPOCK1 gene expression were once again below the detectable limit for all conditions tested and are not displayed. No significant differences in AR expression were detected in differentiated MC3T3-E1 cells in response to treatments, and the slight effects of load and testosterone seen in undifferentiated cells were no longer present (Figure 4.4D). Treatments also did not alter LepR gene expression significantly (Figure 4.4E).

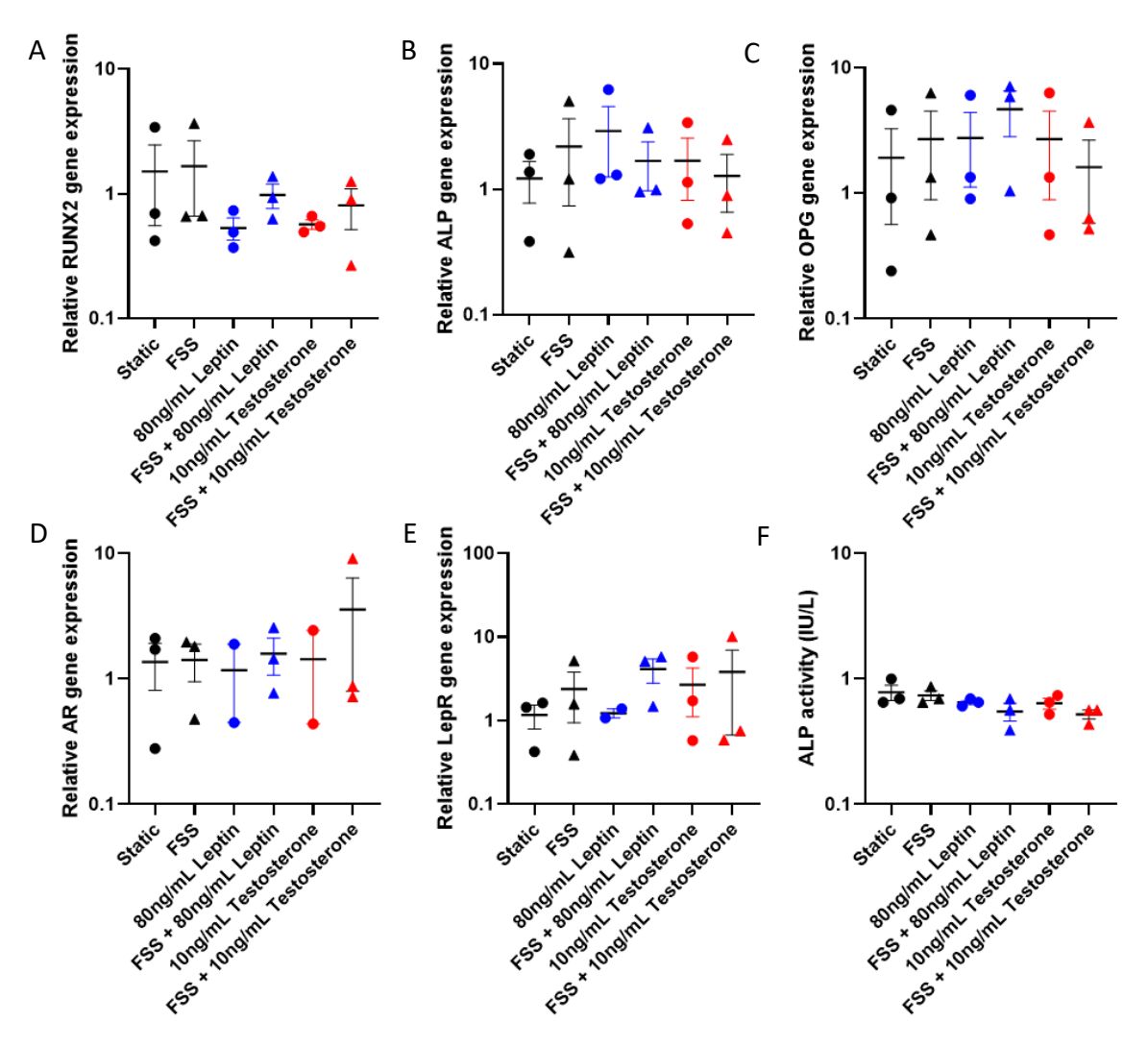


Figure 4.4: Relative gene expression of RUNX2 (A), ALP (B), OPG (C), AR (D), and LepR (E) measured via RT-qPCR, and ALP activity (F) in cell culture media from MC3T3-E1 cells treated with FSS and either 80 ng/mL leptin (n = 3) or 10 ng/mL testosterone (n = 3) alongside static controls (n = 3) after 21 days of culture in differentiation medium.

### 4.3.4. Gene expression of key bone cell markers in MLO-Y4:

A similar set of experiments utilising the same methodology and treatment regimes was performed upon MLO-Y4 cells. This work aimed to investigate whether the effects of hormones and mechanical load upon bone turnover were predominantly due to osteoblastic cells, or those of osteocytic lineage.

Despite clear expression of both housekeeping genes used in this study (Table 4.3), all other genes of interest tested in this study were below the limit of detection. Most

notably, neither AR nor LepR expression were detected in any of the samples tested, and thus they were not used for further studies investigating effects of Leptin and Testosterone.

**Table 4.3:** Average CT values obtained from qRT-PCR analysis of  $\beta$ -Actin and GAPDH gene expression in MLO-Y4 cells subjected to loading and hormone treatment regimes.

	Control	FSS	80 ng/mL	80 ng/mL	10 ng/mL	10 ng/mL
			Leptin	Leptin	Testosterone	Testosterone +
				+ FSS		FSS
β-Actin	27.300	31.920	28.528	33.208	28.024	32.216
GAPDH	27.132	31.630	26.371	33.051	25.509	30.326

# 4.3.5. Suitability of 3D collagen gels for in vitro loading:

Four micron sections of acellular and MG63-laden collagen gels were stained with HandE and assessed microscopically to determine cell viability when cultured in 3D collagen gels, and the suitability of the constructs for histological analysis. HandE stained MG63 cells were evident in the cell laden constructs, and the acellular controls did not demonstrate any false positives or background staining (Figure 4.5). There were consistently more cells present in gels fixed after 4 weeks of culture than those only cultured for 1 week.

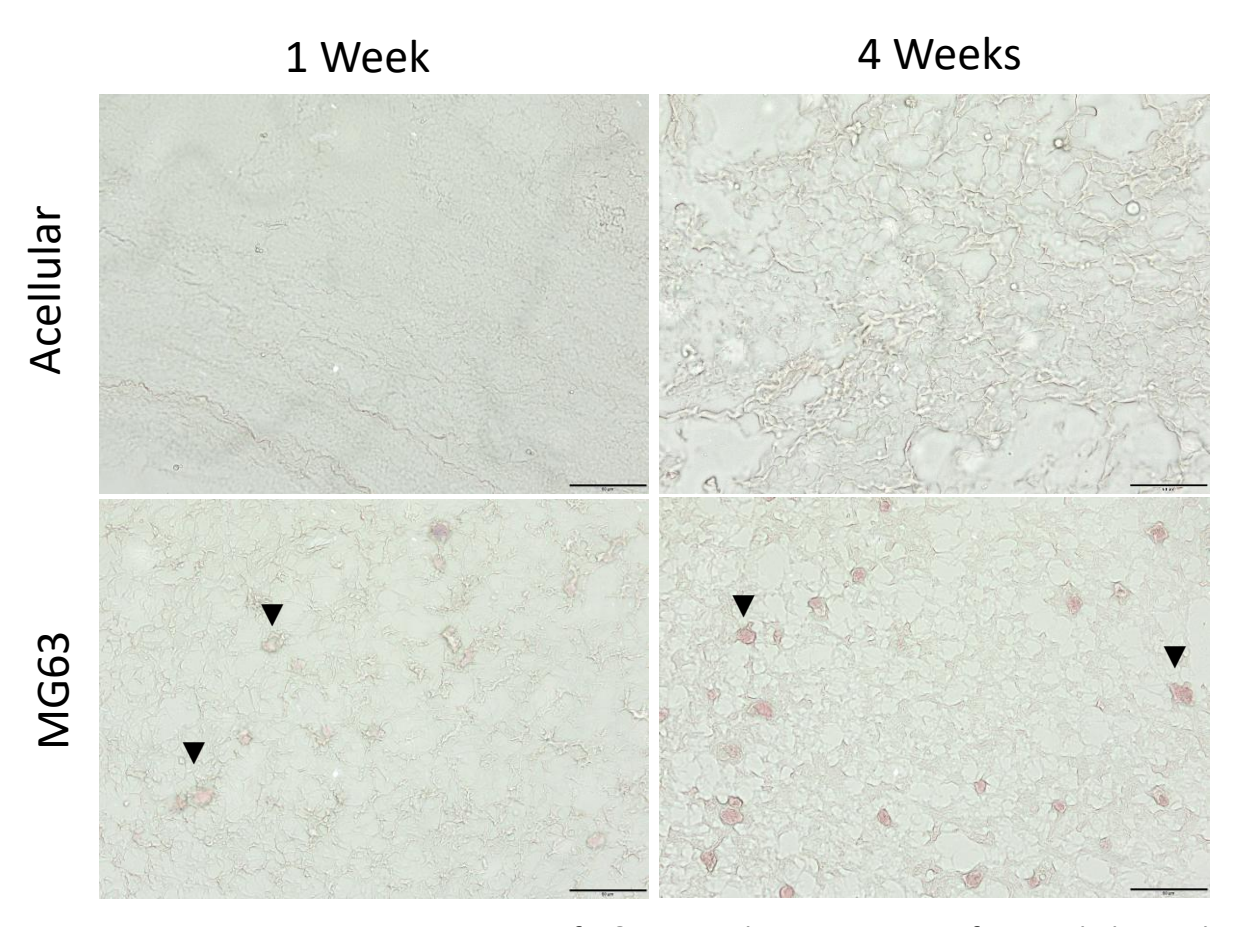


**Figure 4.5**: Representative images of H&E stained 4  $\mu$ m sections of MG63-laden and acellular collagen gel constructs after 1 or 4 weeks of culture. Scale bar = 50  $\mu$ m.  $\blacksquare$  denotes the presence of MG63 cells within the gel.

Additionally, MG63 cells cultured within collagen gels for 4 weeks displayed immunopositivity for both Ki67 (Figure 4.6A) and FAK (Figure 4.6B), indicating that these cells were still proliferating within the gel and were able to detect the presence of mechanical loading.

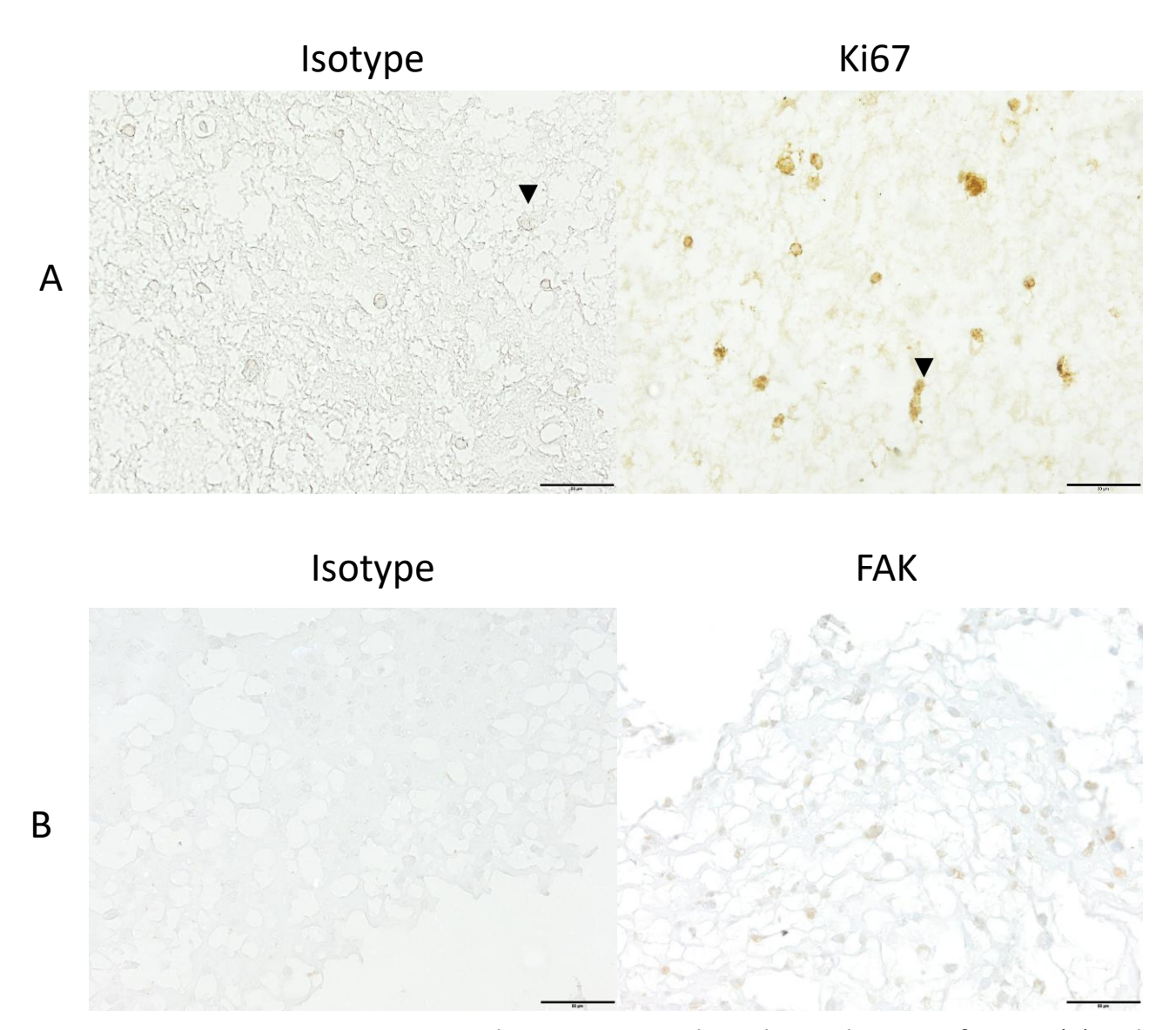


**Figure 4.6:** Representative images depicting immunohistochemical staining for Ki67 (A) and FAK (B) of  $4\mu m$  thick collagen gel sections cultured with MG63 cells for 4 weeks prior to staining. Scale bars are 50  $\mu m$ .

These 3D collagen gels were then subjected to compressive loading *in vitro*, but lacked the mechanical stiffness required to withstand even compressive loading and were destroyed in the process. As a result of this, an alternative, stiffer matrix of hydroxyapatite laden B-Gel was used for all future 3D cultures.

### 4.3.6. Matrix deposition of MC3T3-E1 cells in a 3D in vitro model of bone:

Massons Trichrome and alizarin red staining were used to assess collagen and calcium matrix deposition respectively within 4 µm sections of cell-laden B-gel in response to mechanical loading via *in vitro* hydrostatic loading, alone or in combination with either leptin or testosterone treatment. In addition to this, undifferentiated MC3T3-E1 preosteoblasts were compared to MC3T3-E1 cells in which differentiation had been induced with osteogenic media supplements.

Although these qualitative assessments cannot be reliably quantified, there is a clear trend towards increased collagen deposition, identifiable by deep blue staining, in both loaded and static conditions in undifferentiated MC3T3-E1 cells treated with either leptin or testosterone, compared to untreated controls (Figure 4.7). Conversely, only loading was able to induce increased collagen deposition in MC3T3-E1 cells differentiated in osteogenic medium for 21 days during 3D culture. In these differentiated MC3T3-E1 cells, neither leptin nor testosterone treatment resulted in any observable differences in collagen deposition compared to untreated controls although loaded gels appeared to contain more collagen (Figure 4.7).

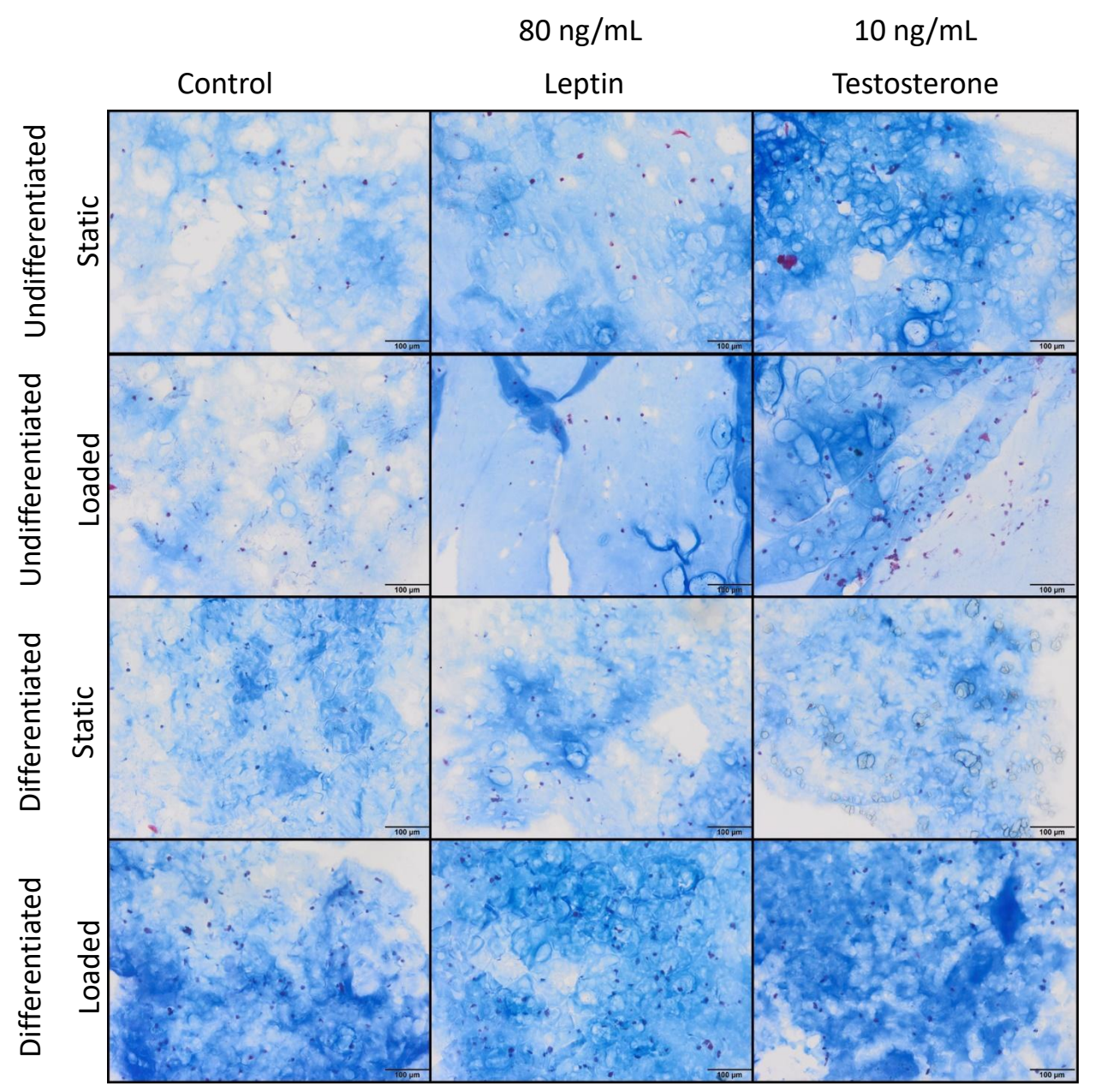


**Figure 4.7:** Representative images depicting Masson's trichrome stained sections of B-gel constructs laden with either undifferentiated MC3T3-E1 cells, or MC3T3-E1 cells that had been differentiated in osteogenic medium for 21 days. Cell-laden constructs either remained unloaded or were subjected to 0.3 mPa of hydrostatic pressure, alongside treatment with either 10 ng/mL testosterone or 80 ng/mL leptin. n = 3 for all groups. Scale bars are 100  $\mu$ m.

Similarly, although unquantifiable, alizarin red staining revealed that both leptin and testosterone staining appeared to slightly increase the presence of calcified nodes highlighted by deep red staining, in static, undifferentiated MC3T3-E1 cells (Figure 4.8). Hydrostatic loading appeared to increase the presence of calcified nodes in both untreated and leptin treated cells, but not in testosterone treated cells, compared to static controls. As observed with collagen deposition, neither leptin nor testosterone treatment appeared to increase calcification in differentiated MC3T3-E1 cells; although in this case load did not appear to significantly alter matrix deposition either (Figure 4.8). Both hormone treatments, but not hydrostatic loading, induce increased matrix deposition in undifferentiated MC3T3-E1 cells. In differentiated MC3T3-E1 cells, hormone treatments no longer induce this effect and load is a more potent inducer of matrix deposition.

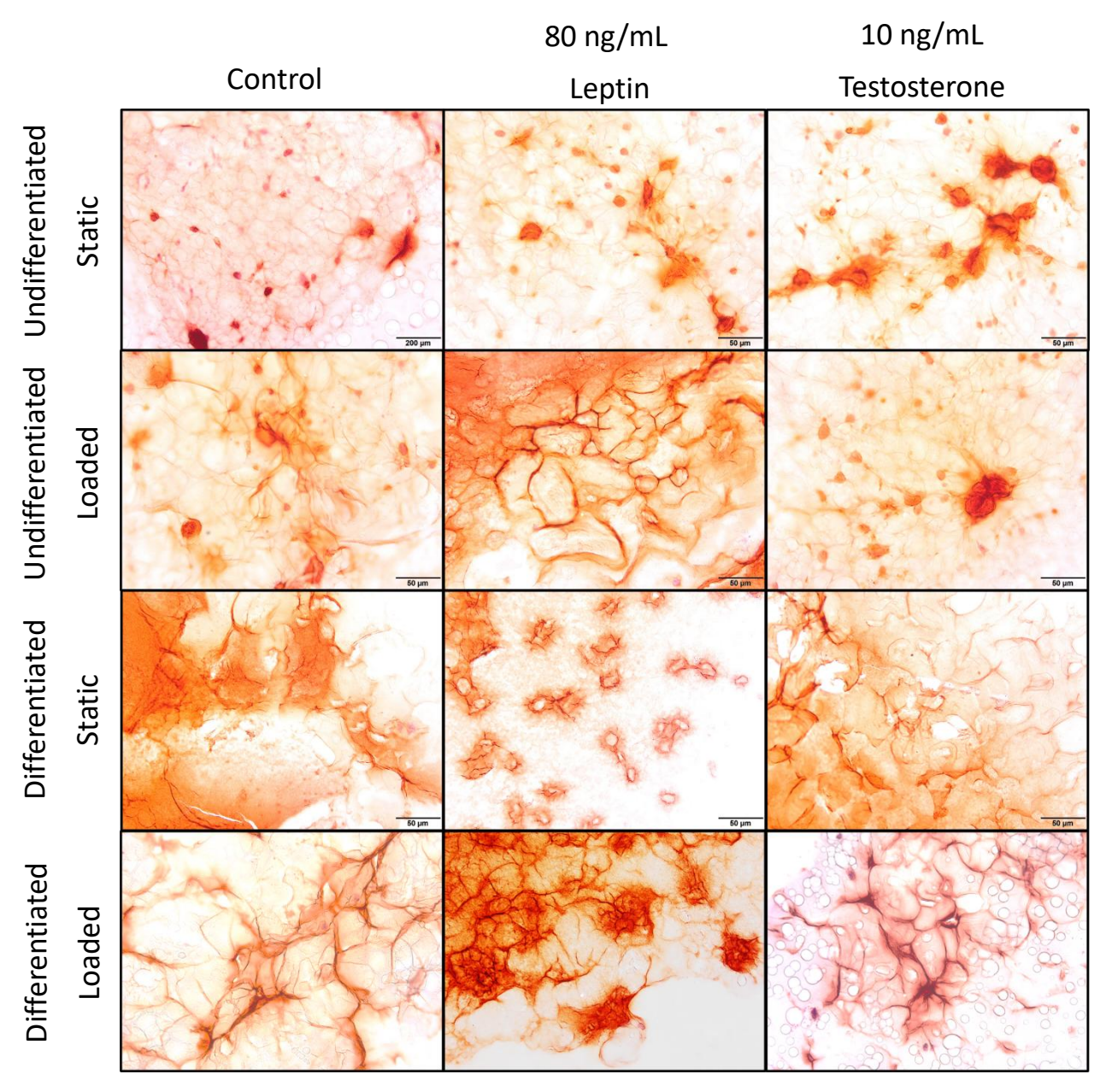


**Figure 4.8:** Representative images depicting Alizarin red stained sections of B-gel constructs laden with either undifferentiated MC3T3-E1 cells, or MC3T3-E1 cells that had been differentiated in osteogenic medium for 21 days. Cell-laden constructs either remained unloaded or were subjected to 0.3 mPa of hydrostatic pressure, alongside treatment with either 10 ng/mL testosterone or 80 ng/mL leptin. n = 3 for all groups. Scale bars are 100  $\mu$ m.

### 4.4. Discussion:

This work aimed to investigate the combined and independent effects of hormones and mechanical load upon murine bone cells *in vitro*, using both 2D and 3D cultures. MC3T3-E1 cells were used primarily in this study to model the response of pre-osteoblasts to *in vitro* mechanical loading with or without leptin or testosterone treatment; including alterations in markers of differentiation and osteogenic activity. Alongside this, MC3T3-E1 cells can also be used as a model of mature, differentiated osteoblasts after culture in osteogenic medium (Hwang and Horton, 2019). Previous studies have shown that, once differentiated, these cells show significant increases in expression of several osteoblastic markers including ALP and RUNX2 (Ju et al., 2022).

The response of undifferentiated and mature MC3T3-E1 cells to hormones and mechanical load was assessed in 2D using *in vitro* FSS, which has been widely used to simulate mechanical loading *in vitro* in a variety of models (Meng et al., 2022; Nile et al., 2023; Wittkowske et al., 2016), notably including MC3T3-E1 cells (Pei et al., 2022). Similarly, cyclical hydrostatic loading was employed to investigate the same conditions a 3D *in vitro* model, using MC3T3-E1 cells seeded within B-gel, a hydroxyapatite nanoparticle containing hydrogel (Thorpe et al., 2016). Hydrostatic loading *in vitro* is used as an alternative model of mechanotransduction *in vitro* (H.-X. Shen et al., 2022), and can also be applied to a 3D gel construct (Mahdi Souzani et al., 2023), unlike FSS.

Outputs from this work include measurements of gene expression and ALP activity in response to mechanical load, with or without hormone treatments, in 2D, and matrix deposition parameters thereof in a 3D gel system. It was hypothesized that leptin and testosterone treatment could attenuate or bolster the effects of mechanical loading.

# 4.4.1. The effect of Hormones and Mechanical Load on MC3T3-E1 and MLO-Y4 Gene Expression *In Vitro*:

Previous studies employing various different loading regimes have revealed that both FSS (Mai et al., 2013) and hydrostatic loading (H.X. Shen et al., 2022) elicit increased expression of osteogenic genes as well as proliferation and growth (Y. Yang et al., 2023) in MC3T3-E1 cells. In contrast, FSS treatment regimens applied to MC3T3-E1 cells in this study, either with or without hormone treatment, did not result in any significant differences in any of the genes tested. Despite no statistical significance, results suggest a relationship between both hormone treatments and mechanical load, although the exact relationship and underpinning mechanisms remain unclear and require further study to elucidate.

It is possible that leptin enhance the responses of MC3T3-E1 cells to FSS induced mechanical loading, as evidenced by the slight trends towards increased OPG, ALP, and AR expression in leptin treated, loaded cells, although further studies with improved statistical power are required to investiaget this relationship further. This suggestion does not align with a previous study in mice, indicating that leptin signalling is a negative modulator of mechanosensitivity *in vivo* (Kapur et al., 2010). Despite results from several previous studies indicating that FSS increases osteogenesis via RUNX2 (Mai et al., 2013; Pei et al., 2022; Yu et al., 2017), this trend was not observed in the present study. Variable factors involved in *in vitro* loading procedures include the length of time cells are subjected to load as well as the amount of force applied; and differences in these factors significantly alter cellular response (Pei et al., 2022). In the present study, MC3T3-E1 cells were subjected to FSS for 24 hours before RNA extraction, which is significantly longer than most studies in the field. A 2020 study by Song *et al.*, indicated

that the osteogenic effect of FSS via Runx2 is achieved via upregulation of PIEZO1 in MC3T3-E1 cells. Interestingly, despite significant increases in PIEZO1 expression shown after five to thirty minutes of FSS, PIEZO1 expression levels had returned to control levels in cells loaded for one hour (Song et al., 2020). Although FSS and hormone treatment did not result in any significant increases in RUNX2 in the present study, results from the study by Song et al., may offer one potential explanation for this unexpected finding. Had the loading regimes in the present study taken place over a shorter duration, it is entirely possible that results obtained would have been more in line with those from similar previous studies. However, these previous studies do not account for the fact that bone is under constant loading forces from body weight, and thus experiments utilising longer loading regimes are necessary to advance our understanding of the effects of load *in vivo*. Furthermore, assessments of protein expression are essential to determine if short term transient responses in mRNA are translated to changes in protein expression.

Despite little differences in ALP or OPG expression in cells treated with either leptin or FSS alone, combined leptin and FSS treatments appeared to increase gene expression of these targets slightly (P = 0.5071 and P = 0.8470 respectively). This finding aligns with previous research suggesting that leptin improves loading-induced bone recovery after a period of unloading in mice (Kawao et al., 2019). However, as RANKL gene expression was consistently below the limit of detection in these samples, and may also have been elevated, no definitive conclusions can be drawn about the potential resulting effects on RANKL:OPG ratio; and therefore osteoclastogenesis. Previous studies have, however, shown that leptin treatment inhibits the expression of RANKL in MC3T3-E1 cells (Lamghari et al., 2006).

AR expression was consistently highest in cells subjected to FSS, indicating that mechanical loading may be a positive modulator of androgen signalling. This hypothesis is consistent with results in humans, showing that mechanical loading from resistance exercise increases AR mRNA concentration in blood serum (Bamman et al., 2001). However, a more recent study found that mechanical loading via resistance exercise did not significantly alter serum androgen or AR, but did increase AR-DNA binding in adult men (Cardaci et al., 2020). Although not statistically significant, undifferentiated MC3T3-E1 cells subjected to FSS displayed slightly reduced LepR expression, indicating a role for mechanical loading in the regulation of leptin signalling in immature osteoblasts. However, this reduction was abolished in cells treated with either leptin or testosterone in combination with mechanical loading. This may be tied to leptin's role in regulating energy expenditure and physical activity, further indicating a two directional dialogue between hormone signalling and mechanotransduction.

The response of differentiated MC3T3-E1 cells to mechanical load have not been reported prior to this study, presenting a gap in current knowledge. Both undifferentiated and differentiated MC3T3-E1 cells were assessed in this study, by employing a well-established method of *in vitro* differentiation in osteogenic medium (Hwang and Horton, 2019) prior to FSS and hormone treatments. This allowed for comparisons between the effects of hormones and mechanical loading upon mature osteoblasts, which are not often assessed, alongside undifferentiated counterparts. These comparisons suggest that, once differentiated, MC3T3-E1 cells exhibit slightly altered responses to FSS and hormone treatments compared to undifferentiated counterparts. For example, Testosterone treatments no longer resulted in slightly increased RUNX2 expression in differentiated MC3T3-E1 cells compared to untreated

controls. This is perhaps due to the fact that the cells had already differentiated, as demonstrated by a peak in RUNX2 expression after 21 days in cell culture medium, and no longer expressed RUNX2 as a result (Hwang and Horton, 2019). Similarly, differentiated MC3T3-E1 cells were overall less affected by hormone treatments along compared to their undifferentiated counterparts, whereas FSS and combination treatments largely induced a response. This could be due to a decline in lepR expression during the advancement of osteoblast differentiation, as suggested by Matic et al., in 2016. Although no such evidence is available to suggest that AR expression also declines with osteoblast maturity, differentiated MC3T3-E1 cells showed no notable responses to androgen therapy. A similar decline of AR expression with osteoblast maturity would provide one possible explanation for the reduced sensitivity of differentiated MC3T3-E1 cells to androgen signalling. With this in mind, it would have been beneficial to this body of work to assess LepR and AR expression at various timepoints throughout the differentiation process. Interestingly, however, FSS consistently had a slight stimulatory effect upon LepR receptor expression, suggesting that mechanical load may sensitise osteoblasts to the effects of leptin signalling. Additionally, a study in LepR deficient Db/Db mice found that mechanical load in the form of vibration mitigates decreases in bone quality associated with leptin deficiency (Jing et al., 2016). Together, these results could imply that the osteogenic effects of leptin and mechanical load upon mature osteoblasts share common downstream pathways. For example, the JAK/STAT pathway has been closely linked to both leptin signalling (Gurzov et al., 2016) and mechanotransduction (Q. Hu et al., 2023). This hypothesis aligns with previous findings that selective STAT3 inactivation in osteoblasts impairs osteogenesis by decreasing osteoblast differentiation (Zhou et al., 2021).

Finally, gene expression levels in MLO-Y4 samples were consistently below the limit of detection for all genes of interest in this study. However, previous studies investigating the cell line have reported expression of RUNX2, ALP, RANKL and OPG among other commonly assessed markers in MLO-Y4 cells (Li et al., 2012; Wittkowske et al., 2016). The primers used to detect expression of target genes were the same as those used for MC3T3-E1 cell samples, which returned positive amplification data. Alongside detectable expression of both housekeeping genes, this suggests that the lack of expression observed was genuine, despite contradictory findings in other studies. Importantly, gene expression of receptors for testosterone and leptin were both below the limits of detection, implying that these cells will have been unaffected by hormone treatments. Conversely, another study of MLO-Y4 cells found that leptin increased proliferation alongside expression of OPG and ALP (Fan et al., 2017). LepR expression was not assessed in the study, but the response to treatment implies that MLO-Y4 cells do typically express this receptor. Similarly, studies investigating the effects of FSS upon MLO-Y4 cells report significant effects of FSS upon gene expression, particularly decreases in RANKL:OPG ratio (Li et al., 2012; Liu et al., 2022; Yan et al., 2018). Again, these results suggest that MLO-Y4 do express these genes in culture. Therefore, it is likely that the lack of expression observed in this study is due to other factors, including perhaps the passage number of the cells, which is unknown.

Additionally, although MLO-Y4 cells have been used extensively in *in vitro* studies of osteocyte mechanobiology, these cells do not express and secrete sufficient levels of sclerostin compared to other osteocyte-like cell lines (Xu et al., 2019), and therefore may not have provided a suitable model for the present study.

Overall, loading regimes employed in this study were not comparable to those used in other studies, meaning that some previously observed alterations in gene expression in response to FSS were not present. Future studies investigating the relationship between hormones and mechanical loading *in vitro* should utilise shorter bouts of *in vitro* loading to relate more closely to previous studies. As expression levels of the genes of interest, importantly including LepR and AR, were below detection limits in MLO-Y4 cells, MC3T3-E1 cells were used for further studies.

## 4.4.2. Collagen Hydrogels Containing MG63 Cells are Not a Viable, Representative Model of Mechanical Loading *In Vitro*:

Initially, the human osteosarcoma cell line MG63 was utilised as a highly proliferative, easily cultured model of osteoblastic-like cells capable of forming ECM attachments (Yoo et al., 2016). These cells were used to in the development of a 3D culture system capable of withstanding and transducing applied mechanical force *in vitro*, initially a collagen hydrogel. In line with a number of previous studies using a variety of cell types within collagen hydrogels (Caliari and Burdick, 2016; Hesse et al., 2010; Ishida-Ishihara et al., 2022), MG63 cells remained viable and proliferative after 4-weeks of culture within the gels. Alongside this MG63 cells are known to express FAK (Lei et al., 2011; Yoo et al., 2016), enabling ECM attachments, and maintained FAK expression measured via immunopositivity in the present study, suggesting that these cells are mechanoresponsive.

Despite this, initial loading experiments revealed that these collagen hydrogels lacked the mechanical stiffness to withstand even a small amount of compressive force. The gels were destroyed completely by as little as 0.1 N, the smallest force applicable by the

load cell used in this study. Previous studies have overcome this drawback of collagen hydrogels by applying compressive loading to gels confined within wells of a silicone well plate (Vazquez et al., 2014). However, attempts to recapitulate this method by culturing collagen gels inside silicone rings prior to loading did not provide a solution. The Young's modulus of gel-containing rings was the same as that of empty rings, suggesting that the collagen gels were not experiencing any of the load applied (data not shown). Instead, future 3D cell culture was performed using B-gel scaffolds to provide more structural support, alongside hydrostatic loading regimes.

Similarly, whilst MG63 cells were viable within the collagen gel, and showed signs of ECM attachment suggesting mechanosensitivity, they are not a wholly representative cell model of normal osteoblastic phenotype due to their tumour origin (Czekanska et al., 2014). Therefore, further investigations were conducted utilising MC3T3-E1 cells to more accurately represent the osteoblastic phenotype.

## 4.4.3. The Effect of Hormones and Mechanical Loading Upon MC3T3-E1 Cell Matrix Deposition in 3D:

Whilst FSS in 2D is a valid model of the effects of mechanical loading *in vitro*, and has been shown to induce a response, these systems do not represent the 3D environment in which bone cells reside. In order to overcome this limitation, cells can be encapsulated within 3D constructs allowing for cell attachment, and therefore transmission of mechanical load, in 3D (Yuste et al., 2021). In the present study, immature or differentiated MC3T3-E1 cells were embedded into a hydroxyapatite-containing hydrogel and subjected to hydrostatic loading with or without hormone treatment. Findings in undifferentiated MC3T3-E1 cells indicate that both leptin and testosterone

treatment increased collagen and calcium deposition within hydrogels, whereas mechanical loading alone did not induce any significant alterations. Conversely, mechanical loading increased matrix deposition in differentiated MC3T3-E1 cells, but neither hormone treatment had a significant effect.

In line with results from this study, leptin has previously been shown to increase collagen type I expression and secretion in human osteoblasts (Reseland et al., 2001) and hepatic stellate cells (Choudhury et al., 2006; García-Ruiz et al., 2012). Increased collagen secretion was observed in both static and loaded conditions treated with mechanical loading, with slightly increased intensity of staining in loaded constructs compared to static controls. However, these differences cannot be reliably quantified, and further work is required to identify the combined effects of leptin and load upon collagen secretion. Similarly, the present study did not identify the form of collagen present in these treatment conditions. This could be assessed for each different collagen subtype using IHC, as performed in previous studies (X. Ren et al., 2017). Findings from a study suggest that leptin deficient mice display decreased expression of Collagen type X (Kishida et al., 2005), implying that leptin treatment may have increased or facilitated collagen type X deposition, alongside collagen type I (García-Ruiz et al., 2012).

Alongside observed increases in blue staining, indicating the presence of collagen in Masson's trichrome stained collagen gel constructs, constructs treated with leptin exhibited increased red staining and nodule size when subjected to Alizarin red staining, indicating calcium deposition in comparison to untreated controls. Increases in mineralisation in response to leptin has also been reported in osteoblasts extracted from rats (Cheng et al., 2018) and bovine aortic smooth muscle cells (Zeadin et al., 2012).

The observed osteogenic effect of leptin was amplified when applied in combination with hydrostatic loading, further suggesting an interaction between the two pathways. Similar increases in both collagen and calcium deposition were observed in undifferentiated MC3T3-E1 cells treated with testosterone regardless of mechanical load. This effect of androgens upon bone cell mineralisation has been observed in previous studies (Balkan et al., 2005; Wiren, 2005), and the anabolic effects of testosterone on bone are well documented (Mohamad et al., 2016).

In contrast to findings in undifferentiated MC3T3-E1 cells, matrix deposition in differentiated MC3T3-E1 cells was instead primarily influenced by mechanical loading, whilst showing reduced responsivity to either hormone treatment alone. Collagen deposition was consistently highest in differentiated MC3T3-E1 cells subjected to hydrostatic loading compared to static controls, regardless of hormone treatment. This aligns with results from 2D assessment of gene expression in these cells under similar conditions, implying that differentiated MC3T3-E1 cells are less sensitive to hormone treatments in favour of increased mechanosensitivity. Despite this, however, results also indicated a synergistic effect of leptin and mechanical load, denoted by increased presence of calcified nodules compared to either treatment alone. However, all measures performed in this study consisted of unquantifiable, qualitative assessments of stained hydrogel sections, and as a result no definitive relationships can be established.

Future work in this field would certainly include IHC evaluation of cell-laden B-gel sections to evaluate differentiation, proliferation and mineralisation profiles of these cells, providing more valuable insights into the mechanisms underpinning the results of this study.

#### 4.4.4. Conclusion:

Together, results from this study further imply a link between leptin and testosterone signalling and mechanical loading. Although the exact relationship between these factors remains unclear, it is suggested that these hormones may influence the response of both immature and differentiated MC3T3-E1 cells to mechanical load *in vitro*. Despite no significant alterations in gene expression, leptin and testosterone treatments in combination with mechanical load influence these cells more significantly than either condition alone, resulting in a response that is greater than the sum of its parts. Moreover, the responses to both hormone and loading regimens differ between undifferentiated and differentiated MC3T3-E1, with undifferentiated cell matrix deposition primarily affected by hormones, and differentiated MC3T3-E1 cells influenced instead by load.

This work has created viable models to assess interactions between hormones and mechanical loading *in vitro* in both 2D utilising fluid shear stress, and 3D via the hydrostatic loading of hydrogel constructs, and provides a foundation for future work to delve deeper into these pathways.

5. Chapter 5: General Discussion and Future Directions:

This work investigated the interconnected roles of testosterone, leptin, and HFD on bone morphology and metabolic regulation, employing a combination of animal models and cell culture studies. The findings of this research contribute to our broader understanding of the endocrine regulation of bone health, particularly in the context of metabolic disorders and hormone deficiencies.

Chapter 2 demonstrated that testosterone deficiency significantly affects bone architecture, particularly by reducing trabecular bone volume and number. Testosterone was found to play a role in suppressing osteoclastogenesis via the RANKL:OPG pathway, resulting in significant morphological alterations in the tibial trabeculae of orchiectomised mice, and these parameters were restored by TRT.

These findings were extended in Chapter 3 by investigating how leptin deficiency and HFD influence bone health. Leptin-deficient (*Ob/Ob*) mice exhibited compromised cortical and trabecular bone structure, independent of body weight. These alterations differ between vertebral and tibial regions, indicating site-specific actions of leptin signalling. Meanwhile, HFD exacerbated bone loss, particularly in trabecular regions, whilst increasing tibial marrow adiposity; suggesting that obesity and leptin resistance contribute to bone loss.

Alongside this, Chapter 4 provided mechanistic insights into the synergistic effects between hormone treatment and mechanical loading in osteoblasts. These effects were assessed in both immature pre-osteoblasts and fully differentiated osteoblasts, providing important mechanistic context. Although no clear mechanisms of action were established, both leptin and testosterone treatments appeared to modulate the responsivity of osteoblasts to mechanical loading, ultimately resulting in subtle differences in gene expression *in vitro*. Together, these findings suggest interplay

between mechanotransduction and leptin or testosterone signalling pathways, indicating that further studies are required to elucidate these shared mechanisms.

#### 5.1. The Role of Testosterone in Bone Metabolism:

Testosterone has long been recognised for its anabolic effects on bone, primarily through its influence on bone formation (Shigehara et al., 2021). However, this work adds an important layer to our understanding by highlighting the potential antiresorptive properties of testosterone via RANKL:OPG ratio modulation, resulting in altered trabecular microarchitecture. Results obtained from the present study emphasise testosterone's protective role in maintaining bone mass and integrity, potentially through indirect effects on osteoclast precursor cells alongside direct effects upon osteogenesis. These findings align with clinical observations of decreased BMD in hypogonadal men (da Costa et al., 2004; Lincoff et al., 2023) and postmenopausal women (Gupta et al., 2012; Ji and Yu, 2015), where declining testosterone and oestrogen respectively are associated with bone loss and increased osteoclast activity. Alongside this, TRT appears to be a viable intervention to prevent the loss of trabecular bone associated with testosterone deficiency, again aligning with results in human trials indicating that TRT increases BMD, especially in the trabeculae (Snyder et al., 2017). However, the observed slight reductions in the mechanical strength of tibiae from orchiectomised mice were not restored by TRT. This indicates that, despite restoring trabecular microarchitecture, TRT may not have any significant effects upon fracture riskin the tibiae. This hypothesis has been investigated in a human trial revealing that TRT did not improve fracture risk in middle-aged and older men, instead resulting in a numerically higher fracture risk than in those treated with placebo (Snyder et al., 2024).

This finding suggests that TRT may be detrimental to bone-related clinical outcomes, despite previously observed benefits to BMD and trabecular parameters. One possible explanation for this observation is the effects of testosterone on bone composition beyond the often-assessed mineral content, owing instead to the presence of various collagens and other ECM components, which also impact fracture risk (Sieverts et al., 2022).

Additionally, results from *in vitro* studies undertaken as part of this work did not reveal any clear relationships between testosterone supplementation and expression of several key markers of gene expression in MC3T3-E1 pre-osteoblast cells, despite a slight trend towards increased RUNX2 expression. This finding aligns with observed slight decreases in RUNX2 immunopositivity in the tibiae of orchiectomised mice in the present study, suggesting that the known increase in osteoblast differentiation in response to androgen signalling (Notelovitz, 2002) may be reliant upon RUNX2 signalling. However, results from this study were inconclusive, and contradictory evidence also suggests that androgen does not increase RUNX2 activity (McCarthy et al., 2003), and further research is required to understand these mechanisms. Testosterone treatment also increased both collagen and calcium matrix deposition within 3D gels in the present study, underscoring the anabolic effects of androgen upon bone (Chen et al., 2019).

Further studies should aim to more broadly assess the effects of testosterone and testosterone deficiency upon bone composition aside from BMD, and further delineate the downstream actions of androgen signalling upon both bone formation and resorption. This will deepen our understanding of the implications of testosterone status

on fracture risk, allowing for more informed use of TRT, and other therapies aimed at improving fracture risk.

#### 5.2. The Role of Leptin in Bone Metabolism:

Leptin's dual role as a metabolic regulator and bone modulator is increasingly recognised. This body of work reinforces the concept that leptin is not merely a satiety hormone but also plays a pivotal role in bone remodelling (Reid et al., 2018). The findings align with past research suggesting leptin influences bone turnover by promoting osteoblast differentiation and inhibiting osteoclastogenesis (Thomas et al., 1999). However, conflicting evidence also suggests leptin may promote adipogenesis over osteogenesis in mesenchymal stromal cells, particularly under high-fat diet (HFD) conditions (Yue et al., 2016). Notably, HFD and especially leptin deficiency led to increased marrow adiposity, further indicating a shift in the bone marrow environment towards adipogenesis at the expense of osteogenesis. The shift towards marrow adiposity in the context of leptin deficiency and obesity further illustrates the complex crosstalk between energy metabolism and bone health, a relationship that is particularly relevant in the growing obesity epidemic.

Additionally, the study highlights the complexities of leptin's role in bone morphology, particularly under HFD conditions, where increased body weight did not correlate with increased bone volume, contrary to expectations. This result suggests that leptin deficiency and HFD may have overlapping negative effects on bone health, complicating the relationship between obesity, bone morphology, and leptin signalling. Technological advances in 3D imaging allowed for a more detailed analysis of trabecular structure, revealing important regional differences in bone morphology that could improve

fracture risk predictions (Sass et al., 2024). Although *in vitro* experiments with MC3T3-E1 cells revealed no significant alterations in gene expression response to leptin treatment in the present study, leptin treatment did appear to increase the deposition of both calcium and collagen matrix by MC3T3-E1 cells in 3D hydrogel constructs. Together with decreases seen in cortical bone volumes of murine tibiae and vertebrae, these findings align with previous suggestions that leptin may be an important regulator of bone formation (Reid et al., 2018).

Leptin deficiency significantly affects bone morphology independent of body weight, with changes similar to those induced by HFD. This study underscored the need for further research to clarify the mechanisms by which leptin and diet influence bone health, particularly using advanced imaging techniques to better understand fracture risk.

# 5.3. Interactions Between Hormones and Mechanical Loading *in vitro*:

It is possible that interactions between hormone signalling and mechanotransduction pathways are responsible for some of the inconsistencies observed in previous studies investigating the relationship between obesity and bone health. This study aimed to investigate the combined and independent effects of hormones (leptin and testosterone) and mechanical load on murine bone cells in both 2D and 3D *in vitro* cultures, focusing on their influence on osteogenic activity and differentiation markers in pre-osteoblasts and mature osteoblasts.

It was found that leptin enhanced the response of MC3T3-E1 cells to mechanical loading in 2D cultures, as indicated by trends toward increased expression of osteogenic markers such as OPG and ALP. Based on previous work in the field, it was expected that FSS alone would induce significant increases in osteogenic genes such as RUNX2 whilst suppressing RANKL:OPG ratio (Li et al., 2012; Pei et al., 2022). However, significant changes in gene expression were not observed in the present study, possibly due to the extended duration of loading applied.

Initial attempts to use MG63 cells within collagen hydrogels for 3D mechanical loading were unsuccessful due to the gels' inability to withstand compressive forces, leading to a shift to a thermoresponsive polymer scaffold (B-gel) which has previously been shown to support osteoblast cell phenotype (Thorpe et al., 2016) and provided a scaffold with improved structural support enabling the application of mechanical loading.

In the 3D culture system, undifferentiated MC3T3-E1 cells treated with leptin and testosterone exhibited increased collagen deposition and mineralization, whereas mechanical loading alone did not produce significant changes. In contrast, matrix deposition in differentiated cells was primarily driven by mechanical load, with hormone treatments having a reduced impact. A synergistic effect was noted when mechanical load and leptin were combined, resulting in increased calcified nodule formation.

Results obtained in this study suggested a complex interaction between hormone signalling and mechanical loading, with differing effects between undifferentiated and differentiated osteoblasts. While the precise mechanisms remained unclear, it was evident that the combination of hormonal treatments and mechanical load had a more pronounced effect than either factor alone. This research provides a foundation for future studies to explore the pathways involved in bone cell mechanotransduction and

hormone interactions using the developed 2D and 3D models. This research should aim to identify shared pathways between hormone signalling and mechanotransduction and provide insights into the mechanisms governing their synergistic effects.

#### **5.4.** Future Directions:

The work detailed in this thesis provides a foundation for further research in the field, which should aim to elucidate the mechanisms facilitating interactions between hormones and mechanical load with respect to bone growth and remodelling. These studies should aim to further isolate the effects of individual hormones from those of diet or mechanical load. Further studies should also strive to elucidate the cellular mechanisms governing interactions between these hormones and mechanical load.

#### **5.4.1.** Elucidating The Role of Testosterone in Bone Remodelling:

This study investigated the role of testosterone deficiency and subsequent testosterone replacement therapy in a murine model of metabolism disorder. One aspect that is not clear from this study, is the contributions of the high fat diet feeding regimes employed throughout this study to the alterations seen in bone parameters. Similarly, whether these effects differ between ApoE-/- animals with a compromised metabolism compared to C57 mice has not been investigated in the present study. Findings from a previous study by Schilling et al., in 2005, it was revealed that ApoE-/- mice exhibit increased bone formation compared to controls, implying that these mice may have had altered bone physiology. To overcome these limitations, future work could include a similar study, this time comparing the effects of orchiectomy and TRT in animals fed a

HFD to those fed a normal diet. Alongside this, C57 mice could be utilised as a control to assess any differences in response between ApoE-/- animals with a compromised metabolism and those without.

Furthermore, in order to assess the role of testosterone's aromatisation to oestrogen, predominantly by fat tissue (Shigehara et al., 2021), these studies could include test groups treated with Tamoxifen, an established oestrogen receptor modulator, or Anastrozole; an aromatase inhibitor (Farrar and Jacobs, 2024), alongside testosterone. This would allow future research to uncouple the effects of these two interlinked sex hormones, providing more important insights into the independent effects of testosterone upon bone remodelling.

Finally, future studies in the field should investigate a wider range of bone regions including hip and vertebral assessments. These inclusions would allow for a more comprehensive view of the effects of testosterone and testosterone deficiency in bone, allowing for more direct comparisons between results obtained and clinical studies. Alongside this, more emphasis should be placed on bone composition beyond BMD. Although decreased BMD is associated with increased fracture risk, this does not mean that the inverse is true in individuals with significantly increased BMD. In fact, higher BMD is sometimes associated with brittle bones and therefore increased fracture risk (Gregson et al., 2013). Alongside this, there are other major contributors to bone mechanical strength besides BMD, including trabecular microarchitecture and bone composition. The immunohistological assessment of collagens, particularly collagen I, within bone samples would provide deeper insights into the likely mechanical properties of the bones. This work would build upon the findings of the present study and provide

important context regarding the implications of testosterone deficiency and TRT for fracture risk.

Alternatively, in the interest of minimising the use of animal models where possible, several strategies have emerged to recapitulate an obese phenotype in vitro (Ghanemi et al., 2022), including altering the lipid and cytokine content of cell culture media. These techniques could be leveraged to investigate interactions between testosterone and bone cells in obese and control conditions in vitro, without the need for any further animal studies. However, in vitro studies in this field may be lacking some important physiological factors present in animal models, including mechanical loading from body weight and the aromatisation of testosterone in fat tissue (Lee et al., 2013). To overcome this, study design could include in vitro FSS and hydrostatic loading regimes, as utilised in the present study, alongside the conditions outlined above. Similarly, coculture studies of bone cells and adipocytes incorporating these conditions would theoretically allow for the effects of testosterone aromatisation to oestrogen to be observed, particularly if conditions with and without oestrogen inhibitors were employed. Oestrogen inhibitors have previously been used in MC3T3-E1 cells, resulting in decreased ALP and RUNX2 expression (Schiavi et al., 2021). Together, this work would provide further insights into links between androgen signalling, metabolism, and diet with respect to bone health.

#### **5.4.2.** Elucidating the Role of Leptin in Bone Remodelling:

The work described in this thesis has provided insights into the effects of leptin deficiency upon bone morphology, drawing attention to regional differences in morphological changes. However, this study did not clarify whether the differences

observed were the result of central or direct actions of leptin. Future studies could address this limitation with the inclusion of conditional, brain specific LepR knockout mice, as utilised in a 2020 study by Ren et al., Utilising these mice, the authors were able to demonstrate that neuronal leptin signalling is essential for the development of an obese phenotype in leptin deficient animals (Z. Ren et al., 2020). Similarly, comparisons between the bone morphologies of brain specific LepR knockout mice and global knockout counterparts would provide insights into the regio-specific effects of leptin signalling on bone metabolism. This work would build upon the findings of the present study and delineate the signalling pathways responsible for the alterations seen in leptin deficient mouse morphology, be they central or direct.

Furthermore, the effects of leptin resistance were not explored in the present study; a factor with potential significance in the obese C57 mice fed a HFD. Blood plasma samples were not available for analysis in the present study, but future studies in the field should aim to assess serum leptin and insulin concentrations and assess leptin resistance in C57 mice. Serum leptin and insulin concentrations could be assessed via a simple ELISA (Burnett et al., 2017) leptin resistance can be further assessed via glucose tolerance tests, measuring glucose metabolism and insulin sensitivity which are often impaired in leptin-resistant states (Enriori et al., 2007).

Additionally, to further separate the effects of leptin from those of load in these animals, it may have been pertinent to assess the calvaria of leptin deficient and control animals alongside the tibiae and lumbar vertebrae. Previous studies have performed calvarial analyses using the same techniques as used for other bone samples in the present study, including micro CT (Shim et al., 2022) and IHC (W.H. Wang et al., 2020). As the calvarium does not bear any load from body weight, the comparisons between leptin deficient and

WT samples would isolate the effects of leptin deficiency. This, in turn, would allow for direct observations regarding the effects of leptin and leptin deficiency.

Finally, the only remaining variable that was not addressed in the present study is the diet fed to the obese control and leptin deficient mice. Leptin deficient mice in the obese group could not be fed a HFD during this study, unlike their C57 counterparts. This is because the food restrictions necessary to weight-pair a leptin deficient mouse to a wild-type mouse would have been far too restrictive and, as a result, unethical. This means that differences in diet nutritional content may have played a role in differences observed in the present study. Future studies should aim to advance our understanding of the impact of diet, particularly HFD, upon bone remodelling despite body weight. This work would allow for more steadfast conclusions to be drawn from the present study.

## 5.4.3. Unravelling Interactions Between Mechanotransduction and Hormone Signalling:

Loading regimes in future FSS studies aiming to establish relationships between hormone signalling and mechanotransduction should aim to more closely align with those demonstrated in previous studies. The work of Pei et al., in 2022 demonstrated that the duration of FSS applied is a crucial factor determining responses in gene and protein expression, and future work should employ a similar strategy, assessing the impact of FSS at various timepoints. This would allow for more direct comparisons between findings to current knowledge in the field and may also reveal more prominent effects of *in vitro* mechanical load.

Whilst results from the present study suggest the presence of interactions between hormones and mechanotransduction with respect to bone cell behaviour *in vitro*, these

findings could be expanded upon further. For example, future studies should assess the expression of various markers of bone turnover, including RUNX2, RANKL, and OPG in the MC3T3-E1-containing B-gel construct sections. This could be achieved via IHC staining of sections, as used for Masson's Trichrome and Alizarin Red histological stains. Additionally, mechanical load is detected and transmitted through different receptors and pathways, as discussed in the introduction to this thesis. It is unclear which of these pathways, if any, is linked to leptin or testosterone signalling, and exactly how these distinct pathways interact with one another.

To assess this, hormone treatments used in conjunction with mechanical load in the present study could be combined with inhibitors of specific mechanoreceptors. One such mechanoreceptor with an established, effective inhibitor is TRPV4, a mechanoreceptor which increases leptin production when activated (Sánchez et al., 2021). It is possible to inhibit TRPV4 signalling using a number of antagonists, including Ruthenium red, Capsazepine, and several others (Kumar et al., 2023). Application of this principle to TRPV4 and other mechanoreceptors would allow for the uncoupling of hormone-induced changes in bone cell behaviour from the effects of mechanical loading, providing important insights into exactly which mechanotransduction pathways overlap with those of hormone signalling.

Due to its commonality between leptin signalling and mechanotransduction pathways, JAK/STAT signalling is a likely candidate to link the effects of the two factors in bone. The JAK/STAT pathway is activated by both leptin signalling (Gurzov et al., 2016) and mechanotransduction (Q. Hu et al., 2023), providing an intriguing avenue for further investigation which has not yet been explored. This relationship could preliminarily be assessed with a relatively straightforward experimental design employing any of the

various inhibitors of the JAK/STAT pathway (Shawky et al., 2022) alongside leptin and mechanical load. This would help determine whether the interplay between leptin and load is mediated by JAK/STAT signalling or if additional mechanisms are also involved. Similarly, JAK/STAT signalling could have been assessed in the present study by assessing STAT3 phosphorylation in protein fractions extracted from the cells (Lee et al., 2002). No clear links have yet been established between androgen signalling pathways and those of mechanotransduction, although androgens do interact with integrins, including the activation of FAK complex (Tsai et al., 2023). This, in turn, presents FAK as a potential mediator in the interplay between testosterone and mechanotransduction, and future studies should aim to assess the effects of androgen signalling on FAK expression and activation. This could be achieved via IHC analysis of FAK in hydrogel sections, allowing for visualisation of cellular FAK expression within the hydrogels (Wei et al., 2020). Deeper understanding of the relationship between testosterone, mechanical load, and bone health will allow for more informed applications of TRT and other measures to aid bone health in ageing, testosterone depleted men.

#### **5.5.** Concluding Remarks:

This thesis has made contributions to our understanding of the hormonal and dietary regulation of bone health, alongside interactions between these factors and mechanical loading. By integrating findings on testosterone, leptin, and HFD, it has provided a view of how these factors influence bone morphology and metabolism, both alone and in combination with mechanical load. The results challenge existing paradigms, particularly regarding the roles of leptin in bone remodelling and underscore the need for a more nuanced approach to studying bone health in the context of metabolic disorders. The differential effects of leptin and testosterone on bone turnover and remodelling suggest potential therapeutic avenues for preventing bone loss. Developing pharmacological agents that mimic or enhance the bone-protective effects of these hormones could offer new treatments for osteoporosis and other metabolic bone diseases. Future research, building on the findings presented here, will be crucial in developing effective strategies to understand, prevent, and treat bone-related complications in individuals with hormonal imbalances and obesity.

### References:

Adachi, T., Aonuma, Y., Tanaka, M., Hojo, M., Takano-Yamamoto, T., and Kamioka, H. (2009). Calcium response in single osteocytes to locally applied mechanical stimulus: Differences in cell process and cell body. *Journal of Biomechanics*, *42*(12), Article 12. https://doi.org/10.1016/j.jbiomech.2009.04.034

Akhter, M. P., Lappe, J. M., Davies, K. M., and Recker, R. R. (2007). Transmenopausal changes in the trabecular bone structure. *Bone*, *41*(1), 111–116. <a href="https://doi.org/10.1016/j.bone.2007.03.019">https://doi.org/10.1016/j.bone.2007.03.019</a>

Akil, L., and Ahmad, H. A. (2011). Relationships between Obesity and Cardiovascular Diseases in Four Southern States and Colorado. *Journal of Health Care for the Poor and Underserved*, 22(5), 61–72.

Al Mukaddam, M., Rajapakse, C. S., Bhagat, Y. A., Wehrli, F. W., Guo, W., Peachey, H., LeBeau, S. O., Zemel, B. S., Wang, C., Swerdloff, R. S., Kapoor, S. C., and Snyder, P. J. (2014). Effects of Testosterone and Growth Hormone on the Structural and Mechanical Properties of Bone by Micro-MRI in the Distal Tibia of Men With Hypopituitarism. *The Journal of Clinical Endocrinology and Metabolism*, *99*(4), 1236–1244. https://doi.org/10.1210/jc.2013-3665

Almeida, M., Han, L., Ambrogini, E., Bartell, S. M., and Manolagas, S. C. (2010). Oxidative Stress Stimulates Apoptosis and Activates NF-κB in Osteoblastic Cells via a PKCβ/p66shc Signaling Cascade: Counter Regulation by Estrogens or Androgens. *Molecular Endocrinology*, 24(10), 2030–2037. https://doi.org/10.1210/me.2010-0189

Ansari, S., Ito, K., and Hofmann, S. (2021). Cell Sources for Human In vitro Bone Models. *Current Osteoporosis Reports*, *19*(1), 88–100. <a href="https://doi.org/10.1007/s11914-020-00648-6">https://doi.org/10.1007/s11914-020-00648-6</a>

Arai, Y., Choi, B., Kim, B. J., Park, S., Park, H., Moon, J. J., and Lee, S.-H. (2021). Cryptic ligand on collagen matrix unveiled by MMP13 accelerates bone tissue regeneration via MMP13/Integrin α3/RUNX2 feedback loop. *Acta Biomaterialia*, 125, 219–230. https://doi.org/10.1016/j.actbio.2021.02.042

Arias, C. F., Herrero, M. A., Echeverri, L. F., Oleaga, G. E., and López, J. M. (2018). Bone remodeling: A tissue-level process emerging from cell-level molecular algorithms. *PLoS ONE*, *13*(9), Article 9. https://doi.org/10.1371/journal.pone.0204171

Arnold, M., Zhao, S., Ma, S., Giuliani, F., Hansen, U., Cobb, J. P., Abel, R. L., and Boughton, O. (2017). Microindentation – a tool for measuring cortical bone stiffness? *Bone and Joint Research*, *6*(9), 542–549. <a href="https://doi.org/10.1302/2046-3758.69.BJR-2016-0317.R2">https://doi.org/10.1302/2046-3758.69.BJR-2016-0317.R2</a>

Avin, K. G., Bloomfield, S. A., Gross, T. S., and Warden, S. J. (2015). Biomechanical Aspects of the Muscle-Bone Interaction. *Current Osteoporosis Reports*, *13*(1), Article 1. https://doi.org/10.1007/s11914-014-0244-x

Baek, K. H., Oh, K. W., Lee, W. Y., Lee, S. S., Kim, M. K., Kwon, H. S., Rhee, E. J., Han, J. H., Song, K. H., Cha, B. Y., Lee, K. W., and Kang, M. I. (2010). Association of oxidative stress with postmenopausal osteoporosis and the effects of hydrogen peroxide on osteoclast formation in human bone marrow cell cultures. *Calcified Tissue International*, *87*(3), 226–235. https://doi.org/10.1007/s00223-010-9393-9

Bagan, L., Jiménez, Y., Leopoldo, M., Rubert, A., and Bagan, J. (2017). Serum levels of RANKL and OPG, and the RANKL/OPG ratio in bisphosphonate-related osteonecrosis of the jaw: Are they useful biomarkers for the advanced stages of osteonecrosis? *Medicina Oral, Patología Oral y Cirugía Bucal, 22*(5), e542–e547. https://doi.org/10.4317/medoral.22128

Bahceci, M., Tuzcu, A., Akkus, M., Yaldiz, M., and Ozbay, A. (1999). The effect of high-fat diet on the development of obesity and serum leptin level in rats. *Eating and Weight Disorders: EWD*, *4*(3), 128–132. <a href="https://doi.org/10.1007/BF03339728">https://doi.org/10.1007/BF03339728</a>

Baker, B. M., and Chen, C. S. (2012). Deconstructing the third dimension – how 3D culture microenvironments alter cellular cues. *Journal of Cell Science*, *125*(13), 3015–3024. <a href="https://doi.org/10.1242/jcs.079509">https://doi.org/10.1242/jcs.079509</a>

Baker, C. (2024). *Obesity statistics*. <a href="https://commonslibrary.parliament.uk/research-briefings/sn03336/">https://commonslibrary.parliament.uk/research-briefings/sn03336/</a>

Balkan, W., Burnstein, K. L., Schiller, P. C., Perez-Stable, C., D'Ippolito, G., Howard, G. A., and Roos, B. A. (2005). Androgen-induced mineralization by MC3T3-E1 osteoblastic cells

reveals a critical window of hormone responsiveness. *Biochemical and Biophysical Research Communications*, 328(3), 783–789. https://doi.org/10.1016/j.bbrc.2004.12.090

Balthasar, N., Coppari, R., McMinn, J., Liu, S. M., Lee, C. E., Tang, V., Kenny, C. D., McGovern, R. A., Chua, S. C., Elmquist, J. K., and Lowell, B. B. (2004). Leptin Receptor Signaling in POMC Neurons Is Required for Normal Body Weight Homeostasis. *Neuron*, 42(6), Article 6. https://doi.org/10.1016/j.neuron.2004.06.004

Bamman, M. M., Shipp, J. R., Jiang, J., Gower, B. A., Hunter, G. R., Goodman, A., McLafferty, C. L., and Urban, R. J. (2001). Mechanical load increases muscle IGF-I and androgen receptor mRNA concentrations in humans. *American Journal of Physiology-Endocrinology and Metabolism*, 280(3), E383–E390. <a href="https://doi.org/10.1152/ajpendo.2001.280.3.E383">https://doi.org/10.1152/ajpendo.2001.280.3.E383</a>

Banes, A. J., Gilbert, J., Taylor, D., and Monbureau, O. (1985). A new vacuum-operated stress-providing instrument that applies static or variable duration cyclic tension or compression to cells in vitro. *Journal of Cell Science*, *75*(1), 35–42. https://doi.org/10.1242/jcs.75.1.35

Baniwal, S. K., Khalid, O., Sir, D., Buchanan, G., Coetzee, G. A., and Frenkel, B. (2009). Repression of Runx2 by Androgen Receptor (AR) in Osteoblasts and Prostate Cancer Cells: AR Binds Runx2 and Abrogates Its Recruitment to DNA. *Molecular Endocrinology*, 23(8), 1203–1214. <a href="https://doi.org/10.1210/me.2008-0470">https://doi.org/10.1210/me.2008-0470</a>

BARREIROS, D., PUCINELLI, C. M., de OLIVEIRA, K. M. H., PAULA-SILVA, F. W. G., NELSON FILHO, P., da SILVA, L. A. B., KÜCHLER, E. C., and da SILVA, R. A. B. (2018). Immunohistochemical and mRNA expression of RANK, RANKL, OPG, TLR2 and MyD88 during apical periodontitis progression in mice. *Journal of Applied Oral Science*, *26*, e20170512. <a href="https://doi.org/10.1590/1678-7757-2017-0512">https://doi.org/10.1590/1678-7757-2017-0512</a>

Bartell, S. M., Rayalam, S., Ambati, S., Gaddam, D. R., Hartzell, D. L., Hamrick, M., She, J.-X., Della-Fera, M. A., and Baile, C. A. (2011). Central (ICV) leptin injection increases bone formation, bone mineral density, muscle mass, serum IGF-1, and the expression of osteogenic genes in leptin-deficient *Ob/Ob* mice. *Journal of Bone and Mineral Research: The Official Journal of the American Society for Bone and Mineral Research*, *26*(8), 1710–1720. https://doi.org/10.1002/jbmr.406

Bateman, L. E. R. (2020). *The anti-inflammatory effects of testosterone on atherosclerosis* [Doctoral, Sheffield Hallam University]. <a href="https://doi.org/10.7190/shuthesis-00351">https://doi.org/10.7190/shuthesis-00351</a>

Belin de Chantemèle, E. J. B., Muta, K., Mintz, J., Tremblay, M. L., Marrero, M. B., Fulton, D., and Stepp, D. W. (2009). Protein Tyrosine Phosphatase 1B, a major regulator of leptin-mediated control of cardiovascular function. *Circulation*, *120*(9), 753–763. https://doi.org/10.1161/CIRCULATIONAHA.109.853077

Bergh, C., Wennergren, D., Möller, M., and Brisby, H. (2020). Fracture incidence in adults in relation to age and gender: A study of 27,169 fractures in the Swedish Fracture Register in a well-defined catchment area. *PLoS ONE*, *15*(12), e0244291. https://doi.org/10.1371/journal.pone.0244291

Bierhals, I. O., dos Santos Vaz, J., Bielemann, R. M., de Mola, C. L., Barros, F. C., Gonçalves, H., Wehrmeister, F. C., and Assunção, M. C. F. (2019). Associations between body mass index, body composition and bone density in young adults: Findings from a southern Brazilian cohort. *BMC Musculoskeletal Disorders*, 20(1), Article 1. https://doi.org/10.1186/s12891-019-2656-3

Blain, H., Vuillemin, A., Guillemin, F., Durant, R., Hanesse, B., de Talance, N., Doucet, B., and Jeandel, C. (2002). Serum Leptin Level Is a Predictor of Bone Mineral Density in Postmenopausal Women. *The Journal of Clinical Endocrinology and Metabolism*, *87*(3), Article 3. https://doi.org/10.1210/jcem.87.3.8313

Blouin, K., Nadeau, M., Perreault, M., Veilleux, A., Drolet, R., Marceau, P., Mailloux, J., Luu-The, V., and Tchernof, A. (2010). Effects of androgens on adipocyte differentiation and adipose tissue explant metabolism in men and women. *Clinical Endocrinology*, 72(2), 176–188. https://doi.org/10.1111/j.1365-2265.2009.03645.x

Blouin, S., Libouban, H., Moreau, M. F., and Chappard, D. (2008). Orchidectomy Models of Osteoporosis. In J. J. Westendorf (Ed.), *Osteoporosis: Methods and Protocols* (pp. 125–134). Humana Press. <a href="https://doi.org/10.1007/978-1-59745-104-8">https://doi.org/10.1007/978-1-59745-104-8</a> 9

Bonewald, L. F. (2011). The Amazing Osteocyte. *Journal of Bone and Mineral Research*, 26(2), Article 2. <a href="https://doi.org/10.1002/jbmr.320">https://doi.org/10.1002/jbmr.320</a>

Bouxsein, M. L., Boyd, S. K., Christiansen, B. A., Guldberg, R. E., Jepsen, K. J., and Müller, R. (2010a). Guidelines for assessment of bone microstructure in rodents using microcomputed tomography. *Journal of Bone and Mineral Research: The Official Journal of the American Society for Bone and Mineral Research*, 25(7), 1468–1486. https://doi.org/10.1002/jbmr.141

Bouxsein, M. L., Boyd, S. K., Christiansen, B. A., Guldberg, R. E., Jepsen, K. J., and Müller, R. (2010b). Guidelines for assessment of bone microstructure in rodents using microcomputed tomography. *Journal of Bone and Mineral Research: The Official Journal of the American Society for Bone and Mineral Research*, 25(7), 1468–1486. https://doi.org/10.1002/jbmr.141

Boyce, B. F., and Xing, L. (2007). Biology of RANK, RANKL, and osteoprotegerin. *Arthritis Research and Therapy*, *9*(Suppl 1), S1. <a href="https://doi.org/10.1186/ar2165">https://doi.org/10.1186/ar2165</a>

Boyce, B. F., and Xing, L. (2008). Functions of RANKL/RANK/OPG in bone modeling and remodeling. *Archives of Biochemistry and Biophysics*, *473*(2), 139–146. <a href="https://doi.org/10.1016/j.abb.2008.03.018">https://doi.org/10.1016/j.abb.2008.03.018</a>

Buettner, C., Pocai, A., Muse, E. D., Etgen, A. M., Myers, M. G., and Rossetti, L. (2006). Critical role of STAT3 in leptin's metabolic actions. *Cell Metabolism*, *4*(1), Article 1. <a href="https://doi.org/10.1016/j.cmet.2006.04.014">https://doi.org/10.1016/j.cmet.2006.04.014</a>

Buo, A. M., and Stains, J. P. (2014). Gap Junctional Regulation of Signal Transduction in Bone Cells. *FEBS Letters*, *588*(8), Article 8. <a href="https://doi.org/10.1016/j.febslet.2014.01.025">https://doi.org/10.1016/j.febslet.2014.01.025</a>

Burnett, L. C., Skowronski, A. A., Rausch, R., LeDuc, C. A., and Leibel, R. L. (2017). Determination of the half life of circulating leptin in the mouse. *International Journal of Obesity (2005)*, *41*(3), 355–359. <a href="https://doi.org/10.1038/ijo.2016.238">https://doi.org/10.1038/ijo.2016.238</a>

Buss, D. J., Kröger, R., McKee, M. D., and Reznikov, N. (2022). Hierarchical organization of bone in three dimensions: A twist of twists. *Journal of Structural Biology: X, 6,* 100057. <a href="https://doi.org/10.1016/j.yjsbx.2021.100057">https://doi.org/10.1016/j.yjsbx.2021.100057</a>

Caliari, S. R., and Burdick, J. A. (2016). A practical guide to hydrogels for cell culture. *Nature Methods*, 13(5), 405–414. https://doi.org/10.1038/nmeth.3839

Campbell, M. J., Bustamante-Gomez, C., Fu, Q., Beenken, K. E., Reyes-Pardo, H., Smeltzer, M. S., and O'Brien, C. A. (2024). RANKL-mediated osteoclast formation is

required for bone loss in a murine model of *Staphylococcus aureus* osteomyelitis. *Bone*, 187, 117181. https://doi.org/10.1016/j.bone.2024.117181

Cao, J. J. (2011). Effects of obesity on bone metabolism. *Journal of Orthopaedic Surgery* and Research, 6, 30. <a href="https://doi.org/10.1186/1749-799X-6-30">https://doi.org/10.1186/1749-799X-6-30</a>

Cao, J. J., Gregoire, B. R., and Gao, H. (2009). High-fat diet decreases cancellous bone mass but has no effect on cortical bone mass in the tibia in mice. *Bone*, *44*(6), 1097–1104. https://doi.org/10.1016/j.bone.2009.02.017

Cardaci, T. D., Machek, S. B., Wilburn, D. T., Heileson, J. L., and Willoughby, D. S. (2020). High-Load Resistance Exercise Augments Androgen Receptor–DNA Binding and Wnt/β-Catenin Signaling without Increases in Serum/Muscle Androgens or Androgen Receptor Content. *Nutrients*, *12*(12), Article 12. https://doi.org/10.3390/nu12123829

Chaves, C., Kay, T., & Anselmo, J. (2022). Early onset obesity due to a mutation in the human leptin receptor gene. Endocrinology, Diabetes & Metabolism Case Reports, 2022, 21–0124. https://doi.org/10.1530/EDM-21-0124

Chen, H. C., and Farese, R. V. (1999). Steroid hormones: Interactions with membrane-bound receptors. *Current Biology*, *9*(13), R478–R481. <a href="https://doi.org/10.1016/S0960-9822(99)80300-5">https://doi.org/10.1016/S0960-9822(99)80300-5</a>

Chen, H., Liu, O., Chen, S., and Zhou, Y. (2022). Aging and Mesenchymal Stem Cells: Therapeutic Opportunities and Challenges in the Older Group. *Gerontology*, *68*(3), 339–352. <a href="https://doi.org/10.1159/000516668">https://doi.org/10.1159/000516668</a>

Chen, H., Zhou, X., Fujita, H., Onozuka, M., and Kubo, K.-Y. (2013). Age-Related Changes in Trabecular and Cortical Bone Microstructure. *International Journal of Endocrinology*, 2013(1), 213234. <a href="https://doi.org/10.1155/2013/213234">https://doi.org/10.1155/2013/213234</a>

Chen, J. C., Hoey, D. A., Chua, M., Bellon, R., and Jacobs, C. R. (2016). Mechanical signals promote osteogenic fate through a primary cilia-mediated mechanism. *The FASEB Journal*, *30*(4), Article 4. <a href="https://doi.org/10.1096/fj.15-276402">https://doi.org/10.1096/fj.15-276402</a>

Chen, J.-F., Lin, P.-W., Tsai, Y.-R., Yang, Y.-C., and Kang, H.-Y. (2019). Androgens and Androgen Receptor Actions on Bone Health and Disease: From Androgen Deficiency to Androgen Therapy. *Cells*, 8(11), 1318. <a href="https://doi.org/10.3390/cells8111318">https://doi.org/10.3390/cells8111318</a>

Chen, X., Wang, Z., Duan, N., Zhu, G., Schwarz, E. M., and Xie, C. (2018). Osteoblast-Osteoclast Interactions. *Connective Tissue Research*, *59*(2), Article 2. <a href="https://doi.org/10.1080/03008207.2017.1290085">https://doi.org/10.1080/03008207.2017.1290085</a>

Chiba, T., Nakazawa, T., Yui, K., Kaneko, E., and Shimokado, K. (2003). VLDL Induces Adipocyte Differentiation in ApoE-Dependent Manner. *Arteriosclerosis, Thrombosis, and Vascular Biology*, 23(8), 1423–1429. https://doi.org/10.1161/01.ATV.0000085040.58340.36

Choudhury, J., Mirshahi, F., Murthy, K. S., Yager, D. R., and Sanyal, A. J. (2006). Physiologic concentrations of leptin increase collagen production by non-immortalized human hepatic stellate cells. *Metabolism: Clinical and Experimental*, *55*(10), 1317–1322. https://doi.org/10.1016/j.metabol.2006.05.016

Chung, E. J., Shah, N., and Shah, R. N. (2013). 11—Nanomaterials for cartilage tissue engineering. In A. K. Gaharwar, S. Sant, M. J. Hancock, and S. A. Hacking (Eds.), *Nanomaterials in Tissue Engineering* (pp. 301–334). Woodhead Publishing. <a href="https://doi.org/10.1533/9780857097231.2.301">https://doi.org/10.1533/9780857097231.2.301</a>

Clarke, B. (2008). Normal Bone Anatomy and Physiology. *Clinical Journal of the American Society of Nephrology*, *3*(Supplement\_3), S131. <a href="https://doi.org/10.2215/CJN.04151206">https://doi.org/10.2215/CJN.04151206</a>
Clément, K., Vaisse, C., Lahlou, N., Cabrol, S., Pelloux, V., Cassuto, D., Gourmelen, M., Dina, C., Chambaz, J., Lacorte, J.-M., Basdevant, A., Bougnères, P., Lebouc, Y., Froguel, P., and Guy-Grand, B. (1998). A mutation in the human leptin receptor gene causes obesity and pituitary dysfunction. *Nature*, *392*(6674), Article 6674. <a href="https://doi.org/10.1038/32911">https://doi.org/10.1038/32911</a>

Coleman, D. L. (1973). Effects of parabiosis of obese with diabetes and normal mice. *Diabetologia*, *9*(4), 294–298. <a href="https://doi.org/10.1007/BF01221857">https://doi.org/10.1007/BF01221857</a>

Colleluori, G., Aguirre, L., Napoli, N., Qualls, C., Villareal, D. T., and Armamento-Villareal, R. (2021). Testosterone Therapy Effects on Bone Mass and Turnover in Hypogonadal Men with Type 2 Diabetes. *The Journal of Clinical Endocrinology and Metabolism*, *106*(8), e3058–e3068. <a href="https://doi.org/10.1210/clinem/dgab181">https://doi.org/10.1210/clinem/dgab181</a>

Corrigan, M. A., Johnson, G. P., Stavenschi, E., Riffault, M., Labour, M.-N., and Hoey, D. A. (2018). TRPV4-mediates oscillatory fluid shear mechanotransduction in mesenchymal

stem cells in part via the primary cilium. *Scientific Reports*, 8(1), Article 1. https://doi.org/10.1038/s41598-018-22174-3

Costa, L. R., Carvalho, A. B., Bittencourt, A. L., Rochitte, C. E., and Canziani, M. E. F. (2020). Cortical unlike trabecular bone loss is not associated with vascular calcification progression in CKD patients. *BMC Nephrology*, *21*(1), 121. https://doi.org/10.1186/s12882-020-01756-2

Costa, S., Fairfield, H., and Reagan, M. R. (2019). Inverse correlation between trabecular bone volume and bone marrow adipose tissue in rats treated with osteoanabolic agents. *Bone*, *123*, 211–223. https://doi.org/10.1016/j.bone.2019.03.038

crossref. (n.d.). Chooser. Retrieved 1 October 2023, from https://chooser.crossref.org/

Czekanska, E. M., Stoddart, M. J., Ralphs, J. R., Richards, R. G., and Hayes, J. S. (2014). A phenotypic comparison of osteoblast cell lines versus human primary osteoblasts for biomaterials testing. *Journal of Biomedical Materials Research Part A*, 102(8), 2636–2643. https://doi.org/10.1002/jbm.a.34937

da Costa, J. V., Semmelmann Pereira-Lima, J. F., and da Costa Oliveira, M. (2004). Bone Mineral Density in Early-Onset Hypogonadism and the Effect of Hormonal Replacement. *Journal of Clinical Densitometry*, 7(3), 334–340. https://doi.org/10.1385/JCD:7:3:334

Dabaja, A. A., Bryson, C. F., Schlegel, P. N., and Paduch, D. A. (2015). The effect of hypogonadism and testosterone-enhancing therapy on alkaline phosphatase and bone mineral density. *BJU International*, *115*(3), 480–485. <a href="https://doi.org/10.1111/bju.12870">https://doi.org/10.1111/bju.12870</a>

Dam, J., and Jockers, R. (2013). Hunting for the functions of short leptin receptor isoforms. *Molecular Metabolism*, 2(4), Article 4. <a href="https://doi.org/10.1016/j.molmet.2013.09.001">https://doi.org/10.1016/j.molmet.2013.09.001</a>

De Bruyn, R., Bollen, R., and Claessens, F. (2011). Identification and characterization of androgen response elements. *Methods in Molecular Biology (Clifton, N.J.)*, 776, 81–93. https://doi.org/10.1007/978-1-61779-243-4 6

De Jonghe, B. C., Hayes, M. R., Zimmer, D. J., Kanoski, S. E., Grill, H. J., and Bence, K. K. (2012). Food intake reductions and increases in energetic responses by hindbrain leptin and melanotan II are enhanced in mice with POMC-specific PTP1B deficiency. *American* 

Journal of Physiology - Endocrinology and Metabolism, 303(5), E644–E651. https://doi.org/10.1152/ajpendo.00009.2012

De Laet, C., Kanis, J. A., Odén, A., Johanson, H., Johnell, O., Delmas, P., Eisman, J. A., Kroger, H., Fujiwara, S., Garnero, P., McCloskey, E. V., Mellstrom, D., Melton, L. J., Meunier, P. J., Pols, H. a. P., Reeve, J., Silman, A., and Tenenhouse, A. (2005). Body mass index as a predictor of fracture risk: A meta-analysis. *Osteoporosis International: A Journal Established as Result of Cooperation between the European Foundation for Osteoporosis and the National Osteoporosis Foundation of the USA*, *16*(11), 1330–1338. https://doi.org/10.1007/s00198-005-1863-y

De Leon-Oliva, D., Barrena-Blázquez, S., Jiménez-Álvarez, L., Fraile-Martinez, O., García-Montero, C., López-González, L., Torres-Carranza, D., García-Puente, L. M., Carranza, S. T., Álvarez-Mon, M. Á., Álvarez-Mon, M., Diaz, R., and Ortega, M. A. (2023). The RANK–RANKL–OPG System: A Multifaceted Regulator of Homeostasis, Immunity, and Cancer. *Medicina*, *59*(10), 1752. <a href="https://doi.org/10.3390/medicina59101752">https://doi.org/10.3390/medicina59101752</a>

De Lorenzo, A., Pellegrini, M., Gualtieri, P., Itani, L., Frank, G., El Ghoch, M., and Di Renzo, L. (2024). The Association between Obesity and Reduced Weight-Adjusted Bone Mineral Content in Older Adults: A New Paradigm That Contrasts with the Obesity Paradox. *Nutrients*, *16*(3), 352. <a href="https://doi.org/10.3390/nu16030352">https://doi.org/10.3390/nu16030352</a>

Deckard, C., Walker, A., and Hill, B. J. F. (2017). Using three-point bending to evaluate tibia bone strength in ovariectomized young mice. *Journal of Biological Physics*, *43*(1), 139–148. <a href="https://doi.org/10.1007/s10867-016-9439-y">https://doi.org/10.1007/s10867-016-9439-y</a>

Delaissé, J.-M., Andersen, T. L., Engsig, M. T., Henriksen, K., Troen, T., and Blavier, L. (2003). Matrix metalloproteinases (MMP) and cathepsin K contribute differently to osteoclastic activities. *Microscopy Research and Technique*, *61*(6), 504–513. https://doi.org/10.1002/jemt.10374

Di Medio, L., and Brandi, M. L. (2021). Chapter Three—Advances in bone turnover markers. In G. S. Makowski (Ed.), *Advances in Clinical Chemistry* (Vol. 105, pp. 101–140). Elsevier. <a href="https://doi.org/10.1016/bs.acc.2021.06.001">https://doi.org/10.1016/bs.acc.2021.06.001</a>

Diez-Escudero, A., Andersson, B., Persson, C., and Hailer, N. P. (2021). Hexagonal pore geometry and the presence of hydroxyapatite enhance deposition of mineralized bone

matrix on additively manufactured polylactic acid scaffolds. *Materials Science and Engineering: C, 125,* 112091. https://doi.org/10.1016/j.msec.2021.112091

do Carmo, J. M., da Silva, A. A., Cai, Z., Lin, S., Dubinion, J. H., and Hall, J. E. (2011). CONTROL OF BLOOD PRESSURE, APPETITE AND GLUCOSE BY LEPTIN IN MICE LACKING LEPTIN RECEPTORS IN POMC NEURONS. *Hypertension*, *57*(5), 918–926. https://doi.org/10.1161/HYPERTENSIONAHA.110.161349

do Carmo, J. M., da Silva, A. A., Dubinion, J., Sessums, P. O., Ebaady, S. H., Wang, Z., and Hall, J. E. (2013). Control of Metabolic and Cardiovascular Function by the Leptin–Brain Melanocortin Pathway. *IUBMB Life*, *65*(8), 692–698. https://doi.org/10.1002/iub.1187

Domazetovic, V., Marcucci, G., Iantomasi, T., Brandi, M. L., and Vincenzini, M. T. (2017). Oxidative stress in bone remodeling: Role of antioxidants. *Clinical Cases in Mineral and Bone Metabolism*, *14*(2), 209–216. https://doi.org/10.11138/ccmbm/2017.14.1.209

Dominic, E., Brozek, W., Peter, R. S., Fromm, E., Ulmer, H., Rapp, K., Concin, H., and Nagel, G. (2020a). Metabolic factors and hip fracture risk in a large Austrian cohort study. *Bone Reports*, *12*. https://doi.org/10.1016/j.bonr.2020.100244

Dominic, E., Brozek, W., Peter, R. S., Fromm, E., Ulmer, H., Rapp, K., Concin, H., and Nagel, G. (2020b). Metabolic factors and hip fracture risk in a large Austrian cohort study. *Bone Reports*, *12*, 100244. <a href="https://doi.org/10.1016/j.bonr.2020.100244">https://doi.org/10.1016/j.bonr.2020.100244</a>

Dong, Y.-F., Soung, D. Y., Schwarz, E. M., O'Keefe, R. J., and Drissi, H. (2006). Wnt induction of chondrocyte hypertrophy through the Runx2 transcription factor. *Journal of Cellular Physiology*, 208(1), Article 1. <a href="https://doi.org/10.1002/jcp.20656">https://doi.org/10.1002/jcp.20656</a>

Driessler, F., and Baldock, P. A. (2010a). Hypothalamic regulation of bone. *Journal of Molecular Endocrinology*, 45(4), 175–181. https://doi.org/10.1677/JME-10-0015

Driessler, F., and Baldock, P. A. (2010b). Hypothalamic regulation of bone. *Journal of Molecular Endocrinology*, 45(4), Article 4. https://doi.org/10.1677/JME-10-0015

Duan, J., Choi, Y.-H., Hartzell, D., Della-Fera, M. A., Hamrick, M., and Baile, C. A. (2007). Effects of subcutaneous leptin injections on hypothalamic gene profiles in lean and *Ob/Ob* mice. *Obesity (Silver Spring, Md.)*, *15*(11), 2624–2633. https://doi.org/10.1038/oby.2007.314

Duan, W., Zou, H., Zang, N., Ma, D., Yang, B., and Zhu, L. (2023). Metformin increases bone marrow adipose tissue by promoting mesenchymal stromal cells apoptosis. *Aging* (Albany NY), 15(2), 542–552. https://doi.org/10.18632/aging.204486

Duan, Y., Zeng, L., Zheng, C., Song, B., Li, F., Kong, X., and Xu, K. (2018). Inflammatory Links Between High Fat Diets and Diseases. *Frontiers in Immunology*, *9*, 2649. https://doi.org/10.3389/fimmu.2018.02649

Ducher, G., Courteix, D., Même, S., Magni, C., Viala, J. F., and Benhamou, C. L. (2005). Bone geometry in response to long-term tennis playing and its relationship with muscle volume: A quantitative magnetic resonance imaging study in tennis players. *Bone*, *37*(4), Article 4. https://doi.org/10.1016/j.bone.2005.05.014

Ducher, G., Jaffré, C., Arlettaz, A., Benhamou, C.-L., and Courteix, D. (2005). Effects of long-term tennis playing on the muscle-bone relationship in the dominant and nondominant forearms. *Canadian Journal of Applied Physiology = Revue Canadianne De Physiologie Appliquee*, *30*(1), 3–17. <a href="https://doi.org/10.1139/h05-101">https://doi.org/10.1139/h05-101</a>

Ducy, P., Amling, M., Takeda, S., Priemel, M., Schilling, A. F., Beil, F. T., Shen, J., Vinson, C., Rueger, J. M., and Karsenty, G. (2000). Leptin inhibits bone formation through a hypothalamic relay: A central control of bone mass. *Cell*, *100*(2), 197–207. https://doi.org/10.1016/s0092-8674(00)81558-5

Duval, K., Grover, H., Han, L.-H., Mou, Y., Pegoraro, A. F., Fredberg, J., and Chen, Z. (2017). Modeling Physiological Events in 2D vs. 3D Cell Culture. *Physiology*, *32*(4), 266–277. <a href="https://doi.org/10.1152/physiol.00036.2016">https://doi.org/10.1152/physiol.00036.2016</a>

E. Kypreos, K., A. Karavia, E., Constantinou, C., Hatziri, A., Kalogeropoulou, C., Xepapadaki, E., and Zvintzou, E. (2018). Apolipoprotein E in diet-induced obesity: A paradigm shift from conventional perception. *Journal of Biomedical Research*, *32*(3), 183–190. <a href="https://doi.org/10.7555/JBR.32.20180007">https://doi.org/10.7555/JBR.32.20180007</a>

Elefteriou, F., Takeda, S., Ebihara, K., Magre, J., Patano, N., Ae Kim, C., Ogawa, Y., Liu, X., Ware, S. M., Craigen, W. J., Robert, J. J., Vinson, C., Nakao, K., Capeau, J., and Karsenty, G. (2004). Serum leptin level is a regulator of bone mass. *Proceedings of the National Academy of Sciences*, 101(9), 3258–3263. https://doi.org/10.1073/pnas.0308744101

Elsheikh, A., and Rothman, M. S. (2023). Testosterone Replacement Therapy for Treatment of Osteoporosis in Men. *Faculty Reviews*, *12*. <a href="https://doi.org/10.12703/r/12-18">https://doi.org/10.12703/r/12-18</a>

Engberg, E., Koivusalo, S. B., Huvinen, E., and Viljakainen, H. (2020). Bone health in women with a history of gestational diabetes or obesity. *Acta Obstetricia Et Gynecologica Scandinavica*, *99*(4), 477–487. <a href="https://doi.org/10.1111/aogs.13778">https://doi.org/10.1111/aogs.13778</a>

Enriori, P. J., Evans, A. E., Sinnayah, P., Jobst, E. E., Tonelli-Lemos, L., Billes, S. K., Glavas, M. M., Grayson, B. E., Perello, M., Nillni, E. A., Grove, K. L., and Cowley, M. A. (2007). Diet-Induced Obesity Causes Severe but Reversible Leptin Resistance in Arcuate Melanocortin Neurons. *Cell Metabolism*, *5*(3), 181–194. <a href="https://doi.org/10.1016/j.cmet.2007.02.004">https://doi.org/10.1016/j.cmet.2007.02.004</a>

Erben, R. G. (2018a). Physiological Actions of Fibroblast Growth Factor-23. *Frontiers in Endocrinology*, 9. <a href="https://doi.org/10.3389/fendo.2018.00267">https://doi.org/10.3389/fendo.2018.00267</a>

Erben, R. G. (2018b). Physiological Actions of Fibroblast Growth Factor-23. *Frontiers in Endocrinology*, *9*. https://doi.org/10.3389/fendo.2018.00267

Eriksen, E. F. (2010). Cellular mechanisms of bone remodeling. *Reviews in Endocrine and Metabolic Disorders*, *11*(4), 219–227. <a href="https://doi.org/10.1007/s11154-010-9153-1">https://doi.org/10.1007/s11154-010-9153-1</a>

Estrada, M., Espinosa, A., Müller, M., and Jaimovich, E. (2003). Testosterone Stimulates Intracellular Calcium Release and Mitogen-Activated Protein Kinases Via a G Protein-Coupled Receptor in Skeletal Muscle Cells. *Endocrinology*, *144*(8), 3586–3597. <a href="https://doi.org/10.1210/en.2002-0164">https://doi.org/10.1210/en.2002-0164</a>

Faienza, M. F., Giardinelli, S., Annicchiarico, A., Chiarito, M., Barile, B., Corbo, F., and Brunetti, G. (2024). Nutraceuticals and Functional Foods: A Comprehensive Review of Their Role in Bone Health. *International Journal of Molecular Sciences*, *25*(11), 5873. <a href="https://doi.org/10.3390/ijms25115873">https://doi.org/10.3390/ijms25115873</a>

Fan, Q., Li, H., Liu, Z., Zhang, Z., Li, H., Ding, J., and Zhang, Z. (2017). Leptin inhibits AMPKα2 down-regulation induced decrease in the osteocytic MLO-Y4 cell proliferation and the expression of osteogenic markers. *International Journal of Clinical and Experimental Pathology*, 10(8), 8544–8552.

Fang, J., Zhang, X., Chen, X., Wang, Z., Zheng, S., Cheng, Y., Liu, S., and Hao, L. (2023). The role of insulin-like growth factor-1 in bone remodeling: A review. *International Journal of Biological Macromolecules*, 238, 124125. <a href="https://doi.org/10.1016/j.ijbiomac.2023.124125">https://doi.org/10.1016/j.ijbiomac.2023.124125</a>

Farroqi, I. S., and O'Rahilly, S. (2014). 20 YEARS OF LEPTIN: Human disorders of leptin action. *Journal of Endocrinology*, 223(1), Article 1. <a href="https://doi.org/10.1530/JOE-14-0480">https://doi.org/10.1530/JOE-14-0480</a>
Farrar, M. C., and Jacobs, T. F. (2024). Tamoxifen. In *StatPearls*. StatPearls Publishing. <a href="http://www.ncbi.nlm.nih.gov/books/NBK532905/">http://www.ncbi.nlm.nih.gov/books/NBK532905/</a>

Felder, A. A., Monzem, S., Souza, R. D., Javaheri, B., Mills, D., Boyde, A., and Doube, M. (2021). *The plate-to-rod transition in trabecular bone loss is elusive* (p. 2020.05.14.081042). bioRxiv. https://doi.org/10.1101/2020.05.14.081042

Feng, X., and McDonald, J. M. (2011). Disorders of Bone Remodeling. *Annual Review of Pathology*, 6, 121–145. <a href="https://doi.org/10.1146/annurev-pathol-011110-130203">https://doi.org/10.1146/annurev-pathol-011110-130203</a>

Fields, A. J., and Keaveny, T. M. (2012). Trabecular architecture and vertebral fragility in osteoporosis. *Current Osteoporosis Reports*, 10(2), 132–140. <a href="https://doi.org/10.1007/s11914-012-0097-0">https://doi.org/10.1007/s11914-012-0097-0</a>

Fitzgibbons, T. P., Kelly, M., Kim, J. K., and Czech, M. P. (2018). *Resistance to diet induced obesity in the apolipoprotein E deficient mouse is associated with an attenuated transcriptional response in visceral fat* (p. 494195). bioRxiv. https://doi.org/10.1101/494195

Fix, C., Jordan, C., Cano, P., and Walker, W. H. (2004). Testosterone activates mitogenactivated protein kinase and the cAMP response element binding protein transcription factor in Sertoli cells. *Proceedings of the National Academy of Sciences*, *101*(30), 10919–10924. <a href="https://doi.org/10.1073/pnas.0404278101">https://doi.org/10.1073/pnas.0404278101</a>

Fontana, F., Hickman-Brecks, C. L., Salazar, V. S., Revollo, L., Abou-Ezzi, G., Grimston, S. K., Jeong, S. Y., Watkins, M., Fortunato, M., Alippe, Y., Link, D. C., Mbalaviele, G., and Civitelli, R. (2017). N-cadherin Regulation of Bone Growth and Homeostasis is Osteolineage Stage-Specific. *Journal of Bone and Mineral Research : The Official Journal of the American Society for Bone and Mineral Research*, 32(6), 1332–1342. https://doi.org/10.1002/jbmr.3112

Forny-Germano, L., De Felice, F. G., and Vieira, M. N. do N. (2019). The Role of Leptin and Adiponectin in Obesity-Associated Cognitive Decline and Alzheimer's Disease. *Frontiers in Neuroscience*, 12. https://doi.org/10.3389/fnins.2018.01027

Franco, M., Khorrami Chokami, K., Albertelli, M., Teti, C., Cocchiara, F., Gatto, F., Trombetta, C., Ferone, D., and Boschetti, M. (2023). Modulatory activity of testosterone on growth pattern and IGF-1 levels in vanishing testis syndrome: A case report during 15 years of follow-up. *BMC Endocrine Disorders*, 23(1), 13. https://doi.org/10.1186/s12902-022-01258-2

Fui, M. N. T., Dupuis, P., and Grossmann, M. (2014). Lowered testosterone in male obesity: Mechanisms, morbidity and management. *Asian Journal of Andrology*, *16*(2), 223–231. <a href="https://doi.org/10.4103/1008-682X.122365">https://doi.org/10.4103/1008-682X.122365</a>

Gandham, A., Zengin, A., Bonham, M. P., Winzenberg, T., Balogun, S., Wu, F., Aitken, D., Cicuttini, F., Ebeling, P. R., Jones, G., and Scott, D. (2020). Incidence and predictors of fractures in older adults with and without obesity defined by body mass index versus body fat percentage. *Bone*, *140*, 115546. <a href="https://doi.org/10.1016/j.bone.2020.115546">https://doi.org/10.1016/j.bone.2020.115546</a>

Gao, K., Wang, X., Liu, Q., Chen, W., Wang, G., Zhang, D., and Liu, L. (2018a). Evaluation of osteoblast differentiation and function when cultured on mesoporous bioactive glass adsorbed with testosterone. *Journal of Cellular Biochemistry*, *119*(7), 5222–5232. https://doi.org/10.1002/jcb.26566

Gao, K., Wang, X., Liu, Q., Chen, W., Wang, G., Zhang, D., and Liu, L. (2018b). Evaluation of osteoblast differentiation and function when cultured on mesoporous bioactive glass adsorbed with testosterone. *Journal of Cellular Biochemistry*, *119*(7), 5222–5232. <a href="https://doi.org/10.1002/jcb.26566">https://doi.org/10.1002/jcb.26566</a>

García-Ruiz, I., Gómez-Izquierdo, E., Díaz-Sanjuán, T., Grau, M., Solís-Muñoz, P., Muñoz-Yagüe, T., and Solís-Herruzo, J. A. (2012). Sp1 and Sp3 Transcription Factors Mediate Leptin-Induced Collagen α1(I) Gene Expression in Primary Culture of Male Rat Hepatic Stellate Cells. *Endocrinology*, *153*(12), 5845–5856. <a href="https://doi.org/10.1210/en.2012-1626">https://doi.org/10.1210/en.2012-1626</a>

Genetos, D. C., Kephart, C. J., Zhang, Y., Yellowley, C. E., and Donahue, H. J. (2007). OSCILLATING FLUID FLOW ACTIVATION OF GAP JUNCTION HEMICHANNELS INDUCES

ATP RELEASE FROM MLO-Y4 OSTEOCYTES. *Journal of Cellular Physiology*, 212(1), Article 1. <a href="https://doi.org/10.1002/jcp.21021">https://doi.org/10.1002/jcp.21021</a>

Ghanemi, A., Yoshioka, M., and St-Amand, J. (2022). In Vitro Mimicking of Obesity-Induced Biochemical Environment to Study Obesity Impacts on Cells and Tissues. *Diseases*, *10*(4), 76. <a href="https://doi.org/10.3390/diseases10040076">https://doi.org/10.3390/diseases10040076</a>

Ghayor, C., Correro, R. M., Lange, K., Karfeld-Sulzer, L. S., Grätz, K. W., and Weber, F. E. (2011). Inhibition of Osteoclast Differentiation and Bone Resorption by N-Methylpyrrolidone \*. *Journal of Biological Chemistry*, *286*(27), 24458–24466. https://doi.org/10.1074/jbc.M111.223297

Gill, R. K., Turner, R. T., Wronski, T. J., and Bell, N. H. (1998). Orchiectomy markedly reduces the concentration of the three isoforms of transforming growth factor beta in rat bone, and reduction is prevented by testosterone. *Endocrinology*, *139*(2), 546–550. https://doi.org/10.1210/endo.139.2.5717

Glatt, V., Canalis, E., Stadmeyer, L., and Bouxsein, M. L. (2007). Age-Related Changes in Trabecular Architecture Differ in Female and Male C57BL/6J Mice. *Journal of Bone and Mineral Research*, 22(8), 1197–1207. https://doi.org/10.1359/jbmr.070507

Goldman, A. L., Bhasin, S., Wu, F. C. W., Krishna, M., Matsumoto, A. M., and Jasuja, R. (2017). A Reappraisal of Testosterone's Binding in Circulation: Physiological and Clinical Implications. *Endocrine Reviews*, *38*(4), 302–324. <a href="https://doi.org/10.1210/er.2017-00025">https://doi.org/10.1210/er.2017-00025</a>

Golds, G., Houdek, D., and Arnason, T. (2017). Male Hypogonadism and Osteoporosis: The Effects, Clinical Consequences, and Treatment of Testosterone Deficiency in Bone Health. *International Journal of Endocrinology*, 2017, 4602129. https://doi.org/10.1155/2017/4602129

Greene, D. A., and Naughton, G. A. (2006). Adaptive skeletal responses to mechanical loading during adolescence. *Sports Medicine (Auckland, N.Z.)*, *36*(9), 723–732. https://doi.org/10.2165/00007256-200636090-00001

Gregson, C. L., Hardcastle, S. A., Cooper, C., and Tobias, J. H. (2013). Friend or foe: High bone mineral density on routine bone density scanning, a review of causes and

management. Rheumatology (Oxford, England), 52(6), 968–985. https://doi.org/10.1093/rheumatology/ket007

Grethen, E., Hill, K. M., Jones, R., Cacucci, B. M., Gupta, C. E., Acton, A., Considine, R. V., and Peacock, M. (2012). Serum leptin, parathyroid hormone, 1,25-dihydroxyvitamin D, fibroblast growth factor 23, bone alkaline phosphatase, and sclerostin relationships in obesity. *The Journal of Clinical Endocrinology and Metabolism*, *97*(5), 1655–1662. https://doi.org/10.1210/jc.2011-2280

Grossmann, M. (2011). Low Testosterone in Men with Type 2 Diabetes: Significance and Treatment. *The Journal of Clinical Endocrinology and Metabolism*, *96*(8), 2341–2353. https://doi.org/10.1210/jc.2011-0118

Gruzdeva, O., Borodkina, D., Uchasova, E., Dyleva, Y., and Barbarash, O. (2019). Leptin resistance: Underlying mechanisms and diagnosis. *Diabetes, Metabolic Syndrome and Obesity: Targets and Therapy*, *12*, 191. <a href="https://doi.org/10.2147/DMSO.S182406">https://doi.org/10.2147/DMSO.S182406</a>

Guilak, F., Leddy, H. A., and Liedtke, W. (2010). Transient Receptor Potential Vanilloid 4: The Sixth Sense of the Musculoskeletal System? *Annals of the New York Academy of Sciences*, 1192, 404–409. https://doi.org/10.1111/j.1749-6632.2010.05389.x

Guo, Y., Xu, C., Wu, X., Zhang, W., Sun, Y., and Shrestha, A. (2021). Leptin regulates OPG and RANKL expression in Gingival Fibroblasts and Tissues of Chronic Periodontitis Patients. *International Journal of Medical Sciences*, 18(11), 2431–2437. https://doi.org/10.7150/ijms.56151

Gupta, R., Al-saeed, O., Azizieh, F., Albusairi, A., Gupta, P., and Mohammed, A. (2012). Evaluation of Bone Mineral Density in Postmenopausal Women in Kuwait. *Journal of Clinical Densitometry*, *15*(2), 211–216. <a href="https://doi.org/10.1016/j.jocd.2011.10.006">https://doi.org/10.1016/j.jocd.2011.10.006</a>

Gurzov, E. N., Stanley, W. J., Pappas, E. G., Thomas, H. E., and Gough, D. J. (2016). The JAK/STAT pathway in obesity and diabetes. *The FEBS Journal*, *283*(16), 3002–3015. <a href="https://doi.org/10.1111/febs.13709">https://doi.org/10.1111/febs.13709</a>

Hadjidakis, D. J., and Androulakis, I. I. (2006). Bone Remodeling. *Annals of the New York Academy of Sciences*, 1092(1), 385–396. https://doi.org/10.1196/annals.1365.035

Hall, J. E., do Carmo, J. M., da Silva, A. A., Wang, Z., and Hall, M. E. (2019). Obesity, kidney dysfunction and hypertension: Mechanistic links. *Nature Reviews. Nephrology*, *15*(6), 367–385. <a href="https://doi.org/10.1038/s41581-019-0145-4">https://doi.org/10.1038/s41581-019-0145-4</a>

Hamrick, M. W. (2004). Leptin, Bone Mass, and the Thrifty Phenotype. *Journal of Bone and Mineral Research*, 19(10), Article 10. <a href="https://doi.org/10.1359/JBMR.040712">https://doi.org/10.1359/JBMR.040712</a>

Hamrick, M. W., Della-Fera, M. A., Choi, Y.-H., Pennington, C., Hartzell, D., and Baile, C. A. (2005). Leptin treatment induces loss of bone marrow adipocytes and increases bone formation in leptin-deficient *Ob/Ob* mice. *Journal of Bone and Mineral Research: The Official Journal of the American Society for Bone and Mineral Research*, 20(6), 994–1001. https://doi.org/10.1359/JBMR.050103

Hamrick, M. W., Pennington, C., Newton, D., Xie, D., and Isales, C. (2004). Leptin deficiency produces contrasting phenotypes in bones of the limb and spine. *Bone*, *34*(3), 376–383. <a href="https://doi.org/10.1016/j.bone.2003.11.020">https://doi.org/10.1016/j.bone.2003.11.020</a>

Han, J., Nepal, P., Odelade, A., Freely, F. D., Belton, D. M., Graves, J. L., and Maldonado-Devincci, A. M. (2021). High-Fat Diet-Induced Weight Gain, Behavioral Deficits, and Dopamine Changes in Young C57BL/6J Mice. *Frontiers in Nutrition*, *7*, 591161. https://doi.org/10.3389/fnut.2020.591161

Handelsman, D. J. (2000). Androgen Physiology, Pharmacology, Use and Misuse. In K. R. Feingold, B. Anawalt, M. R. Blackman, A. Boyce, G. Chrousos, E. Corpas, W. W. de Herder, K. Dhatariya, K. Dungan, J. Hofland, S. Kalra, G. Kaltsas, N. Kapoor, C. Koch, P. Kopp, M. Korbonits, C. S. Kovacs, W. Kuohung, B. Laferrère, ... D. P. Wilson (Eds.), *Endotext*. MDText.com, Inc. <a href="http://www.ncbi.nlm.nih.gov/books/NBK279000/">http://www.ncbi.nlm.nih.gov/books/NBK279000/</a>

Haring, R., Völzke, H., Felix, S. B., Schipf, S., Dörr, M., Rosskopf, D., Nauck, M., Schöfl, C., and Wallaschofski, H. (2009). Prediction of Metabolic Syndrome by Low Serum Testosterone Levels in Men: Results From the Study of Health in Pomerania. *Diabetes*, 58(9), 2027–2031.

Hariri, A. F., Almatrafi, M. N., Zamka, A. B., Babaker, A. S., Fallatah, T. M., Althouwaibi, O. H., and Hamdi, A. S. (2019, April 22). *Relationship between Body Mass Index and T-Scores of Bone Mineral Density in the Hip and Spine Regions among Older Adults with Diabetes: A Retrospective Review* [Research Article]. Journal of Obesity; Hindawi. https://doi.org/10.1155/2019/9827403

Hauger, R. L., Saelzler, U. G., Pagadala, M. S., and Panizzon, M. S. (2022). The role of testosterone, the androgen receptor, and hypothalamic-pituitary–gonadal axis in depression in ageing Men. *Reviews in Endocrine and Metabolic Disorders*, *23*(6), 1259–1273. https://doi.org/10.1007/s11154-022-09767-0

Hesse, E., Hefferan, T. E., Tarara, J. E., Haasper, C., Meller, R., Krettek, C., Lu, L., and Yaszemski, M. J. (2010). Collagen type I hydrogel allows migration, proliferation and osteogenic differentiation of rat bone marrow stromal cells. *Journal of Biomedical Materials Research*. *Part A*, *94*(2), 442–449. <a href="https://doi.org/10.1002/jbm.a.32696">https://doi.org/10.1002/jbm.a.32696</a>

Hileman, S. M., Pierroz, D. D., Masuzaki, H., Bjørbæk, C., El-Haschimi, K., Banks, W. A., and Flier, J. S. (2002a). Characterization of Short Isoforms of the Leptin Receptor in Rat Cerebral Microvessels and of Brain Uptake of Leptin in Mouse Models of Obesity. *Endocrinology*, *143*(3), Article 3. <a href="https://doi.org/10.1210/endo.143.3.8669">https://doi.org/10.1210/endo.143.3.8669</a>

Hileman, S. M., Pierroz, D. D., Masuzaki, H., Bjørbæk, C., El-Haschimi, K., Banks, W. A., and Flier, J. S. (2002b). Characterizaton of Short Isoforms of the Leptin Receptor in Rat Cerebral Microvessels and of Brain Uptake of Leptin in Mouse Models of Obesity. *Endocrinology*, 143(3), Article 3. https://doi.org/10.1210/endo.143.3.8669

Hino, N., Rossetti, L., Marín-Llauradó, A., Aoki, K., Trepat, X., Matsuda, M., and Hirashima, T. (2020). ERK-Mediated Mechanochemical Waves Direct Collective Cell Polarization. *Developmental Cell*, *53*(6), 646-660.e8. <a href="https://doi.org/10.1016/j.devcel.2020.05.011">https://doi.org/10.1016/j.devcel.2020.05.011</a>

Hoey, D. A., Tormey, S., Ramcharan, S., O'Brien, F. J., and Jacobs, C. R. (2012). Primary Cilia-Mediated Mechanotransduction in Human Mesenchymal Stem Cells. *Stem Cells* (*Dayton, Ohio*), *30*(11), Article 11. <a href="https://doi.org/10.1002/stem.1235">https://doi.org/10.1002/stem.1235</a>

Hong, A. R., and Kim, S. W. (2018a). Effects of Resistance Exercise on Bone Health. *Endocrinology and Metabolism*, 33(4), Article 4. <a href="https://doi.org/10.3803/EnM.2018.33.4.435">https://doi.org/10.3803/EnM.2018.33.4.435</a>

Hong, A. R., and Kim, S. W. (2018b). Effects of Resistance Exercise on Bone Health. *Endocrinology and Metabolism*, 33(4), Article 4. <a href="https://doi.org/10.3803/EnM.2018.33.4.435">https://doi.org/10.3803/EnM.2018.33.4.435</a> Hong, X., Arguelles, L. M., Liu, X., Tsai, H.-J., Hsu, Y.-H., Wang, B., Zhang, S., Li, Z., Tang, G., Liu, X., Yang, J., Xu, X., Langman, C., and Wang, X. (2010). Percent Fat Mass Is Inversely Associated With Bone Mass and Hip Geometry in Rural Chinese Adolescents. *Journal of Bone and Mineral Research*, 25(7), 1544–1554. https://doi.org/10.1002/jbmr.40

Horton, M. A., and Helfrich, M. H. (2013). Integrins and Development: Integrins in Skeletal Cell Function and Development. In *Madame Curie Bioscience Database* [Internet]. Landes Bioscience. <a href="https://www.ncbi.nlm.nih.gov/books/NBK6331/">https://www.ncbi.nlm.nih.gov/books/NBK6331/</a>

Hou, J., He, C., He, W., Yang, M., Luo, X., and Li, C. (2020). Obesity and Bone Health: A Complex Link. *Frontiers in Cell and Developmental Biology*, *8*, 600181. https://doi.org/10.3389/fcell.2020.600181

Hu, L., Yin, C., Zhao, F., Ali, A., Ma, J., and Qian, A. (2018). Mesenchymal Stem Cells: Cell Fate Decision to Osteoblast or Adipocyte and Application in Osteoporosis Treatment. *International Journal of Molecular Sciences*, 19(2), 360. <a href="https://doi.org/10.3390/ijms19020360">https://doi.org/10.3390/ijms19020360</a>

Hu, Q., Bian, Q., Rong, D., Wang, L., Song, J., Huang, H.-S., Zeng, J., Mei, J., and Wang, P.-Y. (2023). JAK/STAT pathway: Extracellular signals, diseases, immunity, and therapeutic regimens. *Frontiers in Bioengineering and Biotechnology*, *11*, 1110765. https://doi.org/10.3389/fbioe.2023.1110765

Huang, L., You, Y., Zhu, T. Y., Zheng, L., Huang, X., Chen, H., Yao, D., Lan, H., and Qin, L. (2016). Validity of leptin receptor-deficiency (db/db) type 2 diabetes mellitus mice as a model of secondary osteoporosis. *Scientific Reports*, 6(1), Article 1. <a href="https://doi.org/10.1038/srep27745">https://doi.org/10.1038/srep27745</a>

Huang, Z. H., Reardon, C. A., and Mazzone, T. (2006). Endogenous ApoE Expression Modulates Adipocyte Triglyceride Content and Turnover. *Diabetes*, *55*(12), 3394–3402. <a href="https://doi.org/10.2337/db06-0354">https://doi.org/10.2337/db06-0354</a>

Humphrey, J. D., Dufresne, E. R., and Schwartz, M. A. (2014). Mechanotransduction and extracellular matrix homeostasis. *Nature Reviews. Molecular Cell Biology*, *15*(12), 802–812. https://doi.org/10.1038/nrm3896

Hwang, P. W., and Horton, J. A. (2019). Variable osteogenic performance of MC3T3-E1 subclones impacts their utility as models of osteoblast biology. *Scientific Reports*, *9*(1), 8299. https://doi.org/10.1038/s41598-019-44575-8

Hysaj, O., Marqués-Gallego, P., Richard, A., Elgizouli, M., Nieters, A., Quack Lötscher, K. C., and Rohrmann, S. (2021). Parathyroid Hormone in Pregnancy: Vitamin D and Other Determinants. *Nutrients*, *13*(2), 360. <a href="https://doi.org/10.3390/nu13020360">https://doi.org/10.3390/nu13020360</a>

Ilesanmi-Oyelere, B. L., Coad, J., Roy, N., and Kruger, M. C. (2018). Lean Body Mass in the Prediction of Bone Mineral Density in Postmenopausal Women. *BioResearch Open Access*, 7(1), 150–158. <a href="https://doi.org/10.1089/biores.2018.0025">https://doi.org/10.1089/biores.2018.0025</a>

Ilyés, T., Silaghi, C. N., and Crăciun, A. M. (2022). Diet-Related Changes of Short-Chain Fatty Acids in Blood and Feces in Obesity and Metabolic Syndrome. *Biology*, *11*(11), 1556. <a href="https://doi.org/10.3390/biology11111556">https://doi.org/10.3390/biology11111556</a>

Infante, M., Fabi, A., Cognetti, F., Gorini, S., Caprio, M., and Fabbri, A. (2019). RANKL/RANK/OPG system beyond bone remodeling: Involvement in breast cancer and clinical perspectives. *Journal of Experimental and Clinical Cancer Research*, *38*(1), 12. <a href="https://doi.org/10.1186/s13046-018-1001-2">https://doi.org/10.1186/s13046-018-1001-2</a>

Ishida-Ishihara, S., Takada, R., Furusawa, K., Ishihara, S., and Haga, H. (2022). Improvement of the cell viability of hepatocytes cultured in three-dimensional collagen gels using pump-free perfusion driven by water level difference. *Scientific Reports*, *12*, 20269. <a href="https://doi.org/10.1038/s41598-022-24423-y">https://doi.org/10.1038/s41598-022-24423-y</a>

Isidori, A. M., Giannetta, E., Greco, E. A., Gianfrilli, D., Bonifacio, V., Isidori, A., Lenzi, A., and Fabbri, A. (2005). Effects of testosterone on body composition, bone metabolism and serum lipid profile in middle-aged men: A meta-analysis. *Clinical Endocrinology*, 63(3), 280–293. https://doi.org/10.1111/j.1365-2265.2005.02339.x

Iwaniec, U. T., Dube, M. G., Boghossian, S., Song, H., Helferich, W. G., Turner, R. T., and Kalra, S. P. (2009). Body Mass Influences Cortical Bone Mass Independent of Leptin Signaling. *Bone*, *44*(3), 404–412. <a href="https://doi.org/10.1016/j.bone.2008.10.058">https://doi.org/10.1016/j.bone.2008.10.058</a>

Iwaniec, U. T., and Turner, R. T. (2016). Influence of Body Weight on Bone Mass, Architecture, and Turnover. *The Journal of Endocrinology*, *230*(3), Article 3. https://doi.org/10.1530/JOE-16-0089

Izumiya, M., Haniu, M., Ueda, K., Ishida, H., Ma, C., Ideta, H., Sobajima, A., Ueshiba, K., Uemura, T., Saito, N., and Haniu, H. (2021). Evaluation of MC3T3-E1 Cell Osteogenesis in Different Cell Culture Media. *International Journal of Molecular Sciences*, *22*(14), 7752. https://doi.org/10.3390/ijms22147752

Jansson, J.-O., Palsdottir, V., Hägg, D. A., Schéle, E., Dickson, S. L., Anesten, F., Bake, T., Montelius, M., Bellman, J., Johansson, M. E., Cone, R. D., Drucker, D. J., Wu, J., Aleksic, B., Törnqvist, A. E., Sjögren, K., Gustafsson, J.-Å., Windahl, S. H., and Ohlsson, C. (2018). Body weight homeostat that regulates fat mass independently of leptin in rats and mice. *Proceedings of the National Academy of Sciences of the United States of America*, 115(2), Article 2. <a href="https://doi.org/10.1073/pnas.1715687114">https://doi.org/10.1073/pnas.1715687114</a>

Jensen, V. F. H., Mølck, A.-M., Dalgaard, M., McGuigan, F. E., and Akesson, K. E. (2021). Changes in bone mass associated with obesity and weight loss in humans: Applicability of animal models. *Bone*, *145*, 115781. https://doi.org/10.1016/j.bone.2020.115781

Ji, M.-X., and Yu, Q. (2015). Primary osteoporosis in postmenopausal women. *Chronic Diseases and Translational Medicine*, 1(1), 9–13. https://doi.org/10.1016/j.cdtm.2015.02.006

Jiang, N., Cheng, C. J., Gelfond, J., Strong, R., Diaz, V., and Nelson, J. F. (2023). Prepubertal castration eliminates sex differences in lifespan and growth trajectories in genetically heterogeneous mice. *Aging Cell*, *22*(8), e13891. https://doi.org/10.1111/acel.13891

Jilka, R. L. (2003). Biology of the basic multicellular unit and the pathophysiology of osteoporosis. *Medical and Pediatric Oncology*, *41*(3), Article 3. <a href="https://doi.org/10.1002/mpo.10334">https://doi.org/10.1002/mpo.10334</a>

Jing, D., Luo, E., Cai, J., Tong, S., Zhai, M., Shen, G., Wang, X., and Luo, Z. (2016). Mechanical Vibration Mitigates the Decrease of Bone Quantity and Bone Quality of Leptin Receptor-Deficient Db/Db Mice by Promoting Bone Formation and Inhibiting Bone Resorption. *Journal of Bone and Mineral Research*, 31(9), 1713–1724. <a href="https://doi.org/10.1002/jbmr.2837">https://doi.org/10.1002/jbmr.2837</a>

Jolic, M., Ruscsák, K., Emanuelsson, L., Norlindh, B., Thomsen, P., Shah, F. A., and Palmquist, A. (2023). Leptin receptor gene deficiency minimally affects osseointegration in rats. *Scientific Reports*, *13*, 15631. <a href="https://doi.org/10.1038/s41598-023-42379-5">https://doi.org/10.1038/s41598-023-42379-5</a>

Jonsson, K. B., Frost, A., Nilsson, O., Ljunghall, S., and Ljunggren, Ö. (1999). Three isolation techniques for primary culture of human osteoblast-like cells: A comparison.

Acta Orthopaedica Scandinavica, 70(4), 365–373. 
https://doi.org/10.3109/17453679908997826

Ju, W., Zhang, G., Zhang, X., Wang, J., Wu, T., and Li, H. (2022). Involvement of MiRNA-211-5p and Arhgap11a Interaction During Osteogenic Differentiation of MC3T3-E1 Cells. *Frontiers in Surgery*, *9*. <a href="https://doi.org/10.3389/fsurg.2022.857170">https://doi.org/10.3389/fsurg.2022.857170</a>

Kamel, M. A., Picconi, J. L., Lara-Castillo, N., and Johnson, M. L. (2010). Activation of β–catenin Signaling in MLO-Y4 Osteocytic Cells versus 2T3 Osteoblastic Cells by Fluid Flow Shear Stress and PGE2: Implications for the Study of Mechanosensation in Bone. *Bone*, 47(5), 872–881. https://doi.org/10.1016/j.bone.2010.08.007

Kapur, S., Amoui, M., Kesavan, C., Wang, X., Mohan, S., Baylink, D. J., and Lau, K.-H. W. (2010a). Leptin Receptor (Lepr) Is a Negative Modulator of Bone Mechanosensitivity and Genetic Variations in Lepr May Contribute to the Differential Osteogenic Response to Mechanical Stimulation in the C57BL/6J and C3H/HeJ Pair of Mouse Strains. *The Journal of Biological Chemistry*, 285(48), Article 48. <a href="https://doi.org/10.1074/jbc.M110.169714">https://doi.org/10.1074/jbc.M110.169714</a>

Kapur, S., Amoui, M., Kesavan, C., Wang, X., Mohan, S., Baylink, D. J., and Lau, K.-H. W. (2010b). Leptin Receptor (Lepr) Is a Negative Modulator of Bone Mechanosensitivity and Genetic Variations in Lepr May Contribute to the Differential Osteogenic Response to Mechanical Stimulation in the C57BL/6J and C3H/HeJ Pair of Mouse Strains. *The Journal of Biological Chemistry*, 285(48), 37607–37618. https://doi.org/10.1074/jbc.M110.169714

Kapur, S., Baylink, D. J., and William Lau, K.-H. (2003). Fluid flow shear stress stimulates human osteoblast proliferation and differentiation through multiple interacting and competing signal transduction pathways. *Bone*, *32*(3), Article 3. <a href="https://doi.org/10.1016/S8756-3282(02)00979-1">https://doi.org/10.1016/S8756-3282(02)00979-1</a>

Karim, A., Qaisar, R., Azeem, M., Jose, J., Ramachandran, G., Ibrahim, Z. M., Elmoselhi, A., Ahmad, F., Abdel-Rahman, W. M., and Ranade, A. V. (2022). Hindlimb unloading induces time-dependent disruption of testicular histology in mice. *Scientific Reports*, *12*(1), 17406. https://doi.org/10.1038/s41598-022-22385-9

Karsenty, G., and Khosla, S. (2022). The crosstalk between bone remodeling and energy metabolism: A translational perspective. *Cell Metabolism*, *34*(6), 805–817. <a href="https://doi.org/10.1016/j.cmet.2022.04.010">https://doi.org/10.1016/j.cmet.2022.04.010</a>

Kasperk, C. H., Wergedal, J. E., Farley, J. R., Linkhart, T. A., Turner, R. T., and Baylink. (1989). ANDROGENS DIRECTLY STIMULATE PROLIFERATION OF BONE CELLS IN VITRO. *Endocrinology*, 124(3), 1576–1578. https://doi.org/10.1210/endo-124-3-1576

Kawao, N., Ishida, M., and Kaji, H. (2019). Roles of leptin in the recovery of muscle and bone by reloading after mechanical unloading in high fat diet-fed obese mice. *PLoS ONE*, *14*(10), e0224403. https://doi.org/10.1371/journal.pone.0224403

Kechagia, J. Z., Ivaska, J., and Roca-Cusachs, P. (2019). Integrins as biomechanical sensors of the microenvironment. *Nature Reviews Molecular Cell Biology*, *20*(8), Article 8. <a href="https://doi.org/10.1038/s41580-019-0134-2">https://doi.org/10.1038/s41580-019-0134-2</a>

Kelly, D. M., and Jones, T. H. (2015). Testosterone and obesity. *Obesity Reviews*, *16*(7), 581–606. <a href="https://doi.org/10.1111/obr.12282">https://doi.org/10.1111/obr.12282</a>

Kenkre, J., and Bassett, J. (2018). The bone remodelling cycle. *Annals of Clinical Biochemistry: International Journal of Laboratory Medicine*, *55*(3), Article 3. https://doi.org/10.1177/0004563218759371

Kerckhofs, G., Durand, M., Vangoitsenhoven, R., Marin, C., Van der Schueren, B., Carmeliet, G., Luyten, F. P., Geris, L., and Vandamme, K. (2016). Changes in bone macroand microstructure in diabetic obese mice revealed by high resolution microfocus X-ray computed tomography. *Scientific Reports*, *6*, 35517. <a href="https://doi.org/10.1038/srep35517">https://doi.org/10.1038/srep35517</a>

Khalaf, R. M., and Almudhi, A. A. (2022). The effect of vitamin D deficiency on the RANKL/OPG ratio in rats. *Journal of Oral Biology and Craniofacial Research*, *12*(2), 228–232. https://doi.org/10.1016/j.jobcr.2022.02.004

Khatib, N., Biggs, P., Wilson, C., Williams, R., Mason, D. J., and Holt, C. A. (2019). Dynamic medial knee overloading influences inflammation and bone remodeling in the degenerative knee. *Osteoarthritis and Cartilage*, *27*, S44. <a href="https://doi.org/10.1016/j.joca.2019.02.063">https://doi.org/10.1016/j.joca.2019.02.063</a>

Khodamoradi, K., Khosravizadeh, Z., Seetharam, D., Mallepalli, S., Farber, N., and Arora, H. (2022). The role of leptin and low testosterone in obesity. *International Journal of Impotence Research*, *34*(7), 704–713. <a href="https://doi.org/10.1038/s41443-022-00534-y">https://doi.org/10.1038/s41443-022-00534-y</a>

Khosla, S., Atkinson, E. J., Dunstan, C. R., and O'Fallon, W. M. (2002). Effect of estrogen versus testosterone on circulating osteoprotegerin and other cytokine levels in normal elderly men. *The Journal of Clinical Endocrinology and Metabolism*, 87(4), 1550–1554. https://doi.org/10.1210/jcem.87.4.8397

Khurana, N., and Sikka, S. C. (2019). Interplay Between SOX9, Wnt/β-Catenin and Androgen Receptor Signaling in Castration-Resistant Prostate Cancer. *International Journal of Molecular Sciences*, *20*(9), 2066. https://doi.org/10.3390/ijms20092066

Kim, J., Kigami, H., and Adachi, T. (2021). Comparative gene expression analysis for preosteoblast MC3T3-E1 cells under non-adhesive culture toward osteocyte differentiation. *Journal of Bioscience and Bioengineering*, 132(6), 651–656. <a href="https://doi.org/10.1016/j.jbiosc.2021.09.004">https://doi.org/10.1016/j.jbiosc.2021.09.004</a>

Kim, M., and Kim, I. (2021). Ovariectomy, but not orchiectomy, exacerbates metabolic syndrome after maternal high-fructose intake in adult offspring. *The Korean Journal of Physiology and Pharmacology: Official Journal of the Korean Physiological Society and the Korean Society of Pharmacology,* 25(1), 39–49. <a href="https://doi.org/10.4196/kjpp.2021.25.1.39">https://doi.org/10.4196/kjpp.2021.25.1.39</a>

Kim, N. R., David, K., Corbeels, K., Khalil, R., Antonio, L., Schollaert, D., Deboel, L., Ohlsson, C., Gustafsson, J.-Å., Vangoitsenhoven, R., Van der Schueren, B., Decallonne, B., Claessens, F., Vanderschueren, D., and Dubois, V. (2021). Testosterone Reduces Body Fat in Male Mice by Stimulation of Physical Activity Via Extrahypothalamic ERα Signaling. *Endocrinology*, *162*(6), bqab045. https://doi.org/10.1210/endocr/bqab045

Kim, S., and Lee, M. (2020). Rational design of hydrogels to enhance osteogenic potential. *Chemistry of Materials: A Publication of the American Chemical Society*, 32(22), 9508–9530. https://doi.org/10.1021/acs.chemmater.0c03018

Kim, T.-R., Kim, M.-S., Goh, T. S., Lee, J. S., Kim, Y. H., Yoon, S.-Y., and Lee, C.-S. (2019a). Evaluation of Structural and Mechanical Properties of Porous Artificial Bone Scaffolds Fabricated via Advanced TBA-Based Freeze-Gel Casting Technique. *Applied Sciences*, *9*(9), Article 9. <a href="https://doi.org/10.3390/app9091965">https://doi.org/10.3390/app9091965</a>

Kim, T.-R., Kim, M.-S., Goh, T. S., Lee, J. S., Kim, Y. H., Yoon, S.-Y., and Lee, C.-S. (2019b). Evaluation of Structural and Mechanical Properties of Porous Artificial Bone Scaffolds Fabricated via Advanced TBA-Based Freeze-Gel Casting Technique. *Applied Sciences*, *9*(9), Article 9. https://doi.org/10.3390/app9091965

King, V. L., Hatch, N. W., Chan, H.-W., de Beer, M. C., de Beer, F. C., and Tannock, L. R. (2010). A Murine Model of Obesity With Accelerated Atherosclerosis. *Obesity*, *18*(1), 35–41. https://doi.org/10.1038/oby.2009.176

Kishida, Y., Hirao, M., Tamai, N., Nampei, A., Fujimoto, T., Nakase, T., Shimizu, N., Yoshikawa, H., and Myoui, A. (2005). Leptin regulates chondrocyte differentiation and matrix maturation during endochondral ossification. *Bone*, *37*(5), 607–621. <a href="https://doi.org/10.1016/j.bone.2005.05.009">https://doi.org/10.1016/j.bone.2005.05.009</a>

Klein-Nulend, J., Bacabac, R. G., and Bakker, A. D. (2012). Mechanical loading and how it affects bone cells: The role of the osteocyte cytoskeleton in maintaining our skeleton. *European Cells and Materials*, *24*, 278–291. <a href="https://doi.org/10.22203/ecm.v024a20">https://doi.org/10.22203/ecm.v024a20</a>

Klein-Nulend, J., Burger, E. H., Semeins, C. M., Raisz, L. G., and Pilbeam, C. C. (1997). Pulsating Fluid Flow Stimulates Prostaglandin Release and Inducible Prostaglandin G/H Synthase mRNA Expression in Primary Mouse Bone Cells. *Journal of Bone and Mineral Research*, 12(1), Article 1. <a href="https://doi.org/10.1359/jbmr.1997.12.1.45">https://doi.org/10.1359/jbmr.1997.12.1.45</a>

Koblenzer, M., Weiler, M., Fragoulis, A., Rütten, S., Pufe, T., and Jahr, H. (2022). Physiological Mineralization during In Vitro Osteogenesis in a Biomimetic Spheroid Culture Model. *Cells*, *11*(17), 2702. <a href="https://doi.org/10.3390/cells11172702">https://doi.org/10.3390/cells11172702</a>

Komori, T. (2010). Regulation of Osteoblast Differentiation by Runx2. In Y. Choi (Ed.), Osteoimmunology (pp. 43–49). Springer US. <a href="https://doi.org/10.1007/978-1-4419-1050-95">https://doi.org/10.1007/978-1-4419-1050-95</a>

Kouda, K., Ohara, K., Fujita, Y., Nakamura, H., Tachiki, T., and Iki, M. (2019). Relationships between serum leptin levels and bone mineral parameters in school-aged children: A 3-year follow-up study. *Journal of Bone and Mineral Metabolism*, *37*(1), 152–160. https://doi.org/10.1007/s00774-018-0909-0

Krstic, N., Bishop, N., Curtis, B., Cooper, C., Harvey, N., Lilycrop, K., Murray, R., Owen, R., Reilly, G., Skerry, T., and Borg, S. (2022). Early life vitamin D depletion and mechanical

loading determine methylation changes in the RUNX2, RXRA, and osterix promoters in mice. *Genes and Nutrition*, *17*(1), 7. https://doi.org/10.1186/s12263-022-00711-0

Kumar, M., Zaman, Md. K., Das, S., Goyary, D., Pathak, M. P., and Chattopadhyay, P. (2023). Transient Receptor Potential Vanilloid (TRPV4) channel inhibition: A novel promising approach for the treatment of lung diseases. *Biomedicine and Pharmacotherapy*, *163*, 114861. https://doi.org/10.1016/j.biopha.2023.114861

Laharrague, P., Larrouy, D., Fontanilles, A.-M., Truel, N., Campfield, A., Tenenbaum, R., Galitzky, J., Corberand, J. X., Pénicaud, L., and Casteilla, L. (1998a). High expression of leptin by human bone marrow adipocytes in primary culture. *The FASEB Journal*, *12*(9), Article 9. <a href="https://doi.org/10.1096/fasebj.12.9.747">https://doi.org/10.1096/fasebj.12.9.747</a>

Laharrague, P., Larrouy, D., Fontanilles, A.-M., Truel, N., Campfield, A., Tenenbaum, R., Galitzky, J., Corberand, J. X., Pénicaud, L., and Casteilla, L. (1998b). High expression of leptin by human bone marrow adipocytes in primary culture. *The FASEB Journal*, *12*(9), Article 9. https://doi.org/10.1096/fasebj.12.9.747

Lamghari, M., Tavares, L., Camboa, N., and Barbosa, M. a. (2006). Leptin effect on RANKL and OPG expression in MC3T3-E1 osteoblasts. *Journal of Cellular Biochemistry*, *98*(5), 1123–1129. https://doi.org/10.1002/jcb.20853

Lee, H.-K., Lee, J. K., and Cho, B. (2013). The Role of Androgen in the Adipose Tissue of Males. *The World Journal of Men's Health*, 31(2), 136–140. https://doi.org/10.5534/wjmh.2013.31.2.136

Lee, Y.-J., Park, J.-H., Ju, S.-K., You, K.-H., Ko, J. S., and Kim, H.-M. (2002). Leptin receptor isoform expression in rat osteoblasts and their functional analysis. *FEBS Letters*, *528*(1–3), 43–47. <a href="https://doi.org/10.1016/S0014-5793(02)02889-2">https://doi.org/10.1016/S0014-5793(02)02889-2</a>

Legiran, S., and Brandi, M. L. (2012). Bone mass regulation of leptin and postmenopausal osteoporosis with obesity. *Clinical Cases in Mineral and Bone Metabolism*, *9*(3), Article 3.

Lei, X., Liu, Q., Li, S., Zhang, Z., and Yang, X. (n.d.). Effects of fluid shear stress on expression of focal adhesion kinase in MG-63 human osteoblast-like cells on different surface modification of titanium. *Bioengineered*, 12(1), 4962–4971. <a href="https://doi.org/10.1080/21655979.2021.1962686">https://doi.org/10.1080/21655979.2021.1962686</a>

- Li, J. (2013). JAK-STAT and bone metabolism. *JAK-STAT*, 2(3), Article 3. https://doi.org/10.4161/jkst.23930
- Li, J., Rose, E., Frances, D., Sun, Y., and You, L. (2012). Effect of oscillating fluid flow stimulation on osteocyte mRNA expression. *Journal of Biomechanics*, *45*(2), 247–251. https://doi.org/10.1016/j.jbiomech.2011.10.037
- Li, J., Zuo, B., Zhang, L., Dai, L., and Zhang, X. (2018). Osteoblast versus Adipocyte: Bone Marrow Microenvironment-Guided Epigenetic Control. *Case Reports in Orthopedic Research*, 1(1), Article 1. <a href="https://doi.org/10.1159/000489053">https://doi.org/10.1159/000489053</a>
- Li, L., Rao, S., Cheng, Y., Zhuo, X., Deng, C., Xu, N., Zhang, H., and Yang, L. (2019). Microbial osteoporosis: The interplay between the gut microbiota and bones via host metabolism and immunity. *MicrobiologyOpen*, 8(8), e00810. <a href="https://doi.org/10.1002/mbo3.810">https://doi.org/10.1002/mbo3.810</a>
- Li, M., Thompson, D. D., and Paralkar, V. M. (2007). Prostaglandin E2 receptors in bone formation. *International Orthopaedics*, *31*(6), Article 6. <a href="https://doi.org/10.1007/s00264-007-0406-x">https://doi.org/10.1007/s00264-007-0406-x</a>
- Li, S., Zhao, Y., Yang, Y., Wang, X., Nie, M., Wu, X., and Mao, J. (2020). Metabolic Effects of Testosterone Replacement Therapy in Patients with Type 2 Diabetes Mellitus or Metabolic Syndrome: A Meta-Analysis. *International Journal of Endocrinology*, 2020, 4732021. https://doi.org/10.1155/2020/4732021
- Li, Z., Zheng, Z., Pathak, J. L., Li, H., Wu, G., Xu, S., Wang, T., Cheng, H., Piao, Z., Jaspers, R. T., and Wu, L. (2023). Leptin-deficient *Ob/Ob* mice exhibit periodontitis phenotype and altered oral microbiome. *Journal of Periodontal Research*, *58*(2), 392–402. https://doi.org/10.1111/jre.13099
- Liao, F., Zhang, T. J., Jiang, H., Lefton, K. B., Robinson, G. O., Vassar, R., Sullivan, P. M., and Holtzman, D. M. (2015). Murine versus human apolipoprotein E4: Differential facilitation of and co-localization in cerebral amyloid angiopathy and amyloid plaques in APP transgenic mouse models. *Acta Neuropathologica Communications*, *3*(1), 70. https://doi.org/10.1186/s40478-015-0250-y
- Lincoff, A. M., Bhasin, S., Flevaris, P., Mitchell, L. M., Basaria, S., Boden, W. E., Cunningham, G. R., Granger, C. B., Khera, M., Thompson, I. M., Wang, Q., Wolski, K.,

Davey, D., Kalahasti, V., Khan, N., Miller, M. G., Snabes, M. C., Chan, A., Dubcenco, E., ... Nissen, S. E. (2023a). Cardiovascular Safety of Testosterone-Replacement Therapy. *New England Journal of Medicine*, *389*(2), 107–117. https://doi.org/10.1056/NEJMoa2215025

Lincoff, A. M., Bhasin, S., Flevaris, P., Mitchell, L. M., Basaria, S., Boden, W. E., Cunningham, G. R., Granger, C. B., Khera, M., Thompson, I. M., Wang, Q., Wolski, K., Davey, D., Kalahasti, V., Khan, N., Miller, M. G., Snabes, M. C., Chan, A., Dubcenco, E., ... Nissen, S. E. (2023b). Cardiovascular Safety of Testosterone-Replacement Therapy. *New England Journal of Medicine*, 389(2), 107–117. <a href="https://doi.org/10.1056/NEJMoa2215025">https://doi.org/10.1056/NEJMoa2215025</a>

Liu, G.-Y., Liang, Q.-H., Cui, R.-R., Liu, Y., Wu, S.-S., Shan, P.-F., Yuan, L.-Q., and Liao, E.-Y. (2014). Leptin Promotes the Osteoblastic Differentiation of Vascular Smooth Muscle Cells From Female Mice by Increasing RANKL Expression. *Endocrinology*, *155*(2), 558–567. https://doi.org/10.1210/en.2013-1298

Liu, Z., Tang, Y., He, L., Geng, B., Lu, F., He, J., Yi, Q., Liu, X., Zhang, K., Wang, L., Xia, Y., and Jiang, J. (2022). Piezo1-mediated fluid shear stress promotes OPG and inhibits RANKL via NOTCH3 in MLO-Y4 osteocytes. *Channels*, *16*(1), 127–136. https://doi.org/10.1080/19336950.2022.2085379

Liu, Z., Wang, Q., Zhang, J., Qi, S., Duan, Y., and Li, C. (2023). The Mechanotransduction Signaling Pathways in the Regulation of Osteogenesis. *International Journal of Molecular Sciences*, *24*(18), 14326. <a href="https://doi.org/10.3390/ijms241814326">https://doi.org/10.3390/ijms241814326</a>

Lo Sasso, G., Schlage, W. K., Boué, S., Veljkovic, E., Peitsch, M. C., and Hoeng, J. (2016). The Apoe-/- mouse model: A suitable model to study cardiovascular and respiratory diseases in the context of cigarette smoke exposure and harm reduction. *Journal of Translational Medicine*, *14*(1), 146. https://doi.org/10.1186/s12967-016-0901-1

Lönnqvist, F., Nordfors, L., Jansson, M., Thörne, A., Schalling, M., and Arner, P. (1997). Leptin secretion from adipose tissue in women. Relationship to plasma levels and gene expression. *Journal of Clinical Investigation*, *99*(10), 2398–2404.

Lorincz, C., Reimer, R. A., Boyd, S. K., and Zernicke, R. F. (2010). High-fat, sucrose diet impairs geometrical and mechanical properties of cortical bone in mice. *The British Journal of Nutrition*, *103*(9), 1302–1308. https://doi.org/10.1017/S0007114509993084

Lupsa, B. C., and Insogna, K. (2015). Bone Health and Osteoporosis. *Endocrinology and Metabolism Clinics of North America*, 44(3), 517–530. https://doi.org/10.1016/j.ecl.2015.05.002

Ma, H., Sun, J., Wu, X., Mao, J., and Han, Q. (2024). Percent body fat was negatively correlated with Testosterone levels in male. *PLOS ONE*, *19*(1), e0294567. <a href="https://doi.org/10.1371/journal.pone.0294567">https://doi.org/10.1371/journal.pone.0294567</a>

Mahdi Souzani, A., Rajeshwari, H. R. S., Selvaganapathy, P. R., and Kishen, A. (2023). Impact of 3D collagen-based model and hydrostatic pressure on periodontal ligament fibroblast: A morpho-biochemical analysis. *Journal of the Mechanical Behavior of Biomedical Materials*, *147*, 106092. https://doi.org/10.1016/j.jmbbm.2023.106092

Mai, Z., Peng, Z., Wu, S., Zhang, J., Chen, L., Liang, H., Bai, D., Yan, G., and Ai, H. (2013). Single Bout Short Duration Fluid Shear Stress Induces Osteogenic Differentiation of MC3T3-E1 Cells via Integrin β1 and BMP2 Signaling Cross-Talk. *PLoS ONE*, *8*(4), e61600. https://doi.org/10.1371/journal.pone.0061600

Marcadet, L., Bouredji, Z., Argaw, A., and Frenette, J. (2022). The Roles of RANK/RANKL/OPG in Cardiac, Skeletal, and Smooth Muscles in Health and Disease. *Frontiers in Cell and Developmental Biology*, 10. https://doi.org/10.3389/fcell.2022.903657

Marques, P., Skorupskaite, K., Rozario, K. S., Anderson, R. A., and George, J. T. (2000). Physiology of GnRH and Gonadotropin Secretion. In K. R. Feingold, B. Anawalt, M. R. Blackman, A. Boyce, G. Chrousos, E. Corpas, W. W. de Herder, K. Dhatariya, K. Dungan, J. Hofland, S. Kalra, G. Kaltsas, N. Kapoor, C. Koch, P. Kopp, M. Korbonits, C. S. Kovacs, W. Kuohung, B. Laferrère, ... D. P. Wilson (Eds.), *Endotext*. MDText.com, Inc. <a href="http://www.ncbi.nlm.nih.gov/books/NBK279070/">http://www.ncbi.nlm.nih.gov/books/NBK279070/</a>

Matic, I., Matthews, B. G., Wang, X., Dyment, N. A., Worthley, D. L., Rowe, D. W., Grcevic, D., and Kalajzic, I. (2016). Quiescent Bone Lining Cells Are a Major Source of Osteoblasts During Adulthood. *Stem Cells (Dayton, Ohio)*, 34(12), 2930–2942. <a href="https://doi.org/10.1002/stem.2474">https://doi.org/10.1002/stem.2474</a>

Matthews, B. G., Naot, D., Callon, K. E., Musson, D. S., Locklin, R., Hulley, P. A., Grey, A., and Cornish, J. (2014). Enhanced osteoblastogenesis in three-dimensional collagen gels. *BoneKEy Reports*, *3*, 560. https://doi.org/10.1038/bonekey.2014.55 Mazor, R., Friedmann-Morvinski, D., Alsaigh, T., Kleifeld, O., Kistler, E. B., Rousso-Noori, L., Huang, C., Li, J. B., Verma, I. M., and Schmid-Schönbein, G. W. (2018). Cleavage of the leptin receptor by matrix metalloproteinase—2 promotes leptin resistance and obesity in mice. *Science Translational Medicine*, 10(455), eaah6324. https://doi.org/10.1126/scitranslmed.aah6324

McCabe, L., Britton, R. A., and Parameswaran, N. (2015). Prebiotic and Probiotic Regulation of Bone Health: Role of the Intestine and its Microbiome. *Current Osteoporosis Reports*, *13*(6), 363–371. <a href="https://doi.org/10.1007/s11914-015-0292-x">https://doi.org/10.1007/s11914-015-0292-x</a>

McCarthy, T. L., Chang, W.-Z., Liu, Y., and Centrella, M. (2003). Runx2 Integrates Estrogen Activity in Osteoblasts\*. *Journal of Biological Chemistry*, *278*(44), 43121–43129. https://doi.org/10.1074/jbc.M306531200

McCloskey, E. V., Odén, A., Harvey, N. C., Leslie, W. D., Hans, D., Johansson, H., Barkmann, R., Boutroy, S., Brown, J., Chapurlat, R., Elders, P. J. M., Fujita, Y., Glüer, C.-C., Goltzman, D., Iki, M., Karlsson, M., Kindmark, A., Kotowicz, M., Kurumatani, N., ... Kanis, J. A. (2016). A Meta-Analysis of Trabecular Bone Score in Fracture Risk Prediction and Its Relationship to FRAX. *Journal of Bone and Mineral Research: The Official Journal of the American Society for Bone and Mineral Research*, *31*(5), 940–948. https://doi.org/10.1002/jbmr.2734

McEwan, I. J., and Brinkmann, A. O. (2000). Androgen Physiology: Receptor and Metabolic Disorders. In K. R. Feingold, B. Anawalt, M. R. Blackman, A. Boyce, G. Chrousos, E. Corpas, W. W. de Herder, K. Dhatariya, K. Dungan, J. Hofland, S. Kalra, G. Kaltsas, N. Kapoor, C. Koch, P. Kopp, M. Korbonits, C. S. Kovacs, W. Kuohung, B. Laferrère, ... D. P. Wilson (Eds.), *Endotext*. MDText.com, Inc. <a href="http://www.ncbi.nlm.nih.gov/books/NBK279028/">http://www.ncbi.nlm.nih.gov/books/NBK279028/</a>

Mendoza-Herrera, K., Florio, A. A., Moore, M., Marrero, A., Tamez, M., Bhupathiraju, S. N., and Mattei, J. (2021a). The Leptin System and Diet: A Mini Review of the Current Evidence. Frontiers in Endocrinology, 12. <a href="https://www.frontiersin.org/articles/10.3389/fendo.2021.749050">https://www.frontiersin.org/articles/10.3389/fendo.2021.749050</a>

Mendoza-Herrera, K., Florio, A. A., Moore, M., Marrero, A., Tamez, M., Bhupathiraju, S. N., and Mattei, J. (2021b). The Leptin System and Diet: A Mini Review of the Current

Evidence. Frontiers in Endocrinology, 12, 749050. https://doi.org/10.3389/fendo.2021.749050

Mendoza-Herrera, K., Florio, A. A., Moore, M., Marrero, A., Tamez, M., Bhupathiraju, S. N., and Mattei, J. (2021c). The Leptin System and Diet: A Mini Review of the Current Evidence. *Frontiers in Endocrinology*, *12*. <a href="https://doi.org/10.3389/fendo.2021.749050">https://doi.org/10.3389/fendo.2021.749050</a>

Meng, F., Cheng, H., Qian, J., Dai, X., Huang, Y., and Fan, Y. (2022). In vitro fluidic systems: Applying shear stress on endothelial cells. *Medicine in Novel Technology and Devices*, *15*, 100143. <a href="https://doi.org/10.1016/j.medntd.2022.100143">https://doi.org/10.1016/j.medntd.2022.100143</a>

Meslier, Q. A., and Shefelbine, S. J. (2023). Using Finite Element Modeling in Bone Mechanoadaptation. *Current Osteoporosis Reports*, *21*(2), 105–116. https://doi.org/10.1007/s11914-023-00776-9

Messier, S. P., Beavers, D. P., Loeser, R. F., Carr, J. J., Khajanchi, S., Legault, C., Nicklas, B. J., Hunter, D. J., and DeVita, P. (2014). KNEE-JOINT LOADING IN KNEE OSTEOARTHRITIS: INFLUENCE OF ABDOMINAL AND THIGH FAT. *Medicine and Science in Sports and Exercise*, 46(9), 1677–1683. https://doi.org/10.1249/MSS.00000000000000293

Michael, H., Härkönen, P. L., Väänänen, H. K., and Hentunen, T. A. (2005). Estrogen and testosterone use different cellular pathways to inhibit osteoclastogenesis and bone resorption. *Journal of Bone and Mineral Research: The Official Journal of the American Society for Bone and Mineral Research, 20*(12), 2224–2232. https://doi.org/10.1359/JBMR.050803

Mohamad, N.-V., Soelaiman, I.-N., and Chin, K.-Y. (2016). A concise review of testosterone and bone health. *Clinical Interventions in Aging*, *11*, 1317–1324. https://doi.org/10.2147/CIA.S115472

Montalvany-Antonucci, C. C., Zicker, M. C., Ferreira, A. V. M., Macari, S., Ramos-Junior, E. S., Gomez, R. S., Pereira, T. S. F., Madeira, M. F. M., Fukada, S. Y., Andrade, I., and Silva, T. A. (2018a). High-fat diet disrupts bone remodeling by inducing local and systemic alterations. *The Journal of Nutritional Biochemistry*, *59*, 93–103. https://doi.org/10.1016/j.jnutbio.2018.06.006

Montalvany-Antonucci, C. C., Zicker, M. C., Ferreira, A. V. M., Macari, S., Ramos-Junior, E. S., Gomez, R. S., Pereira, T. S. F., Madeira, M. F. M., Fukada, S. Y., Andrade, I., and

Silva, T. A. (2018b). High-fat diet disrupts bone remodeling by inducing local and systemic alterations. *The Journal of Nutritional Biochemistry*, *59*, 93–103. <a href="https://doi.org/10.1016/j.jnutbio.2018.06.006">https://doi.org/10.1016/j.jnutbio.2018.06.006</a>

Moustafa, A. (2021). Hindlimb unloading-induced reproductive suppression via Downregulation of hypothalamic Kiss-1 expression in adult male rats. *Reproductive Biology and Endocrinology: RBandE*, 19, 37. <a href="https://doi.org/10.1186/s12958-021-00694-4">https://doi.org/10.1186/s12958-021-00694-4</a>

Mulari, M. T. K., Zhao, H., Lakkakorpi, P. T., and Väänänen, H. K. (2003). Osteoclast ruffled border has distinct subdomains for secretion and degraded matrix uptake. *Traffic (Copenhagen, Denmark)*, 4(2), 113–125. <a href="https://doi.org/10.1034/j.1600-0854.2003.40206.x">https://doi.org/10.1034/j.1600-0854.2003.40206.x</a>

Murray, S. L., and Wolf, M. (2024). Calcium and Phosphate Disorders: Core Curriculum 2024. *American Journal of Kidney Diseases*, 83(2), 241–256. https://doi.org/10.1053/j.ajkd.2023.04.017

Mushannen, T., Cortez, P., Stanford, F. C., and Singhal, V. (2019). Obesity and Hypogonadism—A Narrative Review Highlighting the Need for High-Quality Data in Adolescents. *Children*, *6*(5), Article 5. <a href="https://doi.org/10.3390/children6050063">https://doi.org/10.3390/children6050063</a>

Mutabaruka, M.-S., Aoulad Aissa, M., Delalandre, A., Lavigne, M., and Lajeunesse, D. (2010). Local leptin production in osteoarthritis subchondral osteoblasts may be responsible for their abnormal phenotypic expression. *Arthritis Research and Therapy*, 12(1), R20. https://doi.org/10.1186/ar2925

Myers, M. G., Cowley, M. A., and Münzberg, H. (2008). Mechanisms of Leptin Action and Leptin Resistance. *Annual Review of Physiology*, *70*(1), Article 1. <a href="https://doi.org/10.1146/annurev.physiol.70.113006.100707">https://doi.org/10.1146/annurev.physiol.70.113006.100707</a>

Nedresky, D., and Singh, G. (2024). Physiology, Luteinizing Hormone. In *StatPearls*. StatPearls Publishing. <a href="http://www.ncbi.nlm.nih.gov/books/NBK539692/">http://www.ncbi.nlm.nih.gov/books/NBK539692/</a>

Ng Tang Fui, M., Hoermann, R., Bracken, K., Handelsman, D. J., Inder, W. J., Stuckey, B. G. A., Yeap, B. B., Ghasem-Zadeh, A., Robledo, K. P., Jesudason, D., Zajac, J. D., Wittert, G. A., and Grossmann, M. (2021). Effect of Testosterone Treatment on Bone Microarchitecture and Bone Mineral Density in Men: A 2-Year RCT. *The Journal of* 

Clinical Endocrinology and Metabolism, 106(8), e3143–e3158. https://doi.org/10.1210/clinem/dgab149

Nile, M., Folwaczny, M., Wichelhaus, A., Baumert, U., and Janjic Rankovic, M. (2023). Fluid flow shear stress and tissue remodeling—an orthodontic perspective: Evidence synthesis and differential gene expression network analysis. *Frontiers in Bioengineering and Biotechnology*, *11*. https://doi.org/10.3389/fbioe.2023.1256825

Noguchi, T., Ebina, K., Hirao, M., Otsuru, S., Guess, A. J., Kawase, R., Ohama, T., Yamashita, S., Etani, Y., Okamura, G., and Yoshikawa, H. (2018). Apolipoprotein E plays crucial roles in maintaining bone mass by promoting osteoblast differentiation via ERK1/2 pathway and by suppressing osteoclast differentiation via c-Fos, NFATc1, and NF-κB pathway. *Biochemical and Biophysical Research Communications*, *503*(2), 644–650. <a href="https://doi.org/10.1016/j.bbrc.2018.06.055">https://doi.org/10.1016/j.bbrc.2018.06.055</a>

Norvell, S. M., Alvarez, M., Bidwell, J. P., and Pavalko, F. M. (2004). Fluid Shear Stress Induces β-Catenin Signaling in Osteoblasts. *Calcified Tissue International*, *75*(5), Article 5. <a href="https://doi.org/10.1007/s00223-004-0213-y">https://doi.org/10.1007/s00223-004-0213-y</a>

Notelovitz, M. (2002). Androgen effects on bone and muscle. *Fertility and Sterility*, 77, 34–41. https://doi.org/10.1016/S0015-0282(02)02968-0

Odle, B., Dennison, N., Al-Nakkash, L., Broderick, T., and Plochocki, J. (2017). Genistein treatment improves fracture resistance in obese diabetic mice. *BMC Endocrine Disorders*, 17. https://doi.org/10.1186/s12902-016-0144-4

O'Donnell, L., Stanton, P., and de Kretser, D. M. (2000). Endocrinology of the Male Reproductive System and Spermatogenesis. In K. R. Feingold, B. Anawalt, M. R. Blackman, A. Boyce, G. Chrousos, E. Corpas, W. W. de Herder, K. Dhatariya, K. Dungan, J. Hofland, S. Kalra, G. Kaltsas, N. Kapoor, C. Koch, P. Kopp, M. Korbonits, C. S. Kovacs, W. Kuohung, B. Laferrère, ... D. P. Wilson (Eds.), *Endotext*. MDText.com, Inc. <a href="http://www.ncbi.nlm.nih.gov/books/NBK279031/">http://www.ncbi.nlm.nih.gov/books/NBK279031/</a>

Oftadeh, R., Perez-Viloria, M., Villa-Camacho, J. C., Vaziri, A., and Nazarian, A. (2015). Biomechanics and Mechanobiology of Trabecular Bone: A Review. *Journal of Biomechanical Engineering*, 137(1), 0108021–01080215. https://doi.org/10.1115/1.4029176

Oksztulska-Kolanek, E., Znorko, B., Michałowska, M., and Pawlak, K. (2015). The Biomechanical Testing for the Assessment of Bone Quality in an Experimental Model of Chronic Kidney Disease. *Nephron*, *132*(1), 51–58. https://doi.org/10.1159/000442714

Osterhoff, G., Morgan, E. F., Shefelbine, S. J., Karim, L., McNamara, L. M., and Augat, P. (2016). Bone mechanical properties and changes with osteoporosis. *Injury, 47 Suppl* 2(Suppl 2), S11-20. https://doi.org/10.1016/S0020-1383(16)47003-8

Ott, S. M. (2018a). Cortical or Trabecular Bone: What's the Difference? *American Journal of Nephrology*, 47(6), 373–375. <a href="https://doi.org/10.1159/000489672">https://doi.org/10.1159/000489672</a>

Ott, S. M. (2018b). Cortical or Trabecular Bone: What's the Difference? *American Journal of Nephrology*, 47(6), Article 6. https://doi.org/10.1159/000489672

Ottarsdottir, K., Nilsson, A. G., Hellgren, M., Lindblad, U., and Daka, B. (2018). The association between serum testosterone and insulin resistance: A longitudinal study. *Endocrine Connections*, 7(12), 1491. <a href="https://doi.org/10.1530/EC-18-0480">https://doi.org/10.1530/EC-18-0480</a>

Owen, R., and Reilly, G. C. (2018). In vitro Models of Bone Remodelling and Associated Disorders. *Frontiers in Bioengineering and Biotechnology*, *6*, 134. https://doi.org/10.3389/fbioe.2018.00134

Palermo, A., Tuccinardi, D., Defeudis, G., Watanabe, M., D'Onofrio, L., Lauria Pantano, A., Napoli, N., Pozzilli, P., and Manfrini, S. (2016). BMI and BMD: The Potential Interplay between Obesity and Bone Fragility. *International Journal of Environmental Research and Public Health*, *13*(6), 544. <a href="https://doi.org/10.3390/ijerph13060544">https://doi.org/10.3390/ijerph13060544</a>

Palmer, L. C., Newcomb, C. J., Kaltz, S. R., Spoerke, E. D., and Stupp, S. I. (2008). Biomimetic Systems for Hydroxyapatite Mineralization Inspired By Bone and Enamel. *Chemical Reviews*, 108(11), Article 11. https://doi.org/10.1021/cr8004422

Parfitt, A. M. (2002). Targeted and nontargeted bone remodeling: Relationship to basic multicellular unit origination and progression. *Bone*, *30*(1), Article 1. <a href="https://doi.org/10.1016/S8756-3282(01)00642-1">https://doi.org/10.1016/S8756-3282(01)00642-1</a>

Park, J. H., Lee, N. K., and Lee, S. Y. (2017). Current Understanding of RANK Signaling in Osteoclast Differentiation and Maturation. *Moleucles and Cells*, 40(10), 706–713. https://doi.org/10.14348/molcells.2017.0225

Paschall, L., Carrozzi, S., Tabdanov, E., Dhawan, A., and Szczesny, S. E. (2024). Cyclic loading induces anabolic gene expression in ACLs in a load-dependent and sex-specific manner. *Journal of Orthopaedic Research: Official Publication of the Orthopaedic Research Society*, 42(2), 267–276. https://doi.org/10.1002/jor.25677

Patsch, J. M., Kiefer, F. W., Varga, P., Pail, P., Rauner, M., Stupphann, D., Resch, H., Moser, D., Zysset, P. K., Stulnig, T. M., and Pietschmann, P. (2011). Increased bone resorption and impaired bone microarchitecture in short-term and extended high-fat diet—induced obesity. *Metabolism: Clinical and Experimental*, *60*(2), 243–249. <a href="https://doi.org/10.1016/j.metabol.2009.11.023">https://doi.org/10.1016/j.metabol.2009.11.023</a>

Payandeh, N., Peeri, M., Azarbayjani, M. A., and Hosseini, S. (2020). Effect of Resistance Training with Palm Pollen and Testosterone on Runx2 Protein and Gene Expression Levels in Bone Tissue of Adult Male Rats. *Hormozgan Medical Journal*, *24*. https://doi.org/10.5812/hmj.105332

Pei, T., Su, G., Yang, J., Gao, W., Yang, X., Zhang, Y., Ren, J., Shen, Y., and Liu, X. (2022). Fluid Shear Stress Regulates Osteogenic Differentiation via AnnexinA6-Mediated Autophagy in MC3T3-E1 Cells. *International Journal of Molecular Sciences*, *23*(24), 15702. https://doi.org/10.3390/ijms232415702

Piedrahita, J. A., Zhang, S. H., Hagaman, J. R., Oliver, P. M., and Maeda, N. (1992). Generation of mice carrying a mutant apolipoprotein E gene inactivated by gene targeting in embryonic stem cells. *Proceedings of the National Academy of Sciences*, 89(10), 4471–4475. <a href="https://doi.org/10.1073/pnas.89.10.4471">https://doi.org/10.1073/pnas.89.10.4471</a>

Pi-Sunyer, X. (2009). The Medical Risks of Obesity. *Postgraduate Medicine*, 121(6), Article 6. https://doi.org/10.3810/pgm.2009.11.2074

Plotkin, L. I., Speacht, T. L., and Donahue, H. J. (2015). Cx43 and mechanotransduction in bone. *Current Osteoporosis Reports*, *13*(2), Article 2. <a href="https://doi.org/10.1007/s11914-015-0255-2">https://doi.org/10.1007/s11914-015-0255-2</a>

Podrini, C., Cambridge, E. L., Lelliott, C. J., Carragher, D. M., Estabel, J., Gerdin, A.-K., Karp, N. A., Scudamore, C. L., Ramirez-Solis, R., White, J. K., and Sanger Mouse Genetics Project. (2013). High-fat feeding rapidly induces obesity and lipid derangements in C57BL/6N mice. *Mammalian Genome*, *24*(5), 240–251. <a href="https://doi.org/10.1007/s00335-013-9456-0">https://doi.org/10.1007/s00335-013-9456-0</a>

Pollock, N. K., Laing, E. M., Baile, C. A., Hamrick, M. W., Hall, D. B., and Lewis, R. D. (2007). Is adiposity advantageous for bone strength? A peripheral quantitative computed tomography study in late adolescent females. *The American Journal of Clinical Nutrition*, 86(5), 1530–1538. https://doi.org/10.1093/ajcn/86.5.1530

Qaseem, A., Forciea, M. A., McLean, R. M., Denberg, T. D., and for the Clinical Guidelines Committee of the American College of Physicians. (2017). Treatment of Low Bone Density or Osteoporosis to Prevent Fractures in Men and Women: A Clinical Practice Guideline Update From the American College of Physicians. *Annals of Internal Medicine*, *166*(11), Article 11. <a href="https://doi.org/10.7326/M15-1361">https://doi.org/10.7326/M15-1361</a>

Qiao, J., Wu, Y., and Ren, Y. (2021a). The impact of a high fat diet on bones: Potential mechanisms. *Food and Function*, *12*(3), 963–975. <a href="https://doi.org/10.1039/D0FO02664F">https://doi.org/10.1039/D0FO02664F</a>
Qiao, J., Wu, Y., and Ren, Y. (2021b). The impact of a high fat diet on bones: Potential mechanisms. *Food and Function*, *12*(3), 963–975. <a href="https://doi.org/10.1039/d0fo02664f">https://doi.org/10.1039/d0fo02664f</a>
Qiao, Z., Kong, Q., Tee, W. T., Lim, A. R. Q., Teo, M. X., Olieric, V., Low, P. M., Yang, Y., Qian, G., Ma, W., and Gao, Y.-G. (2022). Molecular basis of the key regulator WRINKLED1 in plant oil biosynthesis. *Science Advances*, *8*(34), eabq1211. <a href="https://doi.org/10.1126/sciadv.abq1211">https://doi.org/10.1126/sciadv.abq1211</a>

Ramli, R., Khamis, M. F., and Shuid, A. N. (2012). Bone Micro-CT Assessments in an Orchidectomised Rat Model Supplemented with *Eurycoma longifolia*. *Evidence-Based Complementary and Alternative Medicine*, 2012, e501858. https://doi.org/10.1155/2012/501858

Reid, I. R., Baldock, P. A., and Cornish, J. (2018a). Effects of Leptin on the Skeleton. Endocrine Reviews, 39(6), 938–959. https://doi.org/10.1210/er.2017-00226

Reid, I. R., Baldock, P. A., and Cornish, J. (2018b). Effects of Leptin on the Skeleton. Endocrine Reviews, 39(6), 938–959. https://doi.org/10.1210/er.2017-00226

Ren, X., Fu, X., Zhang, X., Chen, S., Huang, S., Yao, L., and Liu, G. (2017). Testosterone regulates 3T3-L1 pre-adipocyte differentiation and epididymal fat accumulation in mice through modulating macrophage polarization. *Biochemical Pharmacology*, *140*, 73–88. <a href="https://doi.org/10.1016/j.bcp.2017.05.022">https://doi.org/10.1016/j.bcp.2017.05.022</a>

Ren, X., Wang, F., Chen, C., Gong, X., Yin, L., and Yang, L. (2016). Engineering zonal cartilage through bioprinting collagen type II hydrogel constructs with biomimetic chondrocyte density gradient. *BMC Musculoskeletal Disorders*, *17*(1), 301. https://doi.org/10.1186/s12891-016-1130-8

Ren, Z., Liu, Y., Hong, W., Pan, X., Gong, P., Liu, Q., Zhou, G., and Qin, S. (2020). Conditional knockout of leptin receptor in neural stem cells leads to obesity in mice and affects neuronal differentiation in the hypothalamus early after birth. *Molecular Brain*, 13, 109. https://doi.org/10.1186/s13041-020-00647-9

Reseland, J. E., Syversen, U., Bakke, I., Qvigstad, G., Eide, L. G., Hjertner, O., Gordeladze, J. O., and Drevon, C. A. (2001a). Leptin is expressed in and secreted from primary cultures of human osteoblasts and promotes bone mineralization. *Journal of Bone and Mineral Research: The Official Journal of the American Society for Bone and Mineral Research*, 16(8), 1426–1433. <a href="https://doi.org/10.1359/jbmr.2001.16.8.1426">https://doi.org/10.1359/jbmr.2001.16.8.1426</a>

Reseland, J. E., Syversen, U., Bakke, I., Qvigstad, G., Eide, L. G., Hjertner, Ø., Gordeladze, J. O., and Drevon, C. A. (2001b). Leptin Is Expressed in and Secreted from Primary Cultures of Human Osteoblasts and Promotes Bone Mineralization. *Journal of Bone and Mineral Research*, *16*(8), 1426–1433. https://doi.org/10.1359/jbmr.2001.16.8.1426

Rinonapoli, G., Pace, V., Ruggiero, C., Ceccarini, P., Bisaccia, M., Meccariello, L., and Caraffa, A. (2021). Obesity and Bone: A Complex Relationship. *International Journal of Molecular Sciences*, *22*(24), Article 24. <a href="https://doi.org/10.3390/ijms222413662">https://doi.org/10.3390/ijms222413662</a>

Riquelme, M. A., Cardenas, E. R., Xu, H., and Jiang, J. X. (2020). The Role of Connexin Channels in the Response of Mechanical Loading and Unloading of Bone. *International Journal of Molecular Sciences*, *21*(3), Article 3. <a href="https://doi.org/10.3390/ijms21031146">https://doi.org/10.3390/ijms21031146</a>

Rizk, J., Sahu, R., and Duteil, D. (2023). An overview on androgen-mediated actions in skeletal muscle and adipose tissue. *Steroids*, *199*, 109306. <a href="https://doi.org/10.1016/j.steroids.2023.109306">https://doi.org/10.1016/j.steroids.2023.109306</a>

Robling, A. G., and Turner, C. H. (2009a). Mechanical Signaling for Bone Modeling and Remodeling. *Critical Reviews in Eukaryotic Gene Expression*, 19(4), Article 4.

Robling, A. G., and Turner, C. H. (2009b). Mechanical Signaling for Bone Modeling and Remodeling. *Critical Reviews in Eukaryotic Gene Expression*, *19*(4), 319–338.

Rocher, E., Chappard, C., Jaffre, C., Benhamou, C.-L., and Courteix, D. (2008). Bone mineral density in prepubertal obese and control children: Relation to body weight, lean mass, and fat mass. *Journal of Bone and Mineral Metabolism*, *26*(1), 73–78. https://doi.org/10.1007/s00774-007-0786-4

Rosa, N., Simoes, R., Magalhães, F. D., and Marques, A. T. (2015). From mechanical stimulus to bone formation: A review. *Medical Engineering and Physics*, *37*(8), Article 8. <a href="https://doi.org/10.1016/j.medengphy.2015.05.015">https://doi.org/10.1016/j.medengphy.2015.05.015</a>

Roschger, P., Paschalis, E. P., Fratzl, P., and Klaushofer, K. (2008). Bone mineralization density distribution in health and disease. *Bone*, *42*(3), Article 3. https://doi.org/10.1016/j.bone.2007.10.021

Roux, E., Bougaran, P., Dufourcq, P., and Couffinhal, T. (2020). Fluid Shear Stress Sensing by the Endothelial Layer. *Frontiers in Physiology*, 11. <a href="https://doi.org/10.3389/fphys.2020.00861">https://doi.org/10.3389/fphys.2020.00861</a>

Rowe, P., Koller, A., and Sharma, S. (2024). Physiology, Bone Remodeling. In *StatPearls*. StatPearls Publishing. http://www.ncbi.nlm.nih.gov/books/NBK499863/

Rubin, J., Rubin, C., and Jacobs, C. R. (2006). Molecular pathways mediating mechanical signaling in bone. *Gene*, *367*, 1–16. <a href="https://doi.org/10.1016/j.gene.2005.10.028">https://doi.org/10.1016/j.gene.2005.10.028</a>

Ruppert, Z., Neuperger, P., Rákóczi, B., Gémes, N., Dukay, B., Hajdu, P., Péter, M., Balogh, G., Tiszlavicz, L., Vígh, L., Török, Z., Puskás, L. G., Szebeni, G. J., and Tóth, M. E. (2024). Characterization of obesity-related diseases and inflammation using single cell immunophenotyping in two different diet-induced obesity models. *International Journal of Obesity*, 1–9. https://doi.org/10.1038/s41366-024-01584-6

Saad, F., Röhrig, G., von Haehling, S., and Traish, A. (2016). Testosterone Deficiency and Testosterone Treatment in Older Men. *Gerontology*, *63*(2), 144–156. https://doi.org/10.1159/000452499

Sáinz, N., Barrenetxe, J., Moreno-Aliaga, M. J., and Martínez, J. A. (2015). Leptin resistance and diet-induced obesity: Central and peripheral actions of leptin. *Metabolism: Clinical and Experimental, 64*(1), 35–46. <a href="https://doi.org/10.1016/j.metabol.2014.10.015">https://doi.org/10.1016/j.metabol.2014.10.015</a>

Saleh, F. A., Jaber, H., and Eid, A. (2021). Effect of Adipose derived mesenchymal stem cells on multiple Organ Injuries in diet-induced obese mice. *Tissue Barriers*, *9*(4), 1952150. <a href="https://doi.org/10.1080/21688370.2021.1952150">https://doi.org/10.1080/21688370.2021.1952150</a>

Salmon, P. L., Ohlsson, C., Shefelbine, S. J., and Doube, M. (2015). Structure Model Index Does Not Measure Rods and Plates in Trabecular Bone. *Frontiers in Endocrinology*, *6*. https://www.frontiersin.org/articles/10.3389/fendo.2015.00162

Sánchez, J. C., Valencia-Vásquez, A., and García, A. M. (2021). Role of TRPV4 Channel in Human White Adipocytes Metabolic Activity. *Endocrinology and Metabolism*, *36*(5), 997–1006. https://doi.org/10.3803/EnM.2021.1167

Sass, J.-O., Saemann, M., Kebbach, M., Soodmand, E., Wree, A., Bader, R., and Kluess, D. (2024). The Morphology of the Femur Influences the Fracture Risk during Stumbling and Falls on the Hip—A Computational Biomechanical Study. *Life*, *14*(7), Article 7. https://doi.org/10.3390/life14070841

Sato, S., Hanada, R., Kimura, A., Abe, T., Matsumoto, T., Iwasaki, M., Inose, H., Ida, T., Mieda, M., Takeuchi, Y., Fukumoto, S., Fujita, T., Kato, S., Kangawa, K., Kojima, M., Shinomiya, K., and Takeda, S. (2007). Central control of bone remodeling by neuromedin U. *Nature Medicine*, *13*(10), Article 10. <a href="https://doi.org/10.1038/nm1640">https://doi.org/10.1038/nm1640</a>

Savvidis, C., Tournis, S., and Dede, A. D. (2018). Obesity and bone metabolism. Hormones, 17(2), Article 2. <a href="https://doi.org/10.1007/s42000-018-0018-4">https://doi.org/10.1007/s42000-018-0018-4</a>

Saxton, R. A., Caveney, N. A., Moya-Garzon, M. D., Householder, K. D., Rodriguez, G. E., Burdsall, K. A., Long, J. Z., and Garcia, K. C. (2023). Structural insights into the mechanism of leptin receptor activation. *Nature Communications*, *14*(1), 1797. <a href="https://doi.org/10.1038/s41467-023-37169-6">https://doi.org/10.1038/s41467-023-37169-6</a>

Scheller, E. L., Song, J., Dishowitz, M. I., Soki, F. N., Hankenson, K. D., and Krebsbach, P. H. (2010). Leptin Functions Peripherally to Regulate Differentiation of Mesenchymal Progenitor Cells. *Stem Cells (Dayton, Ohio)*, *28*(6), Article 6. https://doi.org/10.1002/stem.432

Schiavi, J., Fodera, D. M., Brennan, M. A., and McNamara, L. M. (2021). Estrogen depletion alters osteogenic differentiation and matrix production by osteoblasts *in vitro*.

Experimental Cell Research, 408(1), 112814. https://doi.org/10.1016/j.yexcr.2021.112814

Schilling, A. F., Schinke, T., Münch, C., Gebauer, M., Niemeier, A., Priemel, M., Streichert, T., Rueger, J. M., and Amling, M. (2005). Increased Bone Formation in Mice Lacking Apolipoprotein E\*. *Journal of Bone and Mineral Research*, 20(2), 274–282. https://doi.org/10.1359/JBMR.041101

Schreyer, S. A., Lystig, T. C., Vick, C. M., and LeBoeuf, R. C. (2003). Mice deficient in apolipoprotein E but not LDL receptors are resistant to accelerated atherosclerosis associated with obesity. *Atherosclerosis*, *171*(1), 49–55. <a href="https://doi.org/10.1016/j.atherosclerosis.2003.07.010">https://doi.org/10.1016/j.atherosclerosis.2003.07.010</a>

Schweizer, L., Rizzo, C. A., Spires, T. E., Platero, J. S., Wu, Q., Lin, T.-A., Gottardis, M. M., and Attar, R. M. (2008). The androgen receptor can signal through Wnt/β-Catenin in prostate cancer cells as an adaptation mechanism to castration levels of androgens. *BMC Cell Biology*, *9*(1), 4. https://doi.org/10.1186/1471-2121-9-4

Selim, M., Mousa, H. M., Abdel-Jaber, G. T., Barhoum, A., and Abdal-hay, A. (2024). Innovative designs of 3D scaffolds for bone tissue regeneration: Understanding principles and addressing challenges. *European Polymer Journal*, *215*, 113251. https://doi.org/10.1016/j.eurpolymj.2024.113251

Sedelaar, J. P. M., Dalrymple, S. S., & Isaacs, J. T. (2013). Of Mice and Men-Warning: Intact Versus Castrated Adult Male Mice as Xenograft Hosts Are Equivalent to Hypogonadal Versus Abiraterone Treated Aging Human Males, Respectively. The Prostate, 73(12), 1316–1325. <a href="https://doi.org/10.1002/pros.22677">https://doi.org/10.1002/pros.22677</a>

Shapses, S. A., Pop, L. C., and Wang, Y. (2017). Obesity is a concern for bone health with aging. *Nutrition Research (New York, N.Y.)*, 39, 1–13. <a href="https://doi.org/10.1016/j.nutres.2016.12.010">https://doi.org/10.1016/j.nutres.2016.12.010</a>

Shapses, S. A., and Sukumar, D. (2012). Bone Metabolism in Obesity and Weight Loss.

Annual Review of Nutrition, 32, 287–309.

https://doi.org/10.1146/annurev.nutr.012809.104655

Shawky, A. M., Almalki, F. A., Abdalla, A. N., Abdelazeem, A. H., and Gouda, A. M. (2022). A Comprehensive Overview of Globally Approved JAK Inhibitors. *Pharmaceutics*, *14*(5), 1001. https://doi.org/10.3390/pharmaceutics14051001

Shen, H.-X., Liu, J.-Z., Yan, X.-Q., Yang, H.-N., Hu, S.-Q., Yan, X.-L., Xu, T., El Haj, A. J., Yang, Y., and Lü, L.-X. (2022). Hydrostatic pressure stimulates the osteogenesis and angiogenesis of MSCs/HUVECs co-culture on porous PLGA scaffolds. *Colloids and Surfaces B: Biointerfaces*, 213, 112419. https://doi.org/10.1016/j.colsurfb.2022.112419

Shen, X., Zhang, M., Cai, H., Leslie, W. D., Lix, L. M., Jiang, D., Feng, L., Cheng, H., Shi, X., Gao, Y., and Yang, S. (2024). Associations of global biomarkers of oxidative stress with osteoporosis, bone microstructure and bone turnover: Evidence from human and animal studies. *Bone*, *183*, 117077. <a href="https://doi.org/10.1016/j.bone.2024.117077">https://doi.org/10.1016/j.bone.2024.117077</a>

Shigehara, K., Izumi, K., Kadono, Y., and Mizokami, A. (2021a). Testosterone and Bone Health in Men: A Narrative Review. *Journal of Clinical Medicine*, *10*(3), 530. <a href="https://doi.org/10.3390/jcm10030530">https://doi.org/10.3390/jcm10030530</a>

Shigehara, K., Izumi, K., Kadono, Y., and Mizokami, A. (2021b). Testosterone and Bone Health in Men: A Narrative Review. *Journal of Clinical Medicine*, *10*(3), 530. https://doi.org/10.3390/jcm10030530

Shigehara, K., Izumi, K., Kadono, Y., and Mizokami, A. (2021c). Testosterone and Bone Health in Men: A Narrative Review. *Journal of Clinical Medicine*, *10*(3), 530. https://doi.org/10.3390/jcm10030530

Shihan, M., Bulldan, A., and Scheiner-Bobis, G. (2014). Non-classical testosterone signaling is mediated by a G-protein-coupled receptor interacting with Gnα11. *Biochimica et Biophysica Acta (BBA) - Molecular Cell Research*, *1843*(6), 1172–1181. https://doi.org/10.1016/j.bbamcr.2014.03.002

Shim, J., Iwaya, C., Ambrose, C. G., Suzuki, A., and Iwata, J. (2022). Micro-computed tomography assessment of bone structure in aging mice. *Scientific Reports*, *12*(1), 8117. https://doi.org/10.1038/s41598-022-11965-4

Shoskes, J. J., Wilson, M. K., and Spinner, M. L. (2016). Pharmacology of testosterone replacement therapy preparations. *Translational Andrology and Urology*, *5*(6), 834–843. https://doi.org/10.21037/tau.2016.07.10

Shu, L., Beier, E., Sheu, T., Zhang, H., Zuscik, M., Puzas, J. E., Boyce, F. B., Mooney, A. R., and Xing, L. (2015). High-fat Diet Causes Bone Loss in Young Mice by Promoting Osteoclastogenesis through Alteration of the Bone Marrow Environment. *Calcified Tissue International*, *96*(4), 313–323. https://doi.org/10.1007/s00223-015-9954-z

Shuid, A. N., El-arabi, E., Effendy, N. M., Razak, H. S. A., Muhammad, N., Mohamed, N., and Soelaiman, I. N. (2012). Eurycoma longifolia upregulates osteoprotegerin gene expression in androgen- deficient osteoporosis rat model. *BMC Complementary and Alternative Medicine*, 12, 152. <a href="https://doi.org/10.1186/1472-6882-12-152">https://doi.org/10.1186/1472-6882-12-152</a>

Sieverts, M., Obata, Y., Rosenberg, J. L., Woolley, W., Parkinson, D. Y., Barnard, H. S., Pelt, D. M., and Acevedo, C. (2022). Unraveling the effect of collagen damage on bone fracture using in situ synchrotron microtomography with deep learning. *Communications Materials*, *3*(1), 1–13. <a href="https://doi.org/10.1038/s43246-022-00296-6">https://doi.org/10.1038/s43246-022-00296-6</a>

Silva, M. A. F. S., Dechichi, P., and Limirio, P. H. J. O. (2020). Impact of Childhood Obesity on Bone Metabolism. *Pediatric Endocrinology Reviews: PER*, *17*(4), 308–316. https://doi.org/10.17458/per.vol17.2020.sdl.childhoodobesitybonemetabolism

Silva, M. J., Eekhoff, J. D., Patel, T., Kenney-Hunt, J. P., Brodt, M. D., Steger-May, K., Scheller, E. L., and Cheverud, J. M. (2019). Effects of High-Fat Diet and Body Mass on Bone Morphology and Mechanical Properties in 1100 Advanced Intercross Mice. *Journal of Bone and Mineral Research*, *34*(4), 711–725. <a href="https://doi.org/10.1002/jbmr.3648">https://doi.org/10.1002/jbmr.3648</a>

Singh, R., Artaza, J. N., Taylor, W. E., Braga, M., Yuan, X., Gonzalez-Cadavid, N. F., and Bhasin, S. (2006). Testosterone Inhibits Adipogenic Differentiation in 3T3-L1 Cells: Nuclear Translocation of Androgen Receptor Complex with β-Catenin and T-Cell Factor 4 May Bypass Canonical Wnt Signaling to Down-Regulate Adipogenic Transcription Factors. *Endocrinology*, *147*(1), 141–154. https://doi.org/10.1210/en.2004-1649

Skowronski, A. A., Ravussin, Y., Leibel, R. L., and LeDuc, C. A. (2017). Energy homeostasis in leptin deficient Lep*Ob/Ob* mice. *PLoS ONE*, *12*(12), e0189784. https://doi.org/10.1371/journal.pone.0189784

Smith, L. B. (2016). Nonclassical Testosterone Signaling: A New Pathway Controlling Spermatogenesis?1. *Biology of Reproduction*, *94*(2), 43, 1–2. https://doi.org/10.1095/biolreprod.115.137950

Solomon, G., Atkins, A., Shahar, R., Gertler, A., and Monsonego-Ornan, E. (2014). Effect of peripherally administered leptin antagonist on whole body metabolism and bone microarchitecture and biomechanical properties in the mouse. *American Journal of Physiology-Endocrinology and Metabolism*, 306(1), E14–E27. <a href="https://doi.org/10.1152/ajpendo.00155.2013">https://doi.org/10.1152/ajpendo.00155.2013</a>

Song, J., Liu, L., Lv, L., Hu, S., Tariq, A., Wang, W., and Dang, X. (2020). Fluid shear stress induces Runx-2 expression via upregulation of PIEZO1 in MC3T3-E1 cells. *Cell Biology International*, *44*(7), 1491–1502. <a href="https://doi.org/10.1002/cbin.11344">https://doi.org/10.1002/cbin.11344</a>

Sophocleous, A., and Idris, A. I. (2019). Ovariectomy/Orchiectomy in Rodents. *Methods in Molecular Biology (Clifton, N.J.)*, 1914, 261–267. <a href="https://doi.org/10.1007/978-1-4939-8997-3">https://doi.org/10.1007/978-1-4939-8997-3</a> 13

Stanworth, R. D., and Jones, T. H. (2008). Testosterone for the aging male; current evidence and recommended practice. *Clinical Interventions in Aging*, *3*(1), 25–44.

Steffens, J. P., Herrera, B. S., Coimbra, L. S., Stephens, D. N., Jr, C. R., Spolidorio, L. C., Kantarci, A., and Dyke, T. E. V. (2014). Testosterone Regulates Bone Response to Inflammation. *Hormone and Metabolic Research*, *46*(03), 193–200. https://doi.org/10.1055/s-0034-1367031

Sun, J., Pan, Y., Li, X., Wang, L., Liu, M., Tu, P., Wu, C., Xiao, J., Han, Q., Da, W., Ma, Y., and Guo, Y. (2022). Quercetin Attenuates Osteoporosis in Orchiectomy Mice by Regulating Glucose and Lipid Metabolism via the GPRC6A/AMPK/mTOR Signaling Pathway. Frontiers in Endocrinology, 13, 849544. <a href="https://doi.org/10.3389/fendo.2022.849544">https://doi.org/10.3389/fendo.2022.849544</a>

Sun, Z., Guo, S. S., and Fässler, R. (2016). Integrin-mediated mechanotransduction. *The Journal of Cell Biology*, *215*(4), 445–456. <a href="https://doi.org/10.1083/jcb.201609037">https://doi.org/10.1083/jcb.201609037</a>

Suresh, S., Alvarez, J. C., Dey, S., and Noguchi, C. T. (2020). Erythropoietin-Induced Changes in Bone and Bone Marrow in Mouse Models of Diet-Induced Obesity. *International Journal of Molecular Sciences*, *21*(5), 1657. <a href="https://doi.org/10.3390/ijms21051657">https://doi.org/10.3390/ijms21051657</a>

Takeda, S., Elefteriou, F., Levasseur, R., Liu, X., Zhao, L., Parker, K. L., Armstrong, D., Ducy, P., and Karsenty, G. (2002). Leptin regulates bone formation via the sympathetic nervous system. *Cell*, *111*(3), 305–317. <a href="https://doi.org/10.1016/s0092-8674(02)01049-8">https://doi.org/10.1016/s0092-8674(02)01049-8</a>

Tamura, Y., Okinaga, H., and Takami, H. (2004). Glucocorticoid-induced osteoporosis. Biomedicine and Pharmacotherapy = Biomedecine and Pharmacotherapie, 58(9), 500–504. https://doi.org/10.1016/j.biopha.2004.08.018

Tan, B. L., and Norhaizan, M. E. (2019). Effect of High-Fat Diets on Oxidative Stress, Cellular Inflammatory Response and Cognitive Function. *Nutrients*, *11*(11), 2579. https://doi.org/10.3390/nu11112579

Tang, S. Y., Herber, R.-P., Ho, S. P., and Alliston, T. (2012). Matrix metalloproteinase-13 is required for osteocytic perilacunar remodeling and maintains bone fracture resistance. *Journal of Bone and Mineral Research: The Official Journal of the American Society for Bone and Mineral Research*, 27(9), 1936–1950. https://doi.org/10.1002/jbmr.1646

Teng, B., Yu, X.-F., Li, J., Udduttula, A., Ismayil, A., Huang, X., Li, J., Zhao, P.-Y., Kerem, G., Long, J., Liu, C., and Ren, P.-G. (2023). Cervical vertebrae for early bone loss evaluation in osteoporosis mouse models. *Quantitative Imaging in Medicine and Surgery*, *13*(4), 2466–2477. <a href="https://doi.org/10.21037/qims-22-717">https://doi.org/10.21037/qims-22-717</a>

Thai, V. L., Mierswa, S., Griffin, K. H., Boerckel, J. D., and Leach, J. K. (2024). Mechanoregulation of MSC spheroid immunomodulation. *APL Bioengineering*, 8(1), 016116. <a href="https://doi.org/10.1063/5.0184431">https://doi.org/10.1063/5.0184431</a>

The Jackson Laboratory. (n.d.). *Body Weight Information for C57BL/6J | The Jackson Laboratory*. Retrieved 1 October 2023, from <a href="https://www.jax.org/jax-mice-and-services/strain-data-sheet-pages/body-weight-chart-000664">https://www.jax.org/jax-mice-and-services/strain-data-sheet-pages/body-weight-chart-000664</a>

Thomas, C. D. L., Mayhew, P. M., Power, J., Poole, K. E., Loveridge, N., Clement, J. G., Burgoyne, C. J., and Reeve, J. (2009). Femoral neck trabecular bone: Loss with aging and role in preventing fracture. *Journal of Bone and Mineral Research: The Official Journal of the American Society for Bone and Mineral Research*, 24(11), 1808–1818. https://doi.org/10.1359/jbmr.090504

Thorpe, A. A., Creasey, S., Sammon, C., and Le Maitre, C. L. (2016). Hydroxyapatite nanoparticle injectable hydrogel scaffold to support osteogenic differentiation of human mesenchymal stem cells. *European Cells and Materials*, *32*, 1–23. https://doi.org/10.22203/ecm.v032a01

Thorpe, A. A., Freeman, C., Farthing, P., Callaghan, J., Hatton, P. V., Brook, I. M., Sammon, C., and Le Maitre, C. L. (2018). In vivo safety and efficacy testing of a thermally triggered injectable hydrogel scaffold for bone regeneration and augmentation in a rat model. *Oncotarget*, *9*(26), 18277–18295. <a href="https://doi.org/10.18632/oncotarget.24813">https://doi.org/10.18632/oncotarget.24813</a>

Touaiher, I., Saadaoui, M., Reynaud, P., Reveron, H., and Chevalier, J. (2023). Mechanical properties of additive-manufactured hydroxyapatite porous scaffolds and follow-up of damage process under compression loading. *Open Ceramics*, *16*, 100498. https://doi.org/10.1016/j.oceram.2023.100498

Traish, A. M., and Morgentaler, A. (2019). Chapter 18—Benefits and Risks of Testosterone Therapy in Men With Testosterone Deficiency. In B. LaMarca and B. T. Alexander (Eds.), *Sex Differences in Cardiovascular Physiology and Pathophysiology* (pp. 321–354). Academic Press. https://doi.org/10.1016/B978-0-12-813197-8.00018-X

Tsai, C.-C., Yang, Y.-C. S. H., Chen, Y.-F., Huang, L.-Y., Yang, Y.-N., Lee, S.-Y., Wang, W.-L., Lee, H.-L., Whang-Peng, J., Lin, H.-Y., and Wang, K. (2023). Integrins and Actions of Androgen in Breast Cancer. *Cells*, *12*(17), 2126. <a href="https://doi.org/10.3390/cells12172126">https://doi.org/10.3390/cells12172126</a>

Turcotte, A.-F., O'Connor, S., Morin, S. N., Gibbs, J. C., Willie, B. M., Jean, S., and Gagnon, C. (2021). Association between obesity and risk of fracture, bone mineral density and bone quality in adults: A systematic review and meta-analysis. *PLoS ONE*, *16*(6), e0252487. <a href="https://doi.org/10.1371/journal.pone.0252487">https://doi.org/10.1371/journal.pone.0252487</a>

Turner, R. T., Kalra, S. P., Wong, C. P., Philbrick, K. A., Lindenmaier, L. B., Boghossian, S., and Iwaniec, U. T. (2013). Peripheral leptin regulates bone formation. *Journal of Bone and Mineral Research: The Official Journal of the American Society for Bone and Mineral Research*, 28(1), 22–34. https://doi.org/10.1002/jbmr.1734

Turner, R. T., Philbrick, K. A., Wong, C. P., Olson, D. A., Branscum, A. J., and Iwaniec, U. T. (2014). Morbid Obesity Attenuates the Skeletal Abnormalities Associated with Leptin Deficiency in Mice. *The Journal of Endocrinology*, *223*(1), M1–M15. <a href="https://doi.org/10.1530/JOE-14-0224">https://doi.org/10.1530/JOE-14-0224</a>

Udagawa, N., Koide, M., Nakamura, M., Nakamichi, Y., Yamashita, T., Uehara, S., Kobayashi, Y., Furuya, Y., Yasuda, H., Fukuda, C., and Tsuda, E. (2021). Osteoclast differentiation by RANKL and OPG signaling pathways. *Journal of Bone and Mineral Metabolism*, *39*(1), 19–26. https://doi.org/10.1007/s00774-020-01162-6

Uto, Y., Kuroshima, S., Nakano, T., Ishimoto, T., Inaba, N., Uchida, Y., and Sawase, T. (2017). Effects of mechanical repetitive load on bone quality around implants in rat maxillae. *PloS One*, *12*(12), e0189893. <a href="https://doi.org/10.1371/journal.pone.0189893">https://doi.org/10.1371/journal.pone.0189893</a>

Vazquez, M., Evans, B. A. J., Riccardi, D., Evans, S. L., Ralphs, J. R., Dillingham, C. M., and Mason, D. J. (2014). A New Method to Investigate How Mechanical Loading of Osteocytes Controls Osteoblasts. *Frontiers in Endocrinology*, *5*, 208. https://doi.org/10.3389/fendo.2014.00208

Viguet-Carrin, S., Garnero, P., and Delmas, P. D. (2006). The role of collagen in bone strength. *Osteoporosis International*, *17*(3), 319–336. <a href="https://doi.org/10.1007/s00198-005-2035-9">https://doi.org/10.1007/s00198-005-2035-9</a>

Vilariño-García, T., Polonio-González, M. L., Pérez-Pérez, A., Ribalta, J., Arrieta, F., Aguilar, M., Obaya, J. C., Gimeno-Orna, J. A., Iglesias, P., Navarro, J., Durán, S., Pedro-Botet, J., and Sánchez-Margalet, V. (2024). Role of Leptin in Obesity, Cardiovascular Disease, and Type 2 Diabetes. *International Journal of Molecular Sciences*, 25(4), Article 4. <a href="https://doi.org/10.3390/ijms25042338">https://doi.org/10.3390/ijms25042338</a>

Walker, W. H. (2011). Testosterone signaling and the regulation of spermatogenesis. *Spermatogenesis*, 1(2), 116–120. <a href="https://doi.org/10.4161/spmg.1.2.16956">https://doi.org/10.4161/spmg.1.2.16956</a>

Wallimann, A., Magrath, W., Thompson, K., Moriarty, T. F., Richards, R. G., Akdis, C. A., O'Mahony, L., and Hernandez, C. J. (2021). Gut microbial-derived short-chain fatty acids and bone: A potential role in fracture healing. *European Cells and Materials*, *41*, 454–470. <a href="https://doi.org/10.22203/eCM.v041a29">https://doi.org/10.22203/eCM.v041a29</a>

Wang, C., and Swerdloff, R. S. (2022). Testosterone Replacement Therapy in Hypogonadal Men. *Endocrinology and Metabolism Clinics of North America*, *51*(1), 77–98. <a href="https://doi.org/10.1016/j.ecl.2021.11.005">https://doi.org/10.1016/j.ecl.2021.11.005</a>

Wang, L. (2018). Solute Transport in the Bone Lacunar-Canalicular System (LCS). *Current Osteoporosis Reports*, *16*(1), 32–41. <a href="https://doi.org/10.1007/s11914-018-0414-3">https://doi.org/10.1007/s11914-018-0414-3</a>

Wang, W.-H., Wang, F., Zhao, H.-F., Yan, K., Huang, C.-L., Yin, Y., Huang, Q., Chen, Z.-Z., and Zhu, W.-Y. (2020). Injectable Magnesium-Zinc Alloy Containing Hydrogel Complex for Bone Regeneration. *Frontiers in Bioengineering and Biotechnology*, 8. https://doi.org/10.3389/fbioe.2020.617585

Wee, N. K. Y., Lima, T. F. C. de, McGregor, N. E., Walker, E. C., Poulton, I. J., Blank, M., & Sims, N. A. (2022). Leptin receptor in osteocytes promotes cortical bone consolidation in female mice. https://doi.org/10.1530/JOE-22-0084

Wei, Z., Schnellmann, R., Pruitt, H. C., and Gerecht, S. (2020). Hydrogel Network Dynamics Regulate Vascular Morphogenesis. *Cell Stem Cell*, *27*(5), 798-812.e6. https://doi.org/10.1016/j.stem.2020.08.005

Weinbaum, S., Cowin, S. C., and Zeng, Y. (1994). A model for the excitation of osteocytes by mechanical loading-induced bone fluid shear stresses. *Journal of Biomechanics*, *27*(3), 339–360. <a href="https://doi.org/10.1016/0021-9290(94)90010-8">https://doi.org/10.1016/0021-9290(94)90010-8</a>

WHO. (n.d.). *Obesity and Overweight Statistics 2024*. Retrieved 1 October 2023, from <a href="https://www.who.int/news-room/fact-sheets/detail/obesity-and-overweight">https://www.who.int/news-room/fact-sheets/detail/obesity-and-overweight</a>

Wilhelmson, A. S., Lantero Rodriguez, M., Svedlund Eriksson, E., Johansson, I., Fogelstrand, P., Stubelius, A., Lindgren, S., Fagman, J. B., Hansson, G. K., Carlsten, H., Karlsson, M. C. I., Ekwall, O., and Tivesten, Å. (2018). Testosterone Protects Against Atherosclerosis in Male Mice by Targeting Thymic Epithelial Cells—Brief Report. *Arteriosclerosis, Thrombosis, and Vascular Biology*, *38*(7), 1519–1527. <a href="https://doi.org/10.1161/ATVBAHA.118.311252">https://doi.org/10.1161/ATVBAHA.118.311252</a>

Williamson, A., da Silva, A., do Carmo, J. M., Le Maitre, C. L., Hall, J. E., and Aberdein, N. (2023). Impact of leptin deficiency on male tibia and vertebral body 3D bone architecture independent of changes in body weight. *Physiological Reports*, *11*(19). <a href="https://doi.org/10.14814/phy2.15832">https://doi.org/10.14814/phy2.15832</a>

Wilson, S., Qi, J., and Filipp, F. V. (2016). Refinement of the androgen response element based on ChIP-Seq in androgen-insensitive and androgen-responsive prostate cancer cell lines. *Scientific Reports*, *6*, 32611. https://doi.org/10.1038/srep32611

Wiren, K. M. (2005). Androgens and bone growth: It's location, location. *Current Opinion in Pharmacology,* 5(6), 626–632. <a href="https://doi.org/10.1016/j.coph.2005.06.003">https://doi.org/10.1016/j.coph.2005.06.003</a>

Wittert, G., and Grossmann, M. (2022). Obesity, type 2 diabetes, and testosterone in ageing men. *Reviews in Endocrine and Metabolic Disorders*, *23*(6), 1233–1242. https://doi.org/10.1007/s11154-022-09746-5

Wu, J., Henning, P., Sjögren, K., Koskela, A., Tuukkanen, J., Movérare-Skrtic, S., and Ohlsson, C. (2019). The androgen receptor is required for maintenance of bone mass in adult male mice. *Molecular and Cellular Endocrinology*, *479*, 159–169. https://doi.org/10.1016/j.mce.2018.10.008

Wu, L., and Pan, Y. (2019). Reactive oxygen species mediate TNF-α-induced inflammatory response in bone marrow mesenchymal cells. *Iranian Journal of Basic Medical Sciences*, *22*(11), 1296–1301. <a href="https://doi.org/10.22038/ijbms.2019.37893.9006">https://doi.org/10.22038/ijbms.2019.37893.9006</a>

Wu, X., and Zhang, M. (2018). Effects of androgen and progestin on the proliferation and differentiation of osteoblasts. *Experimental and Therapeutic Medicine*, *16*(6), 4722–4728. https://doi.org/10.3892/etm.2018.6772

Xu, L. H., Shao, H., Ma, Y.-H. V., & You, L. (2019). OCY454 Osteocytes as an in Vitro Cell Model for Bone Remodeling Under Mechanical Loading. Journal of Orthopaedic Research, 37(8), 1681–1689. https://doi.org/10.1002/jor.24302

Yan, Z., Wang, P., Wu, J., Feng, X., Cai, J., Zhai, M., Li, J., Liu, X., Jiang, M., Luo, E., and Jing, D. (2018). Fluid shear stress improves morphology, cytoskeleton architecture, viability, and regulates cytokine expression in a time-dependent manner in MLO-Y4 cells. *Cell Biology International*, *42*(10), 1410–1422. <a href="https://doi.org/10.1002/cbin.11032">https://doi.org/10.1002/cbin.11032</a>
Yang, Q., Li, Z., Li, W., Lu, L., Wu, H., Zhuang, Y., Wu, K., and Sui, X. (2019). Association of total testosterone, free testosterone, bioavailable testosterone, sex hormone—binding globulin, and hypertension. *Medicine*, *98*(20), e15628.

Yang, Y., Xiao, L., Wu, Y., Xu, Y., Xia, Z., and Wang, S. (2023). Mechanical loading directly regulates the function of osteoblast in multiple ways. *Science and Sports*, *38*(8), 760–768. https://doi.org/10.1016/j.scispo.2022.08.005

https://doi.org/10.1097/MD.0000000000015628

Yeh, P.-S., Lee, Y.-W., Chang, W.-H., Wang, W., Wang, J.-L., Liu, S.-H., and Chen, R.-M. (2019). Biomechanical and tomographic differences in the microarchitecture and strength of trabecular and cortical bone in the early stage of male osteoporosis. *PLoS ONE*, *14*(8), e0219718. <a href="https://doi.org/10.1371/journal.pone.0219718">https://doi.org/10.1371/journal.pone.0219718</a>

Yoo, C.-K., Jeon, J.-Y., Kim, Y.-J., Kim, S.-G., and Hwang, K.-G. (2016). Cell attachment and proliferation of osteoblast-like MG63 cells on silk fibroin membrane for guided bone regeneration. *Maxillofacial Plastic and Reconstructive Surgery*, *38*(1), 17. https://doi.org/10.1186/s40902-016-0062-4

Yu, L., Ma, X., Sun, J., Tong, J., Shi, L., Sun, L., and Zhang, J. (2017). Fluid shear stress induces osteoblast differentiation and arrests the cell cycle at the G0 phase via the ERK1/2 pathway. *Molecular Medicine Reports*, *16*(6), 8699–8708. https://doi.org/10.3892/mmr.2017.7720

Yue, R., Zhou, B. O., Shimada, I. S., Zhao, Z., and Morrison, S. J. (2016). Leptin Receptor Promotes Adipogenesis and Reduces Osteogenesis by Regulating Mesenchymal Stromal Cells in Adult Bone Marrow. *Cell Stem Cell*, *18*(6), 782–796. https://doi.org/10.1016/j.stem.2016.02.015

Yuste, I., Luciano, F. C., González-Burgos, E., Lalatsa, A., and Serrano, D. R. (2021). Mimicking bone microenvironment: 2D and 3D *in vitro* models of human osteoblasts. *Pharmacological Research*, *169*, 105626. <a href="https://doi.org/10.1016/j.phrs.2021.105626">https://doi.org/10.1016/j.phrs.2021.105626</a>

Zarka, M., Etienne, F., Bourmaud, M., Szondi, D., Schwartz, J.-M., Kampmann, K., Helary, C., Rannou, F., Haÿ, E., and Cohen-Solal, M. (2021). Mechanical loading activates the YAP/TAZ pathway and chemokine expression in the MLO-Y4 osteocyte-like cell line. *Laboratory Investigation*, 101(12), 1597–1604. <a href="https://doi.org/10.1038/s41374-021-00668-5">https://doi.org/10.1038/s41374-021-00668-5</a>

Zeadin, M. G., Butcher, M. K., Shaughnessy, S. G., and Werstuck, G. H. (2012). Leptin promotes osteoblast differentiation and mineralization of primary cultures of vascular smooth muscle cells by inhibiting glycogen synthase kinase (GSK)-3β. *Biochemical and Biophysical Research Communications*, 425(4), 924–930. https://doi.org/10.1016/j.bbrc.2012.08.011

Zhang, D., Jian, Y.-P., Zhang, Y.-N., Li, Y., Gu, L.-T., Sun, H.-H., Liu, M.-D., Zhou, H.-L., Wang, Y.-S., and Xu, Z.-X. (2023). Short-chain fatty acids in diseases. *Cell Communication and Signaling*, *21*(1), 212. <a href="https://doi.org/10.1186/s12964-023-01219-9">https://doi.org/10.1186/s12964-023-01219-9</a>

Zhang, P., Hamamura, K., and Yokota, H. (2008). A Brief Review of Bone Adaptation to Unloading. *Genomics, Proteomics and Bioinformatics, 6*(1), 4–7. <a href="https://doi.org/10.1016/S1672-0229(08)60016-9">https://doi.org/10.1016/S1672-0229(08)60016-9</a>

Zhang, Y., Cheng, Z., Hong, L., Liu, J., Ma, X., Wang, W., Pan, R., Lu, W., Luo, Q., Gao, S., and Kong, Q. (2023). Apolipoprotein E (ApoE) orchestrates adipose tissue inflammation and metabolic disorders through NLRP3 inflammasome. *Molecular Biomedicine*, *4*(1), 47. <a href="https://doi.org/10.1186/s43556-023-00158-8">https://doi.org/10.1186/s43556-023-00158-8</a>

Zhang, Z., Zhang, Z., Pei, L., Zhang, X., Li, B., Meng, Y., and Zhou, X. (2022). How high-fat diet affects bone in mice: A systematic review and meta-analysis. *Obesity Reviews*, *23*(10), e13493. <a href="https://doi.org/10.1111/obr.13493">https://doi.org/10.1111/obr.13493</a>

Zheng, R., Byberg, L., Larsson, S. C., Höijer, J., Baron, J. A., and Michaëlsson, K. (2021). Prior loss of body mass index, low body mass index, and central obesity independently contribute to higher rates of fractures in elderly women and men. *Journal of Bone and Mineral Research: The Official Journal of the American Society for Bone and Mineral Research*, 36(7), 1288–1299. https://doi.org/10.1002/jbmr.4298

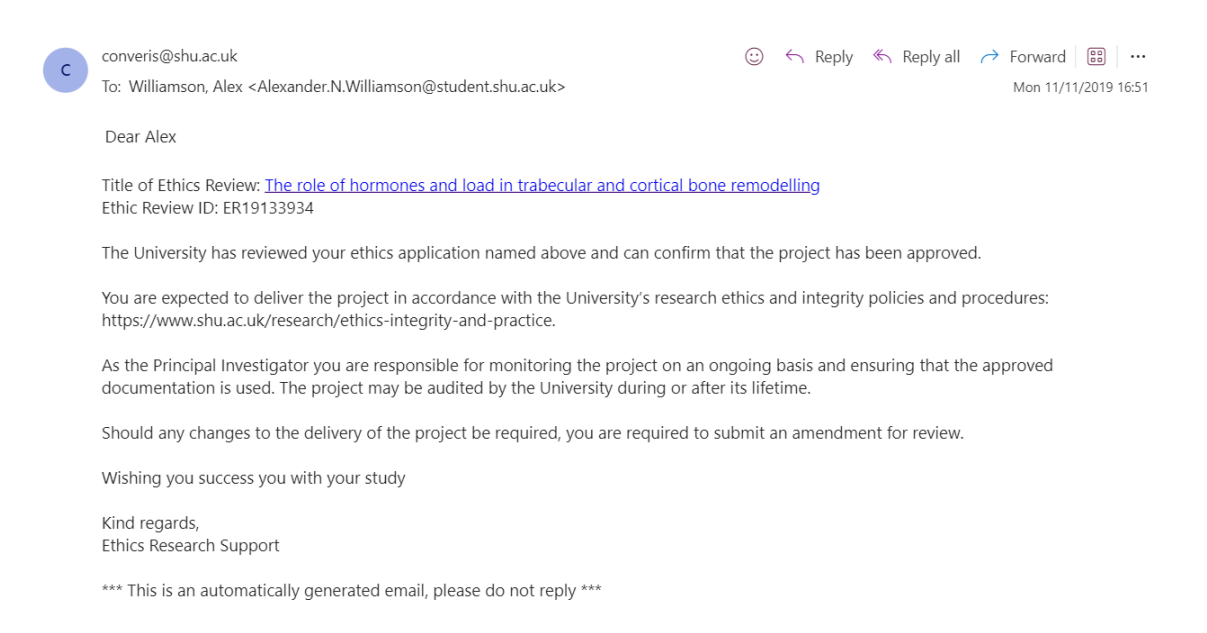
Zhou, S., Dai, Q., Huang, X., Jin, A., Yang, Y., Gong, X., Xu, H., Gao, X., and Jiang, L. (2021). STAT3 is critical for skeletal development and bone homeostasis by regulating osteogenesis. *Nature Communications*, *12*, 6891. <a href="https://doi.org/10.1038/s41467-021-27273-w">https://doi.org/10.1038/s41467-021-27273-w</a>

Zhu, K., Hunter, M., James, A., Lim, E. M., and Walsh, J. P. (2015). Associations between body mass index, lean and fat body mass and bone mineral density in middle-aged Australians: The Busselton Healthy Ageing Study. *Bone*, *74*, 146–152. <a href="https://doi.org/10.1016/j.bone.2015.01.015">https://doi.org/10.1016/j.bone.2015.01.015</a>

Zhu, S., Chen, W., Masson, A., and Li, Y.-P. (2024). Cell signaling and transcriptional regulation of osteoblast lineage commitment, differentiation, bone formation, and homeostasis. *Cell Discovery*, *10*(1), 1–39. <a href="https://doi.org/10.1038/s41421-024-00689-6">https://doi.org/10.1038/s41421-024-00689-6</a>

Zvintzou, E., Skroubis, G., Chroni, A., Petropoulou, P.-I., Gkolfinopoulou, C., Sakellaropoulos, G., Gantz, D., Mihou, I., Kalfarentzos, F., and Kypreos, K. E. (2014). Effects of bariatric surgery on HDL structure and functionality: Results from a prospective trial. *Journal of Clinical Lipidology*, *8*(4), 408–417. <a href="https://doi.org/10.1016/j.jacl.2014.05.001">https://doi.org/10.1016/j.jacl.2014.05.001</a>

# **Ethical Approval Statement:**



## **ApoE study Power calculation:**

**Client: Daniel Kelly** 

Contract number: SSU2017/003P

Date: 22/06/2017

Sample size calculations for study into the effects of testosterone and the drug Rivaroxaban on atherosclerosis

Amy Spencer and Pete Laud

## Experiment

The mice in this experiment are a strain that is prone to atherosclerosis. Six groups will be subjected to various combinations of surgery, replacement testosterone therapy and treatment with Rivaroxaban as follows:

Table 1: Experimental groups

Surgery	Testosterone	Drug
	therapy	
Sham	None	None
Sham	None	Rivaroxaban
Castrated	None	None
Castrated	None	Rivaroxaban
Castrated	Testosterone	None
Castrated	Testosterone	Rivaroxaban
	Sham Sham Castrated Castrated Castrated	therapy  Sham None  Sham None  Castrated None  Castrated None  Castrated Testosterone

Testosterone is known to affect the amount of atherosclerotic plaque. Previous experiments [1] have shown that castrated mice have larger amounts of plaque than non-castrated mice and when castrated mice are treated with replacement testosterone, the amount of plaque is decreased. This experiment will look at this further, and in particular analyse the effects of Rivaroxaban on atherosclerosis in combination with testosterone. This drug has previously been shown to decrease the atherosclerotic plaque in non-castrated mice [2].

# Data from previous studies

A study [1] into the effect of testosterone in atherosclerotic mice had a sham surgery (untreated) group, a castrated (untreated) group and a castrated group treated with replacement testosterone. The mean atherosclerotic plaque observed in these groups was 16.2%, 25.8% and 13.1% of the total area respectively with standard deviations (SDs) of approximately 8% in the sham surgery and 5.5% in the castrated groups. This suggests that castrating mice increases plaque area by around 60% and that treating castrated mice with replacement testosterone decreases plaque area by around 50%.

Another study [2] investigated the effect of Rivaroxaban on mice (these mice were not operated on or given any other treatment). The control group had mean and SD of 5.7% (2.6%) compared to 3.3% (1.4%) for the treated group, suggesting that this treatment reduced plaque areas by around 40%.

It would be expected that the sham surgery group in [1] and the control group in [2] should have similar results, which does not appear to be the case from the percentage plaque areas given. However, this is likely to be due to subjective differences dependent on the individual assessor. Although there is variability between studies, consistency is expected within a study. For the sample size calculations given below we will use the proportional changes observed in the means in both of these studies, but will base the values of the means and SDs on those observed in [2]. We have chosen to do this because the sample sizes were larger in this study suggesting better estimates. Also, although this study does not have any data on castrated mice, the data from [1] suggests that SDs may be smaller in castrated than non-castrated mice, so power calculations based on SDs from [2] should be conservative.

#### **Statistical analysis**

As mentioned above, the effects of testosterone and Rivaroxaban on atherosclerosis independently have been shown in previous studies. Therefore, it has been decided to focus this study on the following comparisons:

- Group 2 vs Group 4: Do mice treated with Rivaroxaban produce a different amount of atherosclerotic plaque dependent on whether or not they are castrated?
- Group 4 vs Group 6: Do castrated mice treated with Rivaroxaban produce a different amount of atherosclerotic plaque dependent on whether or not they are given replacement testosterone therapy?
- Group 5 vs Group 6: Do castrated mice given replacement testosterone therapy produce a different amount of atherosclerotic plaque dependent on whether or not they are treated with Rivaroxaban?

Each of these can be tested using a t-test. As there are three co-primary analyses, and we wish to keep the overall Type I error rate at 5%, a significance level of 5%/3 = 1.67% will be used. There is some evidence from the previous data to suggest that Satterthwaite's t-test for groups with unequal variances might be more appropriate, and under appropriate conditions this would be expected to increase the power of the tests.

Further t-tests, including ones using Groups 1 and 3 may be carried out as secondary analyses, to confirm that the data collected in this study are comparative with those in similar studies, thus validating the experiment, but the sample sizes given below do not power for such tests.

#### Sample size calculations

Group 2 vs Group 4. Based on [2], we expect to see a mean of 3.3% (SD = 1.4%) in the non-castrated group. If there is the same increase of 60% atherosclerotic plaque in castrated mice as was observed in the non-Rivaroxaban treated groups in [1], 12 mice per group would be required to have 80% power to detect this rise to a mean of 5.3% plaque at the 1.67% significance level. To detect a more modest change of 50% (mean = 5.0% plaque), 16 mice per group would be required.

Group 4 vs Group 6. Assuming that the mean plaque area in Group 4 is 5.3% (SD = 1.4), 8 mice would be required to have 80% power to detect a 50% reduction in plaque area (to 2.6%) in Group 6 (addition of testosterone) at the 1.67% level. This is the level of reduction observed in [1] in castrated mice not treated with Rivaroxaban. If it is thought that the effect could be more modest when Rivaroxaban is used, larger sample sizes may be needed. Some alternatives are given in Table 2 below.

Table 2: Possible mean plaque areas for the group given testosterone (and the sample size per group needed) for the test of the addition of testosterone in castrated mice taking Rivaroxaban. Sample sizes calculated assuming 80% power and 1.67% significance level.

Comparative reduction	in Mean plaque a	rea in Group 4 (Castrated +					
plaque in Group 6 (Castrated Rivaroxaban)*							
+ Rivaroxaban	+5%	5.3%					
Testosterone)							
30%	3.5% (20)	3.7% (18)					
40%	3.0% (12)	3.2% (11)					
50%	2.5% (9)	2.6% (8)					

\*These mean plaque areas are based on those discussed in the Group 2 vs Group 4 test section

Group 5 vs Group 6. The data in [2] suggests that Rivaroxaban can reduce the plaque area by 40% in mice that have not been castrated. If this can be assumed to be the same in mice which have been castrated but have had replacement testosterone therapy we can calculate the number of mice per group needed to have 80% power to detect such a change at the 1.67% significance level. If the mean plaque area in Group 6 is 3.2% (SD = 1.4%), this is 40% lower than a mean plaque area of 5.3% in Group 5. In this case the required sample size per group is 11. We may wish to assume different values of the mean plaque area in the two groups and some options are given in Table 3 below, along with the sample sizes needed to detect the differences.

Table 3: Possible mean plaque areas for the group <u>not</u> given Rivaroxaban (and the sample size per group needed) for the test of the addition of Rivaroxaban in castrated mice taking testosterone. Sample sizes calculated assuming 80% power and 1.67% significance level.

Comparative reduction in	Mean plaque area in Group 6 (Castrated + Rivaroxaban +				
plaque in Group 6	Testosterone)** 3.0% 3.2% 3.5% 3.7%				
(Castrated + Rivaroxaban +					
Testosterone)					
30%	4.2% (30)	4.5% (26)	5.0% (20)	5.3% (18)	
35%	4.6% (18)	4.9% (16)	5.3% (15)	5.7% (12)	
40%	5.0% (12)	5.3% (11)	5.8% (10)	6.2% (9)	

<sup>\*\*</sup>These mean plaque areas are based on some of those given in Table 2 in the Group 4 vs Group 6 test section

Overall sample size strategy. The previous studies [1, 2] observed an increase of 60%, a decrease of 50% and a decrease of 40% in the area of atherosclerotic plaque when castration, replacement testosterone therapy (in castrated mice) and Rivaroxaban were added, respectively, in the absence of other factors. We are now looking at those changes when the baseline is already affected by something else. It may therefore be

sensible to look for slightly more modest changes, for example an increase of 50% and decreases of 40% and 35% respectively. This relates to the following mean plaque areas:

• Group 2: 3.3%

• Group 4: 5.0%

• Group 5: 4.6%

• Group 6: 3.0%

Sample sizes needed for the primary analyses with these means are: (2 vs 4) 16, (4 vs 6) 12 and (5 vs 6) 18. This means that while 18 mice would be required in groups 5 and 6, only 16 would be required in groups 2 and 4, and smaller numbers of mice still could be used in groups 1 and 3, which will only be used for secondary analyses. This is only one example of a strategy based on looking for the given changes in the plaque areas.

[1] Testosterone study

[2] Rivaroxaban study

# **Immunohistochemistry Isotype Controls:**

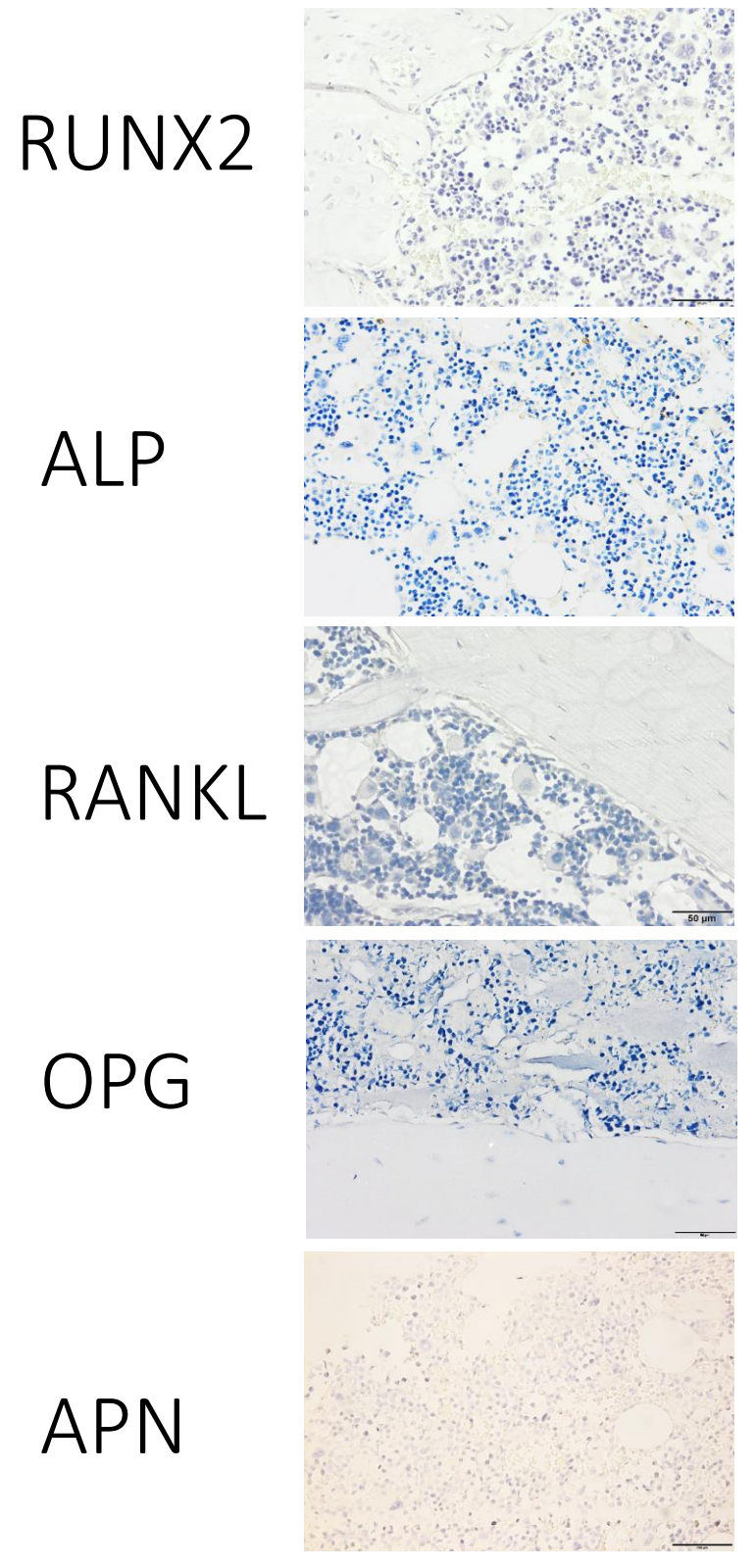


Figure 6.1: Isotype controls from Runx2, ALP, RANKL, OPG, and APN IHC staining procedures. Scale bars are  $50\mu m$ .